



UNIwersytet Śląski
W KATOWICACH

Institute of Chemistry
Faculty of Science and Technology
University of Silesia

mgr inż. Bernadeta Jasiok

Ph.D. Thesis

Approaches based on the theory of thermodynamic fluctuations and molecular dynamics for predicting properties of molecular and ionic liquids under high pressures

Przewidywanie właściwości cieczy molekularnych i jonowych w warunkach wysokiego ciśnienia w oparciu o teorię fluktuacji termodynamicznych i dynamikę molekularną

Doctoral supervisor:

dr hab. Mirosław Chorążewski, prof. UŚ

Scientific tutor provided by PIK — Program for new interdisciplinary elements of education at the doctoral level for a field of chemistry,

POWR.03.02.00–00-I010/17:

Prof. Eugene B. Postnikov

Katowice, 2023

Streszczenie

Niniejsza rozprawa doktorska odnosi się do złożonego problemu dotyczącego opracowania termodynamicznych metod oraz równań stanu celem przewidywania gęstości i jej pochodnych, w tym izobarycznego współczynnika rozszerzalności termicznej, współczynnika ściśliwości izotermicznej, jak i również prędkości propagacji dźwięku w jednofazowych cieczach pod zwiększonym ciśnieniem. Zagadnienie to jest ważne zarówno z punktu widzenia badań podstawowych w obszarze chemii fizycznej czy też ogólnie pojętej fizyki fazy ciekłej, jak i również ma znaczenie w zastosowaniach przemysłowych, np. tam gdzie niezbędna jest wiedza o właściwościach termodynamicznych skompresowanej fazy ciekłej. Te pierwsze wywodzą się z braku ogólnej, uniwersalnej i utylitarnej teorii cieczy, która głównie podaje ilościowe wartości wielkości termodynamicznych w obszarze jednofazowym. Drugie, to choćby między innymi wynikające z potrzeb termodynamicznego modelowania procesów wtrysku paliwa w wysokoprężnych silnikach Diesla typu *common rail*, przeznaczonych do pracy pod ciśnieniem sięgającym wartości kilkuset MPa, a także choćby w problematyce wysokociśnieniowej katalizy chemicznej (np. przetwarzania ligniny z użyciem cieczy jonowych, będących nadal aktualnym kierunkiem badawczym tzw. zielonej chemii).

W ciągu ostatniej dekady (w tym w pracach, w których autorka niniejszej dysertacji jest współautorem) ustalono, że celem opisu właściwości fizykochemicznych cieczy prostych, molekularnych jak i jonowych można podejść analizując ich związek z termodynamicznymi fluktuacjami gęstości, które z kolei można odnieść do zmian objętości swobodnej układu wywołanej ciśnieniem zewnętrznym. Jednocześnie, prace te pozwoliły określić zbiór otwartych problemów, których wyjaśnienie jest głównym celem niniejszej rozprawy.

Niniejsza praca omawia wyznaczone w niej cele przechodząc kolejno od makroskopowego do mikroskopowego obrazu termodynamicznego skompresowanej fazy ciekłej. Pierwszy rozdział dotyczy granic stosowalności podejścia opartego na fluktuacjach gęstości oraz jego ewentualnego rozszerzenia w przypadku aplikacyjności zastosowanych modeli termodynamicznych

do obszarów wysokich ciśnień, jak również wyznaczenia odpowiednich parametrów zaproponowanego izotermicznego równania stanu w warunkach ciśnienia atmosferycznego w taki sposób, aby przewidywane wartości gęstości były porównywalne w granicach niepewności pomiarowych z tymi uzyskanymi drogą bezpośredniego eksperymentu. Drugi rozdział przedstawia szczegółowe podstawy matematyczne i termodynamiczne podejścia zaproponowanego w pierwszym rozdziale. Pozwala to na uogólnienie ich na przypadek własności pochodnych termodynamicznych oraz prędkości propagacji dźwięku, będącej sednem rozważań podjętych w niniejszej dysertacji. Trzeci rozdział łączy makroskopowy obraz termodynamiczny fazy ciekłej z mikroskopowym opartym na wynikach symulacji dynamiki molekularnej. Te ostatnie mają na celu wyjaśnienie anomalii termodynamicznych i kwestii, które pojawiły się w trakcie badań z użyciem modelu fluktuacyjnego. Obejmują one pewien dysonans pomiędzy przewidywaniami opartymi na teorii fluktuacji a wynikami opartymi o pomiary akustyczne i densytometryczne w przebiegu izobarycznej rozszerzalności termicznej halogenopochodnych *n*-alkanów. Synergia podejść opartych na dynamice molekularnej, termodynamice oraz teorii fluktuacji skompresowanej fazy ciekłej, pozwoliła również na zróżnicowanie cech stereochemicznych badanych układów ciekłych, co finalnie przełożyło się na wieloaspektowość dyskusji nad możliwościami przewidywania właściwości termodynamicznych cieczy pod zwiększonym ciśnieniem.

Abstract

This dissertation addresses the complex problem of developing thermodynamic methods and equations of state to predict density and its derivatives, including the isobaric thermal expansion coefficient, the isothermal compressibility, and the speed of sound in single-phase liquids under increased pressure. This issue is important both from the point of view of fundamental research in the area of physical chemistry or liquid phase physics in general, as well as being relevant in industrial applications, such as where knowledge of the thermodynamic properties of the compressed liquid phase is essential. The former derives from lacking a general, universal, and functional theory of liquids, which mainly gives quantitative values of thermodynamic quantities in the single-phase region. The second, among other things, derives from the need for thermodynamic modeling of fuel injection processes in common-rail diesel engines designed to operate at pressures reaching values of several hundred MPa, as well as, for example, in the problems of high-pressure chemical catalysis (e.g., the problem of the ionic liquid-mediated lignin processing that one of the actual directions of Green Chemistry).

During the last decade (including earlier works in which the author of this dissertation is a co-author), it has been established that the goal of describing the physicochemical properties of simple molecular as well as ionic liquids can be approached by analyzing its connection to the thermodynamic density fluctuations, which in turn can be related to changes in the free volume of the system induced by external pressure. At the same time, this work has identified a set of open problems, the clarification of which is the main goal of this dissertation.

This dissertation discusses the objectives sequentially proceeding from the macroscopic to the microscopic thermodynamic picture of the compressed liquid phase. The first section addresses the limits of the applicability of the density fluctuations-based approach and its possible extension in the case of applicability of the applied thermodynamic models to high-pressure regions, as well as the determination of the relevant parameters of the proposed isothermal equation of state at atmospheric pressure in such a way that the predicted density values are comparable within the

limits of measurement uncertainty with those obtained by direct experiment. The second section presents the detailed mathematical and thermodynamic basis of the approach proposed in the first chapter. This allows generalizing them to the case of the properties of thermodynamic derivatives and the speed of sound, which is the essence of the discussion undertaken in this dissertation. The third section combines a macroscopic thermodynamic picture of the liquid phase with a microscopic one based on the results of molecular dynamics simulations. The latter aims to clarify thermodynamic anomalies and issues during the fluctuation model studies. These include some dissonance between predictions based on fluctuation theory and results based on acoustic and densitometric measurements during the isobaric thermal expansion coefficient of halogenated *n*-alkanes. The synergy of approaches based on molecular dynamics, thermodynamics, and the fluctuation theory of the compressed liquid phase, also allowed differentiating the stereochemical characteristics of the liquid systems studied, which ultimately translated into a multifaceted discussion of the possibility of predicting the thermodynamic properties of liquids under increased pressure.

This doctoral dissertation titled "Approaches based on the theory of thermodynamic fluctuations and molecular dynamics for predicting properties of molecular and ionic liquids under high pressures" has been prepared in the form of a guidebook on the collection of the following scientific papers:

- P1. **Bernadeta Jasiok**, Eugene B. Postnikov, Mirosław Chorążewski, The prediction of high-pressure volumetric properties of compressed liquids using the two states model. *Physical Chemistry Chemical Physics* 2019, 21, 15966-15973, DOI: 10.1039/C9CP02448D.
- P2. Eugene B. Postnikov, **Bernadeta Jasiok**, Mirosław Chorążewski, The CATBOOST as a tool to predict the isothermal compressibility of Ionic Liquids. *Journal of Molecular Liquids* 2021, 333, 115889, DOI: 10.1016/j.molliq.2021.115889.
- P3. Eugene B. Postnikov, **Bernadeta Jasiok**, Vyacheslav V. Melent'ev, Olga S. Ryshkova, Vadim I. Korotkovskii, Anton K. Radchenko, Alexander R. Lowe, Mirosław Chorążewski, Prediction of high pressure properties of complex mixtures without knowledge of their composition as a problem of thermodynamic linear analysis. *Journal of Molecular Liquids* 2020, 310, 113016, DOI: 10.1016/j.molliq.2020.113016.
- P4. **Bernadeta Jasiok**, Eugene B. Postnikov, Ivan Yu. Pikalov, Mirosław Chorążewski, Prediction of the speed of sound in ionic liquids as a function of pressure. *Journal of Molecular Liquids* 2022, 363, 119792, DOI: 10.1016/j.molliq.2022.119792.
- P5. **Bernadeta Jasiok**, Mirosław Chorążewski, Eugene B. Postnikov, Claude Millot, Liquid dibromomethane under pressure: a computational study. *Physical Chemistry Chemical Physics* 2021, 23, 2964-2971, DOI: 10.1039/D0CP06458K.
- P6. **Bernadeta Jasiok**, Mirosław Chorążewski, Alexander A. Pribylov, Eugene B. Postnikov, Pascale Friant-Michel, Claude Millot, Thermophysical properties of chloropropanes in liquid phase: Experiments and simulations. *Journal of Molecular Liquids* 2022, 358, 119137, DOI: 10.1016/j.molliq.2022.119137.

Guidebook

Contents

1	Introduction	8
2	Variation of the isothermal compressibility as one of the key parameters allowing predicting the density of liquids at highly elevated pressures	11
3	Substantiation of the approach for predicting the density and the speed of sound as based on the theory of thermodynamic fluctuations: applications to molecular and ionic liquids	18
4	Determination of physicochemical properties of selected halogenoalkanes based on computer simulation methods	24
5	Conclusion	30
6	Publications with statements of co-authors on the contribution	32
7	Appendix – author’s scientific activity	105

1 Introduction

Modern interest in high-pressure liquids studies is motivated by fundamental thermodynamics and statistical physics [1] and prospective industrial applications [2]. Advanced technologies require specialized technical fluids with superior properties as operating mediums in compressors, cooling systems, energy storage systems, or engines. Consequently, many studies have been dedicated to experimental measurements of the density, the speed of sound, the heat capacity of liquids and their mixtures, and methods of their predictions. The effects of temperature and pressure on these properties and their derivatives, such as the isothermal and isentropic compressibilities, have been extensively studied for hundreds of molecular systems and mixtures. At the same time, the recent state of the art indicates that this problem is far from the final resolution due to the complexity of liquid structures heavily dependent on the specificity of particular substances.

Density under high pressure is a critical parameter in engineering studies [3] as well as its derivative, the isobaric thermal expansion coefficient. This coefficient and the heat capacity [4] are crucial for solving energy and continuity equations in fuel injection systems under high pressure, novel diesel injectors, and engine constructions, see, e.g., [5, 6].

From a thermodynamic perspective, the isobaric thermal expansion coefficient is a crucial property due to its high sensitivity to molecular properties of liquids and specific behavior under elevated pressures [7, 8]. As a result, IUPAC recommends checking the accuracy of determining the isobaric thermal expansion coefficient as one of the most demonstrable tests, which needs to be evaluated when developing practically applicable equations of state [9], highlighting its importance as a primary and essential property in thermodynamics.

Another important derivative quantity is isothermal compressibility. It is closely linked to liquids' radial distribution function and structure factor. Also, it can play the role of a starting point for developing isothermal equations of state by integrating along isotherms. Although the high-pressure science of liquids started from exploiting this quantity by P.G. Tait, this problem is still

a challenging task [10] due to the high uncertainty of calculating the first-order derivative of the slightly changing volume [11].

However, it can be indirectly deduced by measuring other physical properties using thermodynamic differential equations. Among the various indirect methods, the most commonly used one relies on the speed of sound, c , which can be accurately measured even at high pressures [3] and also itself provides information on physical and physicochemical properties of molecular [12] and ionic [13] liquids. Simultaneously, the isobaric heat capacity, the adiabatic, and the isobaric thermal expansion coefficient can be obtained when implementing such a method. This forms a basis for developing and testing equations of state.

The primary purpose of equations of state [14] is to provide a theoretical understanding of liquids and enable practical calculations, reducing the need for extensive direct measurements that is of a practical need for various applications in engineering and physical chemistry, which span from fluid mechanics and material engineering to nanotechnology. Among the most popular predictive approaches, one can list a variety of cubic equations of state [15] (however, despite their efficiency at saturated conditions, this kind of equations provides a rather poor accuracy when the calculations are extended to the single-phase region under high elevated pressures) and models based on statistical thermodynamics [16].

The Statistical Association Fluid Theory (SAFT) models, which are molecular-based, are currently the most frequently used equations for predicting the physicochemical properties of compressed liquids [17]. These models have shown significant accuracy in the comprehensive modeling of liquid properties. However, the predictive value of some SAFT approaches may be questionable because their substance-dependent parameters are usually determined by fitting relatively large and sometimes imprecise experimental databases [18, 19].

Thus, one can state a more reduced problem of the search for predictive equations of state, which does not require the necessity to know thermophysical properties under pressure, the structure, composition, or molecular mass of compressed liquids but may use easily measurable macroscopic thermodynamic quantities at ambient atmospheric pressure.

The doctoral thesis aims to investigate such predictive methods *per se* and their relations to the structural changes which may occur in compressed liquids, mainly working and technical liquids, in high-pressure regions. To achieve this, computer simulation methods will be utilized to determine the physicochemical properties of liquids across a broad range of temperatures and pressures. The Molecular Dynamics technique, a deterministic computer simulation tool, can help to explain these issues. Computer simulation methods offer a means to obtain necessary information and bridge the gap between theory and experiment.

Thus, the fluctuation theory-based equations of state and computer simulation techniques offer a better understanding of compressed liquid structures and the prediction of their physicochemical properties across a broad range of thermodynamic parameters.

2 Variation of the isothermal compressibility as one of the key parameters allowing predicting the density of liquids at highly elevated pressures

It has been revealed earlier that the Fluctuation Theory-based Equation of State

$$\rho = \rho_0 + \frac{1}{k} \log [k\rho_0\kappa_T^0 (P - P_0) + 1], \quad (1)$$

correctly predicts the density of liquid ρ over a wide range of pressures P (up to about 200 MPa). Its predictive capabilities have already been proven for molecular liquids, from saturated hydrocarbons to ionic liquids [20–23]. It contains parameters (ρ_0 is the density, k is the parameter described by fitting $(M/(RT\rho_0\kappa_T^0)) = \exp(k\rho_0 + b)$, and κ_T^0 is the isothermal compressibility) determined at atmospheric pressure P_0 from uncomplicated experimental procedures and thermodynamic equalities.

However, Eq. (1) has two weaknesses. The first point relates to the range of pressures for which the isothermal equation of state can be used, i.e., several hundred MPa. For larger pressures, the density and its isothermal derivative, i.e., the isothermal compressibility, significantly deviate from experimental data. On the other hand, the second point relates to the calculation or prediction of the isothermal compressibility at atmospheric pressure since κ_T^0 is a control parameter in Eq. (1) itself and also required to find the second parameter, k . Predicting these parameters can generate higher errors for much lower pressures than the density prediction.

The works addressed in this section propose approaches that can overcome these drawbacks by considering the qualitative changes in the pressure response of the bulk modulus (the inverse isothermal compressibility) of molecular liquids when external pressures tend to the GPa range and proposing a machine learning-based method for predicting κ_T^0 for ionic liquids (ILs). Note that the latter, in turn, is characterized at low pressures by a certain similarity to extremely compressed molecular liquids [24] that gave recent support to the picture considered in this section.

The main message of the **P1**, can be cited as "(...) *the deviation of the reduced bulk modulus from the behavior assuring the FT-EoS validity occurs when the packing fraction defined as the van der Waals volume of molecules with a small nonsphericity reaches the value in between the random loose and random close packing of spheres. This allows the hypothesis of the existence of some kind of structural transition of a liquid state to a state with irregularly closely packed particles, similar to an amorphous solid*".

The literature review discussed the elastic properties of solids and liquids, indicating a certain similarity between them in this respect. This prompted us to consider whether it made sense to link our model with a model related to predicting the properties of solids (the Murnaghan equation of state). Accordingly, we undertook this task. As a result, we obtained a Two State Model that extended the predictive capabilities for the density and the isothermal compressibility to the order of pressures reaching GPa.

In the beginning, we considered two bulk moduli, first for the FT-EoS (K_{FT}), and the second for Murnaghan's approach (K_M):

$$K_{FT} = \left(\frac{\rho}{\rho_0} \right) (\kappa_T^0)^{-1} [1 + \lambda \kappa_T^0 (P - P_0)], \quad (2)$$

$$K_M = (\kappa_T^0)^{-1} [1 + \lambda \kappa_T^0 (P - P_0)']. \quad (3)$$

As can be seen, Eq. (2) differs from Eq. (3) only by one term, $\left(\frac{\rho}{\rho_0} \right)$, which is known as a first reduced density dependent correction in the theory of elasticity [25, 26]. It is also worth noting the packing fraction for liquids. This parameter can be expressed as $\phi = \rho / \rho_{vdW}$, where ρ_{vdW} is the van der Waals density, which is equal to M / V_{vdW} . Here V_{vdW} is the van der Waals molar volume. The parameter ϕ is within the 0.52 – 0.62 range, which corresponds to the range of geometric states from the random, very loose packing to the random close packing of spheres along the saturation curve. Parameter ϕ can also be used for chained liquids like n -alkanes and n -alcohols since V_{vdW} refers to the impenetrable molecular volume independent of a molecule's shape.

When we integrate Eq. 2 along isotherms, we get the formula for predicting density as a function of pressure and temperature, coinciding with the FT-EoS, Eq. (1) above

$$\rho = \rho_0 + \frac{1}{k} \log [\lambda \kappa_T^0 (P - P_0) + 1], \quad (4)$$

but where $\lambda = k\rho_0$.

On the other hand, integration along the isotherms of Eq. 3 will give us the Murnaghan equation:

$$\rho = \rho'_0 [\kappa_T'^0 \lambda (P - P'_0) + 1]^{\lambda^{-1}}, \quad (5)$$

Using Eqs. 4 and 2 and Eqs. 5 and 3, it is not possible to reproduce the experimental values over the entire pressure range since each corresponds to individual pressure ranges. On the other hand, Eqs. 4 and 5 can be written in the form:

$$\exp[k(\rho - \rho_0)] = \kappa_T^0 \lambda (P - P_0) + 1 \quad (6)$$

and

$$\left(\frac{\rho}{\rho'_0}\right)^\lambda = \kappa_T'^0 \lambda (P - P'_0) + 1 \quad (7)$$

The logarithmic right-hand sides of Eqs. 6 and 7 should represent a linear relationship on the plots. However, in the case of Eq. 6, one can see deviations from a straight line for high pressures, while for Eq. 7, deviations occur for low pressures. Thus, it can be said that Eq. 4 reproduces the experimental data in the low-pressure range, while Eq. 5 reproduces the experimental data in the high-pressure range. It should also be noted that there are no phase transitions along the isotherm, so the components of Eqs. 4 and 5 should remain continuous for both the density and the isothermal compressibility. Thus, λ , ρ_0 , and κ_T^0 are inputs at atmospheric pressure for predictions properties at low pressures. In contrast, ρ' and κ_T' are input at reference pressure P' , referring to the transition point between FT-EoS and the Murnaghan equation separately for each isotherm studied.

In the **P1**, we tested the predictive capabilities of the Two States Model for *n*-alkanes, *n*-alcohols, and benzene. The density, ρ , the heat capacity c_P , and the speed of sound c at atmospheric

pressure were used as input data. These properties were used directly to calculate the isothermal compressibility, κ_T , from a well-known thermodynamic relationship

$$\kappa_T = \frac{1}{\rho c^2} + \frac{T \alpha_P^2}{\rho c_P} \quad (8)$$

Using *n*-heptane as an example, it has been demonstrated in detail how the features of the Two State Model are reflected in the experimental data and how this model can be implemented in predictive calculations. In addition, we compared the results obtained by the Two States Model with the density prediction using the FT-EoS equation (where we obtained lower density values) and the Murnaghan equation (where we obtained higher density values). We have also shown a plot of the dependence of the natural logarithm of the reduced density fluctuation as a function of density, where superimposed plots of the linear function can be seen up to about 750 kg·m⁻³. However, above 750 kg·m⁻³, you can see individual straight lines that extend from the 'point' of the FT-EoS – Murnaghan EoS transition.

Next to *n*-alkanes, *n*-alcohols, and benzene, we tested the predictive capabilities of the Two State Model for liquid mixtures, here silicone oil 9981 LTNV-70. Since we do not know the molar mass of this oil, we omitted the *M/R* ratio for the natural logarithm of the reduced density fluctuations because this parallel shift of the fitting line does not affect its slope *k* required as a parameter. Using the Two State Model, the density values obtained for the pressure range larger than several hundred Megapascals were closer to the experimental values than when we used the FT-EoS only.

In addition to density, we verified that the Two State Model could also predict isothermal compressibility. Here, for *n*-heptane, we used the inverse of Eqs. (2) and (3) while considering the transition described above. The results obtained did not differ significantly from the experimental data.

As noted above, both parameters of the predictive model for calculating the density of liquids require knowledge of the isothermal compressibility at the ambient atmospheric pressure. At the same time, the existing data, i.e., the complete set of measurements of the density, the speed of

sound, and the isobaric heat capacity at this state, may not be available, which induces demand for developing predictive methods too.

For this goal, we used machine learning as an algorithm for gradient boosting on decision trees – CATBOOST – manuscript **P2**. We chose the following identifiers as the input quantities: the density at 298.15 K, the critical temperature and pressure, the molar mass, and the acentric coefficient for individual ionic liquids. The target quantity of the machine learning algorithms is isothermal compressibility at 298.15 K.

The quantity given as experiment-based data at this temperature and ambient pressure or interpolated between the data reported for different temperatures were used to form the training and test sets of data.

When density and isothermal compressibility values were not reported in the literature at the input temperature, i.e., 298 K, we used temperature-dependent quadratic polynomials (or a linear function when only three values exist) for the density fitting and the linear fitting of the natural logarithm of the isothermal compressibility, respectively. In addition, the isothermal compressibility data sets were checked for correct behavior with respect to temperature. In the case of excessive data scatter or unphysical behavior, the data were discarded. Thirty-five ionic liquids were selected from the entire data set. Since this number is not so large, taking into account requirements for the standard workflow with the test/training datasets subdivision, an original approach of the complete permutations was applied. It consists of considering all data except one for the training set, predicting this data and comparing it with the actual value, and further repeating this procedure for each substance sequentially.

For the directly predicted values at the temperature of 298.15 K, the average absolute relative deviation over the entire data set is 6.0%. In contrast, for the entire temperature range, for which the experiment-based isothermal compressibilities are known, it was 6.2% when the CATBOOST's predictions were combined with Wada's rule and the known density.

Various parameters can affect the prediction of density and isothermal compressibility. One of the advantages of the CATBOOST algorithm is that information is given on the importance of

individual parameters as affecting the predicted results. Therefore, we found that parameters such as the molar mass, the critical temperature, and the type of cation significantly impact the prediction of the isothermal compressibility for all the ionic liquids studied in this work.

It is worth noting that two parameters, i.e., molar mass and critical temperature, are directly related to the physical chemistry of the liquid. ILs with a larger molar volume are more compressible, and consequently, the isothermal compressibility increases as the alkyl chain of the cation increases. On the other hand, the critical temperature is related to the saturated isothermal compressibility of molecular liquids ($T_c - T$ combination). Wada's rule should also be marked out here, represented by the equation $M/\rho\kappa_T^{1/7} = \text{const.}$ Y. Wada was the first who proposed to predict isothermal compressibility from knowledge of a substance's molar mass, density, and specific chemical groups. Since we determined the isothermal compressibility by the CATBOOST for one temperature, the group contribution term (const in the equation above) is eliminated from the consideration. It should be pointed out also that the power-law dependence of the isothermal compressibility on the density functionally corresponds to Murhaghan's equation for the bulk modulus (the inverse isothermal compressibility), i.e., its usage is also in line with the modern consideration of ionic liquids' properties as resembling properties of the molecular liquids at a very high compression [24] that is coordinated with our Two-State Model. The temperature distance function from the critical point at the saturated conditions affects the density as follows from the Rackett equation. On the other hand, the importance of cations and anions can be related to the occurrence of individual ions.

For three ionic liquids, we obtained the largest deviations: [emim][BF₄], [6,6,6,14-P][bti], and [N-epy][bti]. For the first two ionic liquids, the molar mass and critical temperature are outside the range of the corresponding parameters used for training. In the case of [N-epy][bti], the three parameters are outside those taken for training. Its cation is absent in the training set. Hence we suppose the significant error in predicting the isothermal compressibility for this ionic liquid originates from this fact.

We have shown the position of the isothermal compressibility on the (M, T_c) plane for all the

ionic liquids studied. On this plane, you can find linearly correlated points, which are discussed as corresponding, for example, to homologous series, respectively, to a cation. In this case, it can be seen that isothermal compressibility has a small prediction error, which is the opposite for distantly located pairs of parameters.

We can count isothermal compressibility as one of the most difficult to determine properties of compressed liquids. Purely predictive approaches for this quantity, e.g., phenomenological polynomial equations of state and different versions of the SAFT-based EoS, result, as a rule, in a low prediction accuracy, which can reach up to 20 %. Hence, we conclude that the proposed CATBOOST-based algorithm, whose deviations are about 10 %, can be considered successful and has certain advantages to predict the isothermal compressibility at atmospheric pressure for ionic liquids.

3 Substantiation of the approach for predicting the density and the speed of sound as based on the theory of thermodynamic fluctuations: applications to molecular and ionic liquids

The main purpose of this part of the dissertation is to develop a sequential simultaneous approach based on the theory of thermodynamic fluctuations and Taylor's series expansion of the elevated pressure as a function of either the density or the speed of sound, for the density is aimed to reveal the background for limitations on the FT-EoS's applicability mentioned above. For the speed of sound, there was a problem with a similar development of a new isothermal equation based on the statistical fluctuation theory. Predictive capabilities concurred with reliable literature data for a wide range of molecular liquids and ionic liquids. The main advantage of our approach was, as was the case for the prediction of high-pressure density, no necessity for prior knowledge of other thermophysical properties under high pressure or the chemical composition. This part is based on manuscripts **P3** and **P4**.

Initially, based on previous results [21–23], the fluctuation equation of state by which density can be predicted over a wide range of pressures and temperatures can be successfully applied to fluids of unknown composition, such as SRS Calibration Fluid CV, based on readily available thermodynamic data known at ambient pressure only. Then, we attempted to discover the theoretical basis for this method and generalize it to the case where we would like to predict other thermodynamic properties, primarily – the speed of sound.

However, it is worth noting that Eq. (1) was derived and discussed as based on empiric observations of the universality of the functional form describing the reduced density fluctuations in liquids, i.e., its exponential dependence on the density only that fulfills at atmospheric and moderate elevated density. However, the boundaries of this universality with respect to the pressures as well as its origin were not completely understood.

Here let us look at pressure and density from a slightly different angle. Considering an isothermal equation of state as a mathematical object, which states a functional dependence between the density and the pressure at a constant temperature, the pressure's experimental values can be fitted as a function of the respective density's experimental data by a polynomial, i.e., the excess pressure can be represented as a cubic function of the excess density:

$$P - P_0 = \delta_1 (\rho - \rho_0) + \frac{\delta_2}{2} (\rho - \rho_0)^2 + \frac{\delta_3}{6} (\rho - \rho_0)^3. \quad (9)$$

Theoretically, the data sets can be fitted by a polynomial in two ways, namely 1) P vs. ρ or 2) ρ vs. P . In our considerations, we used the first case because we wrote in textbfP3 that *"the slope of the tangent to the curve $P(\rho)$ is always positive and increasing, and such a curve tends to infinity without any fundamental mathematical and physical constraints."* On the other hand, the $\rho(P)$ curve is decreasing due to decreasing compressibility and increasing pressure. Therefore, the polynomial fit will have a maximum, and next, the curve will decrease, which is physical nonsense.

A form similar to the Eq. 9 was proposed by Sun *et al.* for the speed of sound:

$$P - P_0 = A_1(T)(c - c_0) + A_2(T)(c - c_0)^2 + A_3(T)(c - c_0)^3. \quad (10)$$

Here, $A_j(T)$ are quadratic polynomials as a function of temperature. It can be noted that Eq. 9 also takes the form of a truncated Taylor expansion and thus is always true for the realistic range of state parameters taking into account the data's uncertainty. Assuming that $\left(\frac{\partial P}{\partial \rho}\right)_T = \delta_1 + \delta_2(\rho - \rho_0) + \frac{\delta_3}{2}(\rho - \rho_0)^2$, and performing some mathematical operations that lead us to the ordinary differential equation $\rho_0 \kappa_T^0 \left(\frac{\partial P}{\partial \rho}\right)_T = 1 + k \rho_0 \kappa_T^0 (P - P_0)$, Where $P(\rho_0) = P_0$, which leads us to FT-EoS (see Eq. 1).

It should be pointed out that Eq. (1) obtained as a solution to the formal differential equation stating the reduced density fluctuations as a function of the density, also can be considered from the point of view of the interpolation of a polynomial function by an exponential function. These functions are equal to each other at the initial point $P = P_0$. It can also be seen that

the experimental values and those calculated with FT-EoS are similar for the low-pressure range. On the other hand, for higher pressures, the equations $P - P_0 = (k\rho_0\kappa_T^0)^{-1} [e^{k(\rho-\rho_0)} - 1]$ and $\left(\frac{\partial P}{\partial \rho}\right)_T = (\rho_0\kappa_T^0)^{-1} e^{k(\rho-\rho_0)}$ can be expanded into Taylor series as above. With such an operation, the conditions requiring positivity of δ_1 , δ_2 , and δ_3 are fulfilled automatically due to the properties of the exponential function.

Mathematically, the exponential function and the cubic polynomial function will not coincide. It is known that the exponential function has a steeper curve than the polynomial function. At high temperatures and medium pressures, there may be greater deviations between experimental values and those calculated with FT-EoS, i.e., the $P(\rho)$ curve is more curved. On the other hand, the linearization procedure does not work for high pressures. This can be linked to molecular packing, which this dissertation discusses in **P1**. In conclusion, the polynomial extrapolation will deviate from the experimental data in contrast to the results derived from the exponential function, as proposed during the modified linearization procedure.

The linearization procedure we proposed is also for the speed of sound prediction. However, in this case, we have to operate not with the fluctuations of the density but the fluctuations of the pressures, which are related to the speed of sound [27]. Moreover, the respective reduced adiabatic fluctuation parameter has not exponential but power-law dependence on the density:

$$v_S = \frac{M c^2}{R T} \equiv \frac{M}{RT} \frac{1}{\rho \kappa_S} = \Lambda \rho^\lambda, \quad (11)$$

where M is the molecular mass, R is the gas constant, c is the speed of sound, T is the temperature, ρ is the density, and the κ_S is the isentropic compressibility; Λ and λ as compound-specific constants.

After several transformations and assumptions described in the **P3** and **P4**, it became possible to derive a formula by which it is possible to predict the speed of sound over a wide range of pressures and temperatures. The final expression for the prediction of the high-pressure speed of

sound takes the form:

$$c = c_0 \left[1 + \frac{3}{2} \kappa_T^0 \lambda (P - P_0) \right]^{\frac{1}{3}}. \quad (12)$$

The Equation of State we derived was tested for various groups of liquids, including SRS Calibration Fluid CV, Diesel fuel B0 2015, soybean and rapeseed biodiesels, two alkanes: *n*-heptane and *n*-dodecane, and nine ILs.

However, it was revealed that Eq. (12) also has definite limitations. Although the results obtained for *n*-dodecane and the calibration fluid are reasonable, there are liquids for which an increasing deviation is observed between the calculated and experimental values of the speed of sound (here, for example, *n*-heptane).

Moreover, the density calculated from the speed of sound values predicted by Eq. (12) via equalities for thermodynamic derivatives deviates from experimental values more than the values expected by the FT-EoS. Whence, we decided to modify the equation $c^3(P) = c_0^3 + \delta_s(P - P_0)$ by introducing a temperature-dependent correction factor for the slope of the linear trend $c^3(P)$ along the isotherms as:

$$c^3(P) = c_0^3 \left[1 + \frac{3}{2} \rho_0 \kappa_T^0 k_s k'_s(T) (P - P_0) \right], \quad (13)$$

where $k'_s = k_s^0 (1 + \varepsilon(T - T'_0))$. Here k'_s defined for $T = T'_0$ is close to 1, and ε is quite small.

To find k'_s and ε , we will refer to the fact that FT-EoS predicts density only up to the relative density value $(\rho - \rho_0) / \rho_0$, which is $\approx 1.05 - 1.1$ (even for *n*-alkanes). It is, therefore, necessary to find such correction factors for which the acoustic density calculation method will give values similar to those calculated by FT-EoS, so we used the steps described briefly below.

The first step: density(P, T) was calculated using FT-EoS, and speed of sound(P, T) was calculated using Eq. 12 for *n*-heptane (more compressible) up to $P = 111.4$ MPa and *n*-dodecane (less compressible) up to $P = 196.3$ MPa using as input values of density, speed of sound and isobaric heat capacity at saturated pressure from NIST Chemistry WebBook [28]. Calculations were performed up to the end of the density isotherm's most curved part and at the five isotherms' given temperature range. The third isotherm was chosen as $T = T'_0$.

The second step: recalculation of the speed of sound values for the sample set of $k'_s{}^0$ from 0.7 to 1.3, where the given range was divided into 11 equal steps. The speed of sound was obtained for each of these sample sets, and the density was then calculated using the acoustic method. The average absolute deviation of the calculated density by the acoustic method from the density calculated by FT-EoS along the third isotherm $\langle |\rho_{ac}(P, T') - \rho_{FT-EoS}(P, T')| \rangle$ was also used. Finally, a $k'_s{}^0$ was chosen to minimize this deviation.

The third step: in the last step, the same procedure was repeated with the fixed $k'_s{}^0$ and a set of 35 trial ε uniformly distributed from $6 \cdot 10^{-4}$ to $3 \cdot 10^{-3}$. The minimization procedure was evaluated for all five isotherms and all pressures. Finally, the optimal ε was found.

In the beginning, we tested *n*-heptane and *n*-dodecane. We obtained the corresponding correction factors for both liquids, which were then used in Eq. 13. For *n*-heptane, we got better results for the speed of sound compared to those calculated from Eq. 12. In addition, the density calculated from the speed of sound obtained from Eq. 13 better reproduces the experimental data in the highest pressure range, i.e., $P > 200$ MPa, compared to FT-EoS.

Then we tested the applicability of the above method for SRS Calibration Fluid CV and biofuels. For these fluids, the results obtained improved slightly. Hence, we concluded that for such liquids, Eq. 12 could be used without corrections, as it has adequate accuracy for predicting the speed of sound.

Another class of compounds we have focused our attention on are Ionic Liquids. ILs have been known for more than 100 years. Paul Walden discovered the first IL in 1914, and it was ethylammonium nitrate [29]. These compounds are used in various fields of science and technology due to their unique structure and properties. For example, ILs can be used as electrolytes in lithium-ion batteries, organic synthesis, catalysis, solvent extraction, applications in various biochemical processes, and many others [30–32].

Being aimed at testing the proposed approach respectively to the results of real experimental measurements, we focused on this kind of data using the ILThermo database as a compendium. Accordingly, no additional data, whether calculated or predicted by other models, were considered

in our work. However, experimental data for the speed of sound at high pressures are already scarce; we used the experimental sound speed data for nine ILs that is all such data from the ILThermo database consisting of 589 points used to test the predictive capabilities of Eq. 12.

Simultaneously, experimental data was measured at ambient pressure conditions to get the required parameters. These data were extracted from the ILThermo database and then passed to MATLAB for further calculations using Excel spreadsheets as intermediate data files. These byproduct collections contain information about the experiment, including links to sources of information, composition information, the molar mass of the ionic liquid, and the data themselves. Additionally, a comparative analysis of the available data was carried out. Not all experimental data from the ILThermo database were used in the final calculations since, e.g., for several ILs, extremely scattered and contradicting experimental data were detected and discarded after preliminary data evaluation. Only the high regularity and consistency data were used for predictive calculations that demonstrate highly accurate results.

Using the extended version of the isothermal fluctuation equation of state, very good accuracy can be obtained between the experimental values and the predicted speed of sound for the nine ionic liquids from the ILThermo database, as confirmed by the relative average absolute deviation, which was only 0.85%.

Thus it is possible to conclude that the model proposed model can be used to predict the speed of sound under pressure in its simplest form (12) low compressible liquids and with the temperature-dependent modification (13). It is confirmed by the case studies of a wide set of substances belonging to different classes: SRS Calibration Fluid CV, Diesel fuel B0 2015, soybean and rapeseed biodiesels, *n*-heptane, *n*-dodecane, and nine ILs.

4 Determination of physicochemical properties of selected halogenoalkanes based on computer simulation methods

This part of the dissertation is based on two manuscripts, e.g., **P5** and **P6**. The main goal of this part of the thesis is a systematic investigation of several halogenoalkanes by molecular dynamics (MD) simulations aiming to obtain thermodynamic and structural information in a wide range of temperatures and pressures. We aim to connect experimentally defined thermodynamic peculiarities with the atomistic structure of liquids.

The choice of these compounds was motivated by the following scientific reasons. While the theory of the thermal expansion of solids is well developed, and it is known that the anharmonicity of oscillations mainly causes the thermal expansion in solid condensed systems [33], in the case of liquids, the understanding of this thermodynamic function in terms of molecular behavior is still a challenge. Theoretical investigations by the Fluctuation-based Tait-like Equation of State (FT-EoS) model concluded that the crossing of expansivity isotherms is connected with the structural transition of loose packing liquid to the liquid with irregularly closely packed particles [34, 35]. This hypothesis was pioneered considering discussing the phenomenon of the crossing isotherms of α_P for the series of α , ω -dibromoalkanes starting from dibromomethane. At the same time, the pressure location of the crossing region defined by the FT-EoS exhibited some deviations from the experimental data [36], which are limited and do not reach the target pressure. Simultaneously, the existing limited experimental volumetric data [37] indicated a possibly strict dependence of the crossing pressure on the structure of isomers of other representatives of the same class of haloalkanes – chloropropanes.

Thus, the hypothesis is that the crossing of α_P isotherms is defined by peculiarities of the liquid structure and, first of all, with different molecular packing at low and high pressures. Neither direct experiments nor theoretical models can present mechanisms of molecular packing at different pressures. Therefore, computer simulation methods, which provide information about the positions and interactions of all particles in a molecular ensemble, allow for analyzing the

molecular configurations to solve this problem.

This goal requires a solution to several scientific challenges. As well known, the modeling of liquids is based on existing force fields. To design realistic models, we tested the force fields, which reproduced the experimental properties of liquids at normal conditions or elevated T and P if available. We performed massive computations because our thermodynamic quantities of interest are expressed as derivatives with respect to temperature or pressure. Besides thermodynamics, we had trajectories of all particles of liquids and could calculate structural and dynamical properties.

First, computer simulations were performed for dibromomethane. It was done during a six-month internship under the Wilhelmina Iwanowska program from the National Agency for Academic Exchange at the University of Lorraine in France under Professor Claude Millot's supervision. During the internship, a series of tests were carried out for the experimental density values ($T = 298$ K and 313 K) assuming the model of rigid particles using several calculation methods which are presented in manuscript **P5**, and selecting one for further calculations in the temperature range (268 – 368 K) and pressure range (1 – 3000 bar).

After completing a six-month internship, we ran computer simulations for 1- and 2-chloropropane to explore the possible stereochemical effects affecting thermodynamic properties. Using the results of the MD simulations, we investigated the thermodynamic properties of the above liquids in the temperature range of 293.15 – 373.15 K and the pressure range of 0.1 – 200 MPa. The manuscript **P6** describes the MD simulation details.

In addition to MD simulations in the manuscript **P6**, we also used Span-Wagner EoS. We improved the thermophysical properties already existing in the literature for three haloalkanes: 1-chloropropane, 2-chloropropane, and 1,3-dichloropropane. Such a combination gives all three possible configurations to replace one or two hydrogens with heavier halogen atom(s).

Based on obtained MD computer simulation results in the manuscripts **P5** and **P6**, the thermodynamic properties of dibromomethane, 1-chloropropane, and 2-chloropropane have been studied. We focused primarily on the isobaric thermal expansion coefficient, the isothermal

compressibility, the isobaric and isochoric heat capacities, and the speed of sound. The above physicochemical properties are the basis for characterizing the macroscopic properties of fluids, testing the quality of equations of state, and their modeling can be usefully applied in chemical engineering.

The isobaric thermal expansion coefficient was calculated from the well-known relation:

$$\alpha_P = -\frac{1}{\rho} \left(\frac{\partial \rho}{\partial T} \right)_P. \quad (14)$$

Here, ρ is the density, which equals the ratio between a number of molecules, N , and volume, V . For the eight pressures, we fitted the volume-temperature dependence by a polynomial of order 2 to calculate the partial derivative in Eq. 14.

Next, we calculate the isothermal compressibility, κ_T , using the equation:

$$\kappa_T = \frac{1}{\rho} \left(\frac{\partial \rho}{\partial P} \right)_T \quad (15)$$

To calculate the partial derivative, we used the pressure dependence of the density by a polynomial of order 3. We compared the calculated isothermal compressibility from the MD results with the values obtained using the acoustic method [36] and Heun's predictor-corrector method [22, 38].

In the NVE ensemble, the formula with which it is possible to calculate the isochoric heat capacity is as follows:

$$c_V = \frac{3Nk_B}{1 - \frac{\langle \delta E_{kin}^2 \rangle}{3Nk_B^2 T^2}}, \quad (16)$$

where $\delta E_{kin} = E_{kin} - \langle E_{kin} \rangle$ (E_{kin} is the total kinetic energy of the system of N rigid molecules), k_B is the Boltzmann constant, and T is the temperature.

The constant volume heat capacity can also be calculated from the relation:

$$c_V = \left(\frac{\partial E}{\partial T} \right)_V. \quad (17)$$

Here, E is the internal energy, and V is the volume of the system. The results obtained using these two methods are quite good, considering the amplitude of the error bars.

On the other hand, the isobaric heat capacity c_P can be calculated from the relation:

$$c_P = \left(\frac{\partial H}{\partial T} \right)_P \quad (18)$$

where H is the enthalpy of the system equal to $H = E + PV$.

As a final property, we determined the speed of sound from the equations below:

$$c = \frac{1}{\sqrt{\rho \left(\kappa_T - \frac{TM\alpha_P^2}{\rho c_P} \right)}}, \quad (19)$$

and

$$c = \sqrt{\frac{c_P}{c_V \rho \kappa_T}}, \quad (20)$$

where ρ is the mass density and M is the molar mass.

Since the most interesting property of the above is the isobaric thermal expansion coefficient, α_P , we took a closer look at it based on various methods. Based on the primarily MD simulations, the Span-Wagner EoS, and the Daridon *et al.* method, we calculated α_P . We superposed its value for different isotherms to find a range of elevated pressures where they cross each other.

This effect, which is observed for many molecular liquids at a given pressure or within a particular range of pressures (when a sufficiently wide range of temperatures was considered) – usually below 200 MPa – prompts the question of its occurrence relative to the structure and thermodynamic properties of a liquid [8, 39]. In addition, the reproduction of this phenomenon is denoted by IUPAC as one of the crucial criteria for developing equations of state [9].

Thus, we first wanted to use MD simulations to solve the still unsolved problem concerning the crossing isotherms of the isobaric thermal expansion coefficient. To date, we have only been able to reconstruct the crossing of isotherms of α_P based on the results of MD simulations.

For dibromomethane, the α_P was presented in two ways, i.e., i) from the raw results of computer simulations and ii) using a pressure-dependent linear correlation α_P^{-2} proposed by Randzio *et*

al. [40]. Using the raw results of computer simulations, we get the crossing of the isotherms of α_p between $\simeq 650$ and $\simeq 900$ bar. In contrast, using Randzio *et al.* method, the crossing of isotherm is seen around 780 ± 50 bar. It is also worth noting that Postnikov and Chorążewski predicted, using the fluctuation equation of state, the crossing of isotherms for dibromomethane in the range from $\simeq 650$ to $\simeq 900$ bar [34].

For 1-chloropropane and 2-chloropropane, the crossing of isotherms of the α_p was calculated via three methods: i) MD simulations, ii) Span-Wagner EoS, and iii) the Daridon *et al.* method. It is worth noting that α_p calculated by the Span-Wagner EoS and Daridon *et al.* methods was determined at the points corresponding to the computer simulations. For 1-chloropropane and 2-chloropropane, we obtained very similar results for high pressures by comparing the results obtained using computer simulations and Daridon *et al.* method. The crossing of isotherms is visible around 150 MPa and in the 150 – 200 MPa range for the two isomers of chloropropane. A difference is observed between the α_p values obtained by simulation and the Daridon *et al.* method for the highest temperatures and low pressures simultaneously. This was expected since these points were far from the boiling point.

Crossing of isotherms occurred in the 100 – 122 MPa and 75 – 115 MPa for the two chloropropanes when we used the Span-Wagner EoS. In the case of 1-chloropropane, the crossing of isotherms occurs relatively close to each other. In contrast, in the case of 2-chloropropane, a significant difference in the location of the intersection of α_p isotherms can be seen. This is probably due to obtaining different density values comparing the density from the MD simulation to the density from Span-Wagner EoS; see Fig. 4A and Fig. 5A in **P6**.

In summary, various physicochemical properties of compressed liquids were determined as a function of temperature and pressure, including reproducing the crossing of the isotherms of the isobaric expansivity using MD methods. Despite the fact that the present results of the MD simulations did not reveal specific structural anomalies illustratively corresponding to this phenomenon, we are confident that further research devoted to a more detailed exploration of the collected extensive datasets resulting from the computer simulations will allow us to trace links

between the particular fluid structure and the behavior of the thermal expansion coefficient.

5 Conclusion

Predicting the physicochemical properties of liquids, considering accuracy comparable to a physicochemical experiment, is still a difficult problem. As a rule, it requires the knowledge of at least some reference values measured at elevated pressures, which is a laboratory-intensive task. Although there are equations or methods in the literature that better or worse predict the desired properties, there is no single method by which it is possible to predict a wide range of physicochemical properties of compressed liquids.

The dissertation presented here addressed a more restricted approach, requiring experimental reference data. Still, they should be measured only at the ambient atmospheric pressure, which is significantly more straightforward in realization. However, in consequence, it is possible to predict i) the density and the isothermal compressibility up to very high pressures of the range of GPa using the Two States Model, ii) the speed of sound using an extension of the fluctuating equation of state, and iii) the thermal expansion, the isobaric and isochoric heat capacities, the isothermal compressibility and the speed of sound using MD simulations.

It is worth adding that FT-EoS has been extensively explored over the last few years and has demonstrated a higher degree of universality and allows for predicting the density of under pressures up to some hundreds of MPa for molecular liquids and mixtures varying from simple saturated hydrocarbons to ionic liquids [20–23].

The Two States Model extends the predictive range of the fluctuation equation of state up to the GPa range. However, it requires only knowledge of temperature-dependent, straightforwardly measurable physicochemical properties at atmospheric pressure. The accuracy of both methods remains consistent with the high-pressure experimental data.

Based on the above results, we are convinced that the proposed models will be an important contribution to the understanding of thermodynamic and structural studies of pressurized fluids, as well as that the described research concept will find application potential in the field of engineering technical fluids since the proposed model of Fluctuation Equation of State correctly

predicts the thermodynamic properties of the compressed liquid phase without prior knowledge of any properties of the tested object under elevated pressure. Additionally, the obtained tools allow us to predict and model several engineering-relevant physicochemical properties, which could be used to design new dedicated for specific applications and optimize compressed fluids and their mixtures.

On the other hand, the results of MD simulations were used to determine the physicochemical properties of dibromomethane, 1-chloropropane, and 2-chloropropane. In addition to the demonstration of the ability of the molecular dynamics approach to get a set of data thoroughly characterizing the thermodynamic state of such kind of liquids in the single-phase region, the successful results of the MD simulations provided an alternative source of data for discussing an influence of isomerization on the derivative thermodynamic properties that was a conductive issue in the previous literature sources.

The physicochemical properties of liquid dibromomethane obtained from MD simulations show reasonable agreement compared to experimental values. In addition, it was possible to reproduce the intersection of isotherms of the isobaric thermal expansion coefficient around 780 bar. On the other hand, the Span-Wagner EoS was used to critically evaluate the pre-existing datasets for 1-chloropropane, 2-chloropropane, and 1,3-dichloropropane and improve the accuracy of the representation of their physicochemical properties. Additionally, for the two isomers, i.e., 1-chloropropane and 2-chloropropane, we discussed in detail the intersection of the isobaric thermal expansion coefficient isotherms, which we obtained using MD simulations, the Span-Wagner EoS and the Daridon *et al.* method.

We are convinced the proposed studies will contribute to the scientific development of liquids' physicochemistry under high pressure. Moreover, the research on compressed fluid nature and its thermodynamic properties reflect the worldwide trends in the meaning of interdisciplinary sciences: chemistry and fluids engineering, and the demand for such studies is extremely high. Besides fundamental scientific interests, the indicated topic includes potential applicability in fluids engineering and high-pressure technological process optimization.

6 Publications with statements of co-authors on the contribution



Cite this: DOI: 10.1039/c9cp02448d

The prediction of high-pressure volumetric properties of compressed liquids using the two states model†

Bernadeta Jasiok, *^a Eugene B. Postnikov *^b and Mirosław Chorążewski ^a

In this work, we argue that the volumetric properties of liquids cannot be reproduced by a single isothermal equation of state derived by the compressibility route for the whole pressure region extended up to a GPa pressure but require the consideration of two states associated with qualitatively different molecular packing properties. This is confirmed by examples of polar and non-polar substances within the range of temperatures from 203.15 K to 491.48 K and pressures up to 1200 MPa. The proposed two states model is truly predictive for the high-pressure density and isothermal compressibility using several easily measurable physico-chemical quantities: the density, the isobaric heat capacity, and the speed of sound at atmospheric pressure only. The experimental data on the density for 15 different compressed liquids, given in the literature as a function of temperature and very high-pressures, were used for the comparison and its analysis. The relative absolute average deviation for 2138 experimental data points by a two states model is close to 0.17%.

Received 30th April 2019,
Accepted 27th June 2019

DOI: 10.1039/c9cp02448d

rsc.li/pccp

1 Introduction

Rayleigh¹ was the first who proposed the consideration of the equation of state for liquids based on the macroscopic thermodynamic properties only without any reference to a molecular structure. The main reason was that a liquid is a weakly compressive medium, therefore, there exists a small parameter – from the liquids' compressibility, one can derive *PVT* relations considering small changes of the liquid density (or volume) under small variations of pressure. In particular, Rayleigh derived the van der Waals equation under such assumptions. Furthermore, this approach was developed by M. Smoluchowski, who considered an equation of state derived in such a manner and including macroscopic thermodynamic variables with respect to the particle density fluctuations.² He also introduced the parameter of reduced volume fluctuations defined by a ratio of the isothermal compressibility multiplied by the respective pressure for the amount of particles in a system. The same is taken under the hypothetical case of Boyle's law along the same isotherm and qualitatively discussed a change of this parameter on the concentration growth route from an ideal diluted colloidal system to a gel.³

In fact, the inverse quantity to the reduced compressibility mentioned by Smoluchowski, *i.e.* the reduced bulk modulus defined as

$$\nu = \frac{M}{RT\rho\kappa_T} \quad (1)$$

is more convenient for the consideration of thermodynamic quantities since it does not diverge in the critical point (it is strictly equal to zero there) and allows for a simpler consideration of the pressure dependence. Although eqn (1) can be interpreted from the perspective of a liquids' structure and fluctuations, see ref. 4 for details, it is useful to make quantitative predictions directly with macroscopic thermodynamic quantities: there *M* is the molar mass, *R* is the gas constant, and *T*, ρ , and κ_T are temperature, the density, and the isothermal compressibility, respectively. A specific polynomial fit of the quantity (1) with respect to experimental data is used as the accurate functional representation of a liquid's density in a wide range of temperatures and pressures.⁵

On the other hand, an accurate functional representation of the bulk modulus itself is a function of pressure and is relevant to a general physical approach to the elastic properties of liquids. It has the potential of universal applications for an equations of state constructed on this basis, due to a low compressibility of all liquids irrespective of their composition. In other words, citing Rayleigh's statement on this topic: "a sufficient account can be given without introducing the consideration of molecules, which on this view belong to another stage of the theory".¹

^a Institute of Chemistry, Department of Physical Chemistry, University of Silesia in Katowice, Szkolna 9, 40-006 Katowice, Poland. E-mail: hjasiok@us.edu.pl

^b Department of Theoretical Physics, Kursk State University, Radishcheva St., 33, 305000 Kursk, Russia. E-mail: postnikov@gmail.com

† Electronic supplementary information (ESI) available. See DOI: 10.1039/c9cp02448d

This question was addressed in several detailed reviews^{6,7} including the implications of such fitting for discussing the validity of different classic isothermal equations of state as well as an overview of an extensive set of such appropriations considered from the point of view of sensitivity to the density measurement data.⁸

While solids in the regime of linear elasticity (Hooke's law) can be characterized by a constant bulk modulus $K_0 = (\kappa_T^0)^{-1}$, the regime of small but non-linear deformations typical for liquids may be written in a general form, which includes linear order corrections with respect to the density and the excess pressure,⁹ as

$$K = \kappa_T^{-1} = \rho \left(\frac{\partial P}{\partial \rho} \right)_T = \left(\frac{\rho}{\rho_0} \right)^n [K_0 + K'(P - P_0)], \quad (2)$$

where ρ_0 is the density corresponding to the reference pressure P_0 , and the index n distinguishes between three cases: $n = -1$ corresponds to the classic Tait equation (in Tammann's different form); $n = 1$ results in the so-called Fluctuation Theory-based Tait-like Equation of State (FT-EoS); $n = 0$ represents the Murnaghan equation initially proposed to describe non-linear elasticity of solids but is widely applied to liquids. In fact, there are cases of particular substances, when either Tait's or Murnaghan's is preferable to fit a particular molecular liquid, see the classic comparative review.¹⁰

On the other hand, FT-EoS has been extensively explored over the last few years and has demonstrated a higher degree of universality and allows for predicting liquids density under high pressures for molecular liquids varying from simple saturated hydrocarbons to ionic liquids.^{9,11–13} In addition, it does not require high pressure reference data and can be considered as purely predictive utilizing the data measured at the normal/atmospheric pressure only.

However, it has two weak points: (i) its applicability is limited by several hundreds MPa, and the growing discrepancy originates from the principal deviations of the reduced bulk modulus from eqn (2) with $n = 1$,^{11,12} (ii) an ability to predict the isothermal compressibility itself and speed of sound fails even at smaller elevated pressure than for the density.

It has been first noted¹¹ that the deviation of the reduced bulk modulus from the behaviour assuring the FT-EoS validity occurs when the packing fraction defined as the van der Waals volume of molecules with a small nonsphericity reaches the value inbetween the random loose and random close packing of spheres. This allows the hypothesis of the existence of some kind of structural transition of a liquid state to a state with irregularly closely packed particles, similar to an amorphous solid.

It should be pointed out that the dual picture, which takes into account a duality of the process in liquids comprising solid-like and gas-like features, was discussed recently, including the saturation curve. For example, elastic mode excitations result in a proximity of the isochoric heat capacity behaviour for liquids and solids. Simultaneously the free movement of a liquid's individual particles is what determines its entropic and self-diffusional characteristics.¹⁴ Another example within a similar line of reasoning is the separation of structural processes

accompanying *PVT* changes into evaporation/expansion contributions, which balance voids and "a molecular skeleton" in the bulk.¹⁵

Thus, in this work we introduce a two-state model of liquids which is explicitly based on the physical picture of a change of its elastic properties instead of any artificial *ad hoc* corrections to a single isothermal equation of state. It is aimed at the extension of the predictive capability of the approach, which utilizes the normal pressure reference data only, to the range of pressures up to a GPa range.

The knowledge of a technical fluids thermophysical properties is necessary for modern research. Advanced technologies and continuous technological development require more efficient solutions for several industrial issues, for example, the application of dedicated technical fluids with a better parameter as an operating medium in compressors, cooling systems, energy storage systems or engines. One of the approaches to overcome this obstacle is to estimate the thermophysical properties of new media of engineering significance based on an equation of state. Equation of state enables the prediction of a technical fluid's thermophysical properties that have not been investigated experimentally, so far. As an example, Lopez's work is based on the density scaling concept which requires high-pressure data to generate the fitting parameters to make volumetric predictions.¹⁶ The most novel equation of state models are based on statistical thermodynamics. The two states FT-EoS model, proposed by us, was checked for a wide range of alkanes, alkanols, benzene and silicone oil.

The knowledge of density under high pressure is incredibly important in terms of engineering studies. It is a basic parameter used to determine the isobaric thermal expansion coefficient which is one of the most desired thermophysical properties in terms of physicochemical process design, as well as heat capacity. Both of these are used for the calculation of either heat flow, heat transfer or mass transfer in any significant processes in engineering. The knowledge of the isobaric thermal expansion coefficient as a function of the temperature and the pressure is a significant input value for solving the energy and continuity equations in fuel injection systems under high pressure or novel diesel injectors and engine construction.^{17,18} The high-pressure technologies are used for increasing the efficiency of processes, reducing the emission of pollutants and saving material and energy resources.¹⁹

2 Model

2.1 Two states of elasticity

The bulk moduli defined by the general expression (2) for $n = 1$ and $n = 0$ written in the form that explicitly refers to the isothermal compressibility κ_T^0 corresponding to the reference pressure P_0 can be written as

$$K_{FT} = \left(\frac{\rho}{\rho_0} \right) (\kappa_T^0)^{-1} [1 + \lambda \kappa_T^0 (P - P_0)] \quad (3)$$

and

$$K_M = \left(\kappa_T^0\right)^{-1} \left[1 + \lambda \kappa_T^0 (P - P_0')\right], \quad (4)$$

where $\lambda = K'/K_0$, and the prime symbol is introduced simply to denote that the standard reference thermodynamic conditions may (but not obliged) be different. The parameter λ could also be expressed as $\lambda = k\rho_0$. Here, the coefficient k is the function of density, ρ_0 , and the isothermal compressibility, κ_T^0 , defined as a function of temperature as (see ref. 9):

$$k = -\frac{1}{\rho_0} - \left(\frac{d\rho_0}{dT}\right)^{-1} \left(\frac{1}{T} + \frac{d \log \kappa_T^0}{dT}\right). \quad (5)$$

The expression (4) has a well-motivated thermodynamic background as it keeps the first term in the thermodynamic potential expansion, which results in non-linearity for the stress-strain relation in the case of an isotropic uniform elastic continuum.²⁰ Here this expression is given in Murnaghan's choice of general parameters.²¹

Eqn (3) contains exactly the same expansion with respect to the pressure but it is multiplied by the factor ρ/ρ_0 , which describes a kind of reduced density. Note that this factor is also known in the theory of elasticity as a first reduced density dependent correction obtained within the effective averaged representation of the elastic constants for porous media.^{22,23} It should be pointed out that the packing fraction for liquids determined as $\varphi = \rho/\rho_{vdw}$, where $\rho_{vdw} = M/V_{vdw}$ is the van der Waals density (V_{vdw} is the van der Waals molar volume), varies within the interval from the random close to random very loose packing ($\varphi \approx 0.52-0.62$) from freezing to boiling conditions along the saturation curve. The concept of random packing, which provides definite values for the respective coefficient, can be defined in a strict mathematical way for spherical and slightly aspherical particles, only. But at the same time, the existence of a substance in a liquid state falls in the corresponding range of the density ratios φ for the case of chained liquids too. Thus, we can operate with this parameter as with an averaged characteristic number without the details of the topology of the molecular placement in the bulk volume.

Respectively, moderate external pressures lead to closing holes in the bulk but the medium remains loosely packed and the respective model (3) remains valid. However, this closing of "holes" leads to a faster growth of the effective density, and, as a result, the bulk modulus (3) grows faster too in comparison with (4), which originates from elastic repulsion of the packed molecules themselves. This effect has been qualitatively discussed by P. G. Bridgman in his analysis of experimental data²⁴ for an extremely large change of the applied external pressure to liquids.

The direct integration of eqn (3) and (4) along isotherms from results in the FT-EoS

$$\rho = \rho_0 + k^{-1} \log[\kappa_T^0 \lambda (P - P_0) + 1]. \quad (6)$$

and Murnaghan's equation

$$\rho = \rho_0' \left[\kappa_T^0 \lambda (P - P_0') + 1 \right]^{\lambda^{-1}}, \quad (7)$$

respectively.

Eqn (6) and (7) substituted into (3) and (4) give the relative isothermal compressibility as a function of the relative density:

$$\frac{\kappa_T}{\kappa_T^0} = \frac{\rho_0}{\rho} \exp[-\lambda(\rho - \rho_0)] \quad (8)$$

and

$$\frac{\kappa_T}{\kappa_T^0} = \left(\frac{\rho_0}{\rho}\right)^{-\lambda}. \quad (9)$$

Note that neither (8) and (6) nor (9) and (7) reproduce the experimental data for the whole range of pressures from the atmospheric points up to very high values, but each one covers its own range of pressures. Since the calculated isothermal compressibilities always have larger uncertainties than the directly measured densities (see the discussion in ref. 8), it is more convenient to consider (6) and (7) in the specific co-ordinate representations (along isotherms)

$$\exp[k(\rho - \rho_0)] = \kappa_T^0 \lambda (P - P_0) + 1 \quad (10)$$

and

$$\left(\frac{\rho}{\rho_0}\right)^\lambda = \kappa_T^0 \lambda (P - P_0) + 1 \quad (11)$$

as functions of the pressure optimizing λ in the right-hand side in such a way that the resulting plots are much more close to straight lines within some region of pressures.

Fig. 1 shows an example of the course of the function's variability of $\kappa_T^0 \lambda (P - P_0) + 1$ which is computed using the true experimental data in semi- and double logarithmic scales that should be linear, eqn (10) and (11), respectively. The first case

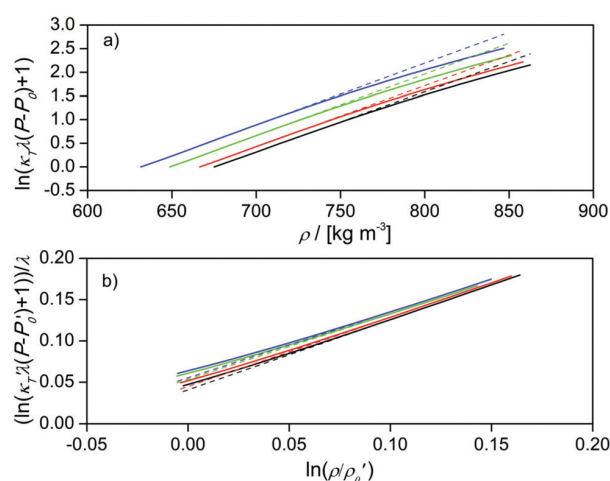


Fig. 1 Deviation of the linear behaviour for the natural logarithm of equations – (a) eqn (10) and (b) eqn (11); solid lines – calculated values for *n*-heptane,²⁵ dash lines – linear fit.

(Fig. 1a) shows a set of straight lines which are added for visual guidance, and there are visible deviations from the linear behaviour beyond some point on each isotherm.

In the second case (Fig. 1b), these visible deviations are observed, in the range of small pressures/densities, while the experimental curves tend to run straight with the increase of pressure up to very high values.

This is the principal point of the two states model approach that curves transit to elastic-solid-like (Murnaghan's behaviour) while packing density tends to an amorphous solid-like liquid. These straight lines which are on the fitting line accurately satisfy experimental data, both for small and high pressures separately. However, due to an absence of any phase transitions along an isotherm, the coefficients in eqn (6) and (7) should be coordinated in such a way that it assures a continuity of the density and the isothermal compressibility (as expressed *via* the first derivative of the density). This means that λ , $\kappa_{T,0}^0$ and ρ_0 apply for the moderately small pressures as calculated from fits to the experimental data measured at atmospheric pressure, while the second set of reference values, ρ_0' and $\kappa_{T,0}'$, should be taken at the reference pressure P_0' corresponding to the transition point between two models of elasticity, separately for each isotherm.

2.2 Method

There are two possible outcomes from the proposed two-state model for practical predictions of thermodynamic quantities of liquids under extremely high pressures: (i) a pure predictive calculation in the case when there is no high pressure reference data and a certain freedom in the choice of an isotherm is required; (ii) a possibility to continue some trend line fitting the experimental density data, measured along an isotherm up to moderately small pressure values, up to extremely high pressure conditions.

Since the most practical goal is to predict high pressure density of liquids without the need of complicated experiments at increased pressures, we concentrate on the purely predictive approach.

For input data, the FT-EoS requires the knowledge of several easily measurable physicochemical quantities: the density, ρ_0 , the isobaric heat capacity, $c_{p,0}$, and the speed of sound, c_0 , at the atmospheric pressure only. The physicochemical quantities mentioned above provide the values of isothermal compressibility at atmospheric pressure, $\kappa_{T,0}$, from a well-known relationship:

$$\kappa_{T,0} = \frac{1}{\rho_0 c_0^2} + \frac{T \alpha_{p,0}^2}{\rho_0 c_{p,0}} \quad (12)$$

Furthermore, the density and the isothermal compressibility at atmospheric pressure should be fitted, generally to square or cubic polynomials: a suitable choice of polynomials is required for the control of accuracy of the $\log(\nu(\rho))$ behaviour. Their differentiation according to eqn (5) provides the principal parameter $\lambda = k\rho_0$, and, respectively, the calculation of the first part of the density curve along an isotherm *via* eqn (6), which should be used up to the transition pressure P_0' . Note that

eqn (5) does not depend on the molar weight and may be applied to liquid mixtures with a complicated composition as well.

This value P_0' may be determined either by finding the density ρ_0' , which corresponds to the packing fraction about the value of $\varphi \approx 0.59$ with respect to the known van der Waals density of the liquid under study, or taking ρ_0' as approximately $\rho_0' = 1.04\rho_{\text{melt}}^0$, where ρ_{melt}^0 is the freezing density at atmospheric pressure.¹² The former criterion is applicable for pure liquids and has some definite uncertainty for strongly non-spherical molecules due to their non-trivial volume tiling. This will be clearly shown in the subsequent prediction results for pure liquids, where this approach was applied. At the same time, this property of molecular arrangement influences the solidification.^{26,27} Thus, this packing criterion can be applied directly as giving solid-like density (although the substance remains in a liquid state due to its temperature is higher than the freezing point at atmospheric pressure) that satisfies the proposed two states model. In addition, this density can be easily determined experimentally for any kind of molecular liquids or their mixtures simply by their cooling and weighing. An example of such an approach will be demonstrated utilizing the technical liquid mixture of silicone oil.

As the final step, this density will be taken as ρ_0' , $\kappa_{T,0}'$ will be found using eqn (3) and they will be substituted into eqn (7) for $P > P_0'$ to find the respective density in the second region.

3 Results

As an example, the two states model was used to predict volumetric properties of *n*-alkanes, *n*-alkanols and benzene, which are typical representatives of non-polar, polar, and aromatic substances. For this work we compared the existing high-pressure data of linear alkanes, primary alkanols and benzene to our model. As input data, the density and isothermal compressibility at atmospheric pressure only were used to predict the density under increased pressures. The isothermal compressibility was usually calculated from eqn (12), when all necessary experimental values existed. Otherwise, the isothermal compressibility was calculated by using an acoustic method.^{28,29} The knowledge of the density, the isobaric heat capacity at atmospheric pressure and the speed of sound as a function of temperature and pressure were used.

To illustrate the typical results in detail, let us consider predictability of different thermodynamic parameters for *n*-heptane, using the experimental data given in ref. 25 for comparison. Fig. 2 shows the experimental density values as a function of the pressure (markers) and the calculated results obtained using eqn (6) and (7) merged according to the continuous transition between them as mentioned above (solid lines). It is worth noting that this transition point occurs for every isotherm in a different point. By using the FT-EoS, the lower values of densities were obtained; on the other hand using Murnaghan's equation of state, higher values of densities were obtained. Therefore, the above results became a contribution to the whole curve within the two states model to

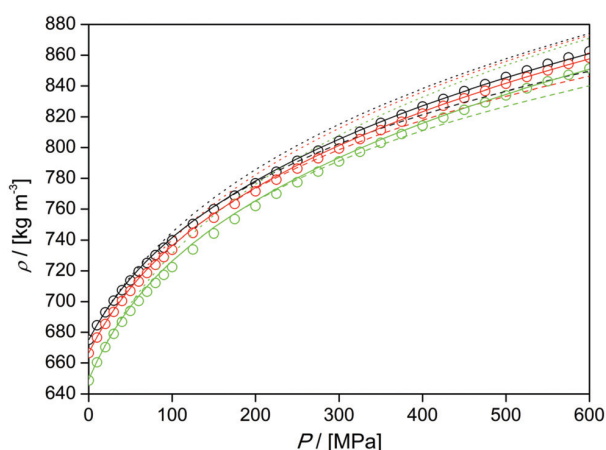


Fig. 2 Plot of experimental values for the density of *n*-heptane²⁵ and their values obtained for three isotherms (black – 303.15 K, red – 313.15 K, green – 333.15 K: dashed lines – eqn (6), dotted lines – eqn (7), solid lines – merger two equations eqn (6) and (7), empty markers – experimental data).²⁵

predict the density as a function of the temperature and pressure. To confirm an advantage of the proposed approach over a single equation considered for the whole wide region of pressures, two additional sets of curves (dashed and dotted lines) are added to Fig. 2. The dashed curves present the result of the FT-EoS which underestimates the density as pressure increases. The dotted curve represents the results of the Murnaghan equation which uses the same atmospheric pressure parameters. In this case, while reproducing the initial range of densities (that is natural since both eqn (6) and (7) have the same polynomial expansion for small P), one can clearly see the overestimation of the density at high pressures. This is explained by the irrelevant assumption of non-linear solid-like elasticity at small increased pressures.

To confirm the basic assumptions of the reduced density fluctuation behaviour change under increasing pressure, we also check the course of the logarithm of this quantity defined by eqn (1) that is shown in Fig. 3. It is seen that up to densities around 750 kg m^{-3} all markers which denote $\ln(\nu)$ are calculated on a base of known experimental data which are reproduced on one straight line. The respective analytical approximation with the determined parameters using the data measured at atmospheric pressure, are shown as the solid line. This reproduces the experimental points with high accuracy. For larger densities, this unique universal line is split into separate dependencies respectively to each isotherm. However, the continuation of the previous analytical line to Murnaghan's functional form applied according to the two states model reproduces this splitting as well.

Additionally, the proposed two states model works also for liquid mixtures. As an example, we presents silicone oil 9981 LTNV-70 which is shown in Fig. 4 for five isotherms and the pressure range up to 860.2227 MPa .³⁰ Here, to show the behaviour of eqn (1), the molar mass (undefined for the substance) and gas constant were omitted. But since the combination M/R is a

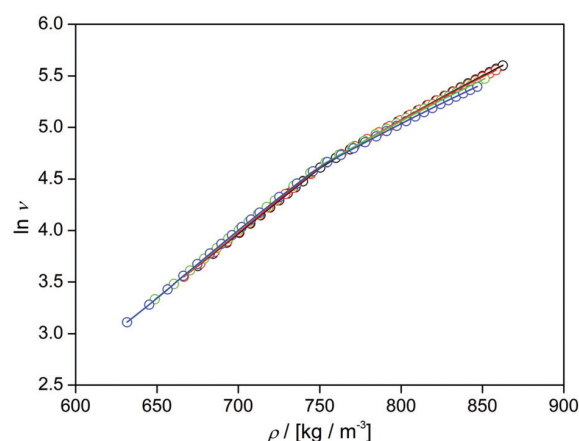


Fig. 3 The behaviour of $\ln(\nu)$ as a function of density for *n*-heptane for four isotherms: 303.15 K – black, 313.15 K – red, 333.15 K – green, 353.15 K – blue.

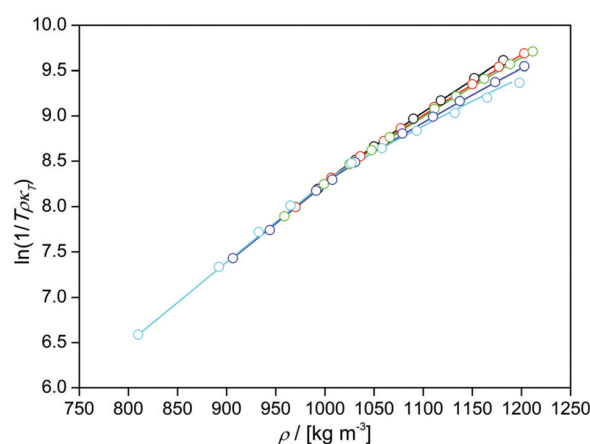


Fig. 4 The behaviour of $\ln(1/(T\rho\kappa_T))$ as a function of density for silicone oil 9981 LTNV-70 for five isotherms: 273.15 K – black, 298.15 K – red, 310.93 K – green, 372.04 K – blue, 491.48 K – cyan.

constant, it's value produces a uniform parallel shift for $\ln(\nu)$ which does not affect its density-dependent behaviour. It is worth noting that this mixture was used in our previous work where we predicted the density only using the FT-EoS.¹² The deviation with using FT-EoS for $T = 491.48 \text{ K}$ and $P = 860.22 \text{ MPa}$ was 3.15% and now with using TSM error decreased to 0.68%. For more details, please see Table S4 in the ESI.†

As a next step, the reproducibility of the isothermal compressibility, κ_T , has been checked. It is an important benchmark since κ_T is a derivative quantity. As a result, it is quite sensitive to various small disturbances even if reproducing the integral quantity, the density, looks reasonable.⁸ The inverse of eqn (3) and (4) was taken to calculate the isothermal compressibility as a function of temperature and pressure with parameters used for the density calculations described above taking into account the transition rule.

Fig. 5 demonstrates the results along isotherms in comparison with the experimental data for the lowest and the highest

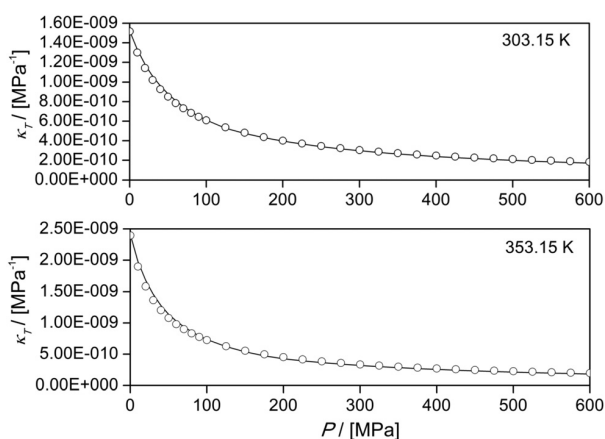


Fig. 5 Plot of calculated isothermal compressibility, κ_T , for *n*-heptane²⁵ as a function of pressure for two isotherms: 303.15 K and 353.15 K; open circle – experimental values, solid lines – calculated values by a two states model.

temperatures given in ref. 25. One can see that this quantity is also reproduced with a good accuracy.

Finally, Fig. 6 shows relative errors of the density predictions for the full set of processed liquids: *n*-alkanes (243.15–433.15 K, up to 1100 MPa), alkanols (203.15–453.15 K, up to 1200 MPa) and benzene (298.09–353.15 K, up to 355.3 MPa)^{25,28,31–37} denoted as markers for each “temperature–pressure” pair. Overall, 2138 data points were processed. The average absolute deviation from experimental data for polar and non-polar liquids are: *n*-alkanes – 0.28%, alkanols – 0.17% and benzene – 0.10%. To assure an additional independence between predicted and raw experimental data, reference values at atmospheric pressure, which are necessary in the proposed method, were taken for a majority of substances from the NIST database.³⁸

In light of this work, we conclude that the proposed two states model approach could be used to truly predict with a

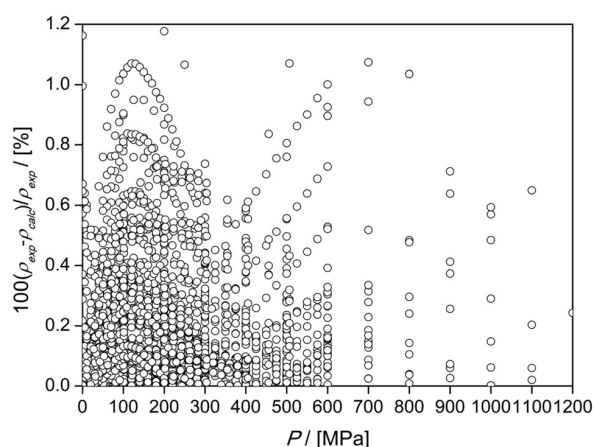


Fig. 6 Absolute deviations between experimental density, ρ_{exp} , and predicted density, ρ_{cal} , data for all liquids^{25,28,31–37} obtained by using the two states model as a function of pressure.

high accuracy the density as a function of temperature and pressure. The detailed report is shown in supplementary tables (ESI†).

4 Discussion

Anomalous thermodynamic properties of highly compressed liquids, including the transition point which occurs in our approach, were already observed and discussed in the context of isotherms of the isobaric expansion coefficient $\alpha_p = -\rho^{-1}(\partial\rho/\partial T)_p$ crossing at certain pressure^{24,39,40} that was hypothesized as a consequence of different excitability of the inner degrees of freedom of molecules brought into too close contact by high degree of compression. A similar effect and its origin were also detected in the behaviour of the dimensionless bulk modulus (reciprocal compressibility).^{41,42} Recently it has been shown¹¹ that the behaviour of the reduced bulk modulus, which can be associated with the fluctuation parameter eqn (1) and isobaric compressibility isotherm can be considered as a consequence of the packing ratio for molecules having their shape close to the spherical one.

Here we can generalize this picture to the case of molecules with sufficiently different shapes and chain lengths. For all of them, the initial region of moderately high densities exhibits the universal exponential behaviour of ν followed by the subsequent formation of separate curves as it is demonstrated in Fig. 3 (certainly, only the shape is kept even though the parameters are substance-dependent). As well, this feature can be reproduced by considering the crossover from FT-EoS to Murnaghan’s isothermal equation of state at some density corresponding to the packing fraction $\varphi = \rho/\rho_{\text{vdW}}$ expressed through the van der Waals density of molecules.

Now, instead of taking this parameter φ as a packing ratio for the random loose packing of spherical (or quasi-spherical) particles or its estimation by the freezing density, let us consider its direct optimization with respect to the best for reproducing the experimental density by the two states model. Specifically, we use the best fit of this parameter resulting in the smallest AAD errors for available experimental density data from atmospheric to the highest available pressures. Table 1 presents the average values of φ and values for parameter k , which is used to determine parameter λ in the next calculations, for *n*-alkanes, *n*-alkanols and benzene obtained in this way.

Table 1 shows that the packing fractions φ belong to a limited range of values for non-polar as well as polar liquids, and this range is expanded from the upper limit of random loose packing and to the range of close random packing density⁴⁵ and parameter k . This confirms the ideas of the close molecular contact^{11,39} as an origin of changes in volumetric response of liquids to the growing applied pressure. In addition, the values of φ , which are higher for *n*-alkohols than for non-polar liquids are supported with physical and chemical arguments,⁴⁶ which indicates the possibility of significant structural transitions in this liquid under high pressures. Table 1 shows also the behaviour of the parameter k . Our applied method takes into account small changes in this parameter as a function of the temperature.⁹

Table 1 The calculated values of parameter ϕ for polar and non-polar liquids

Compound	ϕ	k	AAD/%
<i>n</i> -Pentane ²⁵	0.56	0.0129	0.41
<i>n</i> -Hexane ^{25,31,32}	0.61	0.0122	0.37
<i>n</i> -Heptane ^{25,31,33,43}	0.58	0.0124	0.19
<i>n</i> -Octane ^{25,31,43}	0.59	0.0123	0.43
<i>n</i> -Nonane ^{25,33,43}	0.60	0.0120	0.15
<i>n</i> -Decane ³¹	0.61	0.0120	0.28
<i>n</i> -Dodecane ^{25,43}	0.60	0.0122	0.25
Methanol ^{34,35}	0.59	0.0102	0.08
Ethanol ²⁸	0.60	0.0114	0.11
Butanol ³¹	0.61	0.0114	0.22
Hexanol ^{31,36}	0.65	0.0101–0.0099	0.13
Nonanol ³⁷	0.64	0.0101–0.0119	0.23
Decanol ³⁷	0.65	0.0117–0.0128	0.30
Benzene ^{25,44}	0.59	0.0093–0.0099	0.10
Silicone oil 9981 LTNV-70 ³⁰	—	0.0089–0.0091	0.13

It should be pointed out also that this evidence of necessity is required to operate when a liquid reaches and overcomes some transition density and behaves as a substance with solid-like elastic properties. With some recent results of numerical simulations, similar phenomena to this transition were found. Among them one can note qualitative changes in the corresponding reduced compressibility behaviour of the fluid formed by bowl-shaped particles,⁴⁷ transitions in the character of diffusivity (unavoidably connected with local density fluctuations),^{48–50} viscosity⁵¹ and free volume arguments considering the Murmaghan equation for liquids as an approximation for the small free volume among the volume occupied by particles with their specific bulk modulus.⁵²

5 Conclusions

The search for equation of states, which can be used for predictive calculations of thermodynamic properties, such as derivative, of liquids with accuracy comparable to the respective experimental data has remained for years a challenging task of physics and physical chemistry,^{5,36,53,54} and has resulted in manifold solutions ranging from simple phenomenological models valid for limited ranges of *PVT* parameters to complicated constructions based on extremely multiparametric fitting of experimental data.

In this work, we propose an alternative approach based on the rejection of a single equation of state aimed at reproducing volumetric properties of liquids in the whole interval of pressures of their existence in the liquid state in favour of merging two equations of states which are valid for the separate ranges of the supplied density with the crossover rule for the transition between them, *i.e.* the two states model. This proposal is based on the experimental evidence of the different elastic behaviour of liquids indicated by their bulk moduli and reduced density fluctuations.

The resulting predictive scheme requires only the prior knowledge of some temperature dependent physico-chemical data (the speed of sound, the density and the isobaric heat capacity) at atmospheric pressure, which can be easily obtained

experimentally. The comparative analysis of predictive capacity of this approach was evaluated by the case study of different prototypical molecular liquids. This accuracy is in agreement with real physical high-pressure experiments up to a GPa range.

Finally, this two-state volumetric approach appears to be physically coordinated with a variety of recently revealed arguments in favour of “gas–liquid-like/solid-like” duality of liquid states reflected in the thermophysical¹⁴ and transport properties.⁵¹

Conflicts of interest

There are no conflicts to declare.

Acknowledgements

We are grateful for the financial support based on Decision No. 2016/23/B/ST8/02968 from the National Science Centre (Poland). The author (B. J.) would like to thank Dr Alexander R. Lowe for assisting with the preparation of the final version.

References

- 1 L. Rayleigh, *London Edinburgh Philos. Mag. J. Sci.*, 1892, **33**, 209–220.
- 2 M. Smoluchowski, *Ann. Phys.*, 1908, **330**, 205–226.
- 3 M. Smoluchowski, *Z. Phys.*, 1916, **17**, 557–585.
- 4 A. Goncharov, V. Melent'ev and E. Postnikov, *Eur. Phys. J. B*, 2013, **86**, 357.
- 5 V. Diky, J. P. O'Connell, J. Abildskov, K. Kroenlein and M. Frenkel, *J. Chem. Eng. Data*, 2015, **60**, 3545–3553.
- 6 A. T. J. Hayward, *Br. J. Appl. Phys.*, 1967, **18**, 965.
- 7 H. Gholizadeh, R. Burton and G. Schoenau, *International Journal of Fluid Power*, 2011, **12**, 5–15.
- 8 J.-L. Daridon and J.-P. Bazile, *J. Chem. Eng. Data*, 2018, **63**, 2162–2178.
- 9 M. Chorążewski, E. B. Postnikov, B. Jasiok, Y. V. Nedyalkov and J. Jacquemin, *Sci. Rep.*, 2017, **7**, 5563.
- 10 J. R. Macdonald, *Rev. Mod. Phys.*, 1966, **38**, 669.
- 11 E. B. Postnikov and M. Chorążewski, *Phys. A*, 2016, **449**, 275–280.
- 12 B. Jasiok, A. R. Lowe, E. B. Postnikov, J. Feder-Kubis and M. Chorążewski, *Ind. Eng. Chem. Res.*, 2018, **57**, 11797–11803.
- 13 B. Jasiok, E. B. Postnikov and M. Chorążewski, *Fuel*, 2018, **219**, 176–181.
- 14 K. Trachenko and V. Brazhkin, *Sci. Rep.*, 2013, **3**, 2188.
- 15 C. A. Hunter, *Chem. Sci.*, 2013, **4**, 834–848.
- 16 E. López, O. Fandiño, D. Cabaleiro, L. Lugo and J. Fernández, *Phys. Chem. Chem. Phys.*, 2018, **20**, 3531–3542.
- 17 F. Salvador, J. Gimeno, M. Carreres and M. Crialesi-Esposito, *Fuel*, 2017, **188**, 442–451.
- 18 E. Tahmasebi, T. Lucchini, G. D'Errico, A. Onorati and G. Hardy, *Energy Convers. Manage.*, 2017, **154**, 46–55.
- 19 T. Kobata and H. Kajikawa, *Measurement*, 2019, **131**, 79–84.
- 20 L. D. Landau and E. Lifshitz, *Course of Theoretical Physics*, 1986, vol. 3, p. 109.

- 21 F. Murnaghan, *Proc. Natl. Acad. Sci. U. S. A.*, 1944, **30**, 244–247.
- 22 J. Mackenzie, *Proc. Phys. Soc., London, Sect. B*, 1950, **63**, 2.
- 23 N. Ramakrishnan and V. Arunachalam, *J. Mater. Sci.*, 1990, **25**, 3930–3937.
- 24 P. Bridgman, *Rev. Mod. Phys.*, 1935, **7**, 1.
- 25 Y. Melikhov, PhD thesis, Kursk State University, 1984.
- 26 J. J. van Loef, *Physica B+C*, 1975, **79**, 86–90.
- 27 J. Ram, *Phys. Rep.*, 2014, **538**, 121–185.
- 28 T. Sun, C. Ten Seldam, P. Kortbeek, N. Trappeniers and S. Biswas, *Physics and Chemistry of Liquids an International Journal*, 1988, **18**, 107–116.
- 29 M. Chorążewski and E. B. Postnikov, *Int. J. Therm. Sci.*, 2015, **90**, 62–69.
- 30 R. V. Kleinschmidt, D. Bradbury and M. Mark, *Viscosity and Density of Over Forty Lubricating Fluids of Known Composition at Pressures to 150,000 Psi and Temperature to 425 F*, A Report Prepared with the Assistance of the Advisory Board on Pressure Viscosity of the American Society of Mechanical Engineers, The American Society of Mechanical Engineers, New York, 1953.
- 31 P. W. Bridgman, *Proc. Am. Acad. Arts Sci.*, 1931, 185–233.
- 32 S. Randzio, J.-P. Grolier, J. Quint, D. Eatough, E. Lewis and L. Hansen, *Int. J. Thermophys.*, 1994, **15**, 415–441.
- 33 A. K. Doolittle, *J. Chem. Eng. Data*, 1964, **9**, 275–279.
- 34 T. Sun, S. N. Biswas, N. J. Trappeniers and C. A. Ten Seldam, *J. Chem. Eng. Data*, 1988, **33**, 395–398.
- 35 T. Sun, J. Schouten and S. Biswas, *Ber. Bunsenges. Phys. Chem.*, 1990, **94**, 528–534.
- 36 S. Randzio, J.-P. Grolier and J. Quint, *Fluid Phase Equilib.*, 1995, **110**, 341–359.
- 37 I. Sysoev, *Nauchn. Tr. – Kursk. Gos. Pedagog. Inst.*, 1977, **176**, 185–199.
- 38 <https://webbook.nist.gov/chemistry/fluid/>.
- 39 S. L. Randzio, *Phys. Lett. A*, 1986, **117**, 473–476.
- 40 M. Taravillo, V. G. Baonza, M. Cáceres and J. Núñez, *J. Phys.: Condens. Matter*, 2003, **15**, 2979.
- 41 Y.-H. Huang and J. P. O'Connell, *Fluid Phase Equilib.*, 1987, **37**, 75–84.
- 42 M. Taravillo, M. Cáceres, J. Núñez and V. G. Baonza, *J. Phys.: Condens. Matter*, 2006, **18**, 10213.
- 43 J. Boelhouwer, *Physica*, 1960, **26**, 1021–1028.
- 44 J. Dymond, N. Glen, J. Robertson and J. Isdale, *J. Chem. Thermodyn.*, 1982, **14**, 1149–1158.
- 45 F. A. L. Dullien, *Porous Media: Fluid Transport and Pore Structure*, Academic Press, 2012.
- 46 R. Böhmer, C. Gainaru and R. Richert, *Phys. Rep.*, 2014, **545**, 125–195.
- 47 M. Marechal and M. Dijkstra, *Phys. Rev. E: Stat., Nonlinear, Soft Matter Phys.*, 2010, **82**, 031405.
- 48 S. K. Ghosh, A. G. Cherstvy and R. Metzler, *Phys. Chem. Chem. Phys.*, 2015, **17**, 1847–1858.
- 49 J. Shin, A. G. Cherstvy and R. Metzler, *New J. Phys.*, 2015, **17**, 113028.
- 50 M. Galanti, D. Fanelli and F. Piazza, *Front. Phys.*, 2016, **4**, 33.
- 51 J. Dench, L. Di Mare, N. Morgan and J. Wong, *Phys. Chem. Chem. Phys.*, 2018, **20**, 30267–30280.
- 52 B. Zhang and T. Mawatari, *Proceedings of Asia International Conference on Tribology 2018*, 2018, pp. 208–209.
- 53 J. Greogorowicz, J. O'Connell and C. Peters, *Fluid Phase Equilib.*, 1996, **116**, 94–101.
- 54 I. Polishuk, *Ind. Eng. Chem. Res.*, 2014, **53**, 14127–14141.

Katowice, 11.04.2023 r.

Instytut Chemii
Wydział Nauk Ścisłych i Technicznych
Uniwersytet Śląski w Katowicach
ul. Bankowa 12, 40-007 Katowice

Statement on the contribution to the publication

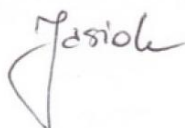
Publication:

B. Jasiok, E.B. Postnikov, M. Chorążewski, The prediction of high-pressure volumetric properties of compressed liquids using the two states model. *Physical Chemistry Chemical Physics* **2019**, 21, 15966-15973, DOI: 10.1039/C9CP02448D.

We hereby state that the contribution to the work published jointly with Bernadeta Jasiok is in accordance with the description below:

Bernadeta Jasiok

I was responsible for: Conceptualization, Methodology, Software, Validation, Formal analysis, Data curation, Writing – Original Draft, Writing – Review & Editing, Visualization, Project administration



Eugene B. Postnikov

I was responsible for: Conceptualization, Methodology, Software, Validation, Writing – Original Draft, Writing – Review & Editing, Supervision



Mirosław Chorążewski

I was responsible for: Conceptualization, Writing – Original Draft, Writing – Review & Editing, Supervision, Funding acquisition





The CATBOOST as a tool to predict the isothermal compressibility of ionic liquids

Eugene B. Postnikov^{a,*}, Bernadeta Jasiok^b, Mirosław Chorażewski^b

^a Theoretical Physics Department, Kursk State University, Radishcheva st., 33, Kursk 305000, Russia

^b Institute of Chemistry, University of Silesia, Szkolna 9, 40-006 Katowice, Poland

ARTICLE INFO

Article history:

Received 1 December 2020

Received in revised form 21 January 2021

Accepted 9 March 2021

Available online 13 March 2021

Keywords:

Isothermal compressibility

Atmospheric pressure

Ionic liquids

CatBoost

ABSTRACT

In this work, we explore the possibility for calculating the isothermal compressibility of Ionic Liquids at atmospheric pressure by combination of the CatBoost machine learning library and Wada's rule. The CatBoost predicts the isothermal compressibility at 298.15 K using the density at the same temperature, the critical temperature and pressure, the molar mass, and the acentric factor. The obtained value plays the role of reference one combined with the power-law dependence on the density to get the target compressibility in a wider temperature range. The isothermal compressibilities for 35 Ionic Liquids, given in literature, were used for the comparison and its analysis. The average result at 298.15 K was 6.0% while for the whole range of temperatures was 6.2%. The influence of machine learning parameters on the prediction is discussed.

© 2021 Elsevier B.V. All rights reserved.

1. Introduction

This work is dedicated to Prof. Emmerich Wilhelm on the occasion of his 80th birthday.

The isothermal compressibility is a key physicochemical property of liquids, and is defined by the first-order derivative of the volume with respect to the pressure:

$$\kappa_T = -\frac{1}{V} \left(\frac{\partial V}{\partial P} \right)_T.$$

This expression can be also given in terms of fluid density, as follows

$$\kappa_T = \frac{1}{\rho} \left(\frac{\partial \rho}{\partial P} \right)_T.$$

The above definitions are the basis for the direct method of κ_T determination based on the high-pressure volumetric (density) liquid experimental data. Additionally, κ_T can be determined by the very well-known indirect rigorous thermodynamic method through the adiabatic compressibility κ_S . Since the propagation of ultrasonic waves in liquids is an adiabatic process, the adiabatic compressibility κ_S can be determined from the speed of sound, u ,

$$\kappa_S = \frac{1}{\rho u^2}$$

and can be related to κ_T through the relationship [1–3]:

$$\kappa_T = \kappa_S + \frac{T\alpha_p^2}{\rho C_p}.$$

The isothermal compressibility is an important physical parameter of liquids, and strongly depends on the structure of the liquid. The investigations of isothermal compressibility of liquids are able to give various information not only on the thermodynamic behavior of different classes of liquids but also on their structure. The isothermal compressibility is connected to the radial distribution function of liquids [4–8].

Some of early works by Professor Emmerich Wilhelm were about isothermal compressibility in the models of simple liquids, which combine hard-sphere system (Carnahan-Starling approximation) with the van der Waals attractive term [9,10] in the case of reproducing realistic experimental data. In his works all mechanical coefficients and the derived quantities were calculated from the relationship which, in principle, have no parameters to be adjusted.

As for the more recent works, an attention to the isothermal compressibility was drawn as to a component of the factor, which is included into the expression for the internal pressure:

$$P_i = T \frac{\alpha_p}{\kappa_T} - P$$

* Corresponding author.

E-mail address: postnikov@kursksu.ru (E.B. Postnikov).

within the context of its connection with intermolecular interactions in pure molecular liquids and mixtures and predictability of their volumetric properties in a wide range of state parameters [1,11,12].

It should be pointed out that the various cubic equations of state well-developed for modelling coexistent multiphase (vapour-liquid as well as mixtures) systems are practically not applicable for the highly compressed uniform substances [13]. This situation induces another approach, which was once called “three-dimensional density correlation system” (TRIDEN) [14]. It operates with three separate equations: one for the saturated density, commonly it is the Rackett equation [15,16] also known as DIPPR 105, the second one is an equation, which defines the saturated pressure P_s (e.g. Wagner's or Antoine's equations) and the third one defines the density of a compressed liquid along isotherms, e.g. by the Tait equation, which can be written in the form, which contains the isothermal compressibility $\kappa_T^s = \kappa_T(P_s)$ at ambient or saturation curve pressure as a parameter:

$$\frac{v}{v_s} = 1 - r^{-1} \ln(r\kappa_T^s(P - P_s) + 1). \quad (1)$$

where v and v_s are the specific volumes at the pressures P and P_s , respectively, and r is the parameter constant for each isotherm but temperature dependent (it can be found only phenomenologically). However, this approach requires knowledge of the high-pressure density measurements and, in fact, implies not a prediction by simple derivation of the isothermal compressibility from the density data.

The first reasonably successful attempt to predict the isothermal compressibility purely from knowledge of constituents of a substance was undertaken by Y. Wada [17], who introduced the concept of molecular compressibility, for which the following statement (now known as the Wada's rule) fulfils:

$$\frac{M}{\rho\kappa_T^{1/7}} = \text{const}, \quad (2)$$

where M is the molar mass and the constant can be calculated by the group contribution method. Later, a number of other empiric correlations considered as universal, was proposed [18–21]. However, they are valid as a rule for non-polar and weakly polar liquids (and not applicable to Ionic Liquids) and may require knowledge of at least some experimental reference point to adjust the coefficients for achieving an acceptable accuracy.

One of the most first attempts similar to the present approach was proposed in the work [22], where the authors consider κ_T at 298.15 K as a linear weighted combination of McGowan's molecular volume, specific volume, the isobaric expansion coefficient and the pressure. However, the results were limited by standard molecular liquids, and variability of required weights for different chemical classes of liquids was noted.

The main aim of this work is to find a tool for prediction the isothermal compressibility for ionic liquids as a function of temperature at atmospheric pressure with accuracy acceptable as comparable with the uncertainty recently known experiment-based data.

For ionic liquids, there was a trial to correlate the isothermal compressibility with the surface tension [23] but a weak correlation has been revealed that was interpreted in terms of a complex packing of the ions and specific properties of cohesive energy density, which drastically differ Ionic Liquids from more conventional molecular liquids.

Gardas and Coutinho reviewed group contribution methods for prediction the isothermal compressibility of ionic liquids, based on the types of cations and anions [24,25]. Similar approach was applied in the work [26] for a wider temperature range, focused on the values of coefficient of the Tait equation, from which, however, the isothermal compressibility can be easily derived. But it should be pointed out that the reference work dealt more with the fitting approach, i.e. the proposed equations were tested respectively to unified reproducing

properties of the substances used for their derivation rather than for true forecast of parameters for liquids completely not included into the set.

It is worth noting that Abildskov et al. proposed two method to predict the isothermal compressibility, first is empirical with 3 parameters, and the second is theoretical approach with 2 parameters, which is connected to a method for predicting gas solubilities in Ionic Liquids [27]. They tested both methods for 28 different ionic liquid systems.

Recently, machine learning algorithms start to attracts attention as a tool for predictive calculations of physical and chemical properties of liquids. This situation is based on the fact that such methods allow operating with a large set of chemical descriptors and, respectively, reveal hidden dependencies affecting the target quantities [28]. Among a variety of machine learning approaches, one can highlight CATBOOST – an algorithm for gradient boosting on decision trees developed by the Yandex corporation, which is specialized in search and information services [29,30] and made free to use an open-source project [31]. During last years, it has been applied to a wide variety of problems in the areas of network systems, medicine, biology and biochemistry, see [32]. The key features, which makes CATBOOST prospective for our goal is the possibility of using both numerical values and categorical features (character strings) as identifiers. This means that a native support of anions and cations names taking into account possible correlations within homologous series without any artificial assignment of numbers (e.g. empiric weights) to them. As for the numerical identifiers, the tree-based subdivision of the parameter space results in a more physically motivated discussion of the identifier's range influence in comparison with purely empiric correlations and “black box” algorithms like numerical networks.

2. Materials and methods

Being based on the correlations between isothermal compressibility and the characteristics of molecular liquids considered earlier [18,22], the following numerical values were chosen as identifiers: the density at 298.15 K, ρ_{298} , the critical temperature and pressure T_c and P_c , the molar mass M , and the acentric factor ω . The isothermal compressibility κ_{T298} as the target quantity for training and forecast was also considered at 298.15 K.

Since the available datasets contain values for the density and the isothermal compressibility provided for various temperatures, they were fitted for uniformity following the scheme proposed and tested for chosen by us Ionic Liquids in the work [33]: by quadratic polynomials of the temperature fitting the density and the natural logarithm of the isothermal compressibility (in several cases when no more than three values were found in the literature, the quadratic polynomial was replaced by the linear one). Thus, the values of ρ_{298} and κ_{T298} given by these polynomials were used in the calculations. It should be pointed out that while for the density the relative average deviation (AAD) between fitted and experimental data does not exceed 0.07% for all substances from the dataset, the regularity of the experimental data values for the isothermal compressibility is sufficiently poorer. After a detailed inspection of the datasets, we excluded the κ_T of those substances, which possessed either an abnormally large scatter that makes impossible to reveal an accurate trend or physically suspicious behavior such as the decrease of the reported isothermal compressibility with rising temperature.

Thus, only 35 ionic liquids were chosen for the further study; for them AAD = 0.07% for the whole dataset, and the maximal deviation from the fitting curve is equal to 0.2%. However, it should be stressed out that these small deviations characterize the fitting procedure only and are not related to the uncertainty of the original data especially taking into account that for the majority of these liquids there is often a unique set of measurements and the values of κ_T were obtained from the coefficients of processed raw data, as a rule, from the Tait's coefficient, see Table 2, that induced additional uncertainty up to 5% end

even more. Note also the work [34], which mentioned frequent discrepancies up to 9% between the results reported by different sources for the internal pressure in Ionic Liquids that primary originates from uncertainty in the values of the isothermal compressibility either reported by different authors or calculated from experimental data by different numerical methods.

All subsequent procedures were carried out using CATBOOST's realisation for Python programming language [31]. The input data formed a pool, which consisted of training parameters (two indices of columns containing the categorical features were denoted), training labels (the experimental values of the isothermal compressibility at 298.15 K), and the training features names.

To be assured of the self-consistency of the applied regression by the tree-based search decomposition, we made the optimization procedure for the CATBOOST's algorithm with respect to the tree depth and L2 regularization taking into account the limited number of points available and avoiding so-called overfitting [31]. The method subdivides the full multi-dimensional parametric space into finite-size cells and associates the output values with the most probable values within such cells determined by the sequential choices along trees. As it is demonstrated in Fig. 1, the regression uncertainty for such a small dataset (the tree depth and the L2 regularization value are equal to 4 and 7, respectively) does not exceed 5% that is acceptable the typical range of the isothermal compressibility determination.

For predictive calculations of the isothermal compressibility at 298.15 K, we applied the following workflow: the full dataset was subdivided into the training set, which contained identifiers and the experimental isothermal compressibilities for all liquids except a particular one and the test set, which contained identifiers for the Ionic Liquid under study, the compressibility of which should be predicted. This procedure was repeated separately for all liquids considered. It should be pointed out that such approach is more preferable than a simple artificial subdivision of the full dataset into two parts, which one is used for training and another – for testing since it allows usage a larger amount of data for training (that is important due to the limited availability of experimental data) and, simultaneously, does not violate the requirement of complete independence of the training dataset and the input parameters for the predictive test.

As a result, 35 possible different combinations (34 + 1) were considered. During this work we were using experimental data available in the

literature from the following sources [35–53]. The critical parameters were taken from [54].

The input data formed a pool, which consisted of training parameters (two indices of columns containing the categorical features were denoted), training labels (experimental values of the isothermal compressibility at 298.15 K), and the training features names. The training process was carried out with this pool applying `CatBoostRegressor` with the depth of trees equal to 4, L2 leaf regularization parameter equal to 7, and the number of iterations was the system's default value 1000 that as controlled by the tracing of the process's convergence. The root mean square error (RMSE) was used as the lost function and the respective learning rate was adjusted automatically. Fig. 2 illustrates the RMSE convergence using the data for all Ionic Liquids except [bmim][tca] as an example of training set. One can see that the RMSE is stabilised up to the threatening process and reaches the value $\Delta\kappa_T = 1.9 \cdot 10^{-11} \text{ Pa}^{-1}$, which is comparable with the standard uncertainty range for the experimental data considered. The resulting RMSE were recorded for all Ionic Liquids and reported. In addition, the sorted list of feature importances normalised to 100% revealed by the CATBOOST's built-in functions was determined and recorded.

The obtained trained model was applied to predict the isothermal compressibility of the Ionic Liquid excluded from the training using identifiers of this liquid as the input dataset. This value $\kappa_T^{\text{pred}}(298.15)$ found for the temperature value 298.15 K was combined with the regression of the experimental data on the density to predict the isothermal compressibility within the temperature range, when the latter exist, accordingly to Wada's rule (2) as follows

$$\kappa_T^{\text{pred}}(T) = \kappa_T^{\text{pred}}(298.15) \left(\frac{\rho(298.15)}{\rho(T)} \right)^7. \quad (3)$$

3. Results

Table 2 presents the estimated relative uncertainty of prediction and well as the comparisons with the test data, which are given as the relative deviation of the CatBoots-predicted data from experimental-based ones at 298.15 K that equal to 6.0% in average over the whole set, and AADs for the whole interval of temperatures, equal to 6.2%, when the prediction uses the combination of CATBOOST predictions with Wada's

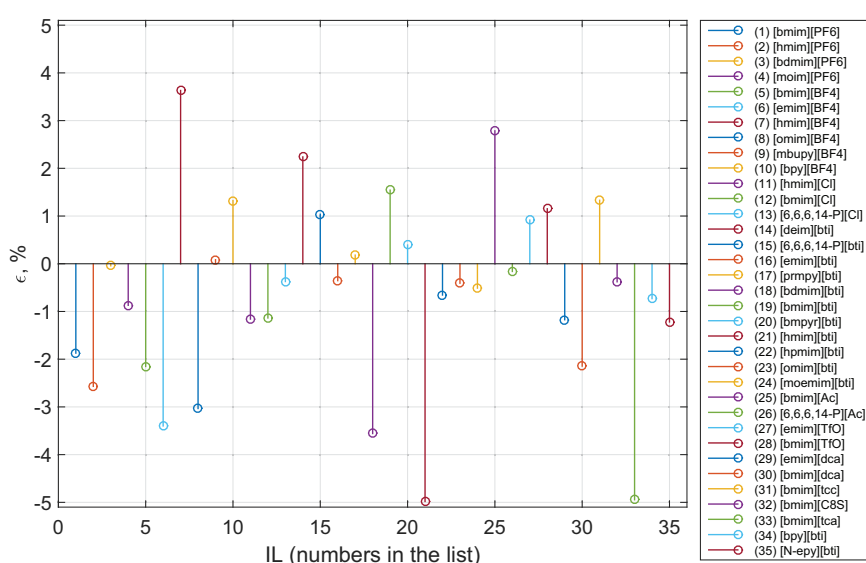


Fig. 1. The test of self-consistency of CATBOOST's data regression model, which indicates relative deviations of the considered experimental compressibilities of ionic liquids used in this study from the model regression data.

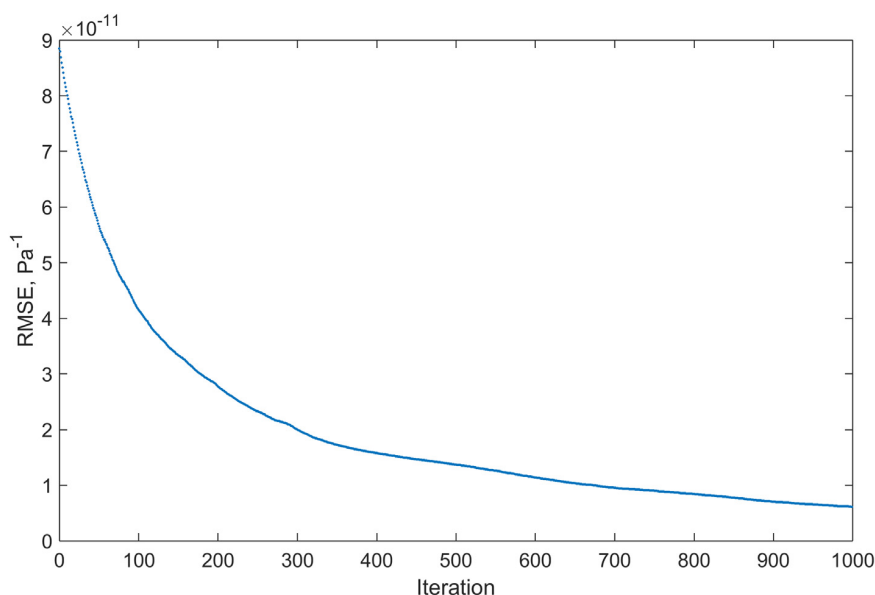


Fig. 2. An example of the root mean square error (RMSE) convergence during the CatBoost's training process.

rule. Note that these values indicate the general characteristic of the applied trained model as a whole, and, in particular is comparable with the uncertainty boundaries determined above within the self-consistency test. At the same time, a separate attention is required to the reproducibility of individual data on the isothermal compressibility, in particular, with respect to interplay of largest individual deviations, see Fig. 3 and the ranges of the input dataset of parameters.

Let us remind that the CatBoost is a generalization of the analysis of trends on the multidimensional space of parameters and multiple overlapping subdivisions of these parametric space as cells, to each of which some most probable value of isothermal compressibility, κ_T , is assigned. Therefore, the prediction of the latter is associated with a kind of interpolation procedure, when the input parameters characterising the

substance under study are within the range of parameters defined for the training set, and is a kind of extrapolation, when some input parameters are outside the range, for which the training procedure was carried out. Naturally, the prediction uncertainty differs for these two qualitatively different cases. In addition, different parameters can have different impact on the results of prediction. One of the main advantages of the CatBoost algorithm in comparison with multiple machine learning approaches is that it explicitly reports importances of the parameters in such subdivisions and/or trends. As it is seen from Table 1, where the average results for feature importances are shown, the molar mass, M , the critical temperature, T_c , and the cation are revealed in particular as the most important parameters for designating isothermal compressibilities for the whole set of ionic liquids considered in this

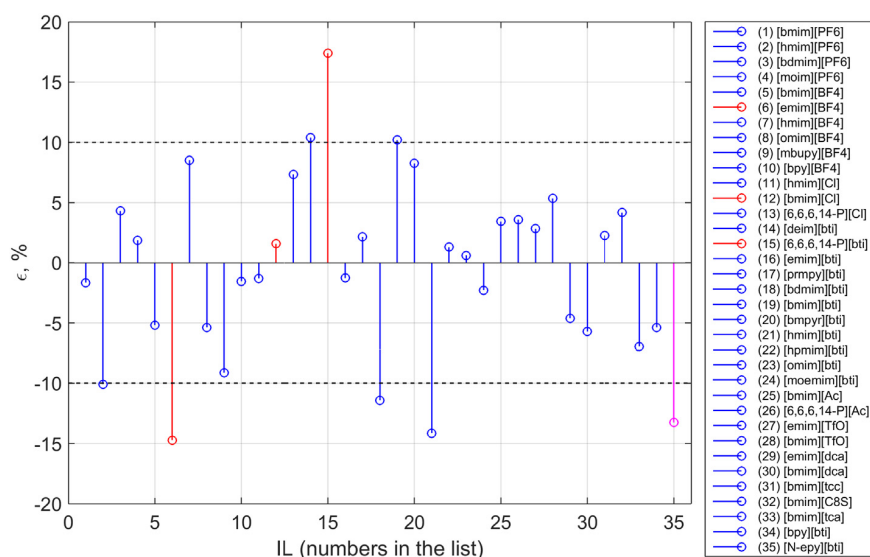


Fig. 3. Relative deviations between the predicted and experiment-based isothermal compressibility at 298.15 K. Red stems highlight those substances, for which either the molar mass or the critical temperature is outside the range of these quantities for the training set; the magenta stem corresponds to the ionic liquid, which has ρ_c , ω , and ρ_{298} outside of the range of training parameters.

Table 1
Average results for feature importances (in per cents) for ILs.

M	Cation	T_c	ρ_c	Anion	ω	ρ_{298}
48.30	16.66	15.92	5.84	4.92	4.81	3.55

work. The detailed report for all liquids studied separately is shown in Table S3 in the Electronic Supplementary Information (ESI). It is seen from this table that this mentioned ranging of the parameter importance fulfils for individual substances too: they vary from (40.43–55.47) % for the molar mass, (11.57–22.16) % for the critical temperature, (9.34–21.02) % for the cation, (3.09–9.46) % for the acentric factor, (3.83–7.41) % for the critical density, (3.02–5.80) % for the density at 298 K, and (2.78–12.96) % for the anion, respectively.

The two most valuable parameters revealed by the CATBOOST, the molar mass and the critical temperature, are well-coordinated with the general concepts of physical chemistry of liquids. In particular, the most strong dependence on the molar mass is coordinated with the fact that the ILs with higher molar volumes are generally more compressible because the isothermal compressibility increases with the alkyl chain length of the cation [55,56]. The second valuable parameter – the critical temperature also follows some established regularities. In particular, it has been noted that the saturated isothermal compressibility of a variety of molecular liquids depends on the combination $T_c - T$ [57]. At the second, Wada's rule (2) declares the dependence on the density, which, in turn, is also a function of the temperature distance from the critical point according to the well-established Rackett equation that fulfils for ionic liquids too [54]. Thus, the predictive method operates with the value of the isothermal compressibility at the fixed temperature $T = 298.15$ K, the value of the critical temperature defines the temperature difference, which is an important control parameters within this line of reasoning. As for the relative importance of cations and anions, it may be connected with the occurrence frequency of the same ions in the training set. Since they are categorical features, the CATBOOST tries to maximise the probability of following ionic homologous series from the available training combinations.

Thus, this line of reasoning gives some hints on the interpretation of the largest deviations shown in Fig. 3. In particular, the two largest ones, revealed for [emim][BF₄], 6,6,6,14-P[bt]i (highlighted in red in Fig. 3) exactly correspond the mentioned case: both the molar mass and the

critical temperature of [6,6,6,14-P][bt]i are outside the range of respective parameters used for training, and same is fulfilled for the critical temperature of [emim][BF₄]. Another outlier, visible for [N-epy][bt]i (highlighted in magenta in Fig. 3) has out-of-training range of less valuable parameters only but for all three of them, and, in addition, its cation (the valuable categorical feature) does not occur in the training set. Whence, the large prediction error is expectable. The detailed graphical representation for all ionic liquids studied in the work and all parameters is shown in Fig. S1 in the Electronic Supplementary Information.

Due to the importance of the molar mass and the critical temperature as numerical parameters, Fig. 4 shows the position of experimental κ_T in the plane (M, T_c). The growing size of numbers corresponds to the growing value of κ_T . Thus, the size of numbers, their location and the errors of predictions, which are shown in Fig. 3, were used for analysis. There could be observed some lines of regularity associated, including, with homologous series with respect to cations already reported by the CATBOOST as a valuable categorical feature. Fig. 4 supports the aforementioned discussion of the origin of the largest deviation in the prediction of the isothermal compressibility for [6,6,6,14-P][bt]i: the respective marker is already located too far from the rest used as the training set. On the other hand, although the relative error of prediction equal to 17.95% is large, it is not catastrophically large because the respective marker in Fig. 4 is biggest, i.e. it follows the regularity of increasing κ_T with growing M and T_c . This also explains, why the substance (12), [bmim][Cl], which is formally marked as red in Fig. 3 has a very small error of the prediction. It is the first in the respective linear sequence of markers in Fig. 4 but is not distant from the accurate next ones, (11, 25) and the growing size of these and subsequent markers is completely regular.

On the contrary, the markers (14, 18, 19, 21) demonstrates the reverse order in size along their sequence with the growing T_c and the respective relative errors of prediction are not small. This is especially demonstrable for the marker (21), which is significantly smaller than the surrounding markers, and, as a result the relative error of approximation is found as 17.15%. But it should be pointed out that the reference value of κ_T was taken not from the direct experimental data processing but from VR-SAFT calculations [36]. This means that this deviation may originate from insufficient accuracy of VR-SAFT for this substance and thermodynamic quantity and call for further studies of this ionic liquid aimed in clarifying its properties. Thus, we can conclude that the proposed (M, T_c) – κ_T representation can serve as a visual

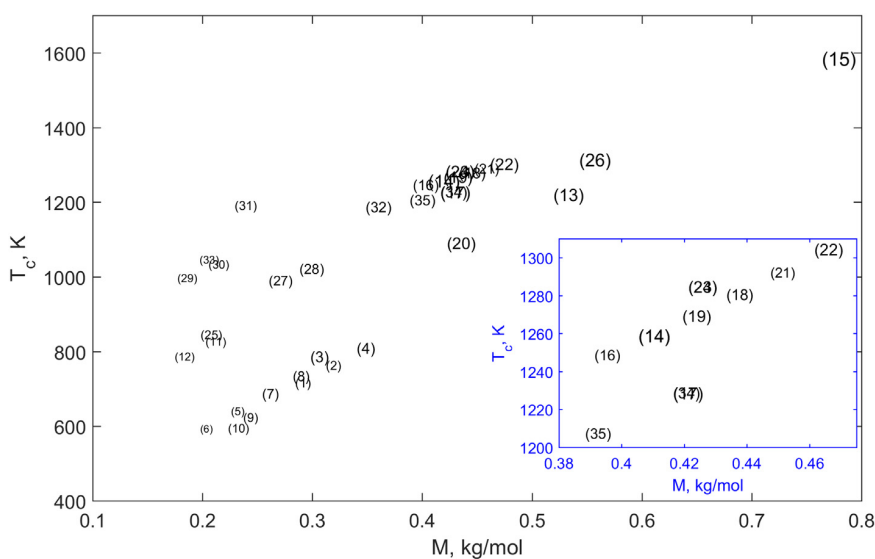


Fig. 4. The position of κ_T in the plane (M, T_c). The inset shows the cloud of overlapping markers in better resolution. Numbers correspond to the legend in Fig. 3.

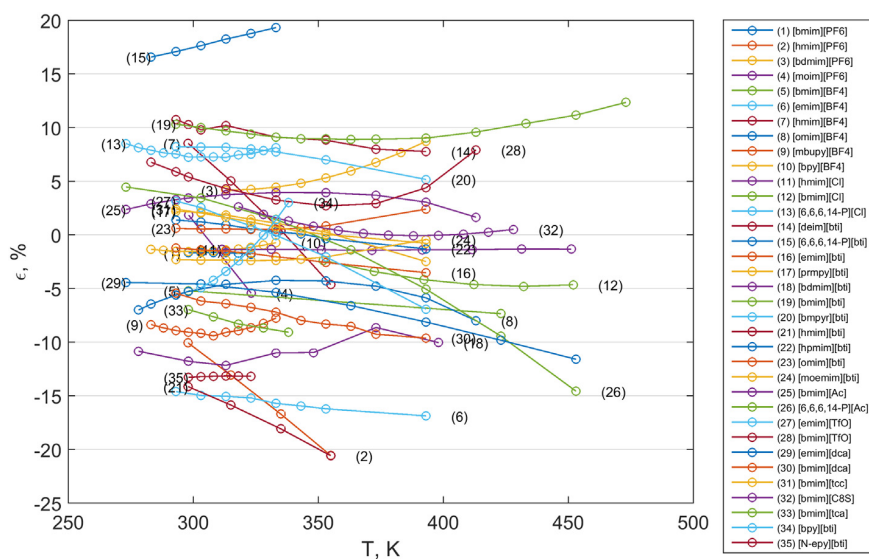


Fig. 5. The relative deviations of the predicted isothermal compressibility – whole range of temperature.

tool, guiding the minimal set of most influencing numerical parameters that is based on the CATBOOST's feature to report feature importances quantitatively.

Finally, Fig. 5 (see also numerical values of AAD in Table 2) represents the relative deviations of the predicted isothermal compressibilities from that ones, which are reported in different sources as results of experimental data processing. This prediction is based on the combination of the CATBOOST-based κ_T prediction at 298.15 K described above and Wada's rule (3) for the rest of temperatures. Note that we keep in Fig. 5 also those ionic liquids, for which the deviation of the isothermal compressibility at 298.15 K are large either due to their input parameters out of the range warrant for the application tree-based regression or questionable values as it is discussed above. This is made just to trace the temperature dependence implicitly taken into account by the usage of the density involved in Wada's rule. For example, the line corresponding to [emim][BF4] exhibit non-growing deviation with the growth of temperature although it is valuably shifted from zero since it starts from the shifted point, see above why. At the same time, it should be pointed out that we did not provide a prediction algorithm for the temperature dependence of the saturated density. As a result, possible deviating trends in the temperature dependence of the density that influence $\kappa_T(T)$ depends on the accuracy of the density data directly used in Eq. (3). However, Fig. 5 demonstrates that such deviations are not too frequent, the majority of curves are located within the same 10% range of deviations as the reference compressibility value given by the CATBOOST-based method for 298.15 K.

The detailed report is shown in the Table S2 in the Supplementary Information (ESI). The tables include all source data, which were collected and used as an input parameters – density at 298.15 K, ρ_{298} , critical density, ρ_{crit} , isothermal compressibility at 298.15 K, κ_{T298} , and relative standard uncertainty.

The standard uncertainty of the algorithm for each ionic liquid varies from 1.26% to 3.33%. The best results for isothermal compressibility at 298.15 K were obtained for eight ionic liquids: [bmim][PF6], [moim][PF6], [bpy][BF4], [hmim][Cl], [bmim][Cl], [emim][bti], [hpmim][bti] and [omim][bti] where the error did not exceed 2.0%. The worst results, where the error exceeded 13%, were for ionic liquids: [emim][BF4, 6,6,6,14-P][bti], [hmim][bti] and [N-epy][bti] that is a direct consequence of the reasons related to their predicted values at 298.15 K discussed above.

4. Discussion

The isothermal compressibility is the mechanical coefficient for which the accuracy is really difficult to estimate even having in hands a moderately large set of experimental data for different thermodynamic quantities. Its value depends on the uncertainty associated with the experimental density data as well as the numerical errors linked to the fitting equations. To avoid mistakes related to the correct determination of isothermal compressibility, a large number of experimental density should be collected [56]. The difference between obtained values for isothermal compressibility could come from the different quantities of water in the sample of ILs [60]. The water content in the ILs affects to experimental density [61], so it has a prior influence on the error of calculations of isothermal compressibility from definition or either from the differential form of Tait equation of state.

The most popular method to determine the isothermal compressibility for ionic liquids is primarily the Tait equation of state which precision of the calculated coefficient is related to the accuracy of the corresponding parameters $A(T)$, $B(T)$, and $C(T)$ [39,47,55,60,62–66]. It is also possible to find thermodynamic relation, PC-SAFT, GMA EoS, or different methods [42,46,53,59,67,68].

For example comparing two values of isothermal compressibility at the same temperature but published by two different groups, the error was 18.57% for [hpy][BF4] (at 303.15 K) [65,69], 15.97% for [bmim][BF4] (at 298.15 K) [40,70], 8.07% for [bmim][bti] (at 293.15 K) [50,70], 9.59% for [bmim][bti] (at 293.15 K) [41,70].

In the Gaciño et al. [64] work we found that the difference between their obtained values for isothermal compressibility for [P-6,6,6,14] [(C2F5)3PF3] in comparison with Ferreira et al. [71] work have an AAD of 14.8%. In the same work, they compare Kiselev's method, where the AAD range from 0.9% for [C1C1im] [(C10)2PO2] up to 4.8% for [P-6,6,6,14] [(C2F5)3PF3, 64]. Also Safarov et al. reported that the average deviation of 14 calculated isothermal compressibility is approximately 6.6% in comparison with the values by Gu and Brennecke [39,72]. The greatest deviations were observed in the work [73] where the authors found the error of the isothermal compressibilities for [C4C1im][TCM] and [4-C4C1py][TCM] even 78.51 and 71.20%, respectively. Gardas et al. were found deviation of 21% for [omim][PF6] at 0.1 MPa and 323.15 K [56].

Thus, the deviations within the range of 10%, which is provided by the predictive CATBOOST-based algorithm seems to be adequate to the

Table 2

The cation and anion for each Ionic Liquid, the isothermal compressibility obtained at 298.15 K by fitting available experimental data with the respective regression method, the relative standard uncertainty of prediction by the CatBoost, the relative deviation of the predicted isothermal compressibility at 298.15 K from the experiment-based one, and the AAD for the predicted isothermal compressibility over the whole temperature interval explored.

No	Cation	Anion	$\kappa_T 10^{10} [\text{Pa}^{-1}]$	κ_T method	$100u_r$	$100e_{298}$	100AAD
1	[bmim]	[PF6]	4.18E-10	therm. Rel. [35]	1.99	-1.65	1.68
2	[hmim]	[PF6]	4.11E-10	SAFT-VR [36]	2.14	-10.09	15.08
3	[bdmim]	[PF6]	4.95E-10	Tait EoS [38]	1.70	4.30	5.80
4	[moim]	[PF6]	4.91E-10	Tait EoS [39]	1.80	1.87	3.64
5	[bmim]	[BF4]	3.60E-10	Tait EoS [40]	2.29	-5.19	6.26
6	[emim]	[BF4]	3.29E-10	Tait EoS [41]	2.58	-14.71	15.56
7	[hmim]	[BF4]	4.46E-10	SAFT-VR [36]	1.71	8.51	4.67
8	[omim]	[BF4]	4.49E-10	Tait EoS [39]	1.88	-5.37	5.60
9	[mbupy]	[BF4]	3.90E-10	Tait and Rackett EoS [42]	2.15	-9.14	8.74
10	[bpy]	[BF4]	3.81E-10	Tait EoS [43]	2.38	-1.54	1.31
11	[hmim]	[Cl]	3.76E-10	Tait EoS [44]	2.80	-1.30	1.36
12	[bmim]	[Cl]	3.68E-10	Tait EoS [45]	2.13	1.59	4.00
13	[6,6,6,14-P]	[Cl]	5.59E-10	GMA EoS [58]	1.38	7.34	7.69
14	[deim]	[bti]	5.81E-10	Tait EoS [47]	1.26	10.38	9.35
15	[6,6,6,14-P]	[bti]	6.23E-10	Tait EoS [48]	1.37	17.39	17.95
16	[emim]	[bti]	4.69E-10	Tait EoS [41]	1.50	-1.27	2.02
17	[prmpy]	[bti]	5.42E-10	Tait EoS [49]	1.43	2.15	1.64
18	[bdmim]	[bti]	4.93E-10	Tait EoS [38]	1.48	-11.43	10.77
19	[bmim]	[bti]	5.23E-10	Tait EoS [50]	1.54	10.19	9.78
20	[bmpyr]	[bti]	5.26E-10	Tait EoS [49]	1.76	8.25	7.51
21	[hmim]	[bti]	4.45E-10	SAFT-VR [36]	2.03	-14.15	17.15
22	[hpmim]	[bti]	5.28E-10	Tait EoS [41]	1.74	1.31	0.77
23	[omim]	[bti]	5.28E-10	Tait EoS [41]	2.29	0.61	0.84
24	[moemim]	[bti]	5.28E-10	Tait EoS [41]	1.94	-2.29	2.05
25	[bmim]	[Ac]	3.93E-10	empiric EoS [51]	2.35	3.44	3.21
26	[6,6,6,14-P]	[Ac]	5.75E-10	Tait EoS [48]	1.56	3.58	5.69
27	[emim]	[TfO]	4.35E-10	Tait EoS [49]	2.37	2.83	2.45
28	[bmim]	[TfO]	4.43E-10	empiric EoS [52]	2.34	5.33	4.85
29	[emim]	[dca]	3.60E-10	GCM Model ^a	3.33	-4.61	7.20
30	[bmim]	[dca]	3.72E-10	Tait EoS [50]	2.89	-5.71	7.55
31	[bmim]	[tcc]	4.03E-10	Tait EoS [41]	2.65	2.25	1.15
32	[bmim]	[C8S]	4.66E-10	Tait and Rackett EoS [53]	2.49	4.16	0.68
33	[bmim]	[tca]	3.56E-10	Tait EoS [55]	2.68	-6.95	8.12
34	[bpy]	[bti]	4.93E-10	Tait EoS [46]	2.13	-5.38	2.58
35	[N-epy]	[bti]	4.70E-10	Tait EoS [49]	2.34	-13.26	13.18

^a Calculated by applying the GCM proposed by Jacquemin et al. [46,59].

isothermal compressibility at atmospheric pressure for ionic liquids with uncertainty comparable to the results, which are provided by the methods of experimental data processing listed in Table 2.

Note that the quite reasonable reproducing the isothermal compressibility within the whole temperature range considered with the usage of Wada's rule (2) as well as Wada's rule itself can be easily explained referring to the class of non-cubic polynomial equations valid along the saturation curve and in the single phase liquids up to moderately high pressures

$$P = -F(T)\rho^n + C\rho^m, \quad (4)$$

where $F(T)$ is some polynomial function of temperature and C is a constant. The first example of this type of equations was proposed by Eucken [74] with $n = 3$, $m = 6$, and $F(T) = A - BT$ but such equations of state not only had been developed further with different polynomial degrees [75] but also used up to now for high-accurate fitting experimental data for molecular and Ionic Liquids in a wide range of thermodynamic conditions, see e.g. [76].

From Eq. (4), the isothermal compressibility is derived as

$$\kappa_T = \frac{1}{(m-n)C\rho^m + P} \quad (5)$$

Under atmospheric pressure conditions, when the ambient pressure P is sufficiently lower than the internal pressure P_i , one can put $P \approx 0$ in Eq. (4) and consider the regression

$$\rho^{(m-n)}(T) = C^{-1}F(T). \quad (6)$$

A test of such fitting for $m = 7$, $n = 4$ and $F(T) = A - BT$ applied to the full set of Ionic Liquids considered in this work gives mean AAD = 0.012% and maximal AAD for individual liquids does not exceed 0.16%. Therefore, one can neglect by P is Eq. (5) and rewrite in the form

$$\frac{M}{\rho(\kappa_T^E)^{1/7}} = M(3C)^{1/7}, \quad (7)$$

which exactly coincides with Wada's Eq. (2).

Finally, it should be pointed out that the uncertainty estimation for the CatBoost-based predictions should necessary take into account the range of parameters used as input ones in their relation to the ones, which are used for the model's training because the regressive type of the algorithm is sensitive to the difference between the interpolation and extrapolation and may fail in the latter case.

5. Conclusion

Estimating the isothermal compressibility coefficient is a very difficult task because it is not a directly measurable quantity. Due to the experimental uncertainty of the primary experimental data, even the application of isothermal derivatives of functions fitting the density [3] can lead to significant errors. The same is true for another indirect approach, which uses the experimental data of the density, speed of

sound and heat capacity and thermodynamic equality. On the other hand, up to date, there is no reliable universal method or equation of state which would allow estimating the isothermal compressibility with very good accuracy from first principles, e.g. from liquid's chemical composition. This problem is especially complicated for Ionic Liquids, which are composed not of neutral molecules.

In this work, we propose to attack this problem with the CatBoost – the modern machine learning approach realizing the gradient boosting regression on trees, which supports the usage of categorical features. In such a way, it is possible to take into account simultaneously the numerical constants, which characterize a liquid with its belonging to chemical homologous series with respect to cations and anions. In addition, the fundamental principle of the tree-based search allows avoiding the typical “black box” problem of machine learning since the known range of parameters used for training as well as the features importances provided by the algorithm make possible the uncertainty quantifications including also the a priori estimation of the validity range of the prediction. One needs to check: i) the self-consistency of the training set, i.e. the uncertainty range assigned to the regression model describing the training set itself, ii) are all of input parameters values located between the maximal and minimal values included into the training set, iii) which parameters are determined as most influencing, and does the test and predicted values satisfy the regularities typical for this reduced set of parameters.

Here we chose the density at 298.15 K, ρ_{298} , the critical temperature, T_c , the critical pressure, P_c , the molar mass, M , and the acentric factor, ω as numerical parameters and the cation and anion names as categorical ones to determine the isothermal compressibility at atmospheric pressure for Ionic Liquids at 298.15 K. For an extended temperature region, Wada's rule combined with the density values at ambient pressure was applied; as a supporting result, the analysis revealing the interplay of this dependence with one of reliable regression of the PVT properties of liquids is obtained.

The data obtained within such an approach have been compared with data from the subject literature with the average result about 6% for AAD and principally bounded by 10% range for those ionic liquids, which are not determined as having parameters out of the range of the direct applicability the algorithm used. This can be considered as quite reasonable taking into account the actual data scattering in the experiment-based sources and recent practical absence of alternative methods for well-confirmed predictive methods for a wide range of different ionic liquids.

Finally, we should point out that these results are not only the first step on the road leading to the quantification of the isothermal compressibility as the thermodynamic property depending on the physical and chemical characteristics of a liquid, but also which provides a quantitative methodology for a quantitatively-supported search for the best set of parameters, which characterize thermodynamic characteristics of complex molecular liquids following the described workflow of this specific kind of machine learning.

Declaration of Competing Interest

The authors declare that they have no competing interests.

Acknowledgements

We are grateful for the financial support based on Decision No. 2016/23/B/ST8/02968 from the National Science Centre (Poland) and PIK - Program for new interdisciplinary elements of education at the doctoral level for a field of chemistry, POWR.03.02.00–00–I010/17 (Poland).

Appendix A. Supplementary data

Supplementary data to this article can be found online at <https://doi.org/10.1016/j.molliq.2021.115889>.

References

- [1] E. Wilhelm, Chemical thermodynamics: a journey of many vistas, *J. Solut. Chem.* 43 (2014) 525–576, <https://doi.org/10.1007/s10953-014-0140-0>.
- [2] E. Wilhelm, What you always wanted to know about heat capacities, but were afraid to ask, *J. Solut. Chem.* 39 (12, 2010) 1777–1818, <https://doi.org/10.1007/s10953-010-9626-6>.
- [3] J.-L. Daridon, J.-P. Bazile, Computation of liquid isothermal compressibility from density measurements: an application to toluene, *J. Chem. Eng. Data* 63 (6) (2018) 2162–2178, <https://doi.org/10.1021/acs.jced.8b00148>.
- [4] J.-L. Burgot, The radial distribution function and the isothermal compressibility coefficient of a system, *Notion Activity Chem.* (2017) 345–351, https://doi.org/10.1007/978-3-319-46401-5_31 Springer.
- [5] D.M. Rogers, Extension of Kirkwood-buff theory to the canonical ensemble, *J. Chem. Phys.* 148 (5) (2018), 054102, <https://doi.org/10.1063/1.5011696>.
- [6] A. Trokhymchuk, I. Nezbeda, J. Jirsák, D. Henderson, Hard-sphere radial distribution function again, *J. Chem. Phys.* 123 (2) (2005), 024501, <https://doi.org/10.1063/1.1979488>.
- [7] R. van Zon, J. Schofield, Constructing smooth potentials of mean force, radial distribution functions, and probability densities from sampled data, *J. Chem. Phys.* 132 (15, 2010) 154110, <https://doi.org/10.1063/1.3366523>.
- [8] S.B. Yuste, A. Santos, Radial distribution function for hard spheres, *Phys. Rev. A* 43 (10, 1991) 5418, <https://doi.org/10.1103/PhysRevA.43.5418>.
- [9] E. Wilhelm, Thermomechanische Eigenschaften eines Systems harter Kugeln mit temperaturabhängigem, effektivem Durchmesser, *Monatsh. Chem.* 105 (1974) 291–301, <https://doi.org/10.1007/BF00907375>.
- [10] E. Wilhelm, Pressure dependence of the isothermal compressibility and a modified form of the Tait equation, *J. Chem. Phys.* 63 (1975) 3379–3381, <https://doi.org/10.1063/1.431774>.
- [11] E. Wilhelm, T. Letcher, *Volume Properties: Liquids, Solutions and Vapours*, Royal Society of Chemistry, 2014.
- [12] E. Wilhelm, Mitigating complexity: cohesion parameters and related topics. I: the Hildebrand solubility parameter, *J. Solut. Chem.* 47 (2018) 1626–1709, <https://doi.org/10.1007/s10953-018-0821-1>.
- [13] J.O. Valderrama, The state of the cubic equations of state, *Ind. Eng. Chem. Res.* 42 (2003) 1603–1618, <https://doi.org/10.1021/ie020447b>.
- [14] E.C. Ihmels, J. Gmehling, Densities of toluene, carbon dioxide, carbonyl sulfide, and hydrogen sulfide over a wide temperature and pressure range in the sub- and supercritical state, *Ind. Eng. Chem. Res.* 40 (2001) 4470–4477, <https://doi.org/10.1021/ie001135g>.
- [15] H.G. Rackett, Equation of state for saturated liquids, *J. Chem. Eng. Data* 15 (1970) 514–517, <https://doi.org/10.1021/je60047a012>.
- [16] T. Yamada, R.D. Gunn, Saturated liquid molar volumes. Rackett equation, *J. Chem. Eng. Data* 18 (1973) 234–236, <https://doi.org/10.1021/je60057a006>.
- [17] Y. Wada, On the relation between compressibility and molal volume of organic liquids, *J. Phys. Soc. Jpn.* 4 (1949) 280–283, <https://doi.org/10.1143/JPSJ.4.280>.
- [18] P.L. Chueh, J.M. Prausnitz, A generalized correlation for the compressibilities of normal liquids, *AIChE J.* 15 (1969) 471–472, <https://doi.org/10.1002/aic.690150335>.
- [19] S.W. Brelvi, J.P. O'Connell, Corresponding states correlations for liquid compressibility and partial molal volumes of gases at infinite dilution in liquids, *AIChE J.* 18 (1972) 1239–1243, <https://doi.org/10.1002/aic.690180622>.
- [20] Y.-H. Huang, J.P. O'Connell, Corresponding states correlation for the volumetric properties of compressed liquids and liquid mixtures, *Fluid Phase Equilib.* 37 (1987) 75–84, [https://doi.org/10.1016/0378-3812\(87\)80044-4](https://doi.org/10.1016/0378-3812(87)80044-4).
- [21] I.C. Sanchez, Dimensionless thermodynamics: a new paradigm for liquid state properties, *J. Phys. Chem. B* 118 (2014) 9386–9397, <https://doi.org/10.1021/jp504140z>.
- [22] Y. Marcus, G.T. Hefter, The compressibility of liquids at ambient temperature and pressure, *J. Mol. Liq.* 73 (1997) 61–74, [https://doi.org/10.1016/S0167-7322\(97\)00057-3](https://doi.org/10.1016/S0167-7322(97)00057-3).
- [23] Y. Marcus, The isothermal compressibility and surface tension product of room temperature ionic liquids, *J. Chem. Thermodyn.* 124 (2018) 149–152, <https://doi.org/10.1016/j.jct.2018.05.002>.
- [24] R.L. Gardas, J.A.P. Coutinho, Group contribution methods for the prediction of thermophysical and transport properties of ionic liquids, *AIChE J.* 55 (2009) 1274–1290, <https://doi.org/10.1002/aic.11737>.
- [25] J.A.P. Coutinho, P.J. Carvalho, N.M.C. Oliveira, Predictive methods for the estimation of thermophysical properties of ionic liquids, *RSC Adv.* 2 (2012) 7322–7346, <https://doi.org/10.1039/C2RA20141K>.
- [26] J. Jacquemin, P. Nancarrow, D.W. Rooney, M.F. Costa Gomes, P. Husson, V. Majer, A.A.H. Pádua, C. Hardacre, Prediction of ionic liquid properties. II. Volumetric properties as a function of temperature and pressure, *J. Chem. Eng. Data* 53 (2008) 2133–2143, <https://doi.org/10.1021/je8002817>.
- [27] J. Abildskov, M.D. Ellegaard, J.P. O'Connell, Densities and isothermal compressibilities of ionic liquids—modeling and application, *Fluid Phase Equilib.* 295 (2) (2010) 215–229, <https://doi.org/10.1016/j.fluid.2010.04.019>.
- [28] H. Tanaka, H. Tong, R. Shi, J. Russo, Revealing key structural features hidden in liquids and glasses, *Nat. Rev. Phys.* 1 (2019) 333–348, <https://doi.org/10.1038/s42254-019-0053-3>.
- [29] L. Prokhorenkova, G. Gusev, A. Vorobev, A.V. Dorogush, A. Gulin, et al., *Adv. Neural Inform. Proces. Syst.* (2018) 6638–6648.
- [30] A.V. Dorogush, V. Ershov, A. Gulin, CatBoost: gradient boosting with categorical features support, arXiv (2018), preprint arXiv:1810.11363.
- [31] <https://catboost.ai/>.
- [32] J. Hancock, T.M. Khoshgoftaar, CatBoost for big data: an interdisciplinary review, *J. Big Data* 7 (2020) 94, <https://doi.org/10.1186/s40537-020-00369-8>.

- [33] M. Chorążewski, E.B. Postnikov, B. Jasiok, Y.V. Nedyalkov, J. Jacquemin, A fluctuation equation of state for prediction of high-pressure densities of ionic liquids, *Sci. Rep.* 7 (2017) 1–9, <https://doi.org/10.1038/s41598-017-06225-9>.
- [34] E. Zorebski, M. Musiał, M. Dzida, Relation between temperature–pressure dependence of internal pressure and intermolecular interactions in ionic liquids—comparison with molecular liquids, *J. Chem. Thermodyn.* 131 (2019) 347–359, <https://doi.org/10.1016/j.jct.2018.11.007>.
- [35] R. Gomes de Azevedo, J.M. Esperança, V. Najdanovic-Visak, Z.P. Visak, H.J. Guedes, M. Nunes da Ponte, L.P. Rebelo, Thermophysical and thermodynamic properties of 1-butyl-3-methylimidazolium tetrafluoroborate and 1-butyl-3-methylimidazolium hexafluorophosphate over an extended pressure range, *J. Chem. Eng. Data* 50 (3) (2005) 997–1008, <https://doi.org/10.1021/je049534w>.
- [36] E. Faramarzi, A. Maghari, Saft-vr modelling of the surface and bulk properties of imidazolium and pyridinium based ionic liquids with ten different anions, *J. Mol. Liq.* 224 (2016) 872–881.
- [37] K.R. Harris, M. Kanakubo, L.A. Woolf, Temperature and pressure dependence of the viscosity of the ionic liquids 1-hexyl-3-methylimidazolium hexafluorophosphate and 1-butyl-3-methylimidazolium bis (trifluoromethylsulfonyl) imide, *J. Chem. Eng. Data* 52 (3) (2007) 1080–1085.
- [38] F.M. Gaciño, T. Regueira, M.J. Comuñas, L. Lugo, J. Fernández, Density and isothermal compressibility for two trialkylimidazolium-based ionic liquids at temperatures from (278 to 398) K and up to 120 MPa, *J. Chem. Thermodyn.* 81 (2015) 124–130, <https://doi.org/10.1016/j.jct.2014.09.014>.
- [39] Z. Gu, J.F. Brennecke, Volume expansivities and isothermal compressibilities of imidazolium and pyridinium-based ionic liquids, *J. Chem. Eng. Data* 47 (2) (2002) 339–345, <https://doi.org/10.1021/je010242u>.
- [40] J. Jacquemin, P. Husson, V. Mayer, I. Cibulka, High-pressure volumetric properties of imidazolium-based ionic liquids: effect of the anion, *J. Chem. Eng. Data* 52 (6) (2007) 2204–2211, <https://doi.org/10.1021/je700224j>.
- [41] R.L. Gardas, M.G. Freire, P.J. Carvalho, I.M. Marrucho, I.M. Fonseca, A.G. Ferreira, J.A. Coutinho, P vs T measurements of imidazolium-based ionic liquids, *J. Chem. Eng. Data* 52 (5) (2007) 1881–1888, <https://doi.org/10.1021/je700205n>.
- [42] H. Guerrero, M. García-Mardones, P. Cea, C. Lafuente, I. Bandrés, Correlation of the volumetric behaviour of pyridinium-based ionic liquids with two different equations, *Thermochim. Acta* 531 (2012) 21–27, <https://doi.org/10.1016/j.tca.2011.12.020>.
- [43] H. Guerrero, S. Martín, V. Pérez-Gregorio, C. Lafuente, I. Bandrés, Volumetric characterization of pyridinium-based ionic liquids, *Fluid Phase Equilib.* 317 (2012) 102–109, <https://doi.org/10.1016/j.fluid.2011.12.029>.
- [44] M. Iguchi, Y. Hiraga, Y. Sato, T.M. Aida, M. Watanabe, R.L. Smith Jr., Measurement of high-pressure densities and atmospheric viscosities of ionic liquids: 1-hexyl-3-methylimidazolium bis (trifluoromethylsulfonyl) imide and 1-hexyl-3-methylimidazolium chloride, *J. Chem. Eng. Data* 59 (3) (2014) 709–717, <https://doi.org/10.1021/je4007844>.
- [45] H. Machida, R. Taguchi, Y. Sato, R.L. Smith Jr., Measurement and correlation of high pressure densities of ionic liquids, 1-ethyl-3-methylimidazolium 1-lactate ([emim][lactate]), 2-hydroxyethyl-trimethylammonium 1-lactate ([[(c2h4oh)(ch3)3n][lactate]]), and 1-butyl-3-methylimidazolium chloride ([bmim][cl]), *J. Chem. Eng. Data* 56 (4) (2010) 923–928, <https://doi.org/10.1021/je1008747>.
- [46] J. Jacquemin, P. Nancarrow, D.W. Rooney, M.F. Costa Gomes, P. Husson, V. Majer, A.A. Pádua, C. Hardacre, Prediction of ionic liquid properties. ii. volumetric properties as a function of temperature and pressure, *J. Chem. Eng. Data* 53 (9) (2008) 2133–2143, <https://doi.org/10.1021/je8002817>.
- [47] L.I. Tomé, P.J. Carvalho, M.G. Freire, I.M. Marrucho, I.M. Fonseca, A.G. Ferreira, J.A. Coutinho, R.L. Gardas, Measurements and correlation of high-pressure densities of imidazolium-based ionic liquids, *J. Chem. Eng. Data* 53 (8) (2008) 1914–1921, <https://doi.org/10.1021/je800316b>.
- [48] L.I. Tomé, R.L. Gardas, P.J. Carvalho, M.J. Pastoriza-Gallego, M.M. Pineiro, J.A. Coutinho, Measurements and correlation of high-pressure densities of phosphonium based ionic liquids, *J. Chem. Eng. Data* 56 (5) (2011) 2205–2217, <https://doi.org/10.1021/je101232g>.
- [49] R.L. Gardas, H.F. Costa, M.G. Freire, P.J. Carvalho, I.M. Marrucho, I.M. Fonseca, A.G. Ferreira, J.A. Coutinho, Densities and derived thermodynamic properties of imidazolium-, pyridinium-, pyrrolidinium-, and piperidinium-based ionic liquids, *J. Chem. Eng. Data* 53 (3) (2008) 805–811, <https://doi.org/10.1021/je700670k>.
- [50] C.A.N. de Castro, E. Langa, A.L. Morais, M.L.M. Lopes, M.J. Lourenço, F.J. Santos, M.S.C. Santos, J.N.C. Lopes, H.I. Veiga, M. Macatrão, et al., Studies on the density, heat capacity, surface tension and infinite dilution diffusion with the ionic liquids [c4mim][ntf2], [c4mim][dca], [c2mim][etos3] and [aliquat][dca], *Fluid Phase Equilib.* 294 (1–2) (2010) 157–179, <https://doi.org/10.1016/j.fluid.2010.03.010>.
- [51] J. Safarov, M. Geppert-Rybczyńska, I. Kul, E. Hassel, Thermophysical properties of 1-butyl-3-methylimidazolium acetate over a wide range of temperatures and pressures, *Fluid Phase Equilib.* 383 (2014) 144–155.
- [52] J. Safarov, A. Guluzade, E. Hassel, Thermophysical properties of 1-butyl-3-methylimidazolium trifluoromethanesulfonate in a wide range of temperatures and pressures, *J. Chem. Eng. Data* 64 (6) (2019) 2247–2258.
- [53] M.J. Dávila, S. Aparicio, R. Alcalde, B. García, J.M. Leal, On the properties of 1-butyl-3-methylimidazolium octylsulfate ionic liquid, *Green Chem.* 9 (3) (2007) 221–232, <https://doi.org/10.1039/B612177B>.
- [54] J.O. Valderrama, R.E. Rojas, Critical properties of ionic liquids, revisited *Ind. Eng. Chem. Res.* 48 (14, 2009) 6890–6900, <https://doi.org/10.1021/ie900250g>.
- [55] M. Królikowska, T. Hofman, Densities, isobaric expansivities and isothermal compressibilities of the thiocyanate-based ionic liquids at temperatures (298.15–338.15 K) and pressures up to 10 MPa, *Thermochim. Acta* 530 (2012) 1–6, <https://doi.org/10.1016/j.tca.2011.11.009>.
- [56] R.L. Gardas, M.G. Freire, P.J. Carvalho, I.M. Marrucho, I.M. Fonseca, A.G. Ferreira, J.A. Coutinho, High-pressure densities and derived thermodynamic properties of imidazolium-based ionic liquids, *J. Chem. Eng. Data* 52 (1) (2007) 80–88, <https://doi.org/10.1021/je060247x>.
- [57] J.C. McGowan, Variation of the isothermal compressibilities of liquids with temperature, *Nature* 210 (1966) 1255–1256, <https://doi.org/10.1038/2101255a0>.
- [58] F. Gonçalves, C. Costa, C. Ferreira, J. Bernardo, I. Johnson, I. Fonseca, A. Ferreira, Pressure–volume–temperature measurements of phosphonium-based ionic liquids and analysis with simple equations of state, *J. Chem. Thermodyn.* 43 (6) (2011) 914–929, <https://doi.org/10.1016/j.jct.2011.01.009>.
- [59] J. Jacquemin, R. Ge, P. Nancarrow, D.W. Rooney, M.F. Costa Gomes, A.A. Pádua, C. Hardacre, Prediction of ionic liquid properties. i. volumetric properties as a function of temperature at 0.1 MPa, *J. Chem. Eng. Data* 53 (3) (2008) 716–726, <https://doi.org/10.1021/je700707y>.
- [60] S. Ghahramani, F. Yousefi, S. Hosseini, S. Aparicio, High-pressure behavior of 2-hydroxyethylammonium acetate ionic liquid: experiment and molecular dynamics, *J. Supercrit. Fluids* 155 (2020) 104664, <https://doi.org/10.1016/j.supflu.2019.104664>.
- [61] A.P. Singh, R.L. Gardas, S. Senapati, How water manifests the structural regimes in ionic liquids, *Soft Matter* 13 (12, 2017) 2348–2361, <https://doi.org/10.1039/C6SM02539K>.
- [62] S. Stevanovic, A. Podgoršek, A.A. Pádua, M.F. Costa Gomes, Effect of water on the carbon dioxide absorption by 1-alkyl-3-methylimidazolium acetate ionic liquids, *J. Phys. Chem. B* 116 (49) (2012) 14416–14425, <https://doi.org/10.1021/jp3100377>.
- [63] Y. Hiraga, A. Kato, Y. Sato, R.L. Smith Jr., Densities at pressures up to 200 MPa and atmospheric pressure viscosities of ionic liquids 1-ethyl-3-methylimidazolium methylphosphate, 1-ethyl-3-methylimidazolium diethylphosphate, 1-butyl-3-methylimidazolium acetate, and 1-butyl-3-methylimidazolium bis (trifluoromethylsulfonyl) imide, *J. Chem. Eng. Data* 60 (3) (2015) 876–885, <https://doi.org/10.1021/je5009679>.
- [64] F.M. Gaciño, T. Regueira, A.V. Bolotov, A. Sharipov, L. Lugo, M.J. Comuñas, J. Fernández, Volumetric behaviour of six ionic liquids from $t=(278$ to $398)$ K and up to 120 MPa, *J. Chem. Thermodyn.* 93 (2016) 24–33, <https://doi.org/10.1016/j.jct.2015.09.013>.
- [65] R. Bounsiar, I. Gascón, F. Amireche, C. Lafuente, Volumetric properties of three pyridinium-based ionic liquids with a common cation or anion, *Fluid Phase Equilib.* 521 (2020) 112732, <https://doi.org/10.1016/j.fluid.2020.112732>.
- [66] O.G. Sas, G.R. Ivanšić, M.L. Kijevčanin, B. González, A. Domínguez, I.R. Radović, Densities and derived volumetric properties of ionic liquids with [mf2] and [ntf2] anions at high pressures, *J. Chem. Eng. Data* 63 (4) (2018) 954–964, <https://doi.org/10.1021/acs.jced.7b00771>.
- [67] J.A. Sarabando, P.J. Magano, A.G. Ferreira, J.B. Santos, P.J. Carvalho, S. Mattedi, I.M. Fonseca, M. Santos, Influence of temperature and pressure on the density and speed of sound of n-ethyl-2-hydroxyethylammonium propionate ionic liquid, *J. Chem. Thermodyn.* 131 (2019) 303–313, <https://doi.org/10.1016/j.jct.2018.11.005>.
- [68] N. Farzi, F. Fateminasab, Average intermolecular interaction in ionic liquids and a new equation of state, *J. Mol. Liq.* 227 (2017) 268–279, <https://doi.org/10.1016/j.molliq.2016.11.091>.
- [69] D. Tomida, S. Kenmochi, K. Qiao, T. Tsukada, C. Yokoyama, Densities and thermal conductivities of n-alkylpyridinium tetrafluoroborates at high pressure, *Fluid Phase Equilib.* 340 (2013) 31–36, <https://doi.org/10.1016/j.fluid.2012.12.008>.
- [70] J. Pandey, A. Shukla, N. Singh, V. Sanguri, Estimation of thermodynamic properties of ionic liquids, *J. Mol. Liq.* 315 (2020) 113585, <https://doi.org/10.1016/j.molliq.2020.113585>.
- [71] C.E. Ferreira, N.M. Talavera-Prieto, I.M. Fonseca, A.T. Portugal, A.G. Ferreira, Measurements of pvt, viscosity, and surface tension of trihexyltetradecylphosphonium tris (pentafluoroethyl) trifluorophosphate ionic liquid and modelling with equations of state, *J. Chem. Thermodyn.* 47 (2012) 183–196, <https://doi.org/10.1016/j.jct.2011.10.012>.
- [72] J. Safarov, K. Suleymanli, A. Aliyev, D.J. Yeadon, J. Jacquemin, M. Bashirov, E. Hassel, (p , ρ , T) data of 1-butyl-3-methylimidazolium hexafluorophosphate, *J. Chem. Thermodyn.* 141 (2020) 105954, <https://doi.org/10.1016/j.jct.2019.105954>.
- [73] P. Navarro, A.M. Palma, J. García, F. Rodríguez, J.A. Coutinho, P.J. Carvalho, High pressure density of tricyanomethanide-based ionic liquids: experimental and pc-saft modelling, *Fluid Phase Equilib.* 520 (2020) 112652, <https://doi.org/10.1016/j.fluid.2020.112652>.
- [74] A. Eucken, Eine halbempirische Zustandsgleichung für Flüssigkeiten, *Forsch. Gebiet Ingenieurwesens* A 12 (1941) 113–116, <https://doi.org/10.1007/BF02584929>.
- [75] K.A. Putilov, Equations of state of gases and liquids. Thermodynamics of the simplest liquids, *Heat Transf. Sov. Res.* 6 (1974) 133–143.
- [76] J. Safarov, K. Suleymanli, A. Aliyev, D.J. Yeadon, J. Jacquemin, M. Bashirov, E. Hassel, (p , ρ , T) data of 1-butyl-3-methylimidazolium hexafluorophosphate, *J. Chem. Thermodyn.* 141 (2020) 105954, <https://doi.org/10.1016/j.jct.2019.105954>.

Katowice, 11.04.2023 r.

Instytut Chemii
Wydział Nauk Ścisłych i Technicznych
Uniwersytet Śląski w Katowicach
ul. Bankowa 12, 40-007 Katowice

Statement on the contribution to the publication

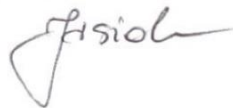
Publication:

E.B. Postnikov, B. Jasiok, M. Chorążewski, The CatBoost as a tool to predict the isothermal compressibility of ionic liquids. *Journal of Molecular Liquids* **2021**,333, 115889, DOI: 10.1016/j.molliq.2021.115889.

We hereby state that the contribution to the work published jointly with Bernadeta Jasiok is in accordance with the description below:

Bernadeta Jasiok

I was responsible for: Formal analysis, Investigation, Data curation, Writing – Original Draft, Writing – Review & Editing, Visualization



Eugene B. Postnikov

I was responsible for: Conceptualization, Methodology, Software, Validation, Formal analysis, Writing – Original Draft, Writing – Review & Editing, Supervision, Project administration



Mirosław Chorążewski

I was responsible for: Conceptualization, Writing – Original Draft, Writing – Review & Editing, Supervision, Funding acquisition





Prediction of high pressure properties of complex mixtures without knowledge of their composition as a problem of thermodynamic linear analysis

Eugene B. Postnikov^{a,*}, Bernadeta Jasiok^b, Vyacheslav V. Melent'ev^c, Olga S. Ryshkova^c, Vadim I. Korotkovskii^c, Anton K. Radchenko^c, Alexander R. Lowe^d, Mirosław Chorążewski^{d,*}

^a Theoretical Physics Department, Kursk State University, Radishcheva st., 33, Kursk 305000, Russia

^b Institute of Chemistry, Department of Physical Chemistry, University of Silesia in Katowice, Szkolna 9, 40-006 Katowice, Poland

^c Laboratory of Molecular Acoustics, Kursk State University, Radishcheva st., 33, Kursk 305000, Russia

^d Institute of Chemistry, Department of Physical Chemistry, University of Silesia in Katowice, Szkolna 9, 40-006 Katowice, Poland

ARTICLE INFO

Article history:

Received 5 January 2020

Received in revised form 26 March 2020

Accepted 28 March 2020

Available online 03 May 2020

Keywords:

Speed of sound

Density

High pressures

Fluctuations

ISO 4113 standard

Diesel injector

ABSTRACT

We propose a mathematical framework, which argues the possibility to predict thermodynamic properties of molecular liquids and their mixtures at elevated pressures using their properties measured at ambient conditions only by considering such procedure as a modified analogue to the linear analysis procedure known from the theory of dynamical system when time is replaced by one of PVT quantities. This approach reveals reasons, why so-called isothermal Fluctuation Theory-based Equation of State has universal effectiveness for different classes of liquid. Further, we generalize this line of reasoning on the case of the speed of sound and other thermodynamic quantities, which can be derived from such data via the acoustic route. This approach is illustrated among others by example of SRS diesel calibrating liquid, for which new original set of experimental data for a wide range of temperatures and pressures is reported.

© 2018 Elsevier B.V. All rights reserved.

1. Introduction

Despite the impressive modern progress in the development of methods for predicting thermodynamic properties of liquids at high pressures [1–5], there is still a high demand for the development of unified approaches to provide quantitative predictions with accuracy comparable to the direct experimental measurement. The intricacy of this problem is based on the extremely complex interplay between intermolecular interactions and disordered structure of molecular liquids. The task is even more problematical for the case of multicomponent liquid mixtures and predicting their thermodynamic properties. This requires taking into account both the volumetric and thermal properties, which also depend on intramolecular interactions and their combinations.

A typical example of these properties is the speed of sound, which is one of the most important quantities, which provides a bridge between molecular physics and thermodynamics. In addition, it provides not only a practical possibility for relatively simple non-invasive measuring in high-pressurized systems but also for calculating the full variety of thermodynamic quantities, which completely characterize the state of fluid under high pressures when the thermodynamic parameters under saturation conditions are known [6–9].

The most popular methods for the computational prediction of the speed of sound belong to different variants of the Perturbed-Chain Statistical Associating Fluid Theory (SAFT). This includes corrections of the original model, which include the usage of the critical constants and the liquid density at the triple point (CP-PC-SAFT) [10], or even the saturated speed of sound itself [11] as reference states for the optimization of PC-SAFT's parameters, introducing a volume shift (VS-PC-SAFT) [12], merging SAFT approach with a cubic equation of state that showed predictive success in the case of heavy hydrocarbons and their mixtures [13]. However, it should be pointed out that the complexity of

* Corresponding authors.

E-mail addresses: postnicov@gmail.com, postnikov@kursksu.ru (E.B. Postnikov), miroslaw.chorazewski@us.edu.pl (M. Chorążewski).

computational procedures and parameters determination increase drastically with the growth of number of components in a liquid mixture.

In general, the approaches built “from bottom to up”, i.e. starting from microscopic level of description and oriented toward to finding desired thermodynamic properties, see [14] for review, require a detailed knowledge of a variety of parameters characterizing individual atomic and/or molecular components and empiric structural models.

Here, we propose to address the problem of predicting the single-phase thermodynamic properties of molecular liquids purely from the macroscopic direction by taking into account the mathematical analogy of thermodynamics equalities expressed as relations between partial derivatives of PVT parameters and the theory of dynamical systems where the time variable is replaced by the change in either temperature or pressure. Note that this idea has some common features with the consideration of the thermodynamic PVT surface from the point of view of a Riemannian geometric model [15], where the thermodynamic derivatives determine the curvature of the PVT surface and, respectively can be interrelated with the characteristics of intermolecular interactions and macroscopic thermodynamic measurements. This approach recently attracts new attention as providing valuable insights also into the proper choice and calibration of potential functions for SAFT-based calculations [16].

It should be noted out that the mentioned geometrical consideration is tightly connected with the behaviour of thermodynamic fluctuations in liquid systems [17]. At the same time, it has been revealed that the dependence of the reduced density fluctuations on the density along the coexistence curve and in the single phase region is the same in a certain range that provide an opportunity for predicting the density under elevated pressures using the thermodynamic quantities [18]. The respective Fluctuation Theory-based Equation of State (FT-EoS) was already demonstrated as a high-accurate too by examples of a wide variety of liquids, from simple ones to polar and ionic substances [19,20] as well as multicomponent liquid mixtures [21,22]. Recently it has been shown that the functional form of the FT-EoS also follows from an assumption of a specific form of liquid's elasticity [23] that also gives some hints for further investigations of these issues from the points of view of dynamical systems theory.

Thus, the first of the goals of this work is to consider the theoretical background and assumptions, which assure the revealed universality of the FT-EoS and its limits of applicability. The next goal is to generalize this approach for the rest of thermodynamic quantities within a two-stage procedure, which consists of predicting the speed of sound along isotherms and then calculating the isobaric heat capacity, the isobaric expansion coefficient within the acoustic route to calculation of the density [24].

As the main illustrating example, we decided to model the thermodynamic properties of SRS diesel calibrating fluid based on newly measured experimental data. This choice is motivated by several reasons. First of all, from the point of view of physics and physical chemistry of molecular liquids, this substance is a complex multicomponent mixture of hydrocarbons. In addition, the exact composition of this fluid is not known and protected by the supplying company. Therefore, one principally can not apply any method, which requires information on molecular components, contributing groups and even reference point like critical conditions (for example, no one from methods described in [25,26]). Thus, the question of whether it is possible to accurately predict thermodynamic properties of such a fluid under the experimental condition with restricted information is a stimulating challenge.

It should be pointed out that accurate thermophysical data for calibration fluids, with the exception of those presented by Lowe [24], Ndiaye [27], and Chorążewski [28], are lacking in the scientific and engineering data bases. Typically, the ISO-4113 standards for calibration fluids present a specific datum of a property for the liquid at a specific temperature. As well these properties are generally measured at below operating conditions of fuel injection for diesel engines which

can compress fuel to its combustions temperature at pressures up to 300 MPa [29,30]. Accurate modelling of the thermophysical properties of calibration fluids can be used to support fuel injection modelling and combustion properties which can help with the design and development of improved engines which are more efficient [31,32]. However, the techniques and equipment required measure the properties accurately are rare, time consuming and can be hazardous. Thus is necessary to overcome these difficulties by developing predictive thermodynamic calculations for SRS and similar industrial fluids.

2. A case study: of SRS calibration fluid CV, experimental data and their primary processing

2.1. Materials and methods

SRS Calibration Fluid CV for diesel injectors was supplied by Hansen & Rosenthal Group (<https://www.hur.com>). The sample was tested and approved by the Technical and Laboratory Department of H&R Group company. The exact composition of the fluid is the propriety of the company and the general composition is provided in their Material Safety Data Sheet, (MSDS) and is provided with the following the identifiers in Table 1.

The measurements were evaluated at the Laboratory of Molecular Acoustics (Kursk State University) using exactly the same equipment and measurement protocols, whose description were published recently in [24]. For this reason, we refer for their details to the mentioned work and give here the basic information on the experimental procedure only.

The density at ambient pressure was measured photometrically for the sample thermostated with a refrigerated thermostat (Kriovist, Termex Russia) for the temperature range below 323.15 K and with the thermostat VIS-T (Termex Russia) for higher temperatures. The specific isobaric heat capacity was measured at ambient pressure conditions using the differential scanning calorimeter assembled on the base of an industrial IT-CP-400 Calorimeter (Russia) and the computer-regulated digital signal processing board by “Tercon” (Russia). The ultrasonic speed of sound was measured by a pulse phase echo method using the patented setup [33] assembled on a base of the the universal digital signal processing board DSP-310-K and the MP-2500 (Russia) dead-weight pressure gauge.

The obtained raw experimental data supplied with their uncertainties are presented in Tables 2, 4.

2.2. Experimental data processing

The experimental values obtained at ambient pressure and represented in Table 2 and in the first row of Table 4 are fitted for the further

Table 1
Composition of SRS Calibration Fluid CV and information on its ingredients according to the safety data sheet.

Identifier numbers	Materials	Quantity
CAS No 1174522-18-19 EC No 920-360-0 REACH No 01-2119448343-41	Hydrocarbons, C14-C18, n-alkanes, isoalkanes, cyclics, aromatics (2–30 w _t %)	85–<90 w _t %
CAS No 64742-46-7 EC No 265-148-2 REACH No 01-2119489867-12	Distillates (petroleum), hydrotreated middle, Gasoil – unspecified	5–<10 w _t %
CAS No 68425-15-0 EC No 270-335-7	Polysulfides, di-tert-dodecyl	1–<5 w _t %

Table 2

The density measured pycnometrically and the isobaric heat capacity at ambient conditions.

T (K) ^a	ρ (kg·m ⁻³) ^b	T (K) ^c	C_p (J·(kg·K) ⁻¹) ^d
287.00	825.2	313.15	2310.1
292.00	821.9	323.15	2366.6
302.00	815.1	333.15	2401.1
323.35	800.5	343.15	2445.4
343.45	786.9	353.15	2496.1
363.35	773.1	363.15	2538.7
383.45	758.9		
403.65	744.7		
423.75	730.2		

^aThe standard uncertainty $u(T) = 0.1$ K; ^bthe standard uncertainty $u(\rho) = 0.1$ kg; ^cThe standard uncertainty $u(T) = 0.5$ K; ^dthe relative standard uncertainty $u_r(C_p) = 0.02$.

use as reference explicit functions of temperature

$$\rho_0(T) = -0.468 \left(\frac{T-346.89}{49.896} \right)^2 - 34.485 \left(\frac{T-346.89}{49.896} \right) + 784.46, \quad (1)$$

$$C_p^0(T) = 84 \left(\frac{T-338.15}{18.71} \right) + 2426, \quad (2)$$

$$c_0(T) = -106.36 \left(\frac{T-338.15}{18.71} \right) + 1212.4, \quad (3)$$

where dimensions of the coefficients correspond to the temperature in K, the density – in kg·m⁻³, the isobaric heat capacity – in J·(kg·K)⁻¹, and the speed of sound – in m·s⁻¹. The fitting procedure was evaluated by MATLAB's routines polyfit supplied the Monte Carlo method of uncertainty quantification: each experimental value was 10⁴ times replicated to form a Gaussian ensemble with each mean and the standard deviation corresponded to the experimental point with the respective standard deviation. The uncertainty characteristics for all coefficients obtained via this procedure are given in Table 3. Fig. 1 illustrates the obtained fitting lines; one can see that they reproduce the course of the points obtained experimentally. The average absolute relative deviations (AAD) are equal to $AAD_\rho = 0.0061\%$, $AAD_{C_p} = 0.13\%$, and $AAD_{c_0} = 0.10\%$ for the density, the isobaric heat capacity and the speed of sound at ambient pressure conditions, respectively.

This set of data provides an opportunity to calculate the isothermal compressibility at ambient pressure conditions as

$$\kappa_T^0 = \frac{1}{\rho_0} \left(\frac{1}{c_0^2} + \frac{T\alpha_{p_0}^2}{C_p^0} \right), \quad (4)$$

where $\alpha_{p_0}(T) = \rho_0^{-1}(\partial\rho_0/\partial T)_{P_0}$ is the isobaric expansion coefficient at $P = P_0$.

The speed of sound under elevated pressure was fitted along each isotherm was represented as the polynomial, which gives an explicit dependence of the speed of sound cubed as a function of the excess pressure applied

$$c(P)^3 = c(P_0)^3 + Y_1(P-P_0) + Y_2(P-P_0)^2, \quad (5)$$

where $c(P_0) = c_0$ is given by Eq. (3) and the values of the coefficients

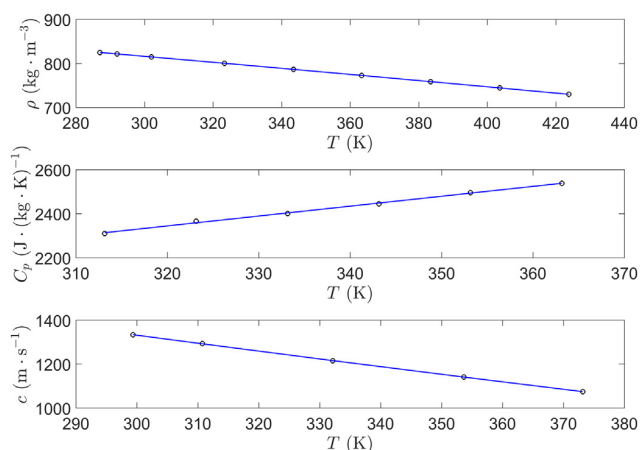


Fig. 1. Thermodynamic quantities of SRS Calibration Fluid CV measured at ambient pressure conditions (circles) and their fitting via Eqs. (1)–(3) shown as lines.

$Y_{1,2}$ and their uncertainties obtained via the Monte Carlo Gaussian ensemble method as described above for the data fitting at ambient pressure conditions are presented in Table 5.

Fig. 2 shows that the cube of the speed of sound depends on the excess pressure practically linearly within the considered pressure range but we prefer to keep the small quadratic term in Eq. (5) too since it assures the fitting with uncertainty comparable with the experimental one; AADs for all isotherm are presented in the last column of Table 5.

To calculate the density and other quantities along these isotherms, the sequential integration of thermodynamic identities

$$\left(\frac{\partial C_p}{\partial P} \right)_T = -\frac{T}{\rho} \left[\alpha_p^2 + \left(\frac{\partial \alpha_p}{\partial T} \right)_p \right], \quad (6)$$

$$\left(\frac{\partial \rho}{\partial P} \right)_T = \left[\frac{T\alpha_p^2}{C_p} - \frac{1}{c^2} \right] \quad (7)$$

By Heun's method was used with the initial values given by functions (1)–(3) and the speed of sound along isotherms given by cubic roots of the functions (5) calculated for all isotherms. The detailed description of the numerical procedure can be found in [24].

The Tables 6–9 report the obtained temperature-pressure dependences for the density, the isobaric heat capacity, the isobaric expansion coefficient, and the isothermal compressibility. Markers in Fig. 3 indicate the obtained values of the density as a function of the pressure.

2.3. Predicting density by the FT-EoS

Following the procedure described in [20], we test accuracy of the density prediction under elevated pressures using the FT-EoS

$$\rho = \rho_0 + k^{-1} \log [k\rho_0\kappa_T^0(P-P_0) + 1], \quad (8)$$

where ρ_0 and κ_T^0 are the density and the isothermal compressibility at

Table 3

Standard deviations of coefficients of Eqs. (1)–(3) for the fitting functions represented in the general form $y(T) = \sum_{n=0}^2 Y_n \left(\frac{T-\bar{T}}{\sigma} \right)^n$.

y	STD(Y_2)	STD(Y_1)	STD(Y_0)	STD(\bar{T})	STD(σ)
ρ	0.060	0.037	0.062	0.033	0.035
C_p		21	20	0.02	0.02
c		0.65	0.58	0.02	0.02

Table 4
The experimental speed of sound values.

T (K) ^a	299.35	310.75	332.15	353.65	373.15
P (MPa) ^b	c (m·s ⁻¹) ^c				
0.1	1334.1	1294.4	1216.1	1141.7	1075.6
9.8	1390.7	1352.9	1278.8	1207.8	1150.2
19.6	1436.8	1402.4	1331.3	1263.3	1207.5
29.4	1482.1	1448.5	1379.4	1314.1	1261.9
39.2	1522.9	1488.3	1425.2	1362.1	1311.7
49.0	1560.7	1529.5	1468.2	1406.5	1357.0
58.8	1600.9	1566.1	1508.9	1448.4	1401.1
68.6	1635.8	1606.6	1547.8	1488.3	1442.6
78.5	1669.9	1638.5	1585.3	1527.7	1483.0
88.3	1702.1	1670.5	1620.2	1563.6	1518.8
98.1	1734.9	1702.1	1653.0	1597.4	
107.9	1762.7	1735.5	1686.1	1630.2	
117.7	1796.0	1766.5	1713.9	1662.4	
127.5	1820.1	1792.8	1745.4	1695.9	
137.3	1846.8	1819.3	1774.8	1722.5	
147.1	1876.0	1844.5	1803.0	1751.4	
156.9	1902.1	1871.1	1828.9	1778.3	
166.7	1929.0	1894.9		1806.7	
176.5	1952.1	1917.2		1832.2	
186.3	1975.7	1943.7		1856.9	
196.1	1994.5	1966.3		1880.7	

^aThe standard uncertainty $u(T) = 0.1$ K; ^bthe standard uncertainty $u(P) = 0.0125$ MPa; ^cthe standard uncertainty $u(c) = 1.3$ m·s⁻¹.

ambient pressure P_0 defined by Eqs. (1)–(4), and

$$k = -\frac{d \log(T\rho_0 k_T^0)}{d\rho_0} \quad (9)$$

which can be easily calculated via the parametric differentiation for the given thermodynamic quantities stated as functions of the temperature, see [21].

The resulted predictions are shown as solid lines in Fig. 3 for all isotherms. The overall high accuracy of prediction is confirmed by AAD = 0.08% for the whole set of data. Visually, one can note small deviations between experimental and predicted data growing at highest available pressures. However, even in the vicinity of 200 MPa, the maximal relative deviation does not exceed 0.29% that about of the experimental uncertainty range.

Thus, FT-EoS can be successfully used for predictive calculation of the density of this fluid with unknown composition basing on the easily obtainable thermodynamic data at ambient pressure only, and our next step is to reveal general theoretical background for this possibility and generalize it on the case of predicting other thermodynamic parameters, especially, the speed of sound.

Table 5

Coefficients of the polynomial fitting the speed of sound cubed, Eq. (5), their standard deviations, and the average absolute relative deviations fitted and experimental values along isotherms explored. The dimensionality of the pressure and the speed of sound for this set of coefficients are MPa and m·c⁻³, respectively.

T, (K)	Y ₂ ·10 ⁻²	Y ₁ ·10 ⁻⁴	STD(Y ₂)·10 ⁻²	STD(Y ₁)·10 ⁻⁴	AAD(%)
299.35	-56.7	2962.9	6.5	9.5	0.10
310.75	-81.0	2924.5	6.3	9.2	0.11
332.15	-28.0	2793.1	9.5	11.2	0.06
353.65	-5.6	2647.6	5.6	8.2	0.06
373.15	-83.0	2636.8	27.3	18.8	0.14

Table 6

Liquid densities calculated by the acoustic method; the combined relative uncertainties are calculated to be $u_{r,c}(\rho) = 0.005$.

T (K)	299.35	310.75	332.15	353.65	373.15
P (MPa)	ρ (kg·m ⁻³)				
0.1	816.9	809.2	794.6	779.8	766.2
10	823.1	815.8	801.9	788.0	775.3
20	828.9	821.9	808.6	795.4	783.5
30	834.3	827.5	814.8	802.3	790.9
40	839.4	832.8	820.6	808.5	797.6
50	844.2	837.8	826.0	814.4	803.9
60	848.8	842.5	831.1	819.8	809.7
70	853.1	847.0	835.9	825.0	815.2
80	857.2	851.3	840.4	829.9	820.3
90	861.2	855.4	844.8	834.5	825.2
100	865.0	859.4	848.9	838.9	829.9
110	868.7	863.2	852.9	843.2	834.3
120	872.2	866.8	856.8	847.2	838.6
130	875.7	870.3	860.5	851.1	842.7
140	879.0	873.8	864.0	854.9	846.6
150	882.2	877.1	867.5	858.5	850.4
160	885.4	880.3	870.9	862.0	854.1
170	888.4	883.4	874.1	865.4	857.7
180	891.4	886.5	877.3	868.7	861.1
190	894.3	889.5	880.3	871.9	864.5
200	897.1	892.4	883.3	875.0	867.8

3. An analogy between thermodynamical equalities derivation and the linear analysis of dynamical systems

3.1. Linearisation for the density prediction

Let us start from the empiric observations on the experimental density behaviour of liquids under moderate elevated pressures along an isotherm. In fact, one can conclude that the cubic fitting the excess pressure as a cubic function of the excess density

$$P - P_0 = \delta_1(\rho - \rho_0) + \frac{\delta_2}{2}(\rho - \rho_0)^2 + \frac{\delta_3}{6}(\rho - \rho_0)^3 \quad (10)$$

is quite accurate to represent experimental data.

Fig. 4 gives an example of such fitting for one isotherm of n-heptane. One can see that deviations between the regression curve and raw data

Table 7

Liquid isobaric heat capacities calculated by the acoustic method; the combined relative standard uncertainties are calculated to be $u_{r,c}(C_p) = 0.02$.

T (K)	299.35	310.75	332.15	353.65	373.15
P (MPa)	C _p (J·(kg·K) ⁻¹)				
0	2252	2303	2399	2496	2584
10	2246	2297	2392	2488	2575
20	2242	2292	2387	2483	2569
30	2239	2289	2384	2479	2565
40	2236	2287	2381	2476	2562
50	2235	2285	2379	2474	2560
60	2233	2283	2378	2472	2558
70	2232	2283	2377	2471	2557
80	2232	2282	2376	2471	2556
90	2232	2282	2376	2470	2556
100	2232	2282	2376	2471	2556
110	2232	2282	2376	2471	2557
120	2232	2283	2377	2472	2557
130	2233	2283	2378	2473	2559
140	2234	2284	2379	2474	2560
150	2235	2286	2380	2476	2562
160	2237	2287	2382	2477	2564
170	2238	2289	2384	2479	2566
180	2240	2291	2386	2482	2569
190	2242	2293	2389	2485	2572
200	2245	2296	2391	2488	2575

Table 8
Liquid isobaric expansion coefficients calculated by the acoustic method; the combined relative standard uncertainties are calculated to be $u_{r,c}(\alpha_p) = 0.01$.

T (K)	299.35	310.75	332.15	353.65	373.15
P (MPa)	$\alpha_p \cdot 10^4 \text{ (T}^{-1}\text{)}$				
0	8.24	8.37	8.63	8.90	9.15
10	7.83	7.91	8.07	8.23	8.39
20	7.47	7.52	7.61	7.71	7.80
30	7.15	7.18	7.23	7.28	7.33
40	6.88	6.89	6.91	6.93	6.95
50	6.63	6.63	6.63	6.62	6.62
60	6.42	6.41	6.38	6.36	6.33
70	6.22	6.20	6.16	6.12	6.08
80	6.05	6.02	5.97	5.91	5.86
90	5.89	5.86	5.79	5.72	5.66
100	5.75	5.71	5.63	5.55	5.47
110	5.62	5.57	5.48	5.39	5.30
120	5.50	5.45	5.35	5.24	5.14
130	5.39	5.33	5.22	5.10	4.99
140	5.29	5.23	5.11	4.98	4.86
150	5.20	5.13	5.00	4.86	4.72
160	5.12	5.04	4.90	4.74	4.60
170	5.05	4.96	4.80	4.64	4.48
180	4.98	4.89	4.72	4.54	4.37
190	4.92	4.82	4.64	4.44	4.26
200	4.87	4.76	4.56	4.35	4.15

is quite small and symmetrically distributed around zero, i.e. there is no a regular trend.

Why it is better to use the fit P vs. ρ but not in and inverse order and it is measured in reality? Note that namely such curve is not only grows monotonically ($\rho(P)$ is growing too) but it is concave downward, i.e. the slope of the tangent to the curve $\rho(P)$ is always positive and growing and such curve goes to infinity without any principal mathematical of physical restrictions. On contrary, the growth speed of the curve $\rho(P)$ is permanently diminishing due to decaying compressibility of liquids with the growing applied pressure that may induce some complications from the point of view of the polynomial fitting since, in the latter case, the finite polynomial will necessary have a maximum after which the fitted density curve will go down that is a physical nonsense. The form (10) is free of such trouble.

Table 9
Liquid isothermal compressibilities calculated by the acoustic method; the combined relative standard uncertainties are calculated to be $u_{r,c}(k_T) = 0.01$.

T (K)	299.35	310.75	332.15	353.65	373.15
P (MPa)	$\alpha_p \cdot 10^{10} \text{ (T}^{-1}\text{)}$				
0	8.24	8.37	8.63	8.90	9.15
10	7.83	7.91	8.07	8.23	8.39
20	7.47	7.52	7.61	7.71	7.80
30	7.15	7.18	7.23	7.28	7.33
40	6.88	6.89	6.91	6.93	6.95
50	6.63	6.63	6.63	6.62	6.62
60	6.42	6.41	6.38	6.36	6.33
70	6.22	6.20	6.16	6.12	6.08
80	6.05	6.02	5.97	5.91	5.86
90	5.89	5.86	5.79	5.72	5.66
100	5.75	5.71	5.63	5.55	5.47
110	5.62	5.57	5.48	5.39	5.30
120	5.50	5.45	5.35	5.24	5.14
130	5.39	5.33	5.22	5.10	4.99
140	5.29	5.23	5.11	4.98	4.86
150	5.20	5.13	5.00	4.86	4.72
160	5.12	5.04	4.90	4.74	4.60
170	5.05	4.96	4.80	4.64	4.48
180	4.98	4.89	4.72	4.54	4.37
190	4.92	4.82	4.64	4.44	4.26
200	4.87	4.76	4.56	4.35	4.15

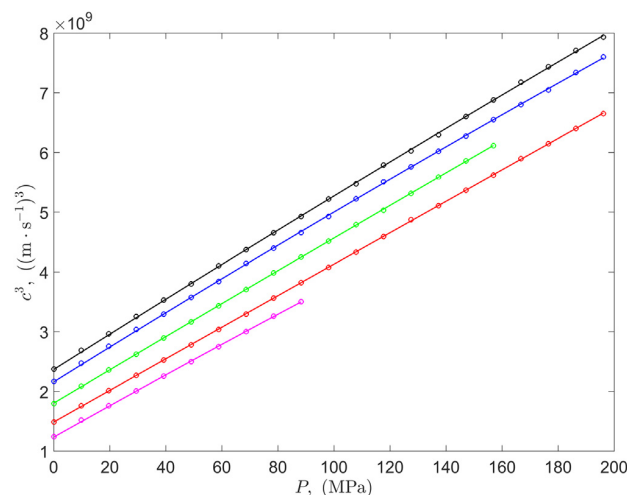


Fig. 2. Experimental speed of sound cubed (markers) for temperatures listed in Table 4 and their fits by Eq. (5) (solid lines). The series of lines from up to down corresponds to sequentially growing temperatures.

Note also that line of reasoning corresponds also to the approach to the speed of sound fitting proposed by Sun et al. [34] as

$$P - P_0 = A_1(T)(c - c_0) + A_2(T)(c - c_0)^2 + A_3(T)(c - c_0)^3, \quad (11)$$

where $a_i(T)$ as some appropriate quadratic polynomials with respect to the temperature. However, in the contexts of the density calculations via Eqs. (6)–(7), this kind of fitting is less convenient because it provides an implicit representation for the speed of sound, i.e. one needs to solve the cubic Eq. (11) for each value of the pressure (and make a proper choice of one of its three roots) to get the speed of sound substituted into Eq. (7) for integration. On contrary, Eq. (5) provides the explicit function of the pressure that simplifies integration. At the same time, from the point of the fitting accuracy, both approaches results practically in the same uncertainty for the full set of the data: AAD = 0.09% for Eq. (5) and AAD = 0.08% for Eq. (11), respectively. Their difference is negligible taking into account the experimental data uncertainty.

Moreover, Eq. (10) can be considered simply as a truncated Taylor series expansion of an arbitrary function $P(\rho)$ around the point (ρ_0, P_0) that is always true irrespectively to any particular form of a physical equation of state. Note that such functional form of Taylor series with respect to the excess (over the saturation) terms is used recently by

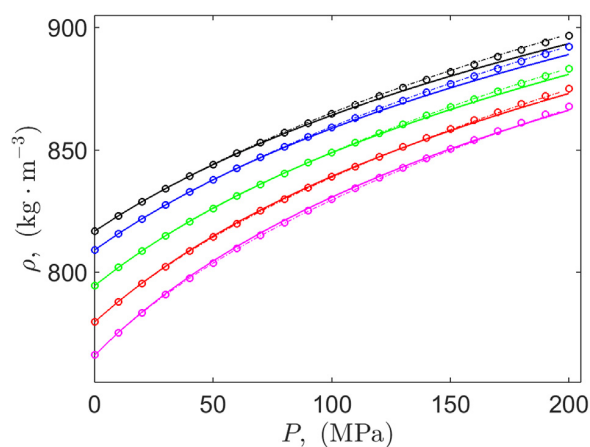


Fig. 3. Experiment-based data (circles) for the density and the respective density curves predicted by FT-EoS along isotherms (solid lines) and calculated from the predicted speed of sound (dash-dotted lines).

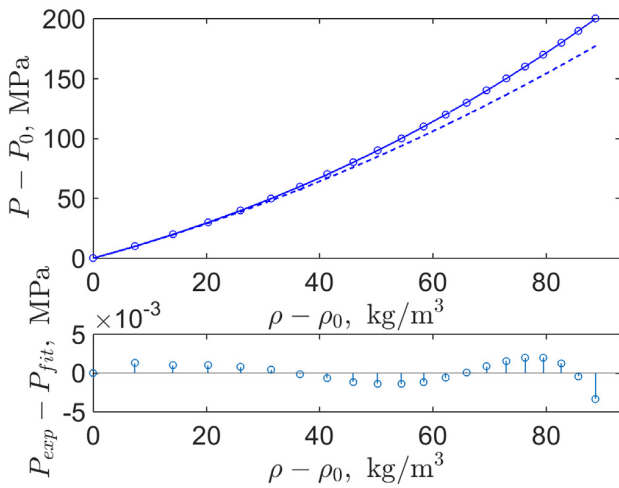


Fig. 4. The experimental data on the excess density (circles) of SRS along the isotherm $T = 332.15$ K and its fitting by the cubic polynomial (solid line) according Eq. (10). The bottom panel demonstrates absolute deviations between experimental data and values fitted by the cubic polynomial. The additional dashed line in the upper panel corresponds to the quadratic polynomial obtained if to put $\delta_3 = 0$ in Eq. (10).

NIST to fit the data; the only difference is a in keeping all term up to the fourth order, see [35]. Thus, it is better motivated from a general mathematical point of view than an empirical choice of selected power indices.

Respectively, the isothermal derivative of the functional expansion given by Eq. (10) is equal to

$$\left(\frac{\partial P}{\partial \rho}\right)_T = \delta_1 + \delta_2(\rho - \rho_0) + \frac{\delta_3}{2}(\rho - \rho_0)^2. \quad (12)$$

But now let us remain that the actual independent variable is the pressure, therefore, we primarily need to consider the partial derivative (directly connected with the isothermal compressibility, which is the response function to the change of conditions by the physical definition of the latter) as a function of the influencing variable, i.e. as a function of the excess pressure.

This can be achieved as follows: since we have not only Eq. (12) but Eq. (10) also, it is possible to express the linear part of the excess density from Eq. (10)

$$(\rho - \rho_0) = \delta_1^{-1} \left[(P - P_0) - \frac{\delta_2}{2}(\rho - \rho_0)^2 - \frac{\delta_3}{6}(\rho - \rho_0)^3 \right] \quad (13)$$

and to substitute it to Eq. (12) that gives

$$\left(\frac{\partial P}{\partial \rho}\right)_T = \delta_1 + \delta_2 \delta_1^{-1} (P - P_0) - \frac{\delta_1^{-1} \rho_0^2}{2} \left(\frac{P}{\rho_0} - 1\right)^2 \left[\delta_2^2 - \delta_3 \delta_1 + \frac{\delta_2 \delta_3}{3} \right] \quad (14)$$

Taking into account that the isothermal compressibility on the saturation curve is equal to $\kappa_T^0 = \rho_0^{-1} (\partial \rho / \partial P)_T|_{P=P_0} = \delta_1^{-1} \rho_0^{-1}$ and denoting $\delta_2 \delta_1^{-1} = \delta_2 \rho_0 \kappa_T^0 = k$, Eq. (14) can be rewritten in a dimensionless form as

$$\rho_0 \kappa_T^0 \left(\frac{\partial P}{\partial \rho}\right)_T = 1 + k \rho_0 \kappa_T^0 (P - P_0) - \frac{(k \rho_0)^2}{2} \left(\frac{P}{\rho_0} - 1\right)^2 \left[1 - \delta_3 \frac{\rho_0 \kappa_T^0}{(k \rho_0)^2} \left\{ 1 - \frac{k \rho_0}{3} \left(\frac{P}{\rho_0} - 1\right) \right\} \right]. \quad (15)$$

Now let us address Eq. (15) using the standard methods of the dynamic systems theory considering the density instead of time. First of all, we can estimate orders of the subsequent terms. Liquids are sufficiently low-compressible, their isothermal compressibility has an

order of 10^{-9} Pa^{-1} . Being combined with the order of saturated densities of $10^3 \text{ kg} \cdot \text{m}^{-3}$ and typical orders of the coefficient k of $10^{-2} \text{ m}^3 \cdot \text{kg}^{-3}$ (this follows from its meaning as the speed of change of the logarithm of the inverse reduced density fluctuations with the change of the density, as it will be shown below in details), the coefficient $k \rho_0 \kappa_T^0$ has an order of 10^{-8} Pa^{-1} , i.e. the second term is less ten one up to tenths Megapascals. Respectively, the coefficient of the third term $(k \rho_0)^2 / 2$ has an order of 10. At the same time, the typical compressions of liquids do not exceed several percents even at extra large pressures applied. This means that the third (non-linear) term in Eq. (15) is always smaller than the second (linear) one. Moreover, the combination in the brackets there is also less than one for $\rho \neq \rho_0$. Although the accurate estimations are impossible due to a priori unknown value of δ_3 , this provides additional arguments that one can consider the third term as negligibly small for the pressures up to some hundreds Megapascals. Fig. 5 illustrates this line of reasoning by a realistic example and demonstrates that the considered derivatives may be estimated as a linear function of the pressure with reasonable accuracy up to sufficiently high pressures (here very accurately up to 70–80 MPa, with not so big deviation even for larger pressures up to 100 MPa). Thus, these plots in Fig. 5 give also a hint for estimations of the warrant validity range for the method of the density prediction: $k \rho_0 \kappa_T^0 (P - P_0) \leq 1$.

Therefore, it is possibly to linearise Eq. (15) that gives the ordinary differential equation

$$\rho_0 \kappa_T^0 \left(\frac{\partial P}{\partial \rho}\right)_T = 1 + k \rho_0 \kappa_T^0 (P - P_0) \quad (16)$$

with the initial conditions stated on the saturation curve $P(\rho_0) = P_0$. The respective solution is precisely the FT-EoS (8).

If to express the pressure as a function of the density and find its respective derivatives, one can see that the experimental polynomial regressions (10) and (12) will be replaced respectively with approximate functional forms representing the exponential continuation of the linearised expressions

$$P - P_0 = (k \rho_0 \kappa_T^0)^{-1} \left[e^{k(\rho - \rho_0)} - 1 \right] \quad (17)$$

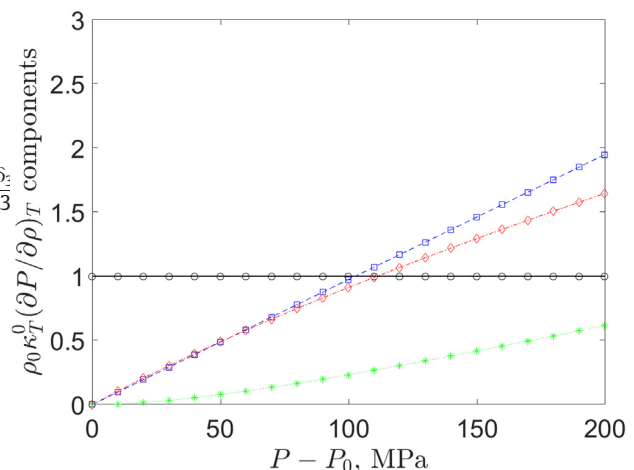


Fig. 5. The experimental components of the right-hand side of Eq. (15) in the case of isotherm shown in Fig. 4: the first equal to one (circles connected by solid line), the second, linear with respect to the pressure (squares connected by the dashed line), and the addition to the unit constant calculated from the polynomial interpolation of the experimental data by Eq. (12), shown as diamonds connected with dash-dotted line. The asterisks connected by dotted curve demonstrate the behaviour of the factor $(k \rho_0)^2 (\rho_0 / \rho - 1)^2 / 2$ at the third term calculated from experimental data.

and

$$\left(\frac{\partial P}{\partial \rho}\right)_T = (\rho_0 k_T^0)^{-1} e^{k(\rho - \rho_0)} \quad (18)$$

Eq. (18) can be rewritten also as

$$(\rho k_T)^{-1} e^{-k\rho} = (\rho_0 k_T^0)^{-1} e^{-k\rho_0} = \text{const} \Big|_{T=\text{const}} \cdot S \quad (19)$$

Note also that the last formula can be multiplied by the combination $M/(RT)$, which is constant along isotherms but also gives the dimensionless fluctuation parameter $\nu(\rho) = M/(RT\rho k_T)$. [18], for which it is known that $\nu(\rho) \exp(-k\rho) = \text{const}$ fulfils not only along isotherms (up to some elevated pressure). This is also true (with a very slightly varying k) along the coexistence curve $P_0 = P_0$ up to temperatures in the vicinity of the boiling point, where the practical measurements are evaluated at the ambient constant (atmospheric) pressure P_0 , see Fig. 6 (upper panel). Its derivative with respect to the density gives the parameter k , Eq. (9) used above.

Thus, the described procedure considered of an initial problem for the ordinary differential equation gives the solution, which is an interpolation of the true polynomial function by the exponential one. They both coincide in the initial value point. For very low pressures applied, the experimental curve and the predicted obtained via FT-EoS coincides with a high accuracy. It is natural, since for $k\rho_0 k_T^0 (P - P_0) \ll 1$ the natural logarithm in Eq. (8) can be expanded into the Taylor series that results just a definition of the forward differentiation of the isothermal compressibility (any k will be simple cancelled by the construction):

$$\rho \approx \rho_0 + k^{-1} k \rho_0 k_T^0 (P - P_0) = \rho(P_0) + \left(\frac{\partial \rho}{\partial P}\right)_T \Big|_{P=P_0} (P - P_0).$$

For larger pressures, the exponential function (17) approximates the cubic polynomial, which is the exact functional dependence. It should be pointed out the exponential functions in Eqs. (17) and (18) can be expanded into the Taylor series with respect to the density and this expansion will contain cubic terms, as in Eqs. (10) and (12). This overcomes the insufficient accuracy if simply to truncate the latter equation keeping only the terms with $\delta_0, \delta_1, \delta_2$ there as it is illustrated by the dashed curve in Fig. 4.

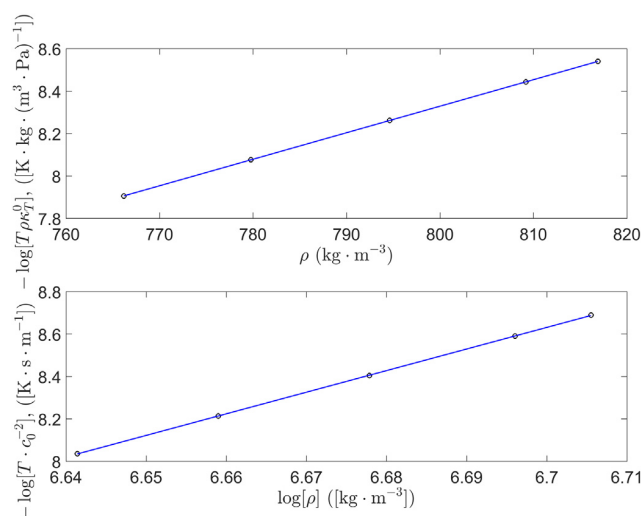


Fig. 6. Logarithms of parameters of the inverse reduced density (upper panel) and the reduced pressure (lower panel) fluctuations and at ambient pressure (circles correspond to the temperatures, at which the speed of sound along isotherms was measured) and their linear fitting with respect to the density and its logarithm.

At the same time, the exact equivalence of the exponential and the cubic polynomial functions is impossible. Since the exponential function grows faster than any polynomial, it can mimic the latter within an interval of its argument wider than one given by the Taylor expansion up to the correspondent maximal degree of the polynomial only if the exponential growth rate will be less than given by the Taylor series expansion. This may results in “hump”-like deviations of the FT-EoS solutions in an intermediate range of pressures, especially for high temperatures, where the curvature of the $P(\rho)$ curve is significant, see, for example the lowest isotherm in Fig. 3. For very large pressures, this linearisation-based procedure goes out of its range of validity, compare the derivative lines (squares connected by the dashed line and diamonds connected with dash-dotted line) in Fig. 5. Note that it is a not pure mathematical feature but also connected with the molecular picture of the transition to the close packing as discussed in [23].

However, it should be pointed out that the procedure (13), which transforms the simple equality for a derivative represented as a polynomial function of its argument, Eq. (12), into the ordinary differential Eq. (16) is crucially important because it results in a significant wider range of an accurate prediction due to the emerging exponential solution, which is not truncated at the low polynomial degree. Since the coefficients δ_1 and δ_2 (the only two, which can be found along the liquid-vapour coexistence curve, or at the ambient pressure), are determined within this approach in the boundary point only, the pure polynomial solution, which will be a pure extrapolation, will deviate from the actual data monotonously and quite fast in contract to the exponential continuation originated from the proposed modified linearisation procedure.

3.2. Linearisation for the speed of sound prediction

Empirical observations starting from the work [36] shows that the speed of sound cubed can be quite accurately fitted up to several hundreds of Megapascals as a linear function of the excess pressure

$$c^3(P) = c_0^3 + \delta_s (P - P_0), \quad (20)$$

where $c_0 = c(P_0)$ is the speed of sound at ambient pressure P_0 , and δ_s is a temperature-dependent constant, which is needed to be defined. The equality (20) holds up to around 100–150 MPa practically for all organic liquids, and even for larger values pressures when the liquid is very low compressible. Better accuracy can be reached by addition of the next, quadratic with respect to the excess pressure term but this addition is sufficiently small in comparison with the linear term and required when one need operate with the pressures higher than 200 MPa and/or to get a fit with accuracy securely within the experimental uncertainty as it has been discussed in [24,37] and used above in the present work.

Eq. (20) can naturally be considered as the truncated Taylor series expansion along an isotherm

$$c^3(P) = c(P_0)^3 + \left(\frac{\partial c^3}{\partial P}\right)_{T,P=P_0} (P - P_0).$$

The partial derivative there, taking into account the interconnection between the speed of sound squared and the adiabatic compressibility $c^2 = (\rho k_S)^{-1} = (\partial \rho / \partial P)_S$, is convenient to represent as

$$\left(\frac{\partial c^3}{\partial P}\right)_{T,P=P_0} = \left(\frac{\partial c^3}{\partial \rho}\right) \left(\frac{\partial \rho}{\partial P}\right)_{T,P=P_0} = \frac{3}{2} \rho_0 k_T^0 c_0 \left(\frac{\partial(\rho k_S)^{-1}}{\partial \rho}\right)_{T,P=P_0}. \quad (21)$$

Now the main question is how to define $\partial(\rho k_S)^{-1} / \partial \rho$ at ambient conditions. Using an analogy with the fluctuation parameter in FT-EoS, the primary idea is to consider the adiabatic fluctuation parameter.

$$\nu_s = \frac{M}{RT} \frac{1}{\rho k_S}, \quad (22)$$

which differs from ν by replacing the isothermal compressibility by the isentropic one. Note that the quantity (22) has a fluctuational character too but describes not the inverse density but reduced inverse pressure fluctuations since (see e.g. [38])

$$\langle (\Delta P)^2 \rangle = -RT \left(\frac{\partial P}{\partial V} \right)_s = \frac{RT}{M} \left(\frac{\partial P}{\partial \rho} \right)_s \rho^2.$$

Let us consider a hypothetical medium, which has the properties of the ideal gas at the same PVT conditions, i.e. $\rho = MP_{ig}/RT$. Substituting this expression into the equation above, we get

$$\frac{\langle (\Delta P)^2 \rangle}{P_{ig}^2} = \frac{M}{RT} \left(\frac{\partial P}{\partial \rho} \right)_s = \nu_s$$

that explains the meaning ν_s as reduced pressure fluctuations.

Fig. 6(lower panel) demonstrates the clear power-law behaviour of this quantity for SRS fluid

$$\nu_s \equiv \frac{M}{RT} \frac{1}{\rho \kappa_s} \equiv \frac{M}{R} \frac{c^2}{T} = \Lambda \rho^\lambda, \quad (23)$$

where M/R , Λ , and λ are constants. Whence,

$$\frac{d\nu_s}{d\rho} = \lambda \Lambda \rho^{\lambda-1} \frac{\lambda}{\rho} \Lambda \rho^\lambda = \frac{M}{RT} \frac{\lambda c^2}{\rho}.$$

Respectively, for the isothermal coefficient from (21)

$$\left(\frac{\partial (c^2)^{3/2}}{\partial \rho} \right)_{T,P=P_0} = \frac{\lambda c_0^2}{\rho_0}$$

and the linear expansion of the speed of sound cubed takes the form

$$c^3(P) = c_0^3 + \frac{3}{2} \rho_0 \kappa_T^0 \frac{\lambda c_0^2}{\rho_0} (P - P_0) = c_0^3 \left[1 + \frac{3}{2} \rho_0 \kappa_T^0 k_s (P - P_0) \right], \quad (24)$$

where $k_s = \lambda/\rho_0$.

It should be stressed that the expression (24) has an interpretation directly connected with FT-EoS in the sense of linearisation. Since

$$\frac{M}{RT} \frac{1}{\rho \kappa_T} = e^{k\rho+b} = \frac{M}{RT} \frac{c^2}{\gamma},$$

using the ratio along an isotherm, the cube of the speed of sound

$$c^3 = c_0^3 \left(\frac{\gamma}{\gamma_0} \right)^{3/2} e^{\frac{3}{2} k(\rho - \rho_0)}.$$

Substituting $k(\rho - \rho_0)$ expressed from the FT-EoS (8)

$$c^3 = c_0^3 \left(\frac{\gamma}{\gamma_0} \right)^{3/2} [1 + \rho_0 \kappa_T k (P - P_0)]^{3/2},$$

after the Taylor series expansion up to the first term we get

$$c^3 = c_0^3 \left(\frac{\gamma}{\gamma_0} \right)^{3/2} \left[1 + \frac{3}{2} \rho_0 \kappa_T k (P - P_0) \right].$$

Note now that the expression above has the factor $(\gamma/\gamma_0)^{3/2}$, which is unknown functions decaying with the growth of the pressure, which also can be expanded up to the linear term as $(\gamma/\gamma_0)^{3/2} \approx 1 - \delta_\gamma (P - P_0)$. Multiplying both factors and keeping the linear terms only,

$$c^3 = c_0^3 \left[1 + \frac{3}{2} \rho_0 \kappa_T (k - \delta_\gamma) (P - P_0) \right], \quad (25)$$

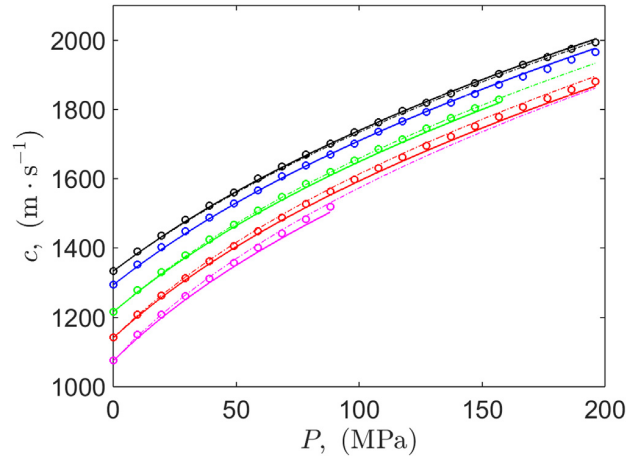


Fig. 7. Experiment-based data (circles) for the speed of sound and the respective curves predicted by Eq. (26) and by the improved method, Eq. (27) (dash-dotted lines) along isotherms.

where the difference $k - \delta_\gamma = k_s$. This implies that $k_s < k$ as it is really observed during the comparative calculations of the speed of sound given below.

Fig. 7 illustrates the speed of sound predicting using the derived formula

$$c = c_0 \left[1 + \frac{3}{2} \rho_0 \kappa_T^0 k_s (P - P_0) \right]^{1/3} \quad (26)$$

and parameters determined using the thermodynamic quantities measured at the normal pressure only and without any information on the fluid's chemical composition. It is visible that the not only the qualitative course of the predicted speed of sound corresponds to the experimental data but a quantitative agreement can be verified too: AAD = 0.47% for the whole set.

As additional tests, Fig. 8 shows the comparison of the speed of sound predictively calculated via the method described above with the experimental data for the Diesel fuel B0 2015 [39] and two kinds of biodiesels based on two vegetable oils, soybean and rapeseed, with methanol [40]. For this three samples AAD = 0.52%, 0.74%, 1.2%, respectively. One can see satisfactory prediction accuracy for these different kinds of fuels too, and note visually that the maximal deviations detected for biodiesels originates from the isotherms with largest temperatures for the Diesel fuel B0 2015 and soybean-based biodiesel and from the isotherms with lowest temperatures for the rapeseed-based biodiesel. This observation induces a necessity in an additional tests on the possible temperature dependence of the parameter k_s and, in general, ranges of applicability of the proposed method for its determination.

4. Speed of sound prediction: caveats and corrections

As it was observed above, a significant curvature of the density as a function of the pressure can result in a growing deviation of the speed of sound predicted via Eq. (26) from experimental data. This follows from the sense of this formula as a linearised around the coexistence curve version of the pressure dependence for all included thermodynamic quantities. Naturally, fluids with which are highly compressible and have a significant dependence of the heat capacity ratio on the temperature, are affected more, compare with the lower value of the molecular packing ratio bounding the direct FT-EoS applicability for such compressed liquid in [23].

The typical example is n-heptane, see Fig. 9, where experimental data are taken from [41]. One can see not only deviations of the density

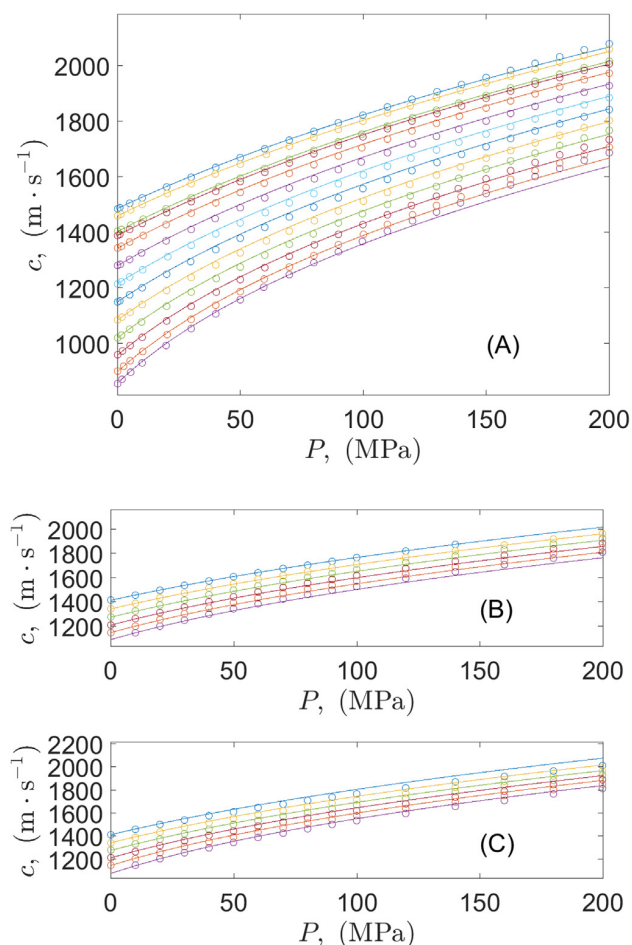


Fig. 8. Experiment-based data (circles) for the speed of sound and the respective curves predicted by Eq. (26) along isotherms for Diesel fuel B0 2015 (A) within the temperature interval $T = (263.15\text{--}468.15)$ K, and soybean (B) and rapeseed (C) biodiesels within the temperature interval $T = (293.15\text{--}393)$ K.

curves from markers for higher pressures but also the significant overestimation of the speeds of sound calculated via (26), which start from very low values of the pressures (they are shown as solid lines), for the whole set $AAD = 1.87\%$ with the maximal relative deviation 3.75%.

The more heavy pure n-alkane, namely, n-dodecane, which sometimes considered as a model or surrogate fuel [42] demonstrate closer similarity between experimental [43] (markers) and predicted (solid lines) data in Fig. 9. The overall $AAD = 0.97\%$ with the maximal relative deviation 2.62%. This confirms the line of reasoning arguing the growth of accuracy of Eq. 26 with lowering response on the applied pressure. Note also that the real diesel calibration fluid as indicated in Table 1 contains even higher hydrocarbons (C14–C18) and respectively, its speed of sound is reproduced better.

In order to improve quality of the speed of sound prediction, let us modify Eq. (24) introducing the correcting temperature-dependent factor for the slope of the linear trend c^3 vs. P along isotherms as

$$c^3(P) = c_0^3 \left[1 + \frac{3}{2} \rho_0 k_7^0 k_s k_s'(T) (P - P_0) \right], \quad (27)$$

where $k_s' = k_s'^0 (1 + \varepsilon(T - T_0'))$. Here k_s' defined for $T = T_0'$ is close to 1, and ε is quite small.

To find two correcting parameters, we refer to the fact that the FT-EoS predicts the density up to relative compressions $(\rho - \rho_0)/$

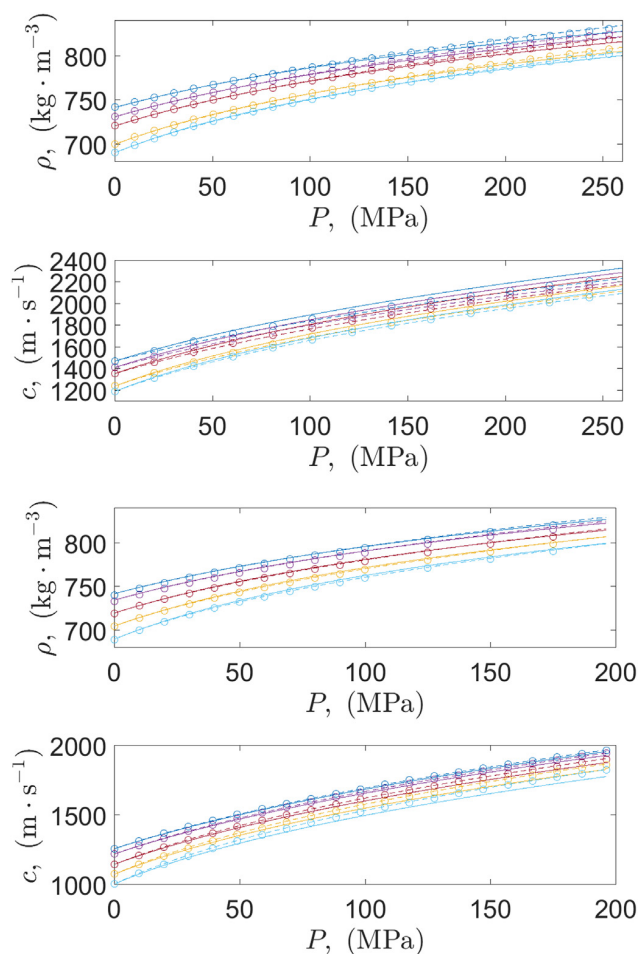


Fig. 9. Experiment-based data (circles) for the density and the speed of sound in comparison with the curves predicted via the direct linearisation approach (lines) and its corrected version (dashed lines). Two upper panels show isotherms $T = (223.35, 236.15, 248.65, 273.75, 285.25)$ K of n-heptane, and two lower panels – isotherms $T = (303.15, 313.15, 333.15, 353.15, 373.15)$ K of n-dodecane.

$\rho_0 \approx 1.05 - 1.1$ even for such highly compressible liquids as light n-alkanes. Thus, the key idea is to use the inverse problem for finding such correcting coefficients for the speed of sound that the acoustic method of the density calculation (6)–(7) will give values close to the predicted by the FT-EoS.

The practical search for the coefficients was organised as follows. At the first step, the density $\rho_{FT-EoS}(P, T)$ via the FT-EoS with the saturated densities, speeds of sound, and isobaric heat capacities taken from NIST Chemistry WebBook [44] as input quantities, and the speed of sound via Eq. (26) were calculated up to the pressure $P = 111.4$ MPa for more compressible n-heptane and up to $P = 196.3$ MPa for less compressible n-dodecane (graphically, up to the end of most curved part of the density isotherm) and the given temperature range of five isotherms. The third isotherm was chosen as $T = T_0'$. Then, the speed of sound was recalculated for a set of trial $k_s'^0$ from 0.7 to 1.3 equispaced subdivided into 11 steps. For each set of obtained speeds of sound, the density ρ_{ac} was calculated for such speeds of sound (6)–(7) using as well as the mean absolute deviation of this density from the density given by the FT-EoS along the third isotherm: $\langle |\rho_{ac}(P, T') - \rho_{FT-EoS}(P, T')| \rangle$. Those value of $k_s'^0$, which minimised this deviation, was determined as the desired value. At the last step the same procedure was repeated with the fixed $k_s'^0$ and a set of 35 trial ε uniformly distributed from $6 \cdot 10^{-4}$ to $3 \cdot 10^{-3}$. In this stage, the minimization procedure was evaluated not

for one but for all five isotherms and all pressures and the respective optimal ε was found.

For n-heptane the obtained correction factors are $k_s'^0=0.88$ and $\varepsilon = 0.0017$ that result in $AAD = 0.34\%$ and the maximal deviation 0.72% of the speed of sound predicted by Eq. (27), shown in Fig. 9 as dashed lines, and the experimental values. As a byproduct, one can also note that the densities calculated from this final speeds of sound (also shown as dashed curves in the respective subpanel) reproduce the experimental ones even better than the FT-EoS for highest available pressures ($P > 200$ MPa > 200 MPa).

For n-dodecane, the improvement made by the same algorithm with the same range and step of trial $k_s'^0$ and ε also leads to the improvement of the predicted speed of sound and the density. The solid curves shown in Fig. 9 correspond to the correcting values $k_s'^0=1.06$ and $\varepsilon = 0.0011$, and the resulting $AAD = 0.19\%$ (the maximal deviation is equal to 0.46%) from the corrected speed of sound. As expected the corrections are significantly smaller because even the uncorrected version (26) gives better result than for n-heptane, the main difference with experimental data is introduced by two most curved isotherms corresponding highest temperatures that is corrected by Eq. (27) reducing deviations down to the experimental uncertainty.

Now we can apply this improved method to diesel fuels too. For SRS Calibration Fluid CV, the procedure completely analogous to the described above gives in Eq. (27) the value $k_s'^0=1.03$ that minimally differs from the initial formula, and the temperature-dependent correction $\varepsilon = 0.0014$, which makes the reproducing high-temperature isotherms better, see the dash-dotted curves in Fig. 7. As a result, the overall $AAD = 0.32\%$ is improved too. However, it should be pointed out that this improvement is not so drastic, and the respective corrections for biofuels are not significant too that confirms the conclusion that for this kind of liquids even the basic predicting formula (26) is applicable with an appropriate predicting accuracy as seen in Fig. 8.

Finally, we complete the considerations of an influence of the correcting procedure on the predicted thermodynamic properties of complex fuel mixtures discussing the resulting density and isobaric expansion coefficient using SRS Calibration Fluid CV, novel data for which are one of the main subjects of this work, as a case study. The densities calculated via the acoustic algorithm (6)–(7) form this predicted speed of sound are added to Fig. 3 as dash-dotted lines. It is visible that the corrected isotherms go better through the experimental points for $P > 100$ –120 MPa, especially for two lowest temperatures as well as the isotherm's curvature for the highest temperature is closer to the experimental one.

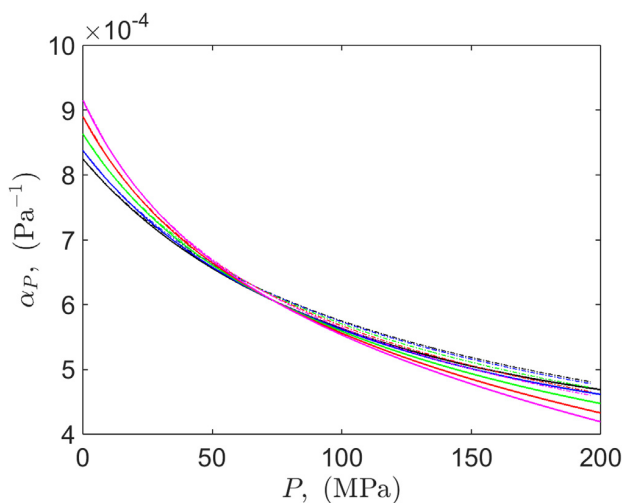


Fig. 10. Experiment-based plot of the isobaric expansion coefficient for SRS Calibration Fluid CV (solid lines) and its course calculated using the acoustic algorithm from the predicted speed of sound.

Although these improvements are not so principal for respect to the pure FT-EoS predictions for the density taking into account the uncertainty of the respective experimental data, the curvature-based issues may affect the quality of predicting the isobaric expansion coefficient. Fig. 10 demonstrates such prediction in comparison with the experiment-based calculations. We can claim very accurate reproducing of the latter, both sets of curves are indistinguishable for $P < 50$ MPa. Moreover, the proposed method of calculations reproduces the crossing of α_P isotherms, not only qualitatively but also quantitatively: the experimental crossing point corresponds to $P \approx 74$ MPa, and the predicted to $P \approx 65$ MPa. The difference between these values is not significant because even in the experimental data the uncertainty of the localizations depends on the number of points along isobars, a degree of the fitting polynomial and can reach several MPa, up to tenths, see the discussion in [45]. For high pressures, i.e. significantly after the crossing point, the calculated isotherms show less divergence than the experimental isotherms but the range of values is still qualitatively reasonable.

5. Conclusion and outlooks

In this work, we explore possibilities for predicting thermodynamic quantities of liquids in the single-phase region (i.e. under high elevated pressures) basing on the data, which can be measured at ambient (i.e. quit low) pressure. The principal possibility of this procedure is based on the introduced analogy between differential equalities of thermodynamics and differential equations of the dynamical system theory in the case when the time variable of the latter is replaced by the density. Mathematical generality of the proposed modified procedure of linear analysis assures its wide applicability to dense liquids, and, as a consequence to the emerging possibility predict properties of complex mixture of molecular liquids even in the case, when the exact composition is not available. One need to measure the density, the speed of sound, and the isobaric heat capacity at ambient conditions only to get all required parameters.

The special attention is attracted to the prediction of the speed of sound that is much more complicated task in comparison with the density prediction. While the density may be treated "geometrically", from the point of view of the molecular packing in space, the speed of sound strictly depends on molecular properties, which determines valuable input from the heat capacity. We proposed the method of prognosis considered from the points of view of linearisation of the expression connecting the density and the pressure to the form of linear dependence of the speed of sound cubed on the pressure. For the latter, there is known some theoretical background for cryogenic liquids [46] be phenomenologically such dependence fulfils for molecular liquids at high temperatures too.

For low compressible liquid mixtures such diesel fuels, the respective coefficient of the linear slope for isotherms is connected with the reduced pressure fluctuations (as a counterpart to the reduced density fluctuations determining parameters for predicting volumetric properties) at compression and isobaric (or saturated) heating. We note that the revealed power-law dependence (23) has common features with so-called Rao-Wada rule [47,48], which can be represented as $c^3 = K_{RW} \rho^0$. Recent studies [49,50] argued that the factor K_{RW} is not a constant and proposed empiric coefficients for the temperature-dependent corrections. On the other hand our expression (23) include the temperature explicitly as motivated by exact thermodynamic fluctuation equalities. As a result, the linearity in double-logarithmic scale, see Fig. 6 (lower panel), is restored. As an outlook, the search for new group-contribution methods for such improved relation can be proposed.

Finally, it should be pointed out that the isobaric and isothermal reduced pressure density universality is not fulfilled for low compressible liquids (the same was observed for the classic Rao-Wada rule, see [51,52]). However, we show that the combination of the density predictions via the Fluctuation Theory-based Equation of State and the

acoustic method of density determination based on the thermodynamic equalities makes possible to introduce a sequential correction procedure, which reduces the prediction error to the range of uncertainty of experiments.

Acknowledgement

The authors would like to acknowledge the following people from the H&R group for providing the sample for this study: we thank Kim Domscheit for organising the sample preparation and shipment and Mr. Hülmann for the quality control of the sample.

This work was supported by a grant from the National Science Centre (Poland) Decision No. 2016/23/B/ST8/02968.

References

- [1] P. Ungerer, C. Nieto-Draghi, B. Rousseau, G. Ahunbay, V. Lachet, Molecular simulation of the thermophysical properties of fluids: from understanding toward quantitative predictions, *J. Mol. Liq.* 134 (2007) 71–89.
- [2] I. Polishuk, Till which pressures the fluid phase EOS models might stay reliable? *J. Supercrit. Fluids* 58 (2011) 204–215.
- [3] J.S. Lopez-Echeverry, S. Reif-Acherman, E. Araujo-Lopez, Peng-Robinson equation of state: 40 years through cubics, *Fluid Phase Equilib.* 447 (2017) 39–71.
- [4] D.C. Johnston, *Advances in Thermodynamics of the Van der Waals Fluid*, Morgan & Claypool Publishers, 2014.
- [5] S.K. Saxena, *Thermodynamic Data: Systematics and Estimation*, Springer Science & Business Media, 2012.
- [6] M. Levy, H. Bass, R. Stern (Eds.), *Modern Acoustical Techniques for the Measurement of Mechanical Properties*, Academic Press, London, 2001.
- [7] Measurement of the thermodynamic properties of single phases, in: A. Goodwin, K.N. Marsh, W.A. Wakeham (Eds.), *IUPAC Experimental Thermodynamics*, VI, Elsevier, Amsterdam, 2003.
- [8] U. Kaatze, F. Eggers, K. Lautscham, Ultrasonic velocity measurements in liquids with high resolution – techniques, selected applications and perspectives, *Meas. Sci. Technol.* 19 (2008), 062001.
- [9] E. Wilhelm, T. Letcher (Eds.), *Volume properties: liquids, solutions and vapours*, Royal Society of Chemistry, London, 2014.
- [10] I. Polishuk, Standardized critical point-based numerical solution of statistical association fluid theory parameters: the perturbed chain-statistical association fluid theory equation of state revisited, *Ind. Eng. Chem. Res.* 53 (2014) 14127–14141.
- [11] X. Liang, B. Maribo-Mogensen, K. Thomsen, W. Yan, G.M. Kontogeorgis, Approach to improve speed of sound calculation within PC-SAFT framework, *Ind. Eng. Chem. Res.* 51 (2012) 14903–14914.
- [12] A.M. Palma, A.J. Queimada, J.A.P. Coutinho, Using a volume shift in perturbed-chain statistical associating fluid theory to improve the description of speed of sound and other derivative properties, *Ind. Eng. Chem. Res.* 57 (2018) 11804–11814.
- [13] I. Polishuk, Generalization of SAFT+ cubic equation of state for predicting and correlating thermodynamic properties of heavy organic substances, *J. Supercrit. Fluids* 67 (2012) 94–107.
- [14] C. Nieto-Draghi, G. Fayet, B. Creton, X. Rozanska, P. Rotureau, J.-C. de Hemptinne, P. Ungerer, B. Rousseau, C. Adamo, A general guidebook for the theoretical prediction of physicochemical properties of chemicals for regulatory purposes, *Chem. Rev.* 115 (24) (2015) 13093–13164.
- [15] G. Ruppeiner, Thermodynamics: a Riemannian geometric model, *Phys. Rev. A* 20 (1979) 1608–1613.
- [16] J. Jaramillo-Gutiérrez, J.L. López, J. Torres-Arenas, R-crossing method applied to fluids interacting through variable range potentials, *J. Mol. Liq.* 295 (2019) 111625.
- [17] G. Ruppeiner, Riemannian geometry in thermodynamic fluctuation theory, *Rev. Mod. Phys.* 67 (1995) 605–659.
- [18] E.B. Postnikov, A.L. Goncharov, V.V. Melent'ev, Tait equation revisited from the entropic and fluctuational points of view, *Int. J. Thermophys.* 35 (2014) 2115–2123.
- [19] E.B. Postnikov, A.L. Goncharov, N. Cohen, I. Polishuk, Estimating the liquid properties of 1-alkanols from C5 to C12 by FT-EoS and CP-PC-SAFT: simplicity versus complexity, *J. Supercrit. Fluids* 104 (2015) 193–203.
- [20] M. Chorażewski, E.B. Postnikov, B. Jasiok, Y.V. Nedyalkov, J. Jacquemin, A fluctuation equation of state for prediction of high-pressure densities of ionic liquids, *Sci. Rep.* 7 (2017) 5563.
- [21] B. Jasiok, E.B. Postnikov, M. Chorażewski, The prediction of high-pressure densities of different fuels using fluctuation theory-based Tait-like equation of state, *Fuel* 219 (2018) 176–181.
- [22] B. Jasiok, A.R. Lowe, E.B. Postnikov, J. Feder-Kubis, M. Chorażewski, High-pressure densities of industrial lubricants and complex oils predicted by the fluctuation theory-based equation of state, *Ind. Eng. Chem. Res.* 57 (34) (2018) 11797–11803.
- [23] B. Jasiok, E.B. Postnikov, M. Chorażewski, The prediction of high-pressure volumetric properties of compressed liquids using the two states model, *Phys. Chem. Chem. Phys.* 21 (2019) 15966–15973.
- [24] A.R. Lowe, B. Jasiok, V.V. Melent'ev, O.S. Ryschkova, V.I. Korotkovskii, A.K. Radchenko, E.B. Postnikov, M. Spinnler, U. Ashurova, J. Safarov, E. Hassel, M. Chorażewski, High-temperature and high-pressure thermophysical property measurements and thermodynamic modelling of an international oil standard: RAVENOL diesel rail injector calibration fluid, *Fuel Process. Technol.* 199 (2020) 106220.
- [25] I.K. Nikolaidis, A. Poursaeidesfahani, Z. Csaszar, M. Ramdin, T.J.H. Vlugt, I.G. Economou, O.A. Moutos, Modeling the phase equilibria of asymmetric hydrocarbon mixtures using molecular simulation and equations of state, *AIChE J.* 65 (2019) 792–803.
- [26] H.B. Rokni, A. Gupta, J.D. Moore, M.A. McHugh, B.A. Bamgbade, M. Gavaises, Purely predictive method for density, compressibility, and expansivity for hydrocarbon mixtures and diesel and jet fuels up to high temperatures and pressures, *Fuel* 236 (2019) 1377–1390.
- [27] E.H.I. Ndiaye, J.-P. Bazile, D. Nasri, C. Boned, J.L. Daridon, High pressure thermophysical characterization of fuel used for testing and calibrating diesel injection systems, *Fuel* 98 (2012) 288–294.
- [28] M. Chorażewski, F. Dergal, T. Sawaya, I. Mokbel, J.-P.E. Grolier, J. Jose, Thermophysical properties of Normafluid (ISO 4113) over wide pressure and temperature ranges, *Fuel* 105 (2013) 440–450.
- [29] Y. Shinohara, K. Takeuchi, O.E. Herrmann, H.J. Laumen, 3000 bar common rail system, *MTZ Worldwide eMagazine* 72 (2011) 4–9.
- [30] J.E. Johnson, S.H. Yoon, J.D. Naber, S.-Y. Lee, G. Hunter, R. Truemmer, T. Harcombe, Characteristics of 3000 bar diesel spray injection under non-vaporizing and vaporizing conditions, Proceedings of the 12th Triennial International Conference on Liquid Atomization and Spray Systems (CLASS), Heidelberg, Germany 2012, pp. 2–6.
- [31] J.A. Wloka, S. Pflaum, G. Wachtmeister, Potential and challenges of a 3000 bar common-rail injection system considering engine behavior and emission level, *SAE Int. J. Engines* 3 (2010) 801–813.
- [32] A.K. Agarwal, A.P. Singh, R.K. Maurya, P.C. Shukla, A. Dhar, D.K. Srivastava, Combustion characteristics of a common rail direct injection engine using different fuel injection strategies, *Int. J. Therm. Sci.* 134 (2018) 475–484.
- [33] V.N. Verveyko, E.B. Boletsky, N.S. Chebrov, Ultrasonic Speed and Densitometer for Fluids, RU 166341 U1, 2016.
- [34] T.F. Sun, S.A.R.C. Bominaar, C.A. Ten Seldam, S.N. Biswas, Evaluation of the thermophysical properties of toluene and n-heptane from 180 to 320 K and up to 260 MPa from speed-of-sound data, *Ber. Bunsenges. Phys. Chem.* 95 (1991) 696–704.
- [35] V. Diky, J.P. O'Connell, J. Abildskov, K. Kroenlein, M. Frenkel, Representation and validation of liquid densities for pure compounds and mixtures, *J. Chem. Eng. Data* 60 (2015) 3545–3553.
- [36] Y.S. Shoitov, N.F. Otpushchennikov, Pressure dependence of the speed of sound in liquids, *Sov. Phys. J.* 11 (1968) 129–130.
- [37] V.V. Melent'ev, M.F. Bolotnikov, Y.A. Neruchev, Speeds of sound, densities, and isentropic compressibilities of 1-iodohexane at temperatures from (293.15 to 413.15) K and pressures up to 200 MPa, *J. Chem. Eng. Data* 50 (2005) 1357–1360.
- [38] L.D. Landau, E.M. Lifshitz, *Statistical physics, part 1, Course of Theoretical Physics*, Volume 5, Elsevier, 2013.
- [39] J. Safarov, U. Ashurova, B. Ahmadov, E. Abdullayev, A. Shahverdiyev, E. Hassel, Thermophysical properties of diesel fuel over a wide range of temperatures and pressures, *Fuel* 216 (2018) 870–889.
- [40] M. Habrioux, S.V.D. Freitas, J.A.P. Coutinho, J.L. Daridon, High pressure density and speed of sound in two biodiesel fuels, *J. Chem. Eng. Data* 58 (2013) 3392–3398.
- [41] M.J.P. Muringer, N.J. Trappeniers, S.N. Biswas, The effect of pressure on the sound velocity and density of toluene and n-heptane up to 2600 bar, *Phys. Chem. Liq.* 14 (1985) 273–296.
- [42] E.W. Lemmon, M.L. Huber, Thermodynamic properties of n-dodecane, *Energy Fuel* 18 (2004) 960–967.
- [43] Y. F. Melikhov, Ph.D. thesis, Kursk State Pedagogical Institute (1984).
- [44] <https://webbook.nist.gov/chemistry/liquid/>.
- [45] M. Taravillo, V.G. Baonza, M. Cáceres, J. Núñez, Thermodynamic regularities in compressed liquids: I. The thermal expansion coefficient, *J. Phys. Condens. Matter* 15 (2003) 2979.
- [46] H.J. Maris, Critical phenomena in ^3He and ^4He at $T = 0$ K, *Phys. Rev. Lett.* 66 (1991) 45.
- [47] M.R. Rao, A relation between velocity of sound in liquids and molecular volume, *Indian Journal of Physics* 14 (1940) 109–116.
- [48] Y. Wada, On the relation between compressibility and molal volume of organic liquids, *J. Phys. Soc. Jpn.* 4 (1949) 280–283.
- [49] J.-L. Daridon, J.A.P. Coutinho, E.H.I. Ndiaye, M.L.L. Paredes, Novel data and a group contribution method for the prediction of the speed of sound and isentropic compressibility of pure fatty acids methyl and ethyl esters, *Fuel* (2013) 466–470.
- [50] S.V.D. Freitas, D.L. Cunha, R.A. Reis, A.S. Lima, J.-L. Daridon, J.A.P. Coutinho, M.L.L. Paredes, Application of Wada's group contribution method to the prediction of the speed of sound of biodiesel, *Energy Fuel* 27 (2013) 1365–1370.
- [51] B.B. Kudryavtsev, G.A. Samgina, Use of ultrasonic measurements in the study of molecular interactions in liquids, *Sov. Phys. J.* 9 (1966) 5–8.
- [52] J. Gmyrek, Erwägungen über die Abhängigkeit der Ausbreitungsgeschwindigkeit der Schallwellen vom Druck in Flüssigkeiten mit konstantem Volumen, *Acta Acustica united with Acustica* 60 (1986) 244–254.

Katowice, 11.04.2023 r.

Instytut Chemii
Wydział Nauk Ścisłych i Technicznych
Uniwersytet Śląski w Katowicach
ul. Bankowa 12, 40-007 Katowice

Statement on the contribution to the publication

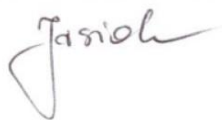
Publication:

E.B. Postnikov, B. Jasiok, V.V. Melent'ev, O.S. Ryshkova, V.I. Korotkovskii, A.K. Radchenko, A.R. Lowe, M. Chorążewski, Prediction of high pressure properties of complex mixtures without knowledge of their composition as a problem of thermodynamic linear analysis. *Journal of Molecular Liquids* **2020**, 310, 113016, DOI: 10.1016/j.molliq.2020.113016.

We hereby state that the contribution to the work published jointly with Bernadeta Jasiok is in accordance with the description below:

Bernadeta Jasiok

I was responsible for: Conceptualization, Methodology, Software, Validation, Formal analysis, Investigation, Data Curation, Writing – Original Draft, Writing – Review & Editing, Visualization



Eugene B. Postnikov

I was responsible for: Conceptualization, Methodology, Software, Validation, Formal analysis, Investigation, Writing – Original Draft, Writing – Review & Editing, Visualization, Project administration



Vyacheslav V. Melent'ev

I was responsible for: Investigation, Resources, Writing – Original Draft, Writing – Review & Editing



Olga S. Ryshkova

I was responsible for: Investigation, Resources, Writing – Original Draft, Writing – Review & Editing



Vadim I. Korotkovskii

I was responsible for: Investigation, Resources, Writing – Original Draft, Writing – Review & Editing



Anton K. Radchenko

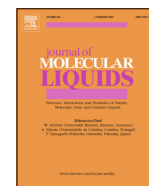
I was responsible for: Investigation, Resources, Writing – Original Draft, Writing – Review & Editing



Mirosław Chorążewski

I was responsible for: Conceptualization, Methodology, Writing – Original Draft, Writing – Review & Editing, Supervision, Funding acquisition





Prediction of the speed of sound in ionic liquids as a function of pressure

Bernadeta Jasiok^{a,*}, Eugene B. Postnikov^{b,*}, Ivan Yu. Pikalov^c, Mirosław Chorążewski^a

^a University of Silesia in Katowice, Institute of Chemistry, ul. 9 Szkolna, 40-006 Katowice, Poland

^b Theoretical Physics Department, Kursk State University, Radishcheva st., 33, Kursk 305000, Russia

^c Center for Information Systems Development and Data Analysis, Kursk State University, Radishcheva st., 33, Kursk 305000, Russia



ARTICLE INFO

Article history:

Received 16 April 2022

Revised 23 June 2022

Accepted 4 July 2022

Available online 5 July 2022

Keywords:

High-pressure

Speed of sound

Ionic liquids

FT-EoS

ABSTRACT

In this work, we demonstrate the possibility of calculating the speed of sound of Ionic Liquids as a function of temperature and pressure using the fluctuation-based approach. The density, speed of sound, and heat capacity at atmospheric pressure are used for the calculations. The collected experimental data from the ILThermo database were used as input. The high-pressure speed of sound for nine ionic liquids was used to compare and analyze. Using the proposed method, the relative average absolute deviation is close to 0.85%.

© 2022 The Authors. Published by Elsevier B.V.

1. Introduction

Thermophysical properties of compressed liquids such as compressibilities, thermal expansivity, and heat capacities are quantities of great interest in several physics and physical chemistry fields. Thus many studies have been devoted to experimental measurements of the thermophysical properties of liquids and mixtures. Significantly, the effect of temperature and pressure on isothermal and isentropic compressibility, isobaric thermal expansivity, constant volume, constant pressure heat capacities, and speed of sound has been investigated by experiments for hundreds of molecular systems and mixtures. The state of any fluid is something engineering chemists often find it necessary to specify clearly. Such a specification for even the simplest fluid must include the amount of substance present, the pressure, and the temperature. The mathematical relationship that links them is the equation of state that remains the basis of thermodynamics. The equations of state were introduced to understand the physical background of liquids and use practical calculations instead of extensive direct measurements. The equations of state, and with them the thermoelastic coefficients, are the starting point for most thermodynamic problems in the field of application and engineering in connection with the molecular nature of the described systems, and the range of their applications is extensive, from

physical chemistry and fluid mechanics, through material engineering to nanotechnology.

However, current knowledge of equations of states in the meaning of practical usefulness indicates that the semi-empirical engineering approach is not entirely correct. It is worth noting that besides all the attempts and efforts devoted to the formulation of the versatile equation of state, none of the derived models, up to date, is efficient enough for the properties prediction of a wide range of liquids in a wide range of pressure changes, especially for novel working fluids with new and vastly improved properties.

On the other hand, complicated statistical mechanics apparatus leads to poor functionality with simultaneous mathematical nature complication of the model, which closes the possibility of broad, easy, and fast applicability for engineers. The interesting approach and the key to explaining these inconsistencies seem to work associating the easiness of equations of states from phenomenological thermodynamics, including the fluctuations phenomenon described by the statistical thermodynamics tools. It also increases the possibility of compiling versatile, fully predictive equations of state.

During this work, we decided to assess the predictive capability for the high-pressure physicochemical properties, primarily the speed of sound for Ionic Liquids (ILs), using an extension of the Fluctuating Equation of State. As has been known for a long time, ILs are liquid organic salts with different physicochemical properties and can therefore be used in various fields of science. For example, ILs can be used as electrolytes in lithium-ion batteries, organic synthesis, catalysis, solvent extraction, they are applied to various biochemical processes and many others [1–3].

* Corresponding authors.

E-mail addresses: bjasiok@us.edu.pl (B. Jasiok), postnikov@kursksu.ru (E.B. Postnikov).

<https://doi.org/10.1016/j.molliq.2022.119792>

0167-7322/© 2022 The Authors. Published by Elsevier B.V.

It is known that ionic liquids have a complicated chemical structure and the nature of intermolecular interactions, so the speed of sound obtained from the experiment under the elevated pressure often does not meet the thermodynamic coherence criteria. Very often, there are relaxation effects in these liquids, which lead to the dispersion of the speed of sound, resulting in a non-thermodynamic speed of sound. This leads to obtaining experimental values not relevant for further thermodynamic modeling. It should be noted that the equation of state derived by us excludes the prediction of non-thermodynamic (i.e., incorrect) speed of sound. Thus, it also verifies the experimental data of speeds of sound.

The speed of sound as a function of a wide range of thermodynamic variables is necessary to determine the complete thermodynamic relations for liquids under high pressure and at elevated temperatures. Even though the speed of sound is not a thermodynamic property *per se*, it is closely related to other thermodynamic properties of a system [4–7]. Moreover, the pressure dependence of the speed of sound provides basic information about compressed liquids, both to investigate the nature of molecular and structural interactions and to obtain thermodynamic properties for applications in industrial processes. It is also essential for deriving and then validating many Equations of State of practical significance.

To date, molecular models belonging to the Statistical Association Fluid Theory (SAFT) family are the primary tools used in the literature to predict the speed of sound of compressed ILs over a wide range of pressures, and temperatures [8–11]. These models can exhibit remarkable accuracy in the comprehensive modeling of liquid properties. On the other hand, the prediction of the speed of sound is also possible using the recently proposed Daridon's method [7]. His approach uses a group contribution method to predict the speed of sound for high molecular weight *n*-alkanes and depict the correlation of speed of sound as a function of temperature and pressure for pure *n*-alkane series.

This work is an extension of the existing Fluctuation Equation of State, which makes it possible to predict the density, the isobaric thermal expansion coefficient, and isothermal compressibility [12–14] and, especially, the approach hypothesized and preliminarily tested for the case of simple hydrocarbons and their mixtures [15].

2. Materials and Method

2.1. Materials

In this study, we used as a primary source the data publicly available in the most comprehensive database of raw experimental measurements of the thermodynamic properties of ionic liquids, ILThermo (v.2.0). It was convenient to create two datasets for further processing for each thermodynamic quantity. The first dataset contains the information on the experiments themselves, i.e., links to information sources, information on the components, and the molar mass of the mixture. The second dataset contains the data of the results of the experiments used for the processing.

The procedure was implemented via the homemade PYTHON code for carrying out requests to the online database and saving the obtained data in Excel spreadsheets for further processing with MATLAB. The general principle of building such a program realization is described in detail elsewhere [16]. Thus, we shortly note only the basic principle of data obtaining.

In order to create the required datasets, it is necessary to request the server where the experiment data is stored, specifying the necessary parameters. In our case, we need to specify the number of mixture components equal to 1 (name on the form: Number

of mixture components, the parameter code is named as `ncmp`) and the property of interest (name on the form: Property, parameter, the parameter's code is `prp`). For example, one needs to execute the following program lines to get the speed of sound:

```
param = 'https://ilthermo.boulder.nist.gov/ILT2/ilsearch?
      cmp=&ncmp = 1&year=&auth=&keyw=&prp = HWGM'
response = requests.get(param)
data = response.json().get('res')
head = ['source_code', 'source_name', 'property',
        'phases', 'fluid_code', 'fluid_code2',
        'fluid_code3', 'col_point', 'fluid_name']
sos_exper = pd.DataFrame(data, columns = head)
```

The result is a dataset with fields containing the code of an experiment used in ILThermo (v.2.0), a reference to the experiment, the property, the phase, the component's code, several measurements, and chemical formulae of components. For further investigation, we only leave the measurements with the phase 'Liquid.' Then, we need to obtain the measurement data for each experiment. A list of experiment codes is generated.

```
sp_sos_exper_liquid = list(sos_exper_liquid
                          ['source_code'])
```

Then queries corresponding to the list of substances was carried out in a loop, and lists with the obtained data were formed:

```
for i in range(len(sp_sos_exper_liquid)):
code_exp = sp_sos_exper_liquid[i]
res = requests.get(main_url + 'ILT2/ilset?set=' +
                  code_exp)
```

Once the necessary lists had been created, the datasets were created and sorted respectively to the lists of unique codes for substances. For these goals, a list of ionic liquids, for which data on the speed of sound exist, was determined as follows:

```
sp_name_fl_unique = sos_exper_liquid
                  ['fluid_code'].unique()
```

and further requests refer to the unique codes, e.g.

```
https://ilthermo.boulder.nist.gov/ILT2/ilsearch?
      cmp=
      2-hydroxy-N-methylethanaminium
      formate&ncmp = 1&year=&auth=&keyw=&
      prp = xXKp
```

After getting all the speed of sound data, we need to get data for the density (and the isobaric heat capacity at the ambient condition in the case of those ionic liquids modeled with the FT-EoS-based approach at high pressures) the selected liquids. In order to do so, the same steps are followed, but with another required property, only in the first query for the experiments we have to substitute the name of the liquid in the loop as well.

2.2. Extraction of experimental data for further calculations

The set of data on the density, the heat capacity, and the speed of sound was downloaded from ILThermo with the PYTHON code operational principles, which are described above. In this particular case, some additional filters were applied: the check that the reported pressure does not exceed 102 kPa, i.e., corresponds to the measurements at ambient conditions, the phase state is strictly denoted as "Liquid", i.e., possible metastable liquids are excluded, strictly one-component compounds, the presence of a liquid's code in both lists (of the density and the speed of sound). Two hundred different ionic liquids were identified at this stage, and the raw data were downloaded.

Nevertheless, it should be pointed out that some of these datasets contain only a few (or even one unique) points and are not applicable for the goal of regression by a non-linear function within an interval of temperatures. Therefore, the secondary check procedures excluded those liquids for which data reported from less than four different temperatures reduced the number of different ionic liquids to 182 compounds.

However, there is still a problem with the coordination of datasets reported in different papers for the same ionic liquid and data uncertainty because some datasets look extremely scattered as functions of the temperature. For this reason, the following procedure was applied: since the change of values is not so drastic within the considered temperature intervals, the linear fitting of all data belonging to each particular ionic liquid was carried out (separately for the density and the speed of sound) and data points, which deviate from this fitting line more than 0.5 % in the relative average absolute deviation for the density and more than 0.2 % for the speed of sound, were excluded. Furthermore, an additional check that the kept values are series, which include not less than four elements (with possible repeating temperatures for the data from different sources), was carried out too to assure the possibility of the further fitting. After this procedure, 139 different ionic liquids remain on the list.

Finally, it should be pointed out that the model considered below operates with the thermodynamic qualities, i.e., it applies to the dispersionless region of ultrasound. For ionic liquids, it is known, see [17] that dispersion effects start to exhibit themselves from several hundreds of MHz. The datasets reported in ILThermo and analyzed in our work do not belong to this range; they explicitly stated their frequencies of ultrasound do not exceed 5 MHz; for those datasets where the frequency is not stated explicitly, the authors of the original works stated that the speed of sound measurements belong to the dispersionless, i.e., thermodynamic, conditions, for which our model is built.

2.3. Description of the procedure for predicting the speed of sound under elevated pressure

Among different mathematical models describing the dependence of the speed of sound as a function of the externally applied pressure [18], one can note that a formula expressing the speed of sound cubed can be fitted as a linear function of the pressure

$$c^3(P) = c_0^3 + \delta_s(P - P_0) \quad (1)$$

that was first described by Shoitov and Otpushchennikov [19] as an empiric observation. Here, $c_0 = c(P_0)$ is the speed of sound at atmospheric pressure P_0 , and δ_s is a temperature-dependence constant, which should be defined. Below, in the section Discussion, we propose a physical picture that leads to such behavior.

For practically all organic liquids, Eq. 1 can be applied up to about 100–150 MPa and sometimes even for higher pressures when the liquid is very low compressibility. For larger pressures,

one needs to expand the pressure dependence that can be achieved, e.g., by adding a quadratic component, to obtain even better accuracy. It is, however, small enough compared to the linear part but is required when testing liquids above 200 MPa, as discussed in [20,21,15].

Within the frames of such a fitting procedure, depending on the pressure range, Eq. (1) can be considered as the first term of a Taylor expansion of the function $c = c^3(P)$ along an isotherm

$$c^3 = c(P_0)^3 + \left(\frac{\partial c^3}{\partial P}\right)_{T,P=P_0} (P - P_0).$$

In the above equation, the partial derivative can be expressed as:

$$\left(\frac{\partial c^3}{\partial P}\right)_{T,P=P_0} = \left(\frac{\partial c^3}{\partial \rho}\right) \left(\frac{\partial \rho}{\partial P}\right)_{T,P=P_0} = \frac{3}{2} \rho_0 \kappa_T^0 c_0 \left(\frac{\partial(\rho \kappa_S)^{-1}}{\partial \rho}\right)_{T,P=P_0}. \quad (2)$$

Thus, to estimate the speed of sound at not extremely high pressures, one need to know the speed of sound and the isothermal compressibility at ambient pressures and, also, the partial derivative of the speed of sound squared $c^2 = (\rho \kappa_S)^{-1}$ considered as a function of the density. The isothermal compressibility can be easily found via the standard thermodynamic equality

$$\kappa_T^0 = \frac{1}{\rho_0} \left(\frac{1}{c_0^2} + \frac{T \alpha_{P,0}^2}{C_{P,0}} \right) \quad (3)$$

when the speed of sound, the density, and the isobaric heat capacity at constant ambient pressure are known (note that in Eq. (3) and further, throughout the work, the mass-related quantities (e.g., the density and the specific heat capacity) are used); under these conditions, the isobaric coefficient of thermal expansion is the simple derivative

$$\alpha_{P,0} = \frac{1}{\rho_0} \left(\frac{\partial \rho_0}{\partial T} \right)_{P,0}. \quad (4)$$

Thus, the main question is in determining the derivative $(\partial(\rho \kappa_S)^{-1} / \partial \rho)_T$ without the usage of the high-pressure data. It is known [22,23] that considering the speed of sound as a pure function of the density is not enough for this goal because of the different values of the respective derivative along the isothermal and isobaric paths. On the other hand, the adiabatic reduced fluctuation parameter

$$v_s = \frac{M}{RT} \frac{1}{\rho \kappa_S}, \quad (5)$$

which is connected with the ratio of pressure fluctuations [24]

$$\langle (\Delta P)^2 \rangle = -RT \left(\frac{\partial P}{\partial V} \right)_S = \frac{RT}{M} \left(\frac{\partial P}{\partial \rho} \right)_S \rho^2.$$

in the actual medium and in the hypothetical case where a substance acts as an ideal gas for the same pressure–temperature–volume (PVT) parameters has the desired invariant property as it has been shown in the work [15].

It can be expressed as a function of the density only

$$v_s = \frac{M}{R} \frac{c^2}{T} \equiv \frac{M}{RT} \frac{1}{\rho \kappa_S} = \Lambda \rho^\lambda, \quad (6)$$

and this power-law scaling fulfils allows considering derivatives with respect to the density independently of the fixed either the pressure or the temperature.

This implies that

$$\frac{dv_s}{d\rho} = \lambda \frac{M}{RT} \frac{c^2}{\rho}.$$

Respectively, along an isotherm, i.e., for $T = \text{const}$, where $M/(RT)$ does not change and can be omitted,

$$\left(\frac{\partial(c^2)^{\frac{3}{2}}}{\partial\rho}\right)_{T,P=P_0} = \frac{3}{2}c_0\left(\frac{\partial c^2}{\partial\rho}\right)_{T,P=P_0} = \frac{3}{2}\lambda\frac{c_0^3}{\rho_0}$$

and the final expression, which will be applied to predict the speed of sound, takes the form

$$c = c_0 \left[1 + \frac{3}{2}\kappa_T^0\lambda(P - P_0)\right]^{\frac{1}{3}}. \quad (7)$$

3. Results

The principal studies aimed an investigation the possibility of application of the approach based on the assumption of the linearity of the pressure dependence of the speed of sound cubed (1) and the power-law scaling of the reduced pressure fluctuations (6) as the premise for searching the principal control parameter of this method, can be subdivided into two particular subtasks. The first one is the test of the validity of Eq. (6) at ambient pressure. Due to a large number of available experimental data, we analyze the universality of such dependence and its power-law parameter. As the next step, we apply the revealed control quantities to the direct test of the predictive capacity of the expression (7).

3.1. Using experimental data under ambient pressure: a test of the power-law scaling

The data on the density and the speed of sound filtered as described in subsection 2.2, were polynomially fitted as functions of the temperature: if a dataset is short (less than five data points), the linear fit was applied; otherwise – the quadratic one; for the sake of numerical stability, the centering and scaling of the data was applied as an intermediate step during the regression procedure. The resulting approximations of the data and the respective data themselves are shown in Fig. 1. One can see that the fitting functions (lines) reproduce the course of data (circles) sufficiently accurately.

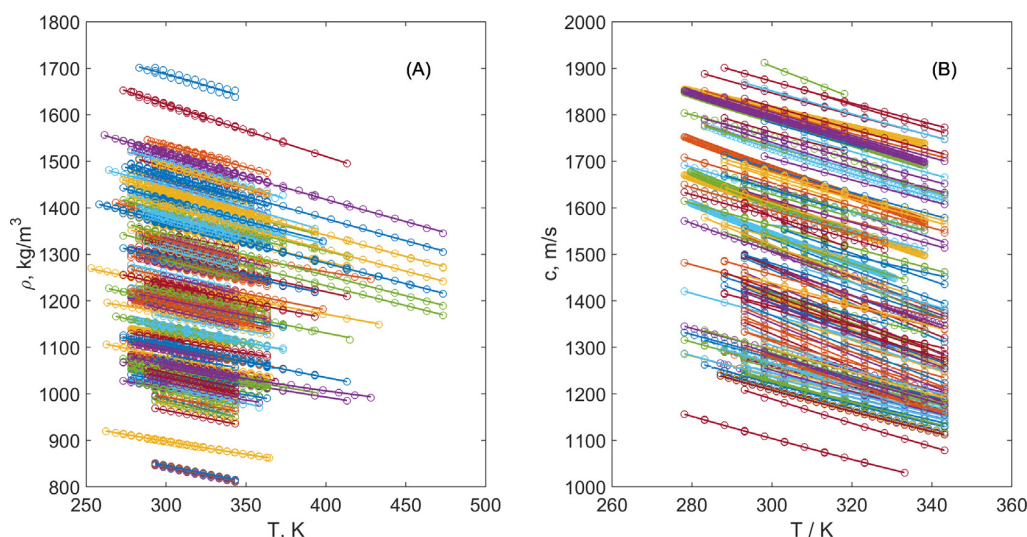


Fig. 1. The temperature dependencies of the density (A) and the speed of sound (B) at ambient pressure for 140 ionic liquids (each liquid is marked by a different color, see the complete list of ILS in Supplementary Information). Circles denote experimental data, and lines show linear or quadratic fits in the least mean squares sense.

The data were filtered in such a way that we used them to check the fulfillment of the power-law dependence on the density, Eq. (6).

For this purpose, the equispaced sets of the density and the speed of sound values were calculated with the polynomial approximations described above from $T = 293.15$ K to $T = 343.15$ K (this interval covers the majority of existing experimental measurements, see Fig. 1(B)), with the step 10 K. Fig. 2 represents the respective plots, where the experimental-based quantities are shown as dot. In double logarithmic coordinates used for demonstrability, one can see that they follow straight lines

$$\ln(v_s) = \ln(A) + \lambda \ln(\rho) \quad (8)$$

as expected from Eq. (6).

The linear regression (shown as a line for each dataset in Fig. 2) gives the slope of such a line, i.e., the desired parameter λ . Even by a naked eye, it is visible that all slopes are very similar. The descriptive statistics confirm this; see the box-and-whiskers plot, Fig. 3(A), which indicates that they are concentrated within a rather narrow range. At the same time, there are several outliers denoted as red pluses, a few already, 7 of 139. This liquids are: N-methyl-2-oxopyrrolidinium formate, trimethylammonium hydrogen sulfate, 2-hydroxy-N,N,N-trimethylethanaminium (S)-2-hydroxypropanoate, N-(2-hydroxyethyl) benzenaminium propionate, 1-hexyl-3-methylimidazolium thiocyanate, 1-ethyl-1-methylpyrrolidinium ethyl sulfate, and 3-hexyl-1-methyl-1H-imidazolium bromide. A more detailed investigation of the respective experimental data revealed that these substances are characterized by a limited number of experimental data, which still have a rather irregular scattering with high uncertainty around the fitting polynomials. Therefore, they should be excluded from consideration from the statistical point of view as requiring additional experimental measurements aimed at the more reliable determination of their thermodynamic properties.

Fig. 3(B) demonstrates the distribution histogram for the rest of 132 ionic liquids, which are accepted as based on reliable data; bins of the histogram are centered in points from 9.25 to 12 with equal widths of 0.25. It can be stated that the range of change of λ for ionic liquids is quite narrow. The distribution has a clear maximum, the model is $\lambda = 9.14$; the mean value is $\lambda = 10.55$, close to

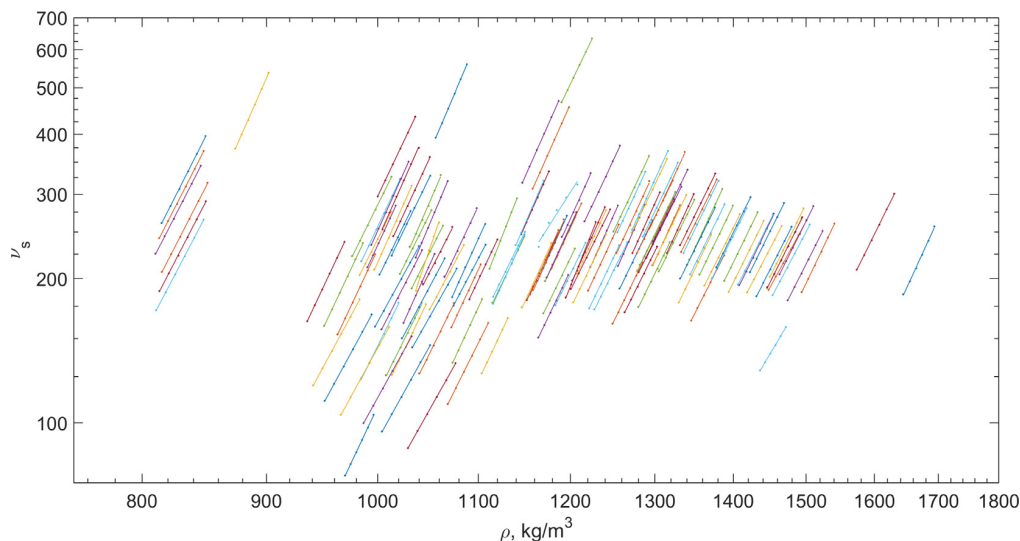


Fig. 2. The dependence of dimensionless reduced pressure fluctuations on the density in 140 ionic liquids (the color coding is the same as in Fig. 1); dots are values calculated with the fits of experimental data, and straight lines are the linear fits of the latter considered in the double logarithmic coordinates.

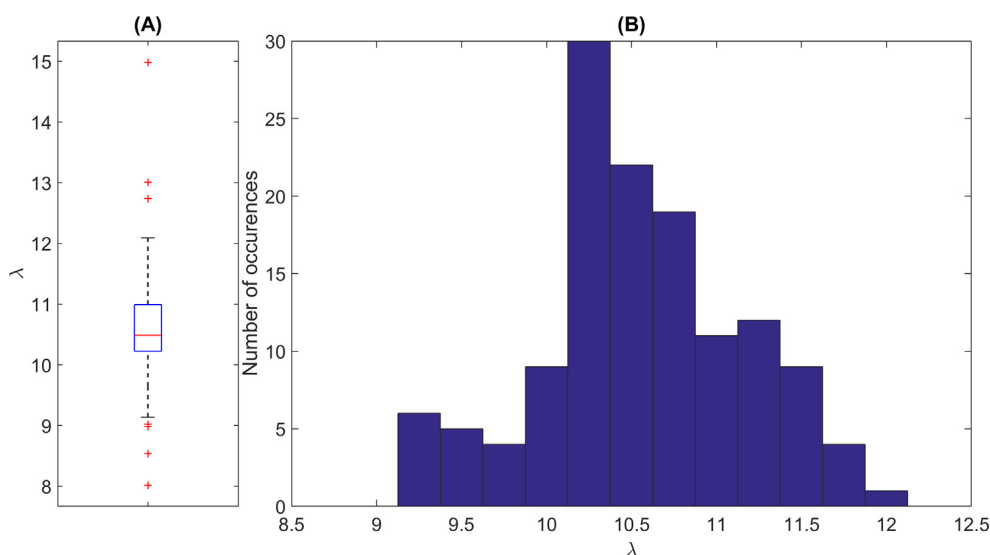


Fig. 3. A standard box-and-whiskers plot describing statistics of the parameter λ for all 139 explored ionic liquids (A) and the distribution of λ values with excluded outliers (B).

the median equal to $\lambda = 10.50$; the standard deviation is equal to $\text{std}(\lambda) = 0.61$.

3.2. The results of calculations of the speed of sound in the high-pressure range

Usually, the experimental data for ILs, the density, and speed of sound at atmospheric pressure, are much more common than experimental data for the speed of sound in the high-pressure range. Our work focused only on experimental data from the ILThermo database intended to not refer to any data either calculated or predicted by any model approaches that are not observed in real measurements. Based on this, the high-pressure values of speed of sound for nine ILs were collected. The speed of sound of ILs was predicted and assessed using 589 data points using Eq.

(7) with parameters found using only the fitting experimental data measured at ambient pressure.

Fig. 4 shows an example of such data preprocessing for 1-ethyl-3-methylimidazolium bis((trifluoromethyl)sulfonyl)imide. It is worth noting that such a filtering procedure is already necessary since it is visible that the experimental data are already very scattered, especially on the density, speed of sound, and isobaric heat capacity. In our approach, large outliers, marked as red 'x,' some of which are beyond any reasonable experimental uncertainty, were excluded from the trend during the evaluation procedure. The rest of the data were used to calculate parameters of Eq. (7) and the speed of sound itself with this formula.

Fig. 5 presents a comparison of the pressure dependence of the speed of sound of 1-ethyl-3-methylimidazolium bis((trifluoromethyl)sulfonyl)imide between the values calculated via this route and collected experimental results. We obtained one of the better

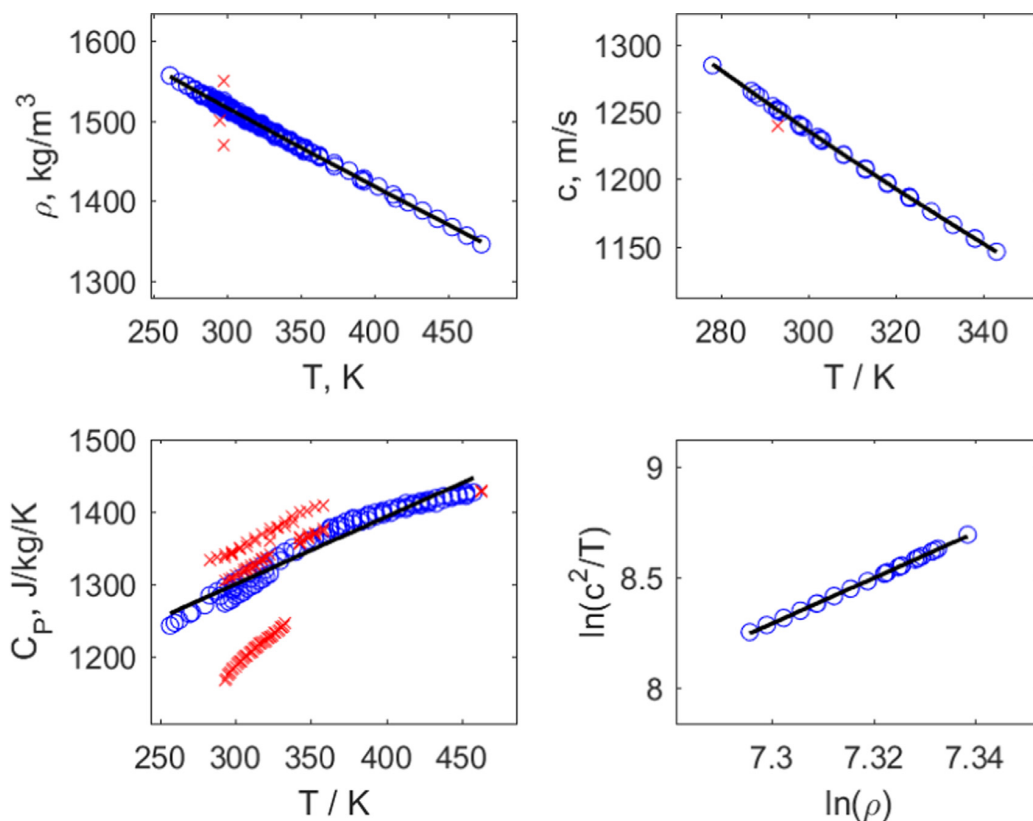


Fig. 4. The density, speed of sound, heat capacity as a function of temperature, and the natural logarithm of the square of the speed of sound to temperature as a function of the natural logarithm of density for 1-ethyl-3-methylimidazolium bis((trifluoromethyl) sulfonyl)imide.

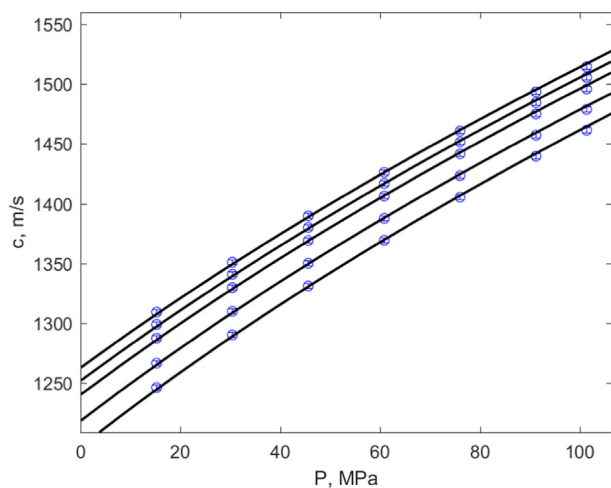


Fig. 5. A comparison of the pressure dependence of the speed of sound between FT-EoS and collected experimental results for 1-ethyl-3-methylimidazolium bis((trifluoromethyl)sulfonyl)imide for (288, 292, 298, 308 and 318) K from up to down.

results for this IL, where the average absolute deviations (AAD) were only 0.1 %.

At the same time, it should be stressed that such a perfect prediction is achieved due to the regularity and consistency of the reference data used for the determination of the parameters. Our second example, 1-butyl-3-methylimidazolium hexafluorophosphate illustrates this caveat. Fig. 6 indicates that the data provided

by different authors are significantly inconsistent that influence the prediction quality even after removing the most deviating ones. In this respect, the uncertainty in the pressure and the speed of sound is most influential for two reasons: 1) the term $1/(\rho_0 \kappa_T^0)$ is leading in Eq. 3 and, respectively, influences the slope of the speed of sound cubed as a function of the pressure; 2) deviations in the speed of sound c_0 directly lead to the displacements in the whole set of the resulting $C(P)$ as it directly follows from Eq. (7). The latter fact is the most obvious: among the data $c_0(T)$ shown in Fig. 6, one can see a sequence of points, which follow the dashed line shifted relatively to other data following the solid line. The fact is that values at ambient pressure correspond to measurements reported for high pressures. As a result, the predicted values obtained using the most consistent regularities in the data at ambient pressure give the relative average absolute deviations 2.5 % from the experimentally reported values. They are shown in Fig. 7 as solid lines and circles, respectively. On the other hand, if to refer to the initial values of the speed of sound, which are 1.5 % less than the other (the dashed line in Fig. 6), the deviation reduces down to 0.94 %, see the dashed curves in Fig. 7. The difference in the slope still kept even, in this case, originates from uncertainty in the density values forming rather a wide stripe than a line in Fig. 6.

The obtained results for all collected ILs with model characteristic λ , average absolute deviations (AAD), and uncertainties of experimental data $unstr_{exp}$ are presented in Table 1. By applying our method, the agreement, well-coordinated with the possibilities of actual experimental methods, is observed between experimental and predicted high-pressure speed of sound data for all collected ILs from the ILThermo database. An overall relative average absolute deviation (RAAD) is close to 0.85 %.

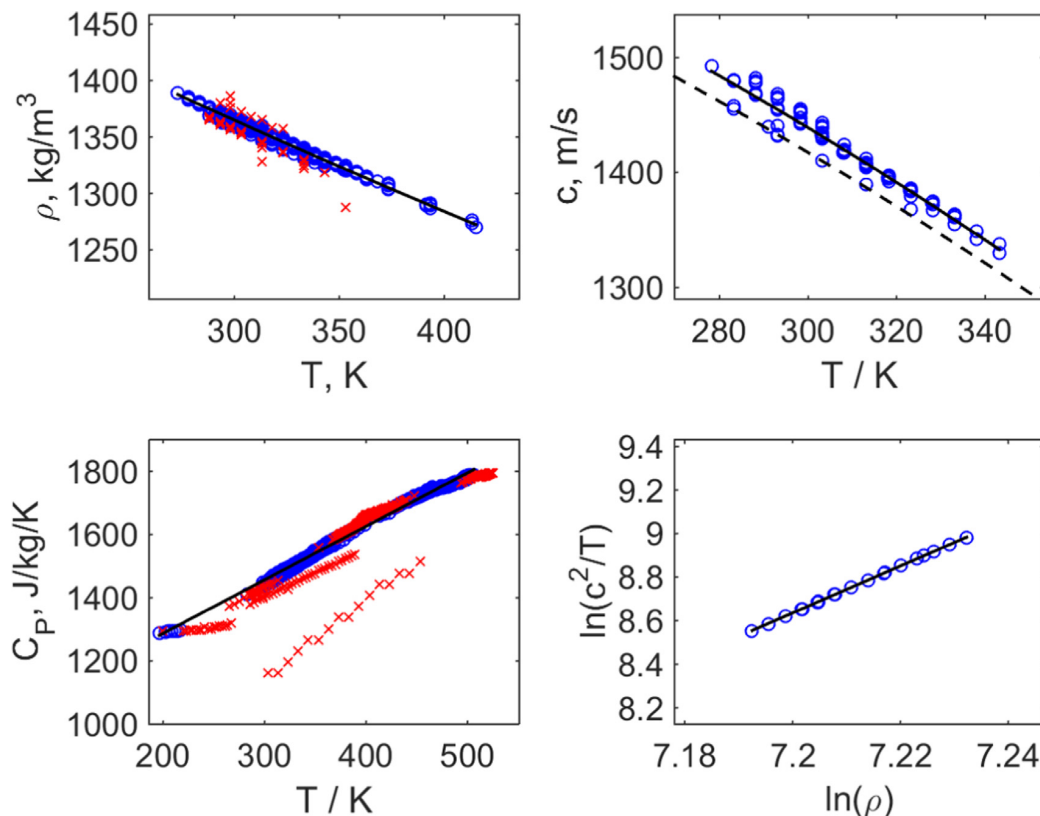


Fig. 6. The density, speed of sound, heat capacity as a function of temperature, and the natural logarithm of the square of the speed of sound to temperature as a function of the natural logarithm of density for 1-butyl-3-methylimidazolium hexafluorophosphate.

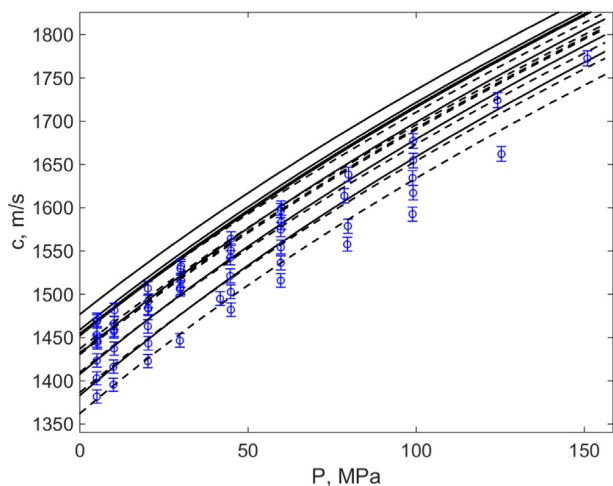


Fig. 7. A comparison of the pressure dependence of the speed of sound between FT-EoS and collected experimental results for 1-butyl-3-methylimidazolium hexafluorophosphate for (283, 291, 293, 294, 303, 313 and 323) K from up to down.

4. Discussion

The possibility of an approximate prediction of the speed of sound in ionic liquids under elevated pressures and on the data obtained at ambient pressure has premises in two kinds of scaling dependencies: between the speed of sound and the pressure, and

Table 1
Obtained results for all collected ILs from ILThermo database with model characteristic λ , average absolute deviations (AAD) and uncertainties of experimental data $unstr_{exp}$. The maximal pressures are either 100 MPa or 150 MPa.

IL name	λ	AAD [%]	$unstr_{exp}$ [%]
1-butyl-3-methylimidazolium dicyanamide	10.2	1.2	1.4
1-butyl-3-methylimidazolium tetrafluoroborate	10.6	1.2	0.43
1-butyl-3-methylimidazolium hexafluorophosphate	10.8	2.4	0.53
1-butyl-3-methylimidazolium hexafluorophosphate	10.8	0.94*	0.53
1-butyl-3-methylimidazolium trifluoromethanesulfonate	10.4	1.1	1.4
1-ethyl-3-methylimidazolium bis((trifluoromethyl) sulfonyl)imide	10.2	0.1	0.15
1-butyl-3-methylimidazolium bis((trifluoromethyl) sulfonyl)imide	10.4	0.16	0.23
1-butyl-1-methylpyrrolidinium bis((trifluoromethyl) sulfonyl)imide	10.6	0.56	1.1
1-methyl-3-pentylimidazolium bis((trifluoromethyl) sulfonyl)imide	10.5	0.43	0.2
1-hexyl-3-methylimidazolium bis((trifluoromethyl) sulfonyl)imide	10.4	0.076	0.47

* When the speeds of sound at ambient pressure are coordinated with the values provided in the same source as for the high-pressure data, their relative difference with the data obtained by averaging over all available sources is about 1.5 %.

between the thermodynamic fluctuations of thermodynamic quantities and the density.

The first kind of scaling is dated back to the empiric Rao rule, which was initially detected for the ambient pressure data [25] in the form

$$\frac{c^{1/3}}{\rho} = K \quad (9)$$

where K is a compound-specific constant. Later, the similar expression

$$\frac{c^{1/3}}{\rho} = K' \quad (10)$$

was found [26] for the dependencies measured along isotherms. However, it should be pointed out that the parameter K' included in Eq. (10) does not coincide with K included in Eq. (9), making impossible the direct transfer of data from the isobaric to the isothermal path [22,23]. At the same time, the isothermal functional form (10) has a more substantial background from the molecular point of view [27,28]. Note that it can be rewritten as

$$c^3 = K' \rho^9, \quad (11)$$

whence one needs to consider the relation of the 9th degree of the density along an isotherm to the pressure applied. Nevertheless, there is no universal power-law dependence valid for all kinds of liquids and pressure range [29] although it can be found for very high pressure. Recently, this fact was explained within the frame of the two-state model [30], which considers the structural difference between the loosely and closely packed structure of a liquid under moderate and high pressures, respectively.

At the same time, there is a more accurate *adiabatic* equation of state first proposed by Brinkley Jr & Kirkwood [31] and well-supported further experimental investigations. It has the form

$$P - P_0 = B(S) \left[\left(\frac{\rho}{\rho_0} \right)^\gamma - 1 \right], \quad (12)$$

as a direct generalization of the adiabatic equation of state of gases but here γ is not the ratio of heat capacities but some empiric coefficient.

It is well-known that the entropy of liquid changes more slowly along isotherms than along the ambient pressure isobar. As a consequence, the expression similar to Eq. (12) is sometimes used for the isothermal change of the density (Murnaghan's equation); in particular, Chueh & Prausnitz [32] considered the dependence

$$\left(\frac{\rho}{\rho_0} \right)^9 = 1 + 9\kappa_T^0 (P - P_0), \quad (13)$$

where κ_T^0 is the isothermal compressibility at ambient (or saturation) pressure for several organic liquids.

The same form as Eq. (13) with $\gamma = 9 \div 11$ has also been actively explored more recently [33–35] within the concept of the density scaling regime of different compressed liquids including ionic ones. The substitution of Eq. (13) in Eq. (11) gives

$$c^3 = K' \rho_0^9 [1 + 9\kappa_T^0 (P - P_0)], \quad (14)$$

i.e. the same dependence of the speed of sound cubed, which we used as the principal assumption in our derivation; here $K' \rho_0^9 = c_0^3$ but the coefficient K' itself is still indefinite.

At the same time, it is worthy that the more accurate is the isobaric equation rather than the isothermal one. Thus, we need to

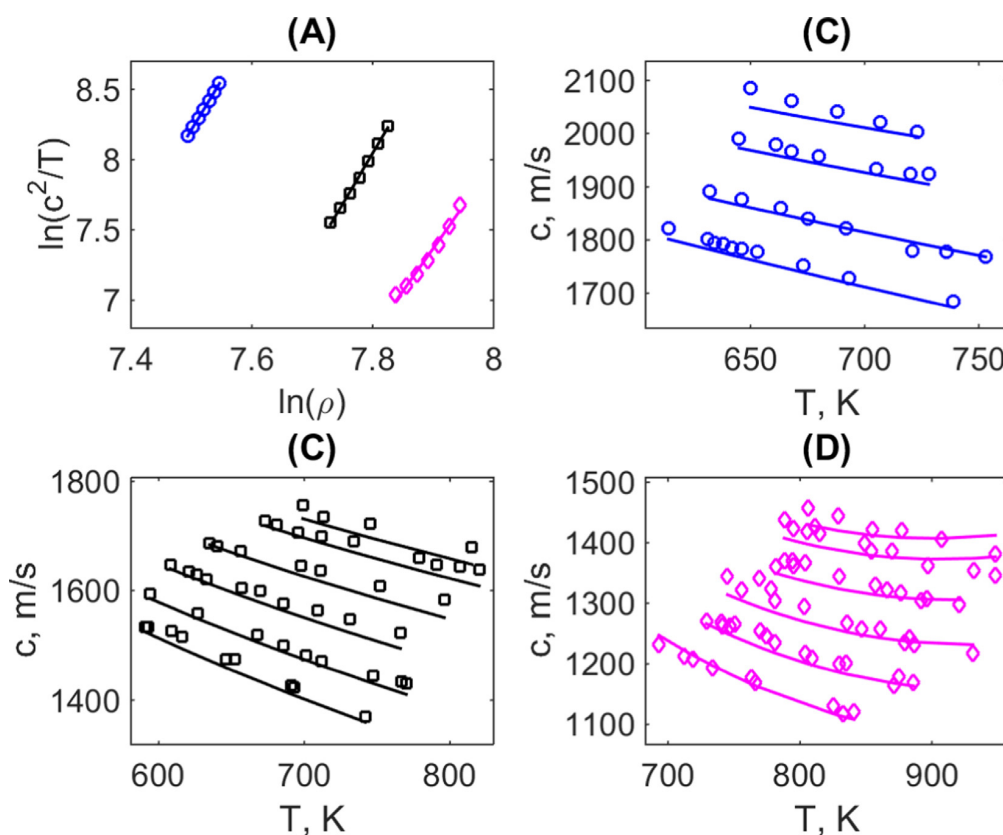


Fig. 8. (A) The plot demonstrating the density scaling of the variable part of the reduced pressure analogues to Fig. 2 NaNO₃ (circles), RbNO₃ (squares), and CsNO₃ (diamonds); comparisons of the predicted and experimental data: (B) for NaNO₃ along isobars (18.6, 100.0, 200.0, and 283.0) MPa ordered from down to up; (C) for RbNO₃ along isobars (25.2, 84.4, 153.0, 227.8, 304.2, and 343.8) MPa ordered down to up; (D) for CsNO₃ along isobars (23.6, 85.4, 153.1, 227.7, 304.2, and 346.4) MPa ordered from down to up.

operate with relations that are less sensitive to the change in thermodynamic path. In this sense, it is crucial that the sound spread is an adiabatic (isentropic) process and fluctuations of the pressure, expressed via the speed of sound Eq. 2, and the fluctuations of entropy are independent [24]. Thus, when we used the fitting of the reduced pressure fluctuations as a power-law function of the density along an isobaric path (where the entropy changes significantly), we are entitled to transfer the obtained power-law index to the isothermal path. This is the main advantage of our approach, based on the fundamental statistical physics, over Rao's (or Rao-Carnevale-Litovitz's) approach, which lacks such invariance.

Finally, as a short additional test, we applied our approach to predict the speed of sound under pressure for molten salts, which, as ionic liquids, belong to the class of substances with strong ionic interaction but exist in liquid state in a much more high range of temperatures. It is worth noting that the number of high-pressure speed of sound data for molten salts is extremely scarce. Thus, as an example for this case study we used high-pressure experimental data for three molten salts, namely i) sodium nitrate, NaNO_3 , ii) rubidium nitrate, RbNO_3 , and iii) cesium nitrate, CsNO_3 reported in the work [36]. The full set of thermodynamic data measured at atmospheric pressure was taken from Refs. [37–40]. The obtained results for these compounds are shown in Fig. 8 as a comparison of the predicted (lines) and the experimental (markers) values.

The primary question, which should be answered as giving the principal criterion of validity of the model (7), is whether the reduced pressure fluctuations scale as a power-law function of the density. Fig. 8 positively answers this question: for NaNO_3 and RbNO_3 linearity of the fit looks perfect, the situation CsNO_3 is less accurate but still acceptable. Note that the original experimental data for this molten salt are also more scattered compared to two others that may originate from complications with the measurements at higher temperatures. The values of the scaling parameter λ are equal to 7.12, 7.24, and 6.04 for NaNO_3 , RbNO_3 , and CsNO_3 , respectively. These values are less than for room-temperature ionic liquids shown in Fig. 3. This fact is in line with the observation that the classic isobaric Rao's parameter is less than most molecular liquids, as discussed in Ref. [37].

However, these diminished values of the scaling parameter do not prevent the possibility of predicting the speed of sound in molten salts at elevated pressures, even up to the higher pressures in comparison with room-temperature ionic liquids, as one can see in Figs. 8 (B)–(D). Note that the data are represented along isobars correspondingly to the procedure of measurements and raw experimental data reported in Ref. [36]. The AADs for NaNO_3 , RbNO_3 , and CsNO_3 are 0.77 %, 1.02 %, and 1.20 %, respectively. We would like to highlight that uncertainty of experimental data themselves is about 1 %. Therefore the predictions are in the range of uncertainty of the measured values (also note a visible scattering of the latter in Figs. 8 (B)–(D)).

Thus, we can conclude that the strong ionic interactions and high temperatures do not hinder the use of the proposed methods, as demonstrated by its application to molten salts.

5. Conclusions

In light of this work, one can conclude that the proposed method can truly predict the speed of sound of ILs under high-pressure conditions with high accuracy. The density, speed of sound, and isobaric heat capacity at atmospheric pressure were used for the calculations. The modifications and modeling of the equation of state based on the fluctuation theory for first density, isobaric thermal expansion coefficient, isothermal compressibility, and second speed of sound are the strong fundamentals of useful

equations of state for the prediction various thermophysical properties. It is worth noting that this proposed model of fluctuation equation of state based on the knowledge of simple physicochemical properties obtained from an uncomplicated experiment at atmospheric pressure correctly predicts the thermodynamic properties of compressed liquid phase without prior knowledge of any properties of the tested object under elevated pressure. At the same time, we need to attract attention to the fact that such an approach requires establishing the consistency of the respective experimental data because the predictive capacity of the model at high pressures is heavily dependent on the accuracy of inputs used for the calculation of its parameters. This mathematical model will be, in the future, the starting point for the construction of relatively easy calculation tools for full and proper thermodynamic descriptions of compressed liquids.

6. Author Contributions

Bernadeta Jasiok – Conceptualization, Methodology, Validation, Formal analysis, Investigation, Resources, Data Curation, Writing - Original Draft, Writing - Review & Editing, Visualization, Project administration; Eugene B. Postnikov – Conceptualization, Methodology, Software, Validation, Formal analysis, Investigation, Resources, Data Curation, Writing - Original Draft, Writing - Review & Editing, Visualization, Supervision, Project administration; Ivan Yu. Pikalov – Software, Resources, Writing - Review & Editing; Mirosław Chorążewski – Conceptualization, Validation, Investigation, Resources, Writing - Review & Editing, Supervision, Funding acquisition.

Declaration of Competing Interest

The authors declare that they have no known competing financial interests or personal relationships that could have appeared to influence the work reported in this paper.

Acknowledgements

This work was supported by a grant from the National Science Centre (Poland) Decision No. 2016/23/B/ST8/02968 and PIK – Program for new interdisciplinary elements of education at the doctoral level for a field of chemistry, POWR.03.02.00–00–1010/17 (Poland).

Appendix A. Supplementary material

Supplementary data associated with this article can be found, in the online version, at <https://doi.org/10.1016/j.molliq.2022.119792>.

References

- [1] D.D. Patel, J.-M. Lee, Applications of ionic liquids, *Chem. Rec.* 12 (2012) 329–355, <https://doi.org/10.1002/tcr.201100036>.
- [2] A.J. Greer, J. Jacquemin, C. Hardacre, Industrial applications of ionic liquids, *Molecules* 25 (2020) 5207, <https://doi.org/10.3390/molecules25215207>.
- [3] A. Ray, B. Saruhan, Application of ionic liquids for batteries and supercapacitors, *Materials* 14 (2021) 2942, <https://doi.org/10.3390/ma14112942>.
- [4] A. Queimada, J. Coutinho, I. Marrucho, J.-L. Daridon, Corresponding-states modeling of the speed of sound of long-chain hydrocarbons, *Int. J. Thermophys.* 27 (4) (2006) 1095–1109.
- [5] K.-J. Wu, Q.-L. Chen, C.-H. He, Speed of sound of ionic liquids: Database, estimation, and its application for thermal conductivity prediction, *AIChE J.* 60 (3) (2014) 1120–1131.
- [6] J. Skowronek, M. Dzida, E. Zorębski, M. Chorążewski, S. Jeżak, M. Żarska, M. Zorębski, P. Goodrich, J. Jacquemin, High pressure speed of sound and related thermodynamic properties of 1-alkyl-3-methylimidazolium bis

- [(trifluoromethyl) sulfonyl] imides (from 1-propyl- to 1-hexyl-), *Journal of Chemical & Engineering Data* 61 (11) (2016) 3794–3805.
- [7] J.-L. Daridon, Predicting and correlating speed of sound in long-chain alkanes at high pressure, *Int. J. Thermophys.* 43 (5) (2022) 1–32.
- [8] J. Pilarz, I. Polishuk, M. Chorążewski, Prediction of sound velocity for selected ionic liquids using a multilayer feed-forward neural network, *J. Mol. Liq.* 347 (2022) 118376, <https://doi.org/10.1016/j.molliq.2021.118376>.
- [9] J. Pilarz, J. Feder-Kubis, V.V. Melent'ev, O.S. Ryshkova, V.I. Korotkovskii, A.K. Radchenko, E.B. Postnikov, M. Chorążewski, I. Polishuk, Speeds of sound in ionic liquids under elevated pressures. new experimental data and cp-pc-saft modelling, *J. Mol. Liq.* 303 (2020) 112669, <https://doi.org/10.1016/j.molliq.2020.112669>.
- [10] Y. Xu, R. Shahriari, Prediction of second order derivative thermodynamic properties of ionic liquids using saft-vr morse equation of state, *Fluid Phase Equilib.* 549 (2021) 113204, <https://doi.org/10.1016/j.fluid.2021.113204>.
- [11] F. Bakhtazma, F. Alavi, Second-order thermodynamic derivative properties of ionic liquids under epc-saft: the effect of partial ionic dissociation, *Industr. Eng. Chem. Res.* 58 (2019) 22408–22417, <https://doi.org/10.1021/acs.iecr.9b05593>.
- [12] M. Chorążewski, E.B. Postnikov, B. Jasiok, Y.V. Nedyalkov, J. Jacquemin, A fluctuation equation of state for prediction of high-pressure densities of ionic liquids, *Scientific Reports* 7 (2017) 1–9, <https://doi.org/10.1038/s41598-017-06225-9>.
- [13] B. Jasiok, E.B. Postnikov, M. Chorążewski, The prediction of high-pressure densities of different fuels using fluctuation theory-based tait-like equation of state, *Fuel* 219 (2018) 176–181, <https://doi.org/10.1016/j.fuel.2018.01.091>.
- [14] B. Jasiok, A.R. Lowe, E.B. Postnikov, J. Feder-Kubis, M. Chorążewski, High-pressure densities of industrial lubricants and complex oils predicted by the fluctuation theory-based equation of state, *Industrial & Engineering Chemistry Research* 57 (34) (2018) 11797–11803, <https://doi.org/10.1021/acs.iecr.8b01542>.
- [15] E.B. Postnikov, B. Jasiok, V.V. Melent'ev, O.S. Ryshkova, V.I. Korotkovskii, A.K. Radchenko, A.R. Lowe, M. Chorążewski, Prediction of high pressure properties of complex mixtures without knowledge of their composition as a problem of thermodynamic linear analysis, *J. Mol. Liq.* 310 (2020) 113016, <https://doi.org/10.1016/j.molliq.2020.113016>.
- [16] E.B. Postnikov, I.T. Pikalov, M. Chorążewski, Thermal conductivity of ionic liquids: recent challenges facing theory and experiment, *Journal of Solution Chemistry*, submitted.
- [17] M. Dzida, E. Zorębski, M. Zorębski, M. Żarska, M. Geppert-Rybczyńska, M. Chorążewski, J. Jacquemin, I. Cibulka, Speed of Sound and Ultrasound Absorption in Ionic Liquids, *Chemical Reviews* 117 (2017) 3883–3929, <https://doi.org/10.1021/acs.chemrev.5b00733>.
- [18] B.A. Oakley, D. Hanna, M. Shillor, G. Barber, Ultrasonic parameters as a function of absolute hydrostatic pressure. II. Mathematical models of the speed of sound in organic liquids, *J. Phys. Chem. Ref. Data* 32 (2003) 1535–1544, <https://doi.org/10.1063/1.1555589>.
- [19] Y.S. Shoitov, N. Otpushchennikov, Pressure dependence of the speed of sound in liquids, *Soviet Physics Journal* 11 (12) (1972) 129–130.
- [20] A.R. Lowe, B. Jasiok, V.V. Melent'ev, O.S. Ryshkova, V.I. Korotkovskii, A.K. Radchenko, E.B. Postnikov, M. Spinnler, U. Ashurova, J. Safarov, E. Hassel, M. Chorążewski, High-temperature and high-pressure thermophysical property measurements and thermodynamic modelling of an international oil standard: Ravenol diesel rail injector calibration fluid, *Fuel Process. Technol.* 199 (2020) 106220, <https://doi.org/10.1016/j.fuproc.2019.106220>.
- [21] V.V. Melent'ev, M.F. Bolotnikov, Y.A. Neruchev, Speeds of sound, densities, and isentropic compressibilities of 1-iodohexane at temperatures from (293.15 to 413.15) K and pressures up to 200 MPa, *Journal of Chemical & Engineering Data* 50 (4) (2005) 1357–1360, doi:10.1021/je050069s.
- [22] B.B. Kudryavtsev, G.A. Samgina, Use of ultrasonic measurements in the study of molecular interactions in liquids, *Soviet Physics Journal* 9 (1966) 5–8, <https://doi.org/10.1007/BF00818478>.
- [23] R.A. Aziz, D.H. Bowman, C.C. Lim, An examination of the relationship between sound velocity and density in liquids, *Can. J. Phys.* 50 (1972) 646–654, <https://doi.org/10.1139/p72-089>.
- [24] L.D. Landau, E.M. Lifshitz, *Statistical Physics*, Vol. 5, Elsevier, 2013.
- [25] M.R. Rao, Velocity of sound in liquids and chemical constitution, *J. Chem. Phys.* 9 (1941) 682–685, <https://doi.org/10.1063/1.1750976>.
- [26] E.H. Carnevale, T.A. Litovitz, Pressure dependence of sound propagation in the primary alcohols, *J. Acoust. Soc. Am.* 27 (1955) 547–550, <https://doi.org/10.1121/1.1907959>.
- [27] R.V.G. Rao, B.S.M. Rao, Variation of sound velocity through liquids with pressure, *Trans. Faraday Soc.* 62 (1966) 2704–2708, <https://doi.org/10.1039/TF9666202704>.
- [28] W. Schaaffs, Molekularakustische Ableitung einer Zustandsgleichung für Flüssigkeiten bei hohen Drucken, *Acustica* 30 (1974) 275–280.
- [29] J.R. Macdonald, Some simple isothermal equations of state, *Rev. Mod. Phys.* 38 (1966) 669–679, <https://doi.org/10.1103/RevModPhys.38.669>.
- [30] B. Jasiok, E.B. Postnikov, M. Chorążewski, The prediction of high-pressure volumetric properties of compressed liquids using the two states model, *Physical Chemistry Chemical Physics* 21 (29) (2019) 15966–15973, <https://doi.org/10.1039/C9CP02448D>.
- [31] S.R. Brinkley Jr, J.G. Kirkwood, Theory of the propagation of shock waves, *Phys. Rev.* 71 (1947) 606–611, <https://doi.org/10.1103/PhysRev.71.606>.
- [32] P.L. Chueh, J.M. Prausnitz, A generalized correlation for the compressibilities of normal liquids, *AIChE J.* 15 (1969) 471–472, <https://doi.org/10.1002/aic.690150335>.
- [33] A. Grzybowski, K. Koperwas, A. Swiety-Pospiech, K. Grzybowska, M. Paluch, Activation volume in the density scaling regime: Equation of state and its test by using experimental and simulation data, *Physical Review B* 87 (2013) 054105, <https://doi.org/10.1103/PhysRevB.87.054105>.
- [34] A. Grzybowski, K. Koperwas, M. Paluch, Equation of state in the generalized density scaling regime studied from ambient to ultra-high pressure conditions, *J. Chem. Phys.* 140 (2014) 044502, <https://doi.org/10.1063/1.4861907>.
- [35] A. Grzybowski, A.R. Lowe, B. Jasiok, M. Chorążewski, Volumetric and viscosity data of selected oils analyzed in the density scaling regime, *J. Mol. Liq.* 353 (2022) 118728, <https://doi.org/10.1016/j.molliq.2022.118728>.
- [36] J. Petitot, L. Denielou, R. Tufeu, Thermodynamic properties of molten nitrates under pressure obtained from velocity of sound, *Physica B+C* 144 (1987) 320–330, [https://doi.org/10.1016/0378-4363\(87\)90013-1](https://doi.org/10.1016/0378-4363(87)90013-1).
- [37] R. Higgs, T. Litovitz, Ultrasonic Absorption and Velocity in Molten Salts, *J. Acoust. Soc. Am.* 32 (1960) 1108–1115, <https://doi.org/10.1121/1.1908357>.
- [38] L. Denielou, J.-P. Petitot, C. Tequi, D. Sirousse-Zia, Masse volumique et coefficient de dilatation des nitrates alcalins fondus et de leurs mélanges, *Journal de Chimie Physique* 74 (1977) 247–248, <https://doi.org/10.1051/jcp/1977740247>.
- [39] P. Cerisier, G. Finiels, Y. Doucet, La célérité des ultra-sons et son exploitation thermodynamique dans les mélanges de sels fondus-II. — Études de quelques halogénures et nitrates alcalins, *Journal de Chimie Physique* 71 (1974) 836–841, <https://doi.org/10.1051/jcp/1974710836>.
- [40] D. Sirousse-Zia, L. Denielou, J. Petitot, C. Tequi, Complément à l'étude thermodynamique de sels fondus à anion polyatomique, *J. de Physique Lett.* 38 (1977) 61–63, <https://doi.org/10.1051/jphyslet:0197700380206100>.

Katowice, 11.04.2023 r.

Instytut Chemii
Wydział Nauk Ścisłych i Technicznych
Uniwersytet Śląski w Katowicach
ul. Bankowa 12, 40-007 Katowice

Statement on the contribution to the publication

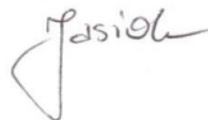
Publication:

B. Jasiok, E.B. Postnikov, I.Yu. Pikalov, M. Chorążewski, Prediction of the speed of sound in ionic liquids as a function of pressure. *Journal of Molecular Liquids* **2022**, 363, 119792, DOI: 10.1016/j.molliq.2022.119792.

We hereby state that the contribution to the work published jointly with Bernadeta Jasiok is in accordance with the description below:

Bernadeta Jasiok

I was responsible for: Conceptualization, Methodology, Validation, Formal analysis, Investigation, Resources, Data Curation, Writing – Original Draft, Writing – Review & Editing, Visualization, Project administration.



Eugene B. Postnikov

I was responsible for: Conceptualization, Methodology, Software, Validation, Formal analysis, Investigation, Resources, Data Curation, Writing – Original Draft, Writing – Review & Editing, Visualisation, Supervision, Project administration.



Ivan Yu. Pikalov

I was responsible for: Software, Resources, Writing – Review & Editing.



Mirosław Chorążewski

I was responsible for: Conceptualization, Methodology, Validation, Investigation, Resources, Writing – Review & Editing, Supervision, Project administration, Funding acquisition.

Mirosław Chorążewski



Liquid dibromomethane under pressure: a computational study†

Cite this: DOI: 10.1039/d0cp06458k

Bernadeta Jasiok,^a Mirostaw Chorazewski,^a Eugene B. Postnikov^b and Claude Millot^c

Received 14th December 2020,
Accepted 2nd January 2021

DOI: 10.1039/d0cp06458k

rsc.li/pccp

Molecular dynamics simulations have been performed on liquid dibromomethane at thermodynamic states corresponding to temperature in the range 268–328 K and pressure varying from 1 bar to 3000 bar. The interaction model is a simple effective two-body pair potential with atom–atom Coulomb and Lennard-Jones interactions and molecules are rigid. Thermodynamic properties have been studied, including the isobaric thermal expansion coefficient, the isothermal compressibility, the heat capacities and the speed of sound. The simulation results exhibit a crossing of the isotherms of the isobaric thermal expansion coefficient at about 800 bar in very good agreement with the prediction of an isothermal fluctuation equation of state predicting such a crossing in the pressure range 650–900 bar, though experimental results up to 1000 bar do not find any crossing.

1 Introduction

Thermophysical properties of liquids such as compressibilities, thermal expansivity and heat capacities are quantities of great interest in several fields of physics and physical chemistry. They are of fundamental interest to characterize the macroscopic properties of fluids, they can be used to test the quality of equation of states and their modeling can find useful applications in chemical engineering. Thus many studies have been devoted to experimental measurements of the thermophysical properties of liquids and mixtures. Particularly, the effect of temperature and pressure on isothermal and isentropic compressibility, isobaric thermal expansivity, constant volume and constant pressure heat capacities, speed of sound has been investigated by experiment for hundreds of molecular systems and mixtures.

For example, analysis of the pressure effects on isobaric thermal expansion coefficient α_p of water has revealed a particular behaviour with an increase of α_p vs. pressure at low temperatures and a decrease of α_p vs. pressure at higher temperatures.^{1,2} Isotherms of

α_p vs. pressure are found to cross in different pressure range (between 2500 and 5000 bar, depending on the temperature varying from 245 to 410 K).² Isobares of α_p vs. temperature cross at a temperature of ≈ 323 K²– ≈ 315 K³. This temperature has been found to correspond to the minimum of isothermal compressibility isobares vs. temperature.³

For many molecular liquids, experiments show that the isobaric thermal expansion coefficient isotherms cross at a given pressure or within a particular range of pressures – usually below 200 MPa –, depending on the explored temperature range, and at low pressure α_p increases as the temperature increases.^{4,5} This has been observed for example for noble gases,^{6–8} *n*-hexane⁹ and longer chain alkanes,¹⁰ bromo-1-alkanes,^{11,12} α,ω -dibromoalkanes except dibromomethane,¹³ quinoline,¹⁴ alkylamines,^{15–17} benzene and tetrachloromethane,¹⁰ ethanol¹⁸ (though no crossing was found in another study¹⁷), toluene.¹⁹ However, for other systems like for example several families of room temperature ionic liquids^{20–22} or 1-phenyldecane and 1-phenylundecane,²³ the crossing of α_p isotherms has not been observed and at low pressures, α_p decreases as the temperature increases. For alcohols like 1-nonanol, the same behaviour have been observed²⁴ whereas for 2-hexanol no crossing has been observed but at low pressures, α_p increases as the temperature increases.²⁵ Isomers of chloropropane have also different behaviours for the thermal expansion coefficient. For both 1-chloropropane and 2-chloropropane, at low pressure, $\partial\alpha_p/\partial T|_p$ is positive, but up to 65 MPa, no crossing of α_p isotherms is observed for 1-chloropropane and a crossing is observed for 2-chloropropane around 12 MPa. For dichloromethane, bromochloromethane and dibromomethane, no crossing of the thermal expansivity isotherms has been found up to 100 MPa²⁶ though a fluctuation model predicts a crossing for

^a Institute of Chemistry, University of Silesia in Katowice, Szkolna 9, 40-006 Katowice, Poland. E-mail: hjasiok@us.edu.pl

^b Department of Theoretical Physics, Kursk State University, Radishcheva St., 33, 305000 Kursk, Russia

^c Université de Lorraine, CNRS, LPCT, F-54000 Nancy, France, Boulevard des Aiguillettes, BP 70239, 54506 Vandoeuvre lès Nancy Cedex, France. E-mail: claudemillot@univ-lorraine.fr; Fax: +33 372745271; Tel: +33 372745281

† Electronic supplementary information (ESI) available: Force fields parameters, technical details characterizing the studies thermodynamic states and numerical values of the thermophysical properties are given in ten tables. See DOI: 10.1039/d0cp06458k

dibromomethane within the pressure range $\approx 65\text{--}90$ MPa.²⁷ In contrast, the experimental results and the predictions of the fluctuation model of α,ω -dibromoalkanes with from two to six carbon atoms exhibit a crossing within a narrow pressure range around 40 MPa.

Explanation of such behaviours of the isobaric thermal expansivity is not yet fully rationalized. Some attempts have been proposed relying on the analysis of the anisotropy of intermolecular vibrations^{11,12} and of the change of shape of the intermolecular potential induced by a pressure increase.²⁸ Apart from thermodynamic models and equation of states, computer simulations offer an alternative route to model thermophysical properties of liquids and potentially should be able to help to find a molecular interpretation of the above mentioned regular and abnormal behaviours in the temperature and pressure evolution of these properties. The thermophysical properties can be obtained from simulation by a thermodynamic route through *PVT* data or by fluctuation formulae in appropriate statistical ensembles.^{29–37} Comparisons of force field performances for modeling the thermophysical properties of organic liquids and mixtures have been published.^{38,39}

In this work, we have been interested in the case of dibromomethane and we chose to analyze its thermophysical properties by molecular dynamics (MD) simulations in the temperature range 268.15–328.15 K and at pressures up to 3000 bar (300 MPa). The choice of this substance among other representatives of the series α,ω -dibromoalkanes is motivated by the fact that dibromomethane allows taking into account an influence of halogen atoms in the most direct way. Especially it relates to the hypothesis connecting the crossing α_p isotherms with the molecular packing. With this respect, the presence of several pure methylene groups in longer α,ω -dibromoalkanes could make their influence more valuable. In particular, the packing ratio at the normal freezing/melting of the series from 1,3-dibromopropane to 1,6-dibromohexane belong to the narrow interval 0.63–0.64 despite different melting temperatures and densities (and even the odd–even effect), while dibromomethane is characterized by the more loose packing 0.59 at this condition. The respective values of the packing ratio has been determined as the product $\phi = \rho_m V_{\text{vdW}}$ of the densities ρ_m estimated at the melting temperatures⁴⁰ and the van der Waals volumes V_{vdW} calculated by the procedure given in ref. 41. Respectively, one can expect that this packing uniformity may be reflected in the uniformity of the isobaric isotherms crossing at higher temperatures and pressures.²⁷ At the same time, more specific packing of simpler molecules of dibromomethane provides expectations that molecular dynamics simulations may provide more direct insight in the microscopic origin of the mentioned phenomenon.

The main aim of this study is to clarify the disagreement between the experimental results showing no crossing of the α_p isotherms up to 100 MPa and the prediction of a fluctuation equation of state predicting a crossing in a relatively wide range of pressure below 100 MPa. In Section 2, details about the simulations are given. Section 3 presents our results for isobaric

thermal expansion coefficient, isothermal compressibility, constant volume and constant pressure heat capacities and speed of sound. The conclusion suggests a possible extension to this work.

2 Simulation details

The molecular geometry has been optimized at Hartree–Fock level with a 6-31G* basis set. The bond lengths are equal to 1.929817 Å for carbon–bromine and 1.071976 Å for carbon–hydrogen bonds. The angles Br–C–Br and H–C–H are equal to 113.1° and 112.1°, respectively. Atomic partial charges have been obtained from *ab initio* calculation at Hartree–Fock (HF) level with the 6-31G* basis set. This level of calculation is consistent with the derivation of the Amber force field parameters. A grid of 10 918 points surrounding a single molecule has been built with a spacing of 0.35 Å in each Cartesian direction with points located at distances between 1.5 and 2.5 times the van der Waals radius of each atom and removing the points located at distances from any atom which are smaller than 1.5 times its van der Waals radius. The electrostatic potential around the molecule has been computed at HF/6-31G* level at each point of the grid. Then, a set a charge has been optimized by the standard minimization of the mean square differences (over the grid of points) between the target *ab initio* electrostatic potential and the one reproduced by the set of atomic charges.^{42,43} The van der Waals radii are taken from Bondi for the carbon and bromine atoms and from Rowland for the hydrogen atom.^{44,45} The Lennard-Jones parameters have been taken from the GAFF2 force field and finely tuned in order to reproduce vaporization enthalpy at 298 and 313 K with the experimental density. After several tests including parameters of different hydrogen and carbon types of the GAFF2 force field and OPLS-AA parameters, a reasonable set has been obtained from the GAFF2 parameters of atoms corresponding to the types c3, br and hc of this force field, and slightly modified. The atomic charges and final Lennard-Jones parameters are gathered in Table S1 of the ESI.† *Ab initio* calculations have been performed with the Gaussian program⁴⁶ and the charges fitted with a home-made code.

MD simulations are performed using periodic boundary conditions (PBC) with $N = 1000$ rigid molecules in the central cubic box interacting through an atom–atom two-body potential containing Lennard-Jones and Coulomb interactions. Equations of motion are solved using center of mass degrees of freedom and a leapfrog quaternion algorithm due to Svanberg⁴⁷ with a time step equal to 2 fs. It is derived from an algorithm proposed by Fincham^{29,48} and improves the conservation of energy significantly. In this approach, the quaternion vector $Q(t + \Delta t/2)$ for each molecule is obtained iteratively. In our implementation of the algorithm, iterations are stopped when the norm of its variation between two consecutive iterations is lower than 10^{-9} . Electrostatic interactions are computed using lattice summations based on the Ladd approach, initially proposed for assemblies of point dipoles^{49–51} and generalized to systems of point charges^{52,53}

leading to expressions equivalent to the ones proposed by other groups.^{54,55} A reaction field contribution is added with the dielectric constant of the surrounding continuum equal to infinity, thus the method is physically equivalent to the standard Ewald approach.⁵¹ As previously, the expansion of the electrostatic interaction energy in cubic harmonics has been truncated at the rank 10, which has been proven to be sufficient to get good accuracy.^{51,56} The van der Waals interactions are truncated beyond a molecular-based cutoff of 20.0 Å. Usual corrections on potential energy and pressure due to this cutoff have been applied.²⁹ MD simulations are performed with home-made simulation codes.

The system has been studied at five temperatures varying from 268.15 to 328.15 K by step of 15 K and densities fitted to get nine pressures, specifically 1, 250, 500, 750, 1000, 1500, 2000, 2500, and 3000 bar (1 bar = 10⁵ Pa = 10⁵ kg m⁻¹ s⁻²). Each simulation, labeled by pressure P and temperature T , is obtained in two stages, an equilibration and thermalizing one and a production one.

During the equilibration and thermalization stage, the system is simulated during periods of 2×10^5 time steps at chosen densities with scaling of velocities and angular momenta every 100 steps in order to bring the system at the chosen temperature. The pressure is computed and used to guide the changes of density iteratively. After three iterations, one get desired pressures in the production runs with a maximum error of 0.7% (except for the runs at 1 bar, for which such an accuracy is unattainable with a reasonable simulation length).

Fig. 1 presents a comparison of the temperature and pressure dependence of the liquid density between our simulations and experimental results in the range 293–313 K and 1–1000 bar.²⁶ At 1 bar, the potential reproduces very well the density and its temperature dependence. As the pressure increases, the potential has the tendency to slightly underestimate the density (by $\simeq 0.3\%$ at 1000 bar) but the temperature evolution remains correct. Thus this potential, though quite simple, is reasonable to tackle a study of thermophysical properties of this liquid.

During the production stage of each simulation, 10⁶ time steps at constant energy (NVE simulation). Additionally, the

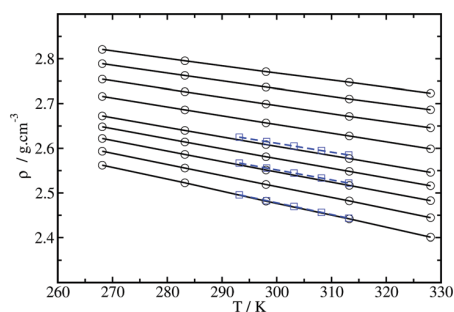


Fig. 1 Temperature dependence of the density of liquid dibromomethane. Black circles: simulation results at nine pressures (from bottom to top: 1, 250, 500, 750, 1000, 1500, 2000, 2500 and 3000 bar). Blue squares: experimental results from ref. 26. The black solid lines and the blue dashed ones are guides for the eye. 1 bar = 10⁵ Pa = 10⁵ kg m⁻¹ s⁻².

total linear momentum of the simulation box is equal to zero. The imposed energy is the average total (internal) energy obtained in the last quarter of the last thermalisation run. In order to correct the small drift in energy due to finite time step and cutoff of Lennard-Jones interactions, a rescaling of velocities and angular momenta is performed every 10³ time steps in order to preserve the energy conservation. As an example, for the simulation at 328 K and 1 bar, the scaling factor distribution function for linear velocities and angular momenta at half-height corresponds to values in the range 1 ± 0.0005 and the extreme values are around 1 ± 0.001 . Averaged translational and rotational temperatures are computed during the simulation from molecular velocities and angular momenta. Tables S2 of the ESI,[†] contain the values of density, imposed internal energy, computed pressure, and computed temperatures of each simulation run.

3 Results

3.1 Isobaric thermal expansion coefficient

The isobaric thermal expansion coefficient α_p has been calculated from the thermodynamic definition. Using the number density $\rho = N/V$ with N the number of molecules and V the volume, α_p is given by:

$$\alpha_p = -\frac{1}{\rho} \left(\frac{\partial \rho}{\partial T} \right)_P \quad (1)$$

where $\rho = N/V$, V , P and T are the density, volume, pressure and temperature of the system. The partial derivative in eqn (1) is obtained, for each of the eight studied pressures, from a fitting of the temperature dependence of the volume (five values) by a polynomial of order 2. The raw MD results are presented in Fig. 2a. One observes the crossings of isotherms in a range of pressures from $\simeq 500$ to $\simeq 1500$ bar. It is interesting to compare this result with a previous study of α, ω -dibromoalkanes by a fluctuation model.²⁷ This model predicts a crossing of isotherms around $\simeq 400$ bar in a narrow pressure range in the series from α, ω -dibromoethane to α, ω -dibromohexane, whereas dibromomethane has a peculiar behaviour: the crossing occurs at higher pressures, between $\simeq 650$ and $\simeq 900$ bar. From extensive studies of experimental data, Randzio *et al.*⁹ proposed a linear correlation between $1/\alpha_p^2$ and the pressure P . Testing this relationship on our MD data, one obtains the graph of $1/\alpha_p^2$ vs. P of Fig. 2b where the circles are the MD values of $1/\alpha_p^2$ and the straight lines are the best linear regression between the MD points. One can observe that MD points are randomly distributed with respect to the best linear regression. Then, using the fitted α_p , the isotherms are modified according to Fig. 2c. Now, the crossing is better located at about 780 ± 50 bar, within the range of pressure predicted by the isothermal fluctuation equation of state.

From this thermodynamic route, it is not direct to obtain error bars on the numerical values of Fig. 2a–c. However, their monotonic character seems to indicate that the error bars are rather small. This observation can be compared to a study of thermophysical properties of CH₄ and CO₂ hydrate mixtures in

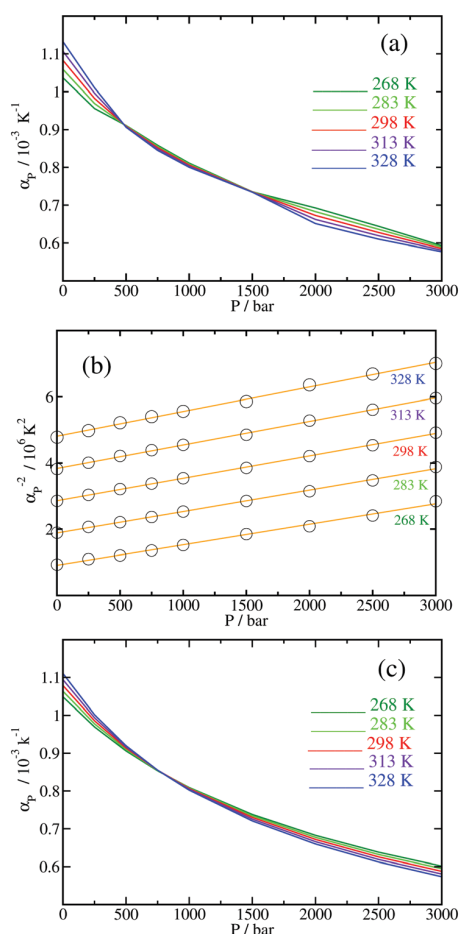


Fig. 2 Isobaric thermal expansivity. (a) α_p isotherms at 268.15, 283.15, 298.15, 313.15 and 328.15 K from raw MD density results. (b) Correlation between $(1/\alpha_p)^2$ and pressure P . Black circles: Raw MD values. Continuous orange line: Best linear regression through the points. The curves are successively shifted by 1.0 along the y axis. (c) Same as graph (a) with α_p fitted according to the linear correlation observed in graph (b).

which the isobaric thermal expansivity and the isothermal compressibility have been obtained through MD simulations by a fluctuation formula in the NPT ensemble and by the thermodynamic route. The thermodynamic route exhibits a regular monotonic behaviour, whereas the fluctuation route gives values much scattered with respect to the average curve.⁵⁷

3.2 Isothermal compressibility

The isothermal compressibility κ_T has been obtained from the thermodynamic definition:

$$\kappa_T = \frac{1}{\rho} \left(\frac{\partial \rho}{\partial P} \right)_T \quad (2)$$

The partial derivative in eqn (2) is obtained, for each of the five studied temperatures, from a fitting of the pressure dependence of the density (nine values) by a polynomial of order 3. The results are given in Fig. 3. In this figure, one also reported experimental determination from literature at 298.15 and

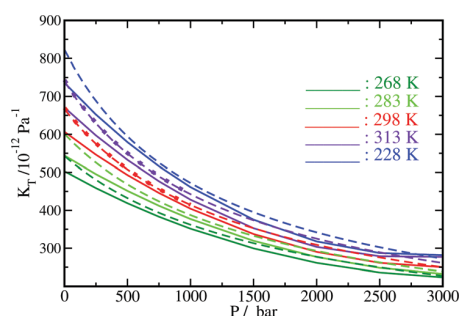


Fig. 3 Isothermal compressibility κ_T . Continuous lines: MD results using thermodynamic definition. Dotted lines: experimental determination at 298.15 and 313.15 K from an acoustic method from ref. 26. Dashed lines: extrapolation of the data based on an acoustic method from ref. 26 using the Heun's predictor-corrector method.^{58,59}

313.15 K up to 1000 bar and an extension of the acoustic method to the other studied temperatures and up to 3000 bar based on the Heun's predictor-corrector method. One can notice a rather good agreement between simulation and experiment except that (i) the model has a tendency to slightly underestimate the isothermal compressibility at the lowest pressures and (ii) at high pressure and above 298 K, the decrease of κ_T observed with an increase of pressure is not well reproduced.

3.3 Constant volume heat capacity

The constant volume heat capacity has been computed from the fluctuation formula in the NVE ensemble:^{29–31}

$$c_V = \frac{3Nk_B}{1 - \frac{\langle \delta E_{\text{kin}}^2 \rangle}{3Nk_B^2 T^2}} \quad (3)$$

where $\delta E_{\text{kin}} = E_{\text{kin}} - \langle E_{\text{kin}} \rangle$, with E_{kin} the total (translational and rotational) kinetic energy of the system of N rigid molecules (having each 3 translational and 3 rotational degrees of freedom), k_B is the Boltzmann constant and T is the temperature. As this formula involves a statistical average, it is trivial to compute an error bar from subaverages. The results are given in Fig. 4. One can see that though our simulations are quite long, the error bars are still larger than the interval between two consecutive plots of the isotherms of the heat capacity. Comparatively, the points are less scattered using the thermodynamic route. From the examination of these curves, one can anticipate that it would be necessary to increase the sampling by about an order of magnitude to bring the errors bars of the fluctuation route at the level of the present thermodynamic route. One can also note that the curves of c_V with the thermodynamic route as a function of pressure are less monotonic than those of α_p and κ_T . This is probably due to a larger uncertainty on the energy caused by the uncertainty on the volume. This uncertainty should be reduced by increasing the sampling to establish the volume vs. pressure curves and by increasing the number of sampled isotherms.

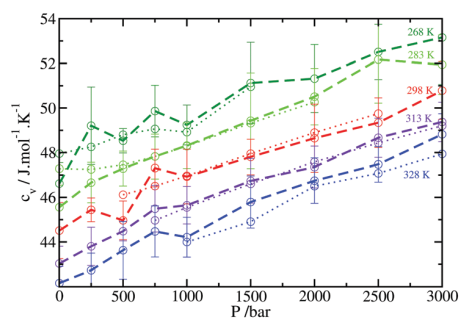


Fig. 4 Constant volume heat capacity c_V obtained from fluctuation formula in NVE ensemble (dashed lines) and from thermodynamic definition (dotted lines). Circles are MD results and lines are guides to the eye.

On the other hand, c_V can also be calculated from the thermodynamic definition:

$$c_V = \left(\frac{\partial E}{\partial T} \right)_V \quad (4)$$

where E is the internal energy (total energy of our MD runs) and V the volume of the system. As our MD thermodynamic states are along isotherms and isobars, the use of eqn (4) is not direct. To use it, one first fits the total energy E vs. volume V using a third-order polynomial for each isotherm. Second, for each MD state characterized by (E, V) , one computes the energy along the isochore V for the four other states located on the four other isotherms. Third, along each isochore, the total energy E is fitted by a second-order polynomial as a function of temperature T , in order to get the partial derivative of eqn (4) at each MD thermodynamic state. Obviously, such a procedure involves to generate thermodynamic states which are outside the range of volume of the simulated states. In order to avoid dubious extrapolations, the third step to get c_V is performed only for the thermodynamic states verifying that the isochore contains at least four values of the volume within the range explored by the MD isotherms. The values obtained by this thermodynamic route are given in the Fig. 4. The agreement is quite good with the results of the fluctuation route according to the amplitude of the error bars.

3.4 Constant pressure heat capacity

The constant pressure heat capacity c_P has been obtained by the thermodynamic definition:

$$c_P = \left(\frac{\partial H}{\partial T} \right)_P \quad (5)$$

where $H = E + PV$ is the enthalpy of the system. In contrast to the calculation of c_V , as our simulated thermodynamic states are adjusted to correspond to selected pressures, along each isobar, one computes H from the values of the energy and the volume and this quantity is directly fitted as a function of temperature by a second-order polynomial to get the partial derivative of eqn (5). This quantity is plotted as a function of pressure in Fig. 5. Here we cannot give easily the error bars, but

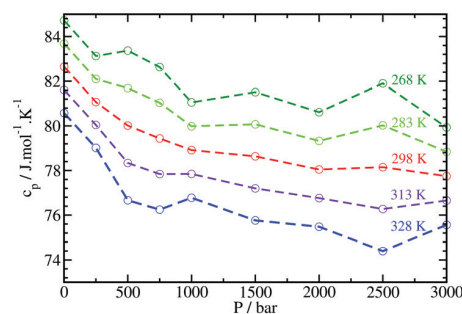


Fig. 5 Constant pressure heat capacity c_P obtained from the thermodynamic definition. Circles are MD results and dashed lines are guides to the eye.

they are of the same order as for c_V , simply increased by a contribution due to the uncertainty on the PV term.

As the molecules are considered as rigid bodies, the contribution of the $n_{\text{vib}} = 9$ vibrational modes per molecule is missing in the determination of heat capacities. We have computed the corresponding corrections using the harmonic oscillator model and the experimental vibrational frequency ν_i ($i = 1, \dots, 9$) of the dibromomethane molecule in gas phase.^{60,61} Defining the vibrational temperature of each vibrational mode by $T_{\nu_i} = h\nu_i/k_B$, where h is the Planck's constant, the corrections are given by:

$$c_{V,\text{vib}} = c_{P,\text{vib}} = \sum_i^{n_{\text{vib}}} \frac{Nk_B \left(\frac{T_{\nu_i}}{2T} \right)^2}{\sinh \left(\frac{T_{\nu_i}}{2T} \right)^2} \quad (6)$$

where N is the number of molecules. The numerical values are 18.61, 19.97, 21.32, 22.65 and 23.95 $\text{J mol}^{-1} \text{K}^{-1}$ from 268.15 to 328.15 K by 15 K steps.

Fig. 6 presents the c_P values obtained by simulation from the thermodynamic definition and augmented by these quantum corrections. Experimental results at 298.15 and 313.15 K at pressures up to 1000 bar from ref. 26 are shown for comparison. Globally, the model gives c_P in reasonable agreement with experiment. However, due to (i) relatively large error bars, (ii) a opposite

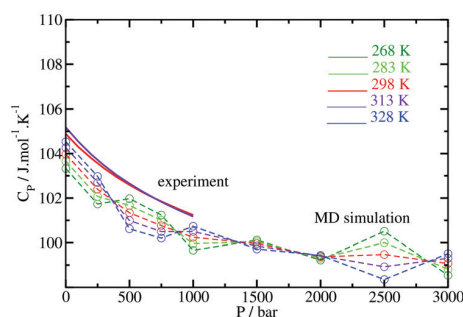


Fig. 6 Constant pressure heat capacity c_P . Simulation: thermodynamic definition with a harmonic oscillator correction for molecular vibrations. Circles are MD results and dashed lines are guides to the eye. Experiment: from ref. 26.

temperature dependence of the uncorrected c_p values and of the quantum correction, the resulting values present an erratic temperature dependence with an uncertainty in the range $\pm 1.5\%$ at least. Comparatively, the experimental results at 298.15 and 313.15 K differ very little, the maximum difference is less than 0.3% at 1 bar. The error bars are not mentioned in ref. 26 but the monotonic behaviour of the curves indicates that it is very small, smaller than 0.3%. Thus, to bring the accuracy of c_p determination by simulation at the level of experiment would require a significantly larger computational effort than in the present study.

Another test of heat capacities is to compute the ratio c_p/c_V . This quantity is related to the compressibility by:

$$\frac{c_p}{c_V} = \frac{\kappa_T}{\kappa_S} \quad (7)$$

where κ_S is the isentropic compressibility. This ratio is presented in Fig. 7 with experimental values at 298.15 and 313.15 K at pressures up to 1000 bar.²⁶ The agreement is reasonable.

3.5 Consistency check

From thermodynamics, heat capacities, isobaric expansivity and isothermal compressibility are related by the relationship:

$$c_p - c_V = \frac{VT\alpha_p^2}{\kappa_T} \quad (8)$$

From our MD data, the values of $c_p - c_V$ are correlated to those of $VT\alpha_p^2/\kappa_T$ in Fig. 8. One can notice a good correlation with largest deviations around 10%. The scattering of points with respect to the perfect expected correlation gives a clear indication of the uncertainty of the global strategy leading to these thermophysical quantities.

3.6 Speed of sound

The speed of sound u can be obtained from the relationship:⁶²

$$u = \frac{1}{\sqrt{\rho \left(\kappa_T - \frac{TM\alpha_p^2}{\rho c_p} \right)}} \quad (9)$$

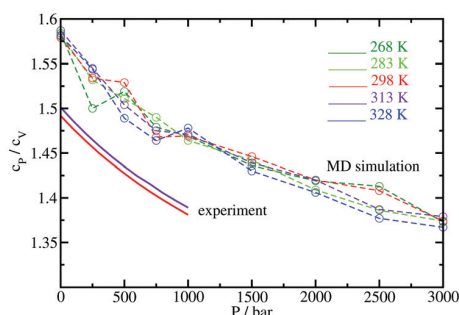


Fig. 7 Ratio c_p/c_V . Simulation: the heat capacities c_p (thermodynamic definition, eqn (5)) and c_V (fluctuation formula, eqn (3)) are corrected by vibrational quantum corrections, eqn (6). Circles are MD results and dashed lines are guides to the eye. Experiment: from ref. 26.

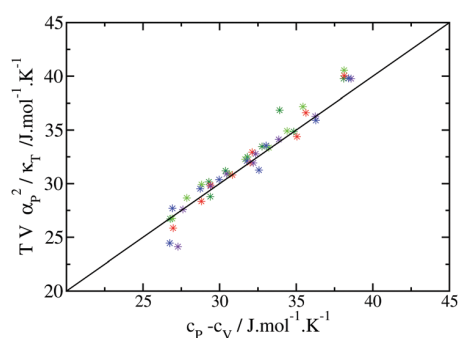


Fig. 8 Correlation between $c_p - c_V$ and $TV\alpha_p^2/\kappa_T$ obtained from MD simulations. Color code: dark green: 268 K, light green: 283 K, red: 298 K, indigo: 313 K and blue: 328 K.

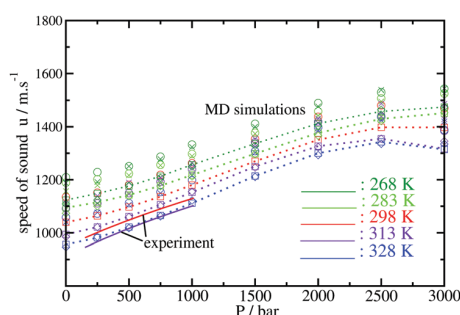


Fig. 9 Speed of sound u . Circles and crosses: u obtained from MD simulations and eqn (9) and (10), respectively. Squares and diamonds: u obtained from MD simulations with quantum corrections for heat capacities eqn (6), (9) and (10), respectively. The dotted curves are given as eye guidance for the case eqn (9) with quantum correction eqn (6). Experiment: from ref. 26.

with ρ the mass density and M the molar mass. Using eqn (8), this relationship is equivalent to

$$u = \sqrt{\frac{c_p}{c_V \rho \kappa_T}} \quad (10)$$

Fig. 9 presents the speed of sound obtained from eqn (9) and (10) from our classical MD simulations. Using eqn (9) and (10) lead to similar values. Compared to experimental values at 298 K and 313 K up to 1000 bar,²⁶ one can note an overestimation of roughly 12–16%. The introduction of quantum corrections for molecular vibrations in heat capacities leads to numerical values a little bit lower, and as shown in Fig. 9, the agreement with the experimental values is improved. For both isotherms at 298 and 313 K, the overestimation is reduced by a factor 2–3.

4 Conclusion

Molecular dynamics simulation have been used to model thermophysical properties of liquid dibromomethane under pressure using a simple five-site effective two-body additive potential with van der Waals parameters slightly tuned from

parameters of the GAFF2 force field. Heat capacities, isobaric thermal expansion coefficient, isothermal compressibility and speed of sound are found in reasonable agreement with available experimental results. The main result of this work is the observation of the crossing of the isotherms of the isobaric thermal expansivity around 780 bar, which is compatible with the prediction of an isothermal fluctuation equation of state but contrasts with experimental results which do not observe any crossing up to 1000 bar, though a crossing at higher pressure can be anticipated from the extrapolation of the experimental data. This suggests that it would be very interesting to reinvestigate the isobaric expansivity of this liquid at pressures above 1000 bar in order to clarify the situation: where is precisely located the crossing of the isotherms?

Conflicts of interest

There are no conflicts of interest to declare.

Acknowledgements

B. Jasiok acknowledges a scholarship from the Iwanowska's Program financed by the National Academic Exchange Agency (Poland) Decision No. PPN/IWA/2018/1/00054/DEC/1 and a grant from the National Science Centre (Poland) Decision No. 2016/23/B/ST8/02968. We are grateful to the University of Silesia in Katowice, the Kursk State University, the University of Lorraine and the CNRS for their support.

References

- P. W. Bridgman, *Proc. Amer. Acad. Arts Sci.*, 1912, **48**, 309–362.
- L. Ter Minassian, P. Pruzan and A. Soulard, *J. Chem. Phys.*, 1981, **75**, 3064–3072.
- F. Mallamace, C. Corsaro and H. E. Stanley, *Sci. Rep.*, 2012, **2**, 993.
- S. L. Randzio, J.-P. Grolier and M. Chorążewski, in *Volume Properties: Liquids, Solutions and Vapours*, ed. E. Wilhelm and T. M. Letcher, The Royal Chemical Society, Cambridge, 2015, pp. 414–438.
- M. Taravillo, V. G. Baonza, M. Cáceres and J. Núñez, *J. Phys.: Condens. Matter*, 2003, **15**, 2979–2989.
- W. B. Streett, *Physica*, 1974, **76**, 59–72.
- W. B. Streett and L. A. K. Staveley, *J. Chem. Phys.*, 1971, **55**, 2495–2506; W. B. Streett and L. A. K. Staveley, *J. Chem. Phys.*, 1975, **62**, 753.
- W. B. Streett, L. S. Sagan and L. A. K. Staveley, *J. Chem. Thermodyn.*, 1973, **5**, 633–650.
- S. L. Randzio, J.-P. E. Grolier, J. R. Quint, D. J. Eatough, E. A. Lewis and L. D. Hansen, *Int. J. Thermophys.*, 1994, **15**, 415–441.
- P. Navia, J. Troncoso and L. Roman, *J. Chem. Eng. Data*, 2010, **55**, 2173–2179.
- G. Jenner and M. Millet, *High Temp. - High Pressures*, 1970, **2**, 205–213.
- G. Jenner and M. Millet, *High Temp. - High Pressures*, 1973, **5**, 145–153.
- M. Chorążewski and E. B. Postnikov, *Int. J. Thermal Sci.*, 2015, **90**, 62–69.
- S. L. Randzio, D. J. Eatough, E. A. Lewis and L. D. Hansen, *Int. J. Thermophys.*, 1996, **17**, 405–422.
- Y. Miyake, A. Baylaucq, F. Plantier, D. Bessières, H. Ushiki and C. Boned, *J. Chem. Thermodyn.*, 2008, **40**, 836–845.
- M. Yoshimura, A. Baylaucq, J.-P. Bazile, H. Ushiki and C. Boned, *J. Chem. Eng. Data*, 2009, **54**, 1702–1709.
- P. Navia, J. Troncoso and L. Roman, *J. Chem. Thermodyn.*, 2010, **42**, 23–27; P. Navia, J. Troncoso and L. Roman, *J. Chem. Thermodyn.*, 2010, **42**, 949.
- F. A. M. M. Gonçalves, A. R. Trindade, C. S. M. F. Costa, J. C. S. Bernardo, I. Johnson, I. M. A. Fonseca and A. G. M. Ferreira, *J. Chem. Thermodyn.*, 2010, **42**, 1039–1049.
- M. Chorążewski, J.-P. E. Grolier and S. L. Randzio, *J. Chem. Eng. Data*, 2010, **55**, 5489–5496; M. Chorążewski, J.-P. E. Grolier and S. L. Randzio, *J. Chem. Eng. Data*, 2011, **56**, 690.
- J. M. S. S. Esperança, H. J. R. Guedes, M. Blesic and L. P. N. Rebelo, *J. Chem. Eng. Data*, 2006, **51**, 237–242.
- R. L. Gardas, M. G. Freire, P. J. Carvalho, I. M. Marrucho, I. M. A. Fonseca, A. G. M. Ferreira and J. A. P. Coutinho, *J. Chem. Eng. Data*, 2007, **52**, 1881–1888.
- R. L. Gardas, H. F. Costa, M. G. Freire, P. J. Carvalho, I. M. Marrucho, I. M. A. Fonseca, A. G. M. Ferreira and J. A. P. Coutinho, *J. Chem. Eng. Data*, 2008, **53**, 805–811.
- M. Milhet, A. Baylaucq and C. Boned, *J. Chem. Eng. Data*, 2005, **50**, 1430–1433.
- A. Pimentel-Rodas, L. A. Galicia-Luna and J. J. Castro-Arellano, *J. Chem. Eng. Data*, 2019, **64**, 324–336.
- R. P. Mendo-Sánchez, C. A. Arroyo-Hernández, A. Pimentel-Rodas and L. A. Galicia-Luna, *Fluid Phase Equil.*, 2020, **514**, 112559.
- M. Chorążewski, J. Troncoso and J. Jacquemin, *Ind. Eng. Chem. Res.*, 2015, **54**, 720–730.
- E. B. Postnikov and M. Chorążewski, *Phys. A*, 2016, **449**, 275–280.
- S. L. Randzio, *Phys. Lett. A*, 1986, **117**, 473–476.
- M. P. Allen and D. J. Tildesley, *Computer Simulation of Liquids*, Oxford University Press, Oxford, 1987.
- J. L. Lebowitz, J. K. Percus and L. Verlet, *Phys. Rev.*, 1967, **153**, 250–254.
- P. S. Y. Cheung, *Mol. Phys.*, 1977, **33**, 519–526.
- J. R. Ray and H. W. Graben, *Mol. Phys.*, 1981, **43**, 1293–1297.
- J. R. Ray, H. W. Graben and J. M. Haile, *Nuovo Cimento*, 1981, **64B**, 191–206.
- R. Lustig, *J. Chem. Phys.*, 1994, **100**, 3048–3059.
- R. Lustig, *J. Chem. Phys.*, 1994, **100**, 3060–3067.
- R. Lustig, *J. Chem. Phys.*, 1994, **100**, 3068–3078.
- K. Meier and S. Kabelac, *J. Chem. Phys.*, 2006, **124**, 064104.

Paper

- 38 C. Caleman, P. J. van Maaren, M. Hong, J. S. Hub, L. T. Costa and D. van der Spoel, *J. Chem. Theory Comput.*, 2012, **8**, 61–74.
- 39 A. W. S. Hamani, J.-P. Bazile, H. Hoang, H. T. Luc, J.-L. Daridon and G. Galliero, *J. Mol. Liq.*, 2020, **303**, 112663.
- 40 C. L. Yaws, *Yaws' Handbook of Thermodynamic and Physical Properties of Chemical Compounds*, McGraw-Hill, New York, 2003.
- 41 Y. H. Zhao, M. H. Abraham and A. M. Zissimos, *J. Org. Chem.*, 2003, **68**, 7368–7373.
- 42 S. R. Cox and D. E. Williams, *J. Comput. Chem.*, 1981, **2**, 304–323.
- 43 J. G. Ángyán and C. Chipot, *Int. J. Quantum Chem.*, 1994, **52**, 17–37.
- 44 A. Bondi, *J. Phys. Chem.*, 1964, **68**, 441–451.
- 45 R. S. Rowland and R. Taylor, *J. Phys. Chem.*, 1996, **100**, 7384–7391.
- 46 M. J. Frisch, G. W. Trucks, H. B. Schlegel, G. E. Scuseria, M. A. Robb, J. R. Cheeseman, G. Scalmani, V. Barone, B. Mennucci, G. A. Petersson, H. Nakatsuji, M. Caricato, X. Li, H. P. Hratchian, A. F. Izmaylov, J. Bloino, G. Zheng, J. L. Sonnenberg, M. Hada, M. Ehara, K. Toyota, R. Fukuda, J. Hasegawa, M. Ishida, T. Nakajima, Y. Honda, O. Kitao, H. Nakai, K. Vreven, J. A. Montgomery, Jr., J. E. Peralta, F. Ogliaro, M. Bearpark, J. J. Heyd, E. Brothers, K. N. Kudin, V. N. Staroverov, T. Keith, R. Kobayashi, J. Normand, K. Raghavachari, A. Rendell, J. C. Burant, S. S. Iyengar, J. Tomasi, M. Cossi, N. Rega, J. M. Millam, M. Klene, J. E. Knox, J. B. Cross, V. Bakken, C. Adamo, J. Jaramillo, R. Gomperts, R. E. Stratmann, O. Yazyev, A. J. Austin, R. Cammi, C. Pomelli, J. W. Ochterski, R. L. Martin, K. Morokuma, V. G. Zakrzewski, G. A. Voth, P. Salvador, J. J. Dannenberg, S. Dapprich, A. D. Daniels, O. Farkas, J. B. Foresman, J. V. Ortiz, J. Cioslowski and D. J. Fox, *Gaussian 09, Revision D.01*, Gaussian Inc., Wallingford CT, 2013.
- 47 M. Svanberg, *Mol. Phys.*, 1997, **92**, 1085–1088.
- 48 D. Fincham, *Mol. Simul.*, 1992, **8**, 165–178.
- 49 A. J. C. Ladd, *Mol. Phys.*, 1977, **33**, 1039–1050.
- 50 A. J. C. Ladd, *Mol. Phys.*, 1978, **36**, 463–474.
- 51 M. Neumann, *Mol. Phys.*, 1987, **60**, 225–235.
- 52 C. Millot, J.-L. Rivail and R. Diguët, *Chem. Phys. Lett.*, 1989, **160**, 228–232.
- 53 F. Dehez, M. T. C. Martins Costa, D. Rinaldi and C. Millot, *J. Chem. Phys.*, 2005, **122**, 234503.
- 54 D. J. Adams and G. S. Dubey, *J. Comput. Phys.*, 1987, **72**, 156–176.
- 55 B. Cichocki, B. U. Felderhof and K. Hinsen, *Phys. Rev. A: At., Mol., Opt. Phys.*, 1989, **39**, 5350–5358.
- 56 C. Millot, J.-C. Soetens and M. T. C. Martins Costa, *Mol. Simul.*, 1997, **18**, 367–383.
- 57 F. L. Ning, K. Glavatskiy, Z. Ji, S. Kjelstrup and T. J. H. Vlugt, *Phys. Chem. Chem. Phys.*, 2015, **17**, 2869–2883.
- 58 A. R. Lowe, B. Jasiok, V. V. Melent'ev, O. S. Ryshkova, V. I. Korotkovskii, A. K. Radchenko, E. B. Postnikov, M. Spinnler, U. Ashurova, J. Safarov, E. Hassel and M. Chorążewski, *Fuel Process. Technol.*, 2020, **199**, 106220.
- 59 E. B. Postnikov, B. Jasiok, V. V. Melent'ev, O. S. Ryshkova, V. I. Korotkovskii, A. K. Radchenko, A. R. Lowe and M. Chorążewski, *J. Mol. Liq.*, 2020, **310**, 113016.
- 60 S. J. Paddison and E. Tschuikow-Roux, *J. Phys. Chem. A*, 1998, **102**, 6191–6199.
- 61 T. Simanouchi, *Tables of Molecular Vibrational Frequencies. Vol. 1.*, National Standard Reference Data Series No. 39, National Bureau of Standards, U. S. Government Printing Office, Washington DC, 1972.
- 62 J. S. Rowlinson, F. L. Swinton, J. E. Baldwin, A. D. Buckingham and S. Danishefsky, *Liquids and Liquid Mixtures: Butterworths. Monographs in Chemistry*, Butterworth-Heinemann, Ltd, London, Boston, 3rd edn, 1982.

Katowice, 11.04.2023 r.

Instytut Chemii
Wydział Nauk Ścisłych i Technicznych
Uniwersytet Śląski w Katowicach
ul. Bankowa 12, 40-007 Katowice

Statement on the contribution to the publication

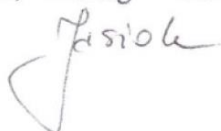
Publication:

B. Jasiok, M. Chorążewski, E.B. Postnikov, C. Millot, Liquid dibromomethane under pressure: a computational study. *Physical Chemistry Chemical Physics* **2021**, 23, 2964-2971, DOI: 10.1039/D0CP06458K.

We hereby state that the contribution to the work published jointly with Bernadeta Jasiok is in accordance with the description below:

Bernadeta Jasiok

I was responsible for: Conceptualization, Methodology, Formal analysis, Investigation, Data Curation, Writing – Original Draft, Writing – Review & Editing, Visualization, Project administration



Mirosław Chorążewski

I was responsible for: Conceptualization, Investigation, Writing – Original Draft, Writing – Review & Editing, Supervision, Funding acquisition

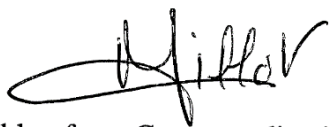


Eugene B. Postnikov

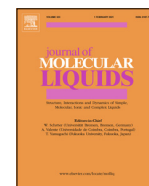
I was responsible for: Conceptualization, Methodology, Formal analysis, Investigation, Writing – Original Draft, Writing – Review & Editing, Visualization, Supervision



Claude Millot

A handwritten signature in black ink, appearing to read 'C. Millot', with a large, sweeping underline that extends to the left.

I was responsible for: Conceptualization, Methodology, Software, Formal analysis, Investigation, Data Curation, Writing – Original Draft, Writing – Review & Editing, Visualization, Supervision, Project administration



Thermophysical properties of chloropropanes in liquid phase: Experiments and simulations



Bernadeta Jasiok^a, Mirosław Chorążewski^a, Alexander A. Pribylov^b, Eugene B. Postnikov^{c,*}, Pascale Friant-Michel^d, Claude Millot^{d,*}

^a University of Silesia in Katowice, Institute of Chemistry, ul. 9 Szkolna, 40-006 Katowice, Poland

^b Southwest State University, 50 Let Oktyabrya st., 94, Kursk 305040, Russia

^c Department of Theoretical Physics, Kursk State University, Radishcheva St., 33, 305000 Kursk, Russia

^d Université de Lorraine, CNRS, LPCT, F-54000 Nancy, France, Boulevard des Aiguillettes, BP 70239, 54506 Vandoeuvre lès Nancy Cedex, France

ARTICLE INFO

Article history:

Received 11 December 2021

Revised 25 February 2022

Accepted 8 April 2022

Available online 18 April 2022

This work is dedicated to Prof. Gábor Pálínkás on the occasion of his 80th birthday.

Keywords:

Chloropropanes

High-pressures

Thermophysical properties

Span–Wagner EoS

MD simulations

Daridon's method

ABSTRACT

In this work, the properties of liquid 1-chloropropane, 2-chloropropane and 1,3-dichloropropane are investigated. The Span–Wagner equation of state (EoS) is used to improve the existing thermophysical properties as a function of the temperature and pressure of these chloropropanes. For 1-chloropropane and 2-chloropropane, the thermophysical properties are compared with Molecular Dynamics simulation results performed in the range of temperature 293.15–373.15 K and the range of pressure 0.1–200 MPa. In addition, for both monochloropropanes, the isobaric thermal expansion coefficient obtained from Span–Wagner EoS and MD simulations is compared with the one obtained from the recently proposed Daridon's method.

© 2022 Elsevier B.V. All rights reserved.

1. Introduction

The interplay of functional forms and parameters of equations of state with macroscopic thermoelastic coefficients and the microscopic molecular nature of the described system is not only of fundamental interest of condensed matter physics and physical chemistry but also is the starting point for most thermodynamic issues related to engineering applications from chemistry and fluid mechanics to materials engineering and nanotechnology. The knowledge of an effective and predictive equation of state and thermoelastic coefficients for a wide range of liquid systems is becoming essential in the context of designing technological processes under high pressure. Therefore, the analysis of the anomalous thermodynamic properties of liquids (thermodynamic

response functions) in connection with the molecular structure of liquids acquires an entirely new meaning.

Within this context, a particular interest can be focused on halogenated propanes. They provide an opportunity to explore the influence of the qualitative change of pure *n*-alkane originating from the introduction of the heavy atom. It is possible either symmetrically (with two opposite kinds of effects: in the middle of chain for 2-halogen-propane; and at the end of the molecule for 1,3-halogen-propane) or asymmetrically for 1-halogen-propane. This work focused primarily on one class of chloroalkanes, namely 1-chloropropane, 2-chloropropane, and 1,3-dichloropropane. Experimental datasets are determined in a similar range of thermodynamic conditions intended to validate modeling approaches. In addition, it should be pointed out that haloalkanes have a practical application; namely, they are used, for example, as solvents, propellants, fumigants, disinfectants, or refrigerants [1–4].

However, the prediction of fluid properties over a wide range of thermodynamic states is a complex scientific task. Direct experimental measurement of parameters at high temperature and pressure requires sophisticated equipment. Generally, theoretical

* Corresponding authors at: Department of Theoretical Physics, Kursk State University, Radishcheva St., 33, 305000 Kursk, Russia (E.B. Postnikov), Université de Lorraine, CNRS, LPCT, F-54000 Nancy, France (C. Millot)

E-mail addresses: postnikov@kursksu.ru (E.B. Postnikov), claudio.millot@univ-lorraine.fr (C. Millot).

<https://doi.org/10.1016/j.molliq.2022.119137>

0167-7322/© 2022 Elsevier B.V. All rights reserved.

methods work well for simple systems. Some experimental data are needed to use semi-empirical methods using correlations and approximations. The use of computer simulation methods can generate valuable information and bridge the gap between experiment and theory. This work will apply the Span–Wagner Equation of State (Span–Wagner EoS), known as one of the most accurate empiric correlations that can reproduce the thermodynamic properties in a wide range of temperatures and pressures with an accuracy comparable to the one of practical experimental measurements. Respectively, obtaining parameters of this EoS that allow analytical calculating of primary and derivative thermodynamic quantities gives a background for discussing direct molecular features revealed by MD simulations.

This work will look specifically at the isobaric thermal expansion coefficient $\alpha_p = -\rho^{-1}(\partial\rho/\partial T)_p$, which is known as a thermodynamic quantity quite sensitive to the data and its processing. In particular, the IUPAC recommends paying attention to the reproducibility of α_p 's behavior when developing data regression and modeling with equations of state [5]. One of such features of importance is that isotherms of α_p intersect at a given pressure or within a specific range of pressures. In general, they cross below 200 MPa, depending on the temperature range studied [6,7] and the nature of the liquid system [8–10]. In other words, there exist a curve on the thermodynamic plane, where $(\partial\alpha_p/\partial T)_p = 0$. To simplify, we will call this feature as the "intersection of isotherms" instead of the long sentence "zeroing the temperature derivative of the isobaric thermal expansion coefficient".

The experimental data evaluation of three chloropropanes is shown in Section 2. Section 3 is focused on the MD simulations' details. The following section shows how we used experimental data to apply Span–Wagner's method and calculate the fundamental thermodynamic properties from computer simulation results. The discussion section presents the fitting of coefficients and their uncertainty in the Span–Wagner method and different views on calculating the thermal expansion coefficient.

2. Experimental data evaluation

2.1. 1-chloropropane

The experimental data presented in work [11] and other literature sources referenced therein were evaluated using the ThermoData Engine (TDE) [12,13]. It has been revealed that the density data along isotherms $T \geq 333.15$ K, i.e., larger than the boiling temperature $T_b = 319.8$ K, and pressures $P \geq 10$ MPa looks inconsistent with the rest of the data as it exhibits deviations toward large densities. Thus, these data were rejected, and we need to redetermine the respective values. At the same time, the course of isotherms of the speed of sound satisfies the self-consistent overall picture of the available PVT data. Thus, we decided to redetermine the densities based on the modified acoustic route described in details in Lowe et al.'s work [14].

To integrate the thermodynamic equalities

$$\left(\frac{\partial C_p}{\partial P}\right)_T = -\frac{T}{\rho} \left[\alpha_p^2 + \left(\frac{\partial \alpha_p}{\partial T}\right)_p \right], \quad (1)$$

$$\left(\frac{\partial \rho}{\partial P}\right)_T = \left[\frac{T \alpha_p^2}{C_p} - \frac{1}{c^2} \right], \quad (2)$$

where C_p and α_p are the isobaric heat capacity and the coefficient of thermal expansion supplied with the experimental data of the speed of sound, which cubed value is fitted by cubic polynomials along isotherms $c^3(P) = \sum_{n=1}^2 \sum_{j=0}^2 A_{jn}(T)(P - P_0)^n$, it is required to

state initial conditions along an isobar P_0 . Since the temperature interval, $T = (293.15 - 373.15)$ K covers the significant range after the boiling point of 1-chloropropane, the isobar $P_0 = 4.9$ MPa was chosen. Evaluating the data from [11,15] along all these temperature regions and the data from [9] for its part below the boiling point indicates good consistency between these sources. The speed of sound along this isobar was taken from Melent'ev and Postnikov's work [11].

For the isobaric heat capacity, we applied a two-step procedure. The data evaluation demonstrated that the data presented in work [11] need to be slightly shifted by adding a constant value $\Delta C_p = 1.7$ J/(mol · K). In this case, the data at 298.15 K are centred concerning the set of available experimental data for this temperature. The whole sequence of C_p values follows a smooth continuous curve formed by the rest of the experimental data and TDE-based predictions for the saturated heat capacity. Note that the shift applied is within the uncertainty range defined for the original data in Melent'ev and Postnikov's work [11]; therefore, this procedure does not out-throw redefined values supplied with the uncertainty range bounded by the original data from the validity range of the experiment. As the next step, the Span–Wagner equation of state for polar substances was fitted to the whole set of available (and not rejected due to large deviations) data using the standard TDE procedure. As a result, the desired heat capacity data for the isobar $P_0 = 4.9$ MPa were obtained.

2.2. 2-chloropropane

As done for 1-chloropropane, the recalculation of the density via the acoustic route was carried out. Again, the isobar $P = 4.5$ MPa was chosen as the reference one for the initial conditions; the density ρ_0 and the speed of sound c_0 were taken from the Melent'ev and Postnikov's work [16]. As for the isobaric heat capacity at this pressure, the following procedure was applied. The values at the ambient atmospheric pressure C_p^0 were reported in Melent'ev and Postnikov's work [17]. We used the second-order polynomial interpolation for ρ_0 , c_0 , and C_p^0 and one step of integration of Eq. (1). As a result, the values of $C_p(4.9$ MPa) for temperatures lower than the boiling point were obtained; in turn, they were interpolated by the second-order polynomial to end the values extrapolated to the temperatures exceeding the boiling temperature. The resulting density at high pressures was found as described above for 1-chloropropane by integrating the system (1) and (2) with the simultaneous uncertainty quantification and applying the processing 10^4 times replicated Monte Carlo ensemble.

2.3. 1,3-dichloropropane

A unique example of halogenated propanes is 1,3-dichloropropane, for which the direct measurements of the isobaric expansion coefficient at high pressures are available [18]. It means that these values can play a role in the reference set since they are not connected to any density approximation method.

At the same time, to the best of our knowledge, despite relatively extensive amounts of saturated data and the data measured at ambient atmospheric pressure [19], the data on the density itself at elevated pressure is absent. However, there exists a dataset of the speed of sound data [20]. Thus, the acoustic route for the density determination, analogous to the one described above, has been carried out. Moreover, the third-order polynomial interpolation was used to determine the isobaric thermal expansion coefficient during the intermediate steps, possibly due to the higher temperature points.

3. Simulation details

MD simulations are performed with home-made simulation codes in periodic boundary conditions (PBC) with $N = 1000$ rigid molecules in the central cubic box interacting through an atom-atom two-body potential containing Lennard-Jones and Coulomb interactions. The choice of using rigid molecules has been made in order to increase the value of the time step. The molecular geometries have been optimized at Hartree-Fock level with a 6-31G* basis set. In the case of 1-chloropropane, the molecule has three important conformational isomers corresponding to different values of the torsion angle C-C-Cl: one trans ($\approx 180^\circ$) and two gauche ($\approx 60^\circ$ and $\approx 300^\circ$) conformers. In order to approximate the experimental situation as close as possible for each studied thermodynamic state, the experimental percentages of each conformer trans, gauche⁺, and gauche⁻ have been used. These populations at different temperatures and pressures have been interpolated from the results of a Raman study [21]. The number of 1-chloropropane conformers and the molecular geometries are given in Tables S1 and S2 of the [Supplementary Information](#), respectively.

Atomic partial charges have been fitted from ab initio calculation at Hartree-Fock level with the 6-31G* basis set in order to reproduce the electrostatic potential around the molecule (ESP charges). Points are located around the molecule with a spacing of 0.35 Å in each Cartesian direction with points located at distances between 1.0 and 2.0 times the van der Waals radius of each atom and removing points closer from any atom than 1.0 times its van der Waals radius. The van der Waals radii are taken from Bondi for the carbon and chlorine atoms and Rowland for the hydrogen atom [22,23]. The grids around the three conformers of trans, gauche⁺, gauche⁻ 1-chloropropane, and 2-chloropropane have 6659, 6563, 6563, and 6506 points, respectively. Charges of hydrogen atoms of each CH₂, of each CH₃ groups, and terminal carbon atoms in 2-chloropropane are fitted with a constraint of equality. Then, for 1-chloropropane, an average is taken over the three conformers in order to use a single charge-set. Charges of 1-chloropropane are eventually scaled by 0.99. The ratio of the dipole moment of both isomers of chloropropane would be equal to the value obtained with the ab initio values of the dipole moments. Ab initio calculations have been performed using the Gaussian package [24], and atomic charges are fitted using a home-made code based on the standard minimization of mean-square deviation between the electrostatic potential obtained from the ab initio calculation and the one obtained from the atomic-charge model. The Lennard-Jones parameters have been taken from the OPLS-AA force field, and consistently geometric combination rules are applied for ϵ_{ab} and σ_{ab} parameters for pairs of dissimilar atoms a and b [25]. The atomic charges and Lennard-Jones parameters are gathered in Table S3 of the [Supplementary Information](#).

Equations of motion are solved using the center of mass degrees of freedom and a leapfrog quaternion algorithm due to Svanberg [26] with a time step equal to 4 fs. This scheme improves a previous algorithm developed by Fincham [27,28]. In this approach, each molecule's quaternion vector $\mathbf{Q}(t+\Delta t/2)$ is obtained iteratively.

In our code, iterations are stopped when the norm of its variation between two consecutive iterations is lower than 10^{-9} . Electrostatic interactions are computed using lattice summations based on the Ladd approach, initially proposed for assemblies of point dipoles [29–31] and generalized to systems of point charges [32,33], leading to expressions equivalent to the ones proposed by other groups [34,35]. A reaction field contribution is added with the dielectric constant of the surrounding continuum equal to infinity, making the method physically equivalent to the standard Ewald approach [31]. It has been observed that the truncation at rank 10 of the expansion of the electrostatic interaction energy in cubic harmonics leads to good accuracy even for highly polar and polarizable systems [31,36]. The van der Waals interactions are truncated beyond a molecular-based cutoff of 20.0 Å. Usual corrections on potential energy and pressure due to this cutoff have been applied [28].

4. Results

4.1. 1-chloropropane

The complete set of the initial data used for solving Eqs. 1,2 is listed in Table 1. The resulting density was found by integrating the (1) and (2) system using the Heun's method with these initial conditions applying the second-order polynomials along isobars for determining the coefficient of thermal expansion and its derivative with respect to pressure. Table S4 in the [Supplementary Information](#) presents the obtained values. The standard uncertainty of the data was determined by the Monte Carlo method of uncertainty quantification [37,38]. Each initial condition was replicated 10^4 times to form a Gaussian ensemble with the dispersions corresponding to the values listed in Table 1.

Fig. 1 presents the density values compared to other known data for some of these isotherms. One can see that the behavior of the isotherms for temperatures $T > T_b$ significantly deviates from the values listed in the table of densities in Melent'ev and Posnikov's work [11]. On the contrary, for $T < T_b$, the values of both sets are reasonably consistent, with an average absolute deviation AAD = 0.002. The same is true in a direct comparison with the data from [9] for two isotherms with coinciding temperatures AAD = 0.001, i.e., the correspondence is even better, which is also visible in Fig. 1, where asterisks are practically overlapped with circles. As an additional criterion, isotherms from Bridgman's work [39] are shown. They correspond to the temperatures that do not coincide with those we considered. However, the position, slope, and curvature of these intermediate curves support the accuracy of the new proposed dataset. In particular, when comparing the highest pressure region for the isotherm $T = 293.15\text{K}$ and Bridgman's isotherm $T = 273.15\text{K}$, we can conclude that the deviation of crosses (previous data from Ref. [11]) from new (circles) is irrelevant and new (more extensive and less curved) data should be preferred. Finally, it can be pointed out that comparison of the data listed in Table 1 for $P \geq 10$ MPa with the prediction of the initial TDE's Span-Wagner model built by fitting the data (except the

Table 1

Thermodynamic parameters at the pressure $P_0 = 4.9\text{MPa}$, which play the role of initial conditions for the system 1,2. Their standard uncertainties are $u(\rho) = 2.2\text{kg} \cdot \text{m}^{-3}$, $u(c) = 3.4\text{m} \cdot \text{s}^{-1}$, $u(C_p) = 1.8\text{J} \cdot \text{mol}^{-1} \cdot \text{K}^{-1}$.

T/K	293.15	313.15	333.15	353.15	373.15
$\rho(P_0)/\text{kg} \cdot \text{m}^{-3}$	896.5	871.6	846.3	820.5	794.3
$c(P_0)/\text{m} \cdot \text{s}^{-1}$	1117.4	1028.3	943.1	862.8	788.0
$C_p(P_0)/\text{J} \cdot \text{mol}^{-1} \cdot \text{K}^{-1}$	128.2	132.5	137.2	142.3	147.9

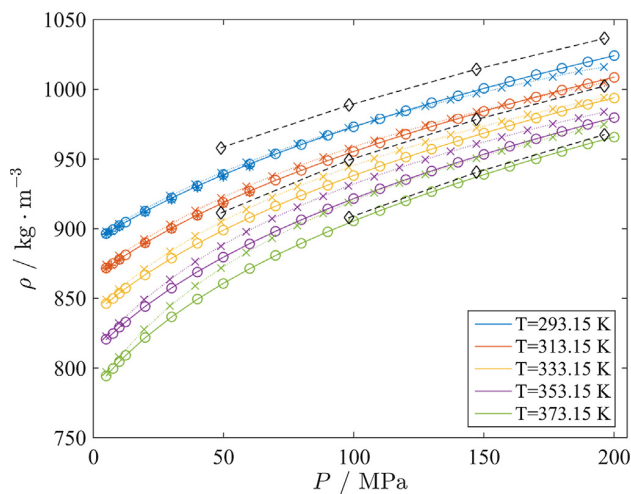


Fig. 1. The density found via the speed of sound-based thermodynamic route (circles), the data from [11] (crosses) for isotherms listed in Table S4 in the Supplementary Information (from up to down). For comparison, the data from [9] for $T = 293.15\text{ K}$ and $T = 313.15\text{ K}$ are shown as asterisks and the data from [39] for $T = 273.15\text{ K}$, $T = 323.15\text{ K}$, and $T = 368.15\text{ K}$ as black diamonds. Lines connect markers for visual guidance.

speed of sound) at temperatures not exceeding T_b for such pressures deviates from these new determined densities with $\text{AAD} = 0.002$.

Thus, we can conclude that the dataset for the density of 1-chloropropane published in work [11] should be rejected and replaced with the new dataset given in Table S4.

4.2. 2-chloropropane

Fig. 2 illustrates the pressure dependence of the density obtained via acoustic route presented in Table S5 in the Supplementary Information compared to the data given in Ref. [16] and three isotherms from Ref. [9]. Unfortunately, there is no other data related to this compound at high pressures. One can see that again, newly obtained values are well-coordinated with the previously reported ones for temperatures below the boiling point as it was noted for 1-chloropropane. However, one can see deviations for $P > 100\text{ MPa}$. Nevertheless, for lower pressures, the correspondence is quite accurate; in particular $\text{AAD} = 0.1\%$ ($1.06\text{ kg}\cdot\text{m}^{-3}$ in the dimensional form) that is reliably within the experimental uncertainty for the isotherm 293.15 K from [9], the only one which coincides with these data in the temperature value. Two other isotherms, which go on both sides from the mentioned one, also demonstrate coordinated position and shape with the newly obtained one. For the two largest temperatures in the studied interval, there is the visible deviation of data from Ref. [16] in the intermediate region of pressures that we can associate with the possible instrumental inaccuracies affecting the results of volumetric density determination in the cited work.

4.3. 1,3-dichloropropane

The obtained results are listed in Table S6 in the Supplementary Information. Unfortunately, to the best of our knowledge, there are no other data for this liquid.

4.4. MD Simulations

1-chloropropane and 2-chloropropane have been studied at six temperatures (293.15 , 303.15 , 313.15 , 333.15 , 353.15 and

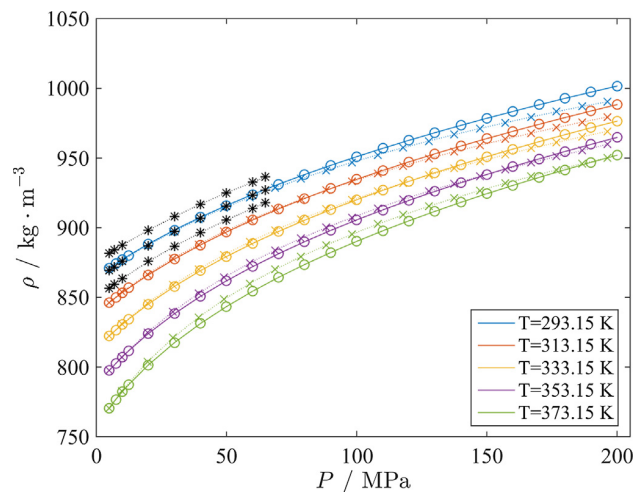


Fig. 2. The density found via the speed of sound-based thermodynamic route (circles), the data from [16] (crosses) for isotherms listed in Table S5 in the Supplementary Information (from up to down). For comparison, the data from [9] for $T = 283.15\text{ K}$, $T = 293.15\text{ K}$ and $T = 303.15\text{ K}$ are shown as black asterisks. Lines connect markers for visual guidance.

373.15 K) and densities have been fitted to get eight pressures (0.1 , 12.5 , 25.0 , 50.0 , 75.0 , 100 , 150.0 and 200.0 MPa). In the first stage, the volume is adjusted to get the desired pressure using constant volume simulation with frequent scaling of velocities and angular momenta to impose the desired temperature. Pressure is averaged over 50000 – 100000 time step periods and used iteratively to guide volume change. When the right density is obtained, the system is simulated at constant energy and volume during a production period of 400000 time steps. The imposed energy is the average total (internal) energy obtained in the last 25000 time steps of the last thermalization run (see Table S8 of the Supplementary Information). Due to finite time step and cutoff of Lennard-Jones interactions, a rescaling of velocities and angular momenta is performed every 500 -time step in order to maintain the total energy constant. Among the 48 thermodynamical states of both systems, the root-mean-square deviation between the imposed energies and the MD averaged energies (over 1.6 ns) is around 0.6 J/mol and the maximum deviation is 1.6 J/mol . Averaged translational and rotational temperatures, computed during the simulation from molecular velocities and angular momenta, are very close to the target values. The root-mean-square deviations of the translation and rotational temperatures for the 96 MD runs for the target values is $\approx 0.3\text{ K}$. The maximum deviation is 0.75 K . The averaged pressures differ from the target values by less than 1% for the systems under pressure. At 0.1 MPa , the deviations are within the range $\pm 0.2\text{ MPa}$.

5. Discussion

5.1. Span–Wagner EoS for chloropropanes: coefficients fitting and uncertainty evaluation

With the datasets prepared in the previous sections supplied additionally with the other available experimental data given in the NIST standard reference database 103b [19], the fitting of polar Span–Wagner EoS for 1-chloropropane, 2-chloropropane, and 1,3-dichloropropane was carried out with the TDE fitting tool by employing the "simulated annealing" fitting procedure.

The Span–Wagner EoS operates with the Helmholtz free energy per unit mass A_m as a thermodynamic potential for obtaining other

thermodynamic properties of the substance, written in the following form:

$$a(\delta, \tau) = \frac{A_m}{RT} = a^0(\delta, \tau) + a^r(\delta, \tau) \quad (3)$$

where $\delta = \rho/\rho_c$, $\tau = T_c/T$ with ρ_c as the critical density and T_c as the critical temperature, R is the specific gas constant, a^0 is the ideal gas part of the Helmholtz free energy, and a^r is the residual part.

For the polar Span–Wagner EoS, the residual part of Eq. (3) is usually found as the following sum:

$$a^r(\delta, \tau) = \sum_{i=1}^5 n_i \delta^{d_i} \tau^{t_i} + \sum_{i=6}^{12} n_i \delta^{d_i} \tau^{t_i} e^{-\delta^i} \quad (4)$$

The ideal gas part of Eq. (3) is usually obtained from the ideal gas heat capacity function $C_p^0(T)$ by calculating the integrals in the following expression:

$$a^0(\delta, \tau) = \frac{1}{RT} \left(\int_{T_0}^T C_p^0 dT + h_0^0 \right) - 1 - \frac{1}{R} \left(\int_{T_0}^T \frac{C_p^0 - R}{T} dT + R \ln \left(\frac{\rho}{\rho_0^0} \right) + s_0^0 \right) \quad (5)$$

where all variables with the lower index "0" refer to an arbitrary reference state and do not contribute to the derived liquid's properties, the $C_p^0(T)$ functions for all studied substances are provided by TDE as a 4-degree polynomial $C_p^0(T)/R = \sum_{i=0}^4 C_i T^i$. Thus, the integration of Eq. (5) gives the following form of $a^0(\delta, \tau)$ for this type of the $C_p^0(T)$ fitting function:

$$a^0(\delta, \tau) = \ln \delta + a_0 \ln \tau + a_1 \tau^{-1} + a_2 \tau^{-2} + a_3 \tau^{-3} + a_4 \tau^{-4} \quad (6)$$

For 1-chloropropane, the following constants were used for fitting: $T_c = 503.305$ K, $\rho_c = 3.733$ mol/l and $R = 105.862$ J/kg K. The coefficients, obtained for the ideal gas part in the form of Eq. (6), are the following: $a_0 = 4.21713431$, $a_1 = 0.93881713$, $a_2 = -4.95589391$, $a_3 = 2.04005711$ and $a_4 = -0.32740601$.

For 2-chloropropane, the following constants were used for fitting: $T_c = 482.401$ K, $\rho_c = 4.079$ mol/l and $R = 105.862$ J/kg K. The coefficients, obtained for the ideal gas part in the form of Eq. (6), are the following: $a_0 = 5.10191966$, $a_1 = 2.65807121$, $a_2 = -5.88923338$, $a_3 = 2.47291938$ and $a_4 = -0.41940059$.

For 1,3-dichloropropane, the following constants were used for fitting: $T_c = 614.600$ K, $\rho_c = 3.473$ mol/l and $R = 73.589$ J/kg K. The coefficients, obtained for the ideal gas part in the form of Eq. (6), are the following: $a_0 = 6.76492505$, $a_1 = 3.25768226$, $a_2 = -8.92941215$, $a_3 = 4.54996311$ and $a_4 = -0.91194098$.

The coefficients of Eq. (4), obtained from the fitting procedure, are listed in Table S7 (note that coefficients d_i , t_i , and c_i are specific for the polar type of the Span–Wagner EoS and do not vary from one substance to another).

To evaluate the uncertainties of all obtained EoS, the experimental data for density and the speed of sound for compressed and saturated liquid, the heat capacity at constant pressure and the heat capacity at saturation pressure, were used. All data were taken from the TDE database [19], except for the points rejected after performing the Data Evaluation procedure or replaced to the corrected values in the previous sections. The theoretical predictions of the density values at particular pressure and temperature were made by choosing the ρ value that predicts the closest value of pressure by the formula $p(\delta, \tau) = \rho RT(1 + \delta a_\delta^r)$, with a ρ increment of $10^{-6} \rho_c$. The equations for the heat capacity per unit mass at constant pressure, heat capacity per unit mass at satura-

tion pressure, and the speed of sound via derivatives of the Helmholtz free energy are following:

$$\frac{C_p(\delta, \tau)}{R} = -\tau^2(a_{\tau\tau}^0 + a_{\tau\tau}^r) + \frac{(1 + \delta a_\delta^r - \delta \tau a_{\delta\tau}^r)^2}{1 + 2\delta a_\delta^r + \delta^2 a_\delta^r} \quad (7)$$

$$\frac{C_s(\delta, \tau)}{R} = -\tau^2(a_{\tau\tau}^0 + a_{\tau\tau}^r) + \frac{(1 + \delta a_\delta^r - \delta \tau a_{\delta\tau}^r)^2}{1 + 2\delta a_\delta^r + \delta^2 a_\delta^r}$$

$$\left[(1 + \delta a_\delta^r - \delta \tau a_{\delta\tau}^r) - \frac{\rho_c}{R\delta} \frac{dp_s}{dT} \right] \quad (8)$$

$$\frac{c^2(\delta, \tau)}{RT} = 1 + 2\delta a_\delta^r + \delta^2 a_\delta^r - \frac{(1 + \delta a_\delta^r - \delta \tau a_{\delta\tau}^r)^2}{\tau^2(a_{\tau\tau}^0 + a_{\tau\tau}^r)} \quad (9)$$

with $p_s(T)$ as the phase boundary pressure function. In equations above, subscripts δ and τ denote partial derivatives respectively to these reduced variables. To evaluate the uncertainties at the saturation curve, the experimental phase boundary pressure data provided by the TDE database were fitted by the Wagner vapor pressure equation. Using this equation, the values of boundary pressure were added to each data point so that it would be possible to apply the Span–Wagner EoS for calculations. The deviations of the density values, calculated by obtained EoS, from respective experimental values at elevated pressure for all studied liquids are shown in Fig. S1 of the [Supplementary Information](#). The deviations of predicted density values at the saturation curves from the experimental ones are shown in Fig. S2 of the [Supplementary Information](#).

AAD calculation was made for all above-counted quantities in the range of temperatures from 273.15 K to 373.15 K, and for all values of the temperatures presented in considered datasets. Table S10 of the [Supplementary Information](#) summarizes the AAD values obtained for all considered substances in compressed liquid and saturated liquid states.

5.2. The isobaric thermal expansion intersection curves and the thermodynamic curvature isolines

Using the Span–Wagner EoS with the obtained coefficients, the isobaric thermal expansion intersection curve and the thermodynamic Riemannian curvature contours were plotted for all studied liquids by the procedure described in the [Supplementary Information](#) of Pribylov and Postnikov's work [40]. Fig. S3 of the [Supplementary Information](#) shows the obtained isolines of the Riemannian curvature R and the α_p intersection curve on the (P, T) plane, as well as the contours of dimensionless thermodynamic curvature $R^* = R/V_{vdW}$, where V_{vdW} is the van der Waals molecular volume characterizing the size of molecules in (ρ^*, T) coordinates, where $\rho^* = \rho/\rho_{vdW}$ with $\rho_{vdW} = M/N_a V_{vdW}$ as the van der Waals density, where M – molar mass and N_a – Avogadro constant.

One can see that the intersection curve behaves for these liquids in the manner typical of n -alkanes, it coincides with an isoline of the thermodynamic curvature when the liquid tends to melt. Around the melting point, such a coincidence is observed for substances with longer chains starting from n -pentane rather than for n -propane, characterized by the specificity of packing near the melting point [40]. However, this observation is in line with the analysis of the cohesive energy density [41], which indicates that for 1-haloalkanes, introducing chlorine atom (which is significantly heavier than the replaced hydrogen) is equivalent from the point of view of the energy of intermolecular interactions to the ascending shift along with pure alkane's homologous series on just about three members of it, see [42].

Thus, the α_p intersection curves for 1-chloropropane, 2-chloropropane and 1,3-dichloropropane obtained in the present study can be compared to each other and to the one of *n*-propane reported in Pribylov and Postnikov's work [40], by plotting in both dimensionless (ρ^*, T^*) with $T^* = T/T_c$, and (P, T) sets of coordinates. Fig. S4 of the [Supplementary Information](#) shows those intersection curves in chosen coordinates. One can see that despite the different position of the intersection curves on the (P, T), three out of four of them are almost merged practically in one narrow stripe on the (ρ^*, T^*) plane. As discussed in [40], this stripe can be interpreted as the universality of molecular packing properties corresponding to the thermodynamic state, where $(\partial\alpha_p/\partial T)_p = 0$. This is also related to the reasons mentioned above that the chlorine atom replacing the hydrogen in the methyl group is equivalent, to the certain extent, to a simple elongation of the alkane's chain. On the contrary, introducing chlorine into the middle methylene group results in the some displacement of the $(\partial\alpha_p/\partial T)_p = 0$ line at low reduced temperatures and its more linear character.

5.3. Comparison of the isobaric thermal expansions obtained in different ways

To compare α_p for two isotherms whose temperatures coincide in the direct measurements [18] and for the acoustic route based on the speed of sound data [20], the acoustic route of the density determination was applied to determine the isobaric thermal expansion coefficient at the same values of pressure that in Chorążewski et al. [18]. Since this interval of pressures overcomes available data in Yebra et al. [20], the second-order polynomial extrapolation of the cubed speed of sound was used for $P > 95$ MPa and the same order of polynomial was used in the extrapolated region for partial derivatives with respect to the temperature. The Span–Wagner EoS obtained in the previous section also allows to calculate α_p by the following formula:

$$\alpha_p = -\frac{\delta\tau}{T_c} \frac{\tau(a_{\delta\tau}^0 + a_{\delta\tau}^T) - a_{\delta}^0 - a_{\delta}^T}{1 + 2\delta a_{\delta}^0 + \delta^2 a_{\delta\delta}^T}. \tag{10}$$

In this way, it is possible to compare the values of α_p , obtained by these three different methods at the values of the temperature of 303.15 K and 323.15 K (these values are only common for both sources [18,20], the latter was used to obtain α_p through the acoustic route), and the values of pressure, where the experimental measurements were made. The uncertainties of calculations were estimated for each point by the Monte Carlo method for the acoustic route calculations, and by the TDE's EoS calculation instrument for the Span–Wagner EoS calculations. The comparison of the experimental and calculated values of α_p is provided in Fig. S5 of the [Supplementary Information](#).

A comparison of the results of α_p calculations using the previously described acoustic route method and the Span–Wagner EoS can also be done in a wider range of temperatures, where the experimental measurements of the speed of sound in [20] are made. To avoid using extrapolation, the comparison is made only in the interval of pressures, where the values of the speed of sound were measured. Fig. S6 of the [Supplementary Information](#) shows the result of calculations of the α_p values with the acoustic route method and the Span–Wagner EoS, carried out at the points where the speed of sound was measured.

Finally, we look at a recently published numerical method, where a limited number of experimental data were used to estimate the isobaric thermal expansion coefficient and its uncertainty [43]. It is based on a proper power-law transformation of variables (density and temperature) that linearizes the experimental points in such a representation. In comparison with the other method

where a proper polynomial degree is needed, it is unnecessary here. For the calculations, we used the MD results. To calculate the isobaric thermal expansion coefficient, we used the following equation proposed by Daridon et al. [43]:

$$\alpha_p = -\frac{T_m}{mnT} \frac{a_1}{\rho_n} \tag{11}$$

where T_m and ρ_n are the temperature and density re-expressed as a power transformation ($T_m = T^{1/m}$; $\rho_n = (\frac{\rho}{1000})^n$), T is the temperature, and a_1 is the slope of the expression $\rho_n(T_m)$.

The results of MD simulations, carried out for 1-chloropropane and 2-chloropropane, also allow to calculate α_p by making a polynomial interpolation of the obtained values of density from the thermodynamic definition $\alpha_p = (-\frac{1}{\rho})(\frac{\partial\rho}{\partial T})_p$, with the temperature dependence of the density fitted using a polynomial of order 2. Thus, the comparison of the MD results, the ones predicted by fitting on the experimental data Span–Wagner EoS, and the ones predicted by the Daridon et al. method can be provided. The respective values of α_p for 1- and 2-chloropropane were calculated from the results of the MD simulations by the Span–Wagner EoS' and Daridon et al. method at the points where the simulations were made are shown in Fig. 3.

Using the polynomial interpolation of the obtained MD values of density compared to the Daridon et al. method [43], we obtained very similar results in the high-pressure region. Here, the crossing occurs around 150 MPa and in the range of pressures 150–200 MPa for 1-chloropropane and 2-chloropropane, respectively. There is a difference between polynomial and Daridon et al. method for the highest temperatures at small pressures. Such behavior is understandable because it corresponds to the state far after the boiling point. The results obtained by the Span–Wagner method differ from those previously mentioned. Here, the crossing occurs in the range 100–122 MPa and 75–115 MPa for two isomers of chloropropane. The intersection ranges occur in relatively close ranges for 1-chloropropane. However, a significant intersection shift is seen for 2-chloropropane. This may be due to obtaining a more significant discrepancy in the MD density results compared to the data obtained with Span–Wagner EoS.

5.4. The other thermodynamic quantities calculated from the MD results

The computer simulations were used to obtain the thermophysical properties for 1-chloropropane, and 2-chloropropane, such as the density, the isothermal compressibility, constant volume and constant pressure heat capacities, and the speed of sound.

The density was calculated using the formula $\rho = \frac{N}{V}$, where N is the number of molecules, and V is the volume. The isothermal compressibility, κ_T , was computed from the thermodynamic definition $\kappa_T = (\frac{1}{\rho})(\frac{\partial\rho}{\partial P})_T$ with the density dependence of density modeled by the functional form used in the Tait equation.

The constant volume heat capacity was obtained from the fluctuation formula in the NVE ensemble [44,45,28]:

$$C_V = \frac{3Nk_B}{1 - \frac{\langle \delta E_{kin}^2 \rangle}{3Nk_B^2 T^2}} \tag{12}$$

where $\delta E_{kin} = E_{kin} - \langle E_{kin} \rangle$, with E_{kin} the total (translational and rotational) kinetic energy of the system of N rigid molecules, k_B being the Boltzmann constant and T is the temperature. The constant pressure heat capacity is computed from the formula $C_p = (\frac{\partial H}{\partial T})_p$ where the temperature dependence of the enthalpy H is fitted using a polynomial of order 2. Quantum corrections due to vibrational degrees of freedom for heat capacities are computed

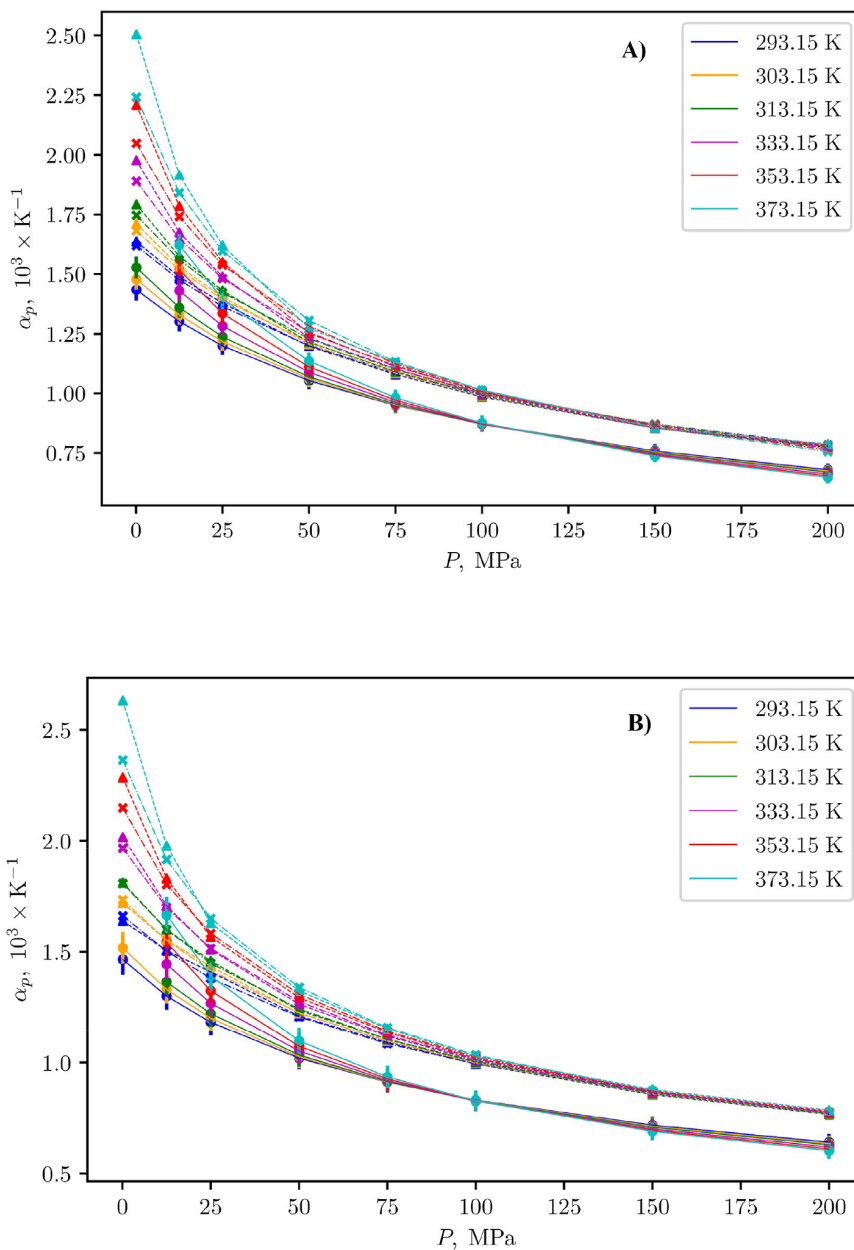


Fig. 3. The isobaric thermal expansion coefficients of 1-chloropropane (A) and 2-chloropropane (B), found from the MD simulations data (crosses), by the obtained Span–Wagner EoS (circles) and the Daridon *et al.* method (triangles) at the points where the simulations were made. Lines connect markers for visual guidance.

assuming a harmonic oscillator model for the molecular vibrations. Values of the vibrational frequencies are taken from the literature. For 1-chloropropane gauche and trans rotamers they are taken from an infrared (IR) study in gas phase; the missing values for the trans rotamer being estimated from the corresponding modes of the gauche conformer and ab initio values from $V_{estimatedIR,trans} = \frac{V_{IR,gauche} \cdot V_{abinitio,trans}}{V_{abinitio,gauche}}$ [46]. For 2-chloropropane, observed frequencies from the gas phase and liquid phase IR data are used [47]. Using vibrationally quantum corrected heat capacities, the speed of sound is obtained from the equation:

$$c = \sqrt{\frac{C_p}{C_v} \frac{V}{M \kappa_T}} \quad (13)$$

where M is the mass of the system, the numerical values of the density are given in Table S9 of the [Supplementary Information](#).

The comparison of the thermodynamic quantities obtained from the MD simulations to the respective Span–Wagner EoS is provided in [Fig. 4](#) for 1-chloropropane and [Fig. 5](#) for 2-chloropropane, respectively. The colors of markers and lines match the same temperature values as in [Fig. 3](#).

First, we look at the density ([Fig. 4\(A\)](#)) and [Fig. 5\(A\)](#)). As seen, better results for 1-chloropropane compared to 2-chloropropane were obtained. This is due to a smaller error for 1-chloropropane than 2-chloropropane, for which the density plot is more “elongated”. This also explains the behavior of the thermal expansion coefficient discussed above. On the other hand, for both heat capacities, the “almost” monotonic functions from MD results

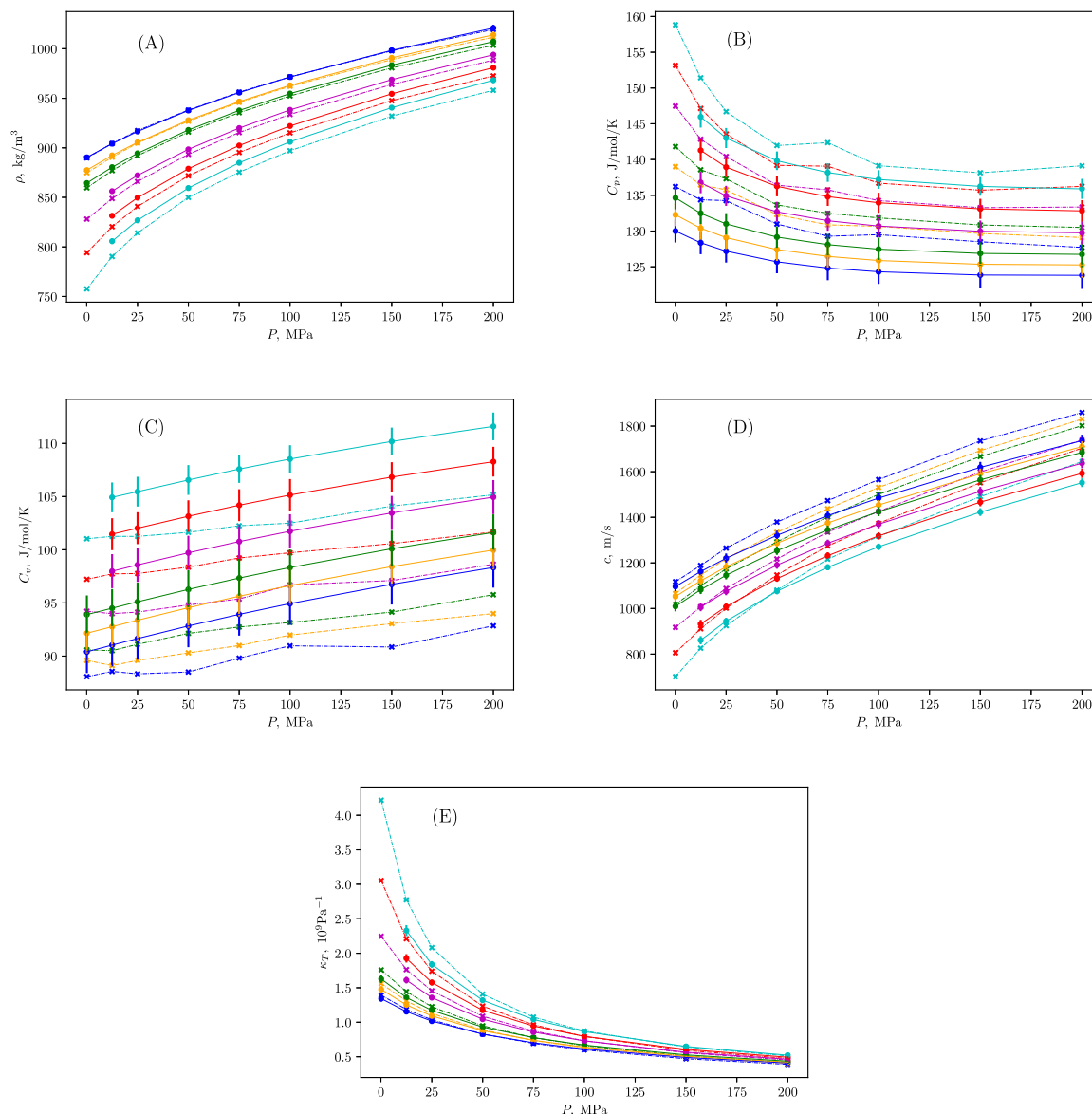


Fig. 4. The comparison of the values of density (A), heat capacity at constant pressure (B), heat capacity at constant volume (C), speed of sound (D) and isothermal compressibility (E) of 1-chloropropane, found from the MD Simulations data (crosses) and by the obtained Span–Wagner EoS (circles) at the points where the simulations were made. Lines connect markers for visual guidance.

(Figs. 4(B), (C)) and Figs. 5(B), (C)) were obtained. This may be due to the use of a small number of energy isotherms used to calculate the constant pressure and constant volume heat capacities. As the temperature increases, the error increases for C_p , while for C_v for each isotherm, the error remains approximately constant. The speed of sound calculated from Eq. 13 is shown in Fig. 4(D) and Fig. 5(D). Here also, we obtained better results for 1-chloropropane, which may be due to the use of the values with error used to calculate the speed of sound from the thermodynamic equation. The Fig. 4(E) and Fig. 5(E) show the results for isothermal compressibility.

For both chloropropanes, we obtain acceptable results except for the results for $P = 0.1$ MPa. Several temperatures are larger than the boiling temperature in these points, which explains the larger deviations. In Table 2 the Absolute Average Deviations

(AADs) for each thermodynamic properties of two chlorinated propanes are shown.

One may wonder why simulation results differ between liquids composed of isomers that do not differ significantly. The OPLS force field and ESP/HF-6-31G* charges give a very similar density for both liquids in a given thermodynamic state. In contrast, experimentally, 2-chloropropane has a density lower than 1-chloropropane by a few per cents. Focusing on the four extreme state points explored in the simulation: 293.15 K – 0.1 MPa, 293.15 K – 200 MPa, 373.15 K – 0.1 MPa and 373.15 K – 200 MPa, the extrapolation of experimental densities of this work through a polynomial fitting of order 6 gives 'experimental' values of the density at these four states, respectively: 890.7, 1024.2, 783.7 and 965.9 $\text{kg}\cdot\text{m}^{-3}$ for 1-chloropropane and 864.7, 1001.6, 758.5 and 952.1 $\text{kg}\cdot\text{m}^{-3}$ for 2-chloropropane, respectively 2.9,

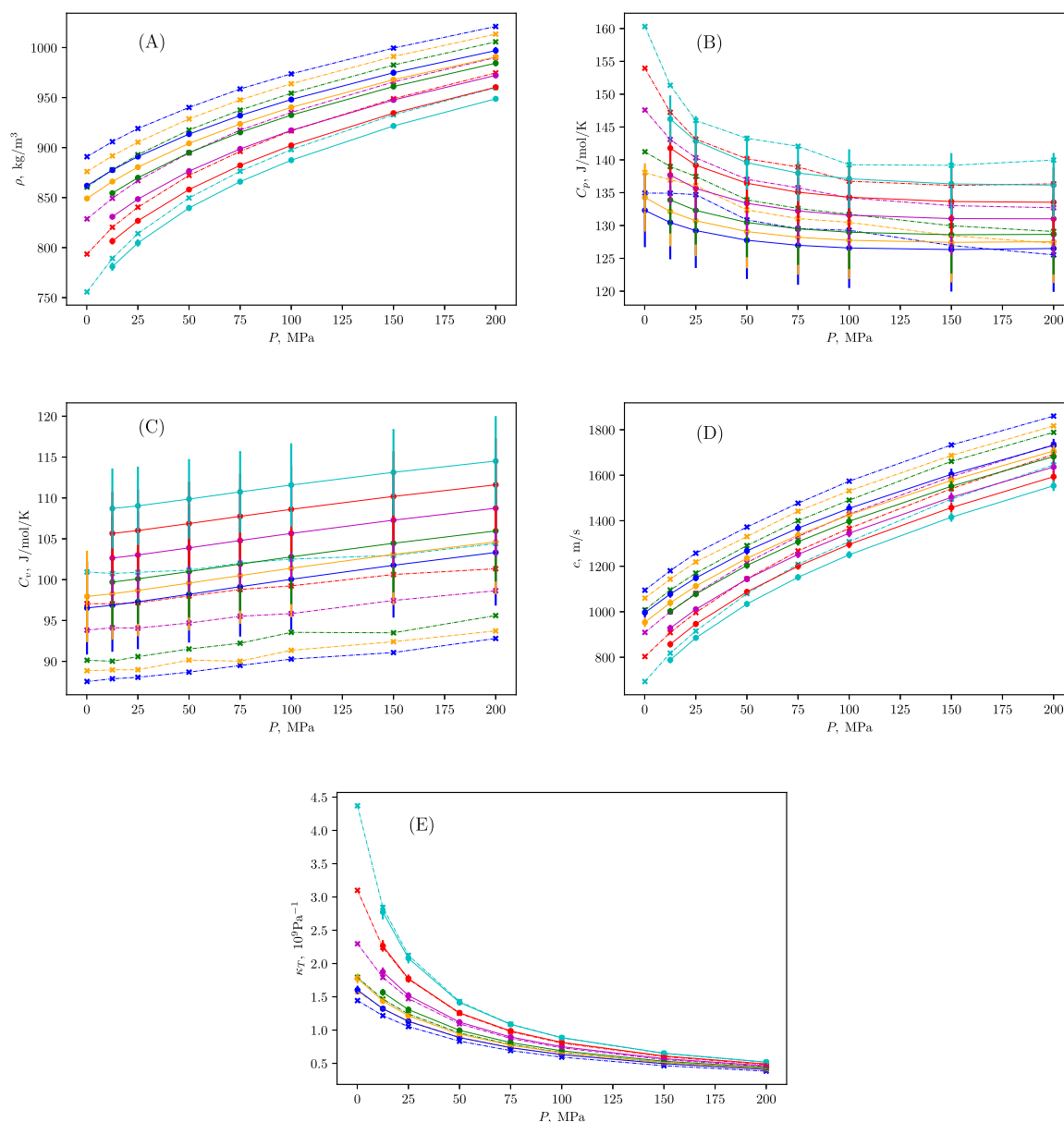


Fig. 5. The comparison of the values of density (A), heat capacity at constant pressure (B), heat capacity at constant volume (C), speed of sound (D) and isothermal compressibility (E) of 2-chloropropane, found from the MD simulation data (crosses) and by the obtained Span–Wagner EoS (circles) at the points where the simulations were made. Lines connect markers for visual guidance.

Table 2

The AADs for the thermodynamic properties of 1-chloropropane and 2-chloropropane from the MD simulations and Span–Wagner EoS.

AADs	1-chloropropane	2-chloropropane
$\rho/\%$	0.543	2.141
$C_p/\%$	3.415	2.407
$C_v/\%$	4.734	9.128
$c/\%$	3.820	26.928
$\kappa_T/\%$	4.206	3.661

2.2, 3.2 and 1.4 % lower than for 1-chloropropane. The OPLS/ESP-HF/6-31G* model we have used gives densities for both liquids 1-chloropropane/2-chloropropane equal to 890/891, 1019/1021, 758/756, 988/960 kg·m⁻³ in the four states, respectively. Let us

remind that in this work, the simulations of 1-chloropropane and 2-chloropropane are performed with rigid molecules.

In order to model the volume-dependent thermophysical properties accurately, it is crucial to get a very accurate reproduction of the density as a function of temperature and pressure. To see the effect of the force field, we did a *NPT* simulation with the AMBER package (release 18) and the GAFF2 force field [48,49] coupled to our set of charges of both liquids in the four previous states. After thermalization, with 150 ps runs, we got densities for both liquids 1-chloropropane/2-chloropropane equal to 885/883, 1006/1005, 765/763, 947/947 kg·m⁻³. Doing the simulation with the same GAFF2 potential and our set of charges using the Lammmps package [50] (the Oct. 2020 version), the densities were found to be equal to 862/859, 997/995, 717/718, 937/937 kg·m⁻³, the error bars being around ± 5 kg·m⁻³ except for the third state where it is around

$\pm 10 \text{ kg}\cdot\text{m}^{-3}$. The differences are due to differences in algorithmic features used in both packages. These tests also differ from our simulations because they fully include molecular flexibility.

Additionally, we performed another test to examine the effect of a charge model. We fitted a new set of ESP charges but we chose the grid points differently. The points where the electrostatic potential is computed are restrained with distances from atoms ranging from 1.00 to 1.01 times an atom's van der Waals radius. The simulation with the GAFF2 potential and the new charges using the LAMMPS package give densities equal to 858/859, 997/995, 722/711, 936/935 $\text{kg}\cdot\text{m}^{-3}$. The effect of the set of the set of charges is thus very small, which is not unexpected because the electrostatic interaction energy is a small fraction of the cohesive energy for these liquids. The interesting information we get from these comparisons is that whatever the model one uses, the densities of both 1-chloropropane and 2-chloropropane remain very close at any thermodynamic state. Thus such models cannot be good for both liquids simultaneously. It thus seems that to improve the interaction model significantly, it will be necessary to modify the functional form and/or reconsider the transferability of parameters between both isomers. This task is a challenge for molecular modeling far beyond the scope of the present work.

6. Conclusions

In this work, we modeled the thermophysical properties of 1-chloropropane, 2-chloropropane, and 1,3-dichloropropane as a function of temperature and pressure using thermodynamic and molecular dynamics modeling. The study was motivated by the fact that halogenated propanes represent the most straightforward systems, which makes it possible to explore the effect on the thermodynamic properties of the liquid caused by the changes in molecular symmetry originating from the replacement of hydrogen by a heavy atom. Therefore, the study requires (i) the building of a high-accurate equation of state, which would be valid for a wide range of states. It would be based on a comprehensive critical evaluation of the existing experimental data and (ii) direct molecular dynamics simulations whose purpose is to test the conventional MD force fields. The differences associated with the various positions of a halogen atom allow us to capture the respective specificity of thermodynamic functions.

Thus, the main results can be formulated as follows:

1. we have found parameters for the Span–Wagner Equation of State, which has recently been considered the most accurate empiric multiparametric EoS (implemented in particular in the REFPROP system providing the standard reference data by the National Institute of Standard and Technologies), for all studied substances;
2. while building the model mentioned above, we critically evaluated the complete set of experimental data existing in the literature. We noted these data, which demonstrably deviate from the self-consistent thermodynamic model. We, therefore, proposed appropriate corrections that included their tabular form;
3. we explored the behavior of the thermal expansion coefficients in detail. Indeed, the IUPAC recommended this as a sensitive criterion for testing the accuracy of equations of state and was noted earlier as an open problem exhibiting a big difference between the compressed states of 1-chloropropane and 2-chloropropane. It is of specific fundamental interest to discuss the universality of its zero temperature isobaric derivative respective to the molecular packing and thermodynamic curvature;
4. in addition to this thermodynamic consideration, we reported and analyzed the results of the molecular dynamics simulations, which indicated the validity ranges of conventional force

fields for reproducing the thermodynamics of 1-chloropropane and 2-chloropropane and posed required directions for future studies outside of these ranges.

Author Contributions

The manuscript was written through contributions of all authors. All authors have given approval to the final version of the manuscript.

Declaration of Competing Interest

The authors declare that they have no known competing financial interests or personal relationships that could have appeared to influence the work reported in this paper.

Acknowledgements

We are grateful for the financial support based on Decision No. 2016/23/B/ST8/02968 from the National Science Centre (Poland). We are grateful to the University of Silesia in Katowice, the Kursk State University, the University of Lorraine, the EXPLOR mesocentre and the CNRS for their support. PFM and CM thank Kanika Anand and Gérald Monard for their help in using the LAMMPS and Amber packages, respectively.

Appendix A. Supplementary material

Supplementary data associated with this article can be found, in the online version, at <https://doi.org/10.1016/j.molliq.2022.119137>.

References

- [1] L. Xie, J. Zan, Z. Yang, Q. Wu, X. Chen, X. Ou, C. Lin, Q. Chen, H. Yang, A perovskite-based paper microfluidic sensor for haloalkane assays. *Front. Chem.* 9 (2021) 236, <https://doi.org/10.3389/fchem.2021.682006>.
- [2] B. Li, L. Cui, C. Li, Macrocyclic co-crystals showing vapochromism to haloalkanes, *Angew. Chem. Int. Ed.* 59 (49) (2020) 22012–22016, <https://doi.org/10.1002/anie.202010802>.
- [3] X. Wang, E. Wright, N. Gao, Y. Li, Evaluation on excess entropy scaling method predicting thermal transport properties of liquid hfc/hfo refrigerants, *J. Therm. Sci.* (2020) 1–11, <https://doi.org/10.1007/s11630-020-1383-2>.
- [4] I. Polishuk, M. Katz, Y. Levi, H. Lubarsky, Implementation of pc-saft and saft+cubic for modeling thermodynamic properties of haloalkanes. i. 11 halomethanes, *Fluid Ph. Equilibria* 316 (2012) 66–73, <https://doi.org/10.1016/j.fluid.2011.12.003>.
- [5] U.K. Deiters, K.M. De Reuck, Guidelines for publication of equations of state I. Pure fluids (Technical Report), *Pure Appl. Chem.* 69 (1997) 1237–1250.
- [6] S.L. Randzio, J.-P. Grolier, M. Chorążewski, High-Pressure 'Maxwell Relations' Measurements, The Royal Chemical Society, London, 2015, pp. 414–438.
- [7] M. Taravillo, V.G. Baonza, M. Cáceres, J. Núñez, Thermodynamic regularities in compressed liquids: I. the thermal expansion coefficient, *J. Phys.: Condens. Matter* 15 (19) (2003) 2979, <https://doi.org/10.1088/0953-8984/15/19/302>.
- [8] P. Navia, J. Troncoso, L. Román, Isobaric thermal expansivity for nonpolar compounds, *J. Chem. Eng. Data* 55 (6) (2010) 2173–2179, <https://doi.org/10.1021/jje900757k>.
- [9] H. Guerrero, L.M. Ballesteros, M. García-Mardones, C. Lafuente, I. Gascón, Volumetric properties of short-chain chloroalkanes, *J. Chem. Eng. Data* 57 (2012) 2076–2083, <https://doi.org/10.1021/jje3003805>.
- [10] M. Chorążewski, J. Troncoso, J. Jacquemin, Thermodynamic properties of dichloromethane, bromochloromethane, and dibromomethane under elevated pressure: Experimental results and saft-vr mie predictions, *Ind. Eng. Chem. Res.* 54 (2) (2015) 720–730, <https://doi.org/10.1021/ie5038903>.
- [11] V.V. Melent'ev, E.B. Postnikov, Speed of sound and density of 1-chloropropane in the range of temperatures 180–373 K and pressures up to 196.1 MPa, *J. Chem. Eng. Data* 62 (2017) 3409–3413, <https://doi.org/10.1021/acs.jced.7b00443>.
- [12] M. Frenkel, R.D. Chirico, V. Diky, X. Yan, Q. Dong, C. Muzny, ThermoData Engine (TDE): software implementation of the dynamic data evaluation concept, *J. Chem. Inf. Model.* 45 (2005) 816–838, <https://doi.org/10.1021/ci050067b>.
- [13] V. Diky, C.D. Muzny, E.W. Lemmon, R.D. Chirico, M. Frenkel, ThermoData Engine (TDE): Software implementation of the dynamic data evaluation concept. 2. Equations of state on demand and dynamic updates over the web, *J. Chem. Inf. Model.* 47 (2007) 1713–1725, <https://doi.org/10.1021/ci700071t>.

- [14] A.R. Lowe, B. Jasiok, V.V. Melent'ev, O.S. Ryschkova, V.I. Korotkovskii, A.K. Radchenko, E.B. Postnikov, M. Spinnler, U. Ashurova, J. Safarov, E. Hassel, M. Chorążewski, High-temperature and high-pressure thermophysical property measurements and thermodynamic modelling of an international oil standard: RAVENOL diesel rail injector calibration fluid, *Fuel Process. Technol.* 199 (2020) 106220, <https://doi.org/10.1016/j.fuproc.2019.106220>.
- [15] W.M. Rutherford, Viscosity and density of some lower alkyl chlorides and bromides, *J. Chem. Eng. Data* 33 (1988) 234–237, <https://doi.org/10.1021/je00053a003>.
- [16] V.V. Melent'ev, E.B. Postnikov, Density and speed of sound of 2-chloropropane in the range of temperatures 293.15–373.15 K and pressures up to 196.2 MPa, *Chem. Data Collect.* 24 (2019) 100270, <https://doi.org/10.1016/j.cdc.2019.100270>.
- [17] V.V. Melent'ev, E.B. Postnikov, Influence of isomerization on acoustic and fluctuation properties of chloropropanes according to experimental and model studies, in: Proceedings of the XXXII Session of the Russian Acoustical Society, Moscow, October 14–18, 2019, GEOS (Moscow), 2019, pp. 1245–1250. URL: <http://rao.akin.ru/images/32%20isbn.zip>.
- [18] M. Chorążewski, A. Grzybowski, M. Paluch, The complex, non-monotonic thermal response of the volumetric space of simple liquids, *Phys. Chem. Chem. Phys.* 16 (2014) 19900–19908, <https://doi.org/10.1039/C4CP02350A>.
- [19] ThermoData Engine (TDE)Version 10: NIST standard reference database 103b (2015).
- [20] F. Yebra, K. Zemánková, J. Troncoso, Speed of sound as a function of temperature and pressure for propane derivatives, *J. Chem. Thermodyn.* 109 (2017) 117–123, <https://doi.org/10.1016/j.jct.2016.12.016>.
- [21] Y. Meléndez-Pagaán, B.E. Taylor, D. Ben-Amotz, Cavity formation and dipolar contribution to the gauche-trans isomerization of 1-chloropropane and 1,2-dichloroethane, *J. Phys. Chem. B* 105 (2001) 520–5262, <https://doi.org/10.1021/jp002781w>.
- [22] A. Bondi, Van der waals volumes and radii, *J. Phys. Chem.* 68 (1964) 441–451.
- [23] R.S. Rowland, R. Taylor, Intermolecular nonbonded contact distances in organic crystal structures: Comparison with distances expected from van der waals radii, *J. Phys. Chem.* 100 (1996) 7384–7391, <https://doi.org/10.1021/jp953141+>.
- [24] M.J. Frisch, G.W. Trucks, H.B. Schlegel, G.E. Scuseria, M.A. Robb, J.R. Cheeseman, G. Scalmani, V. Barone, B. Mennucci, G.A. Petersson, H. Nakatsuji, M. Caricato, X. Li, H.P. Hratchian, A.F. Izmaylov, J. Bloino, G. Zheng, J.L. Sonnenberg, M. Hada, M. Ehara, K. Toyota, R. Fukuda, J. Hasegawa, M. Ishida, T. Nakajima, Y. Honda, O. Kitao, H. Nakai, K. Vreven, J.A. Montgomery, Jr., J.E. Peralta, F. Ogliaro, M. Bearpark, J.J. Heyd, E. Brothers, K.N. Kudin, V.N. Staroverov, T. Keith, R. Kobayashi, J. Normand, K. Raghavachari, A. Rendell, J.C. Burant, S.S. Iyengar, J. Tomasi, M. Cossi, N. Rega, J.M. Millam, M. Klene, J.E. Knox, J.B. Cross, V. Bakken, C. Adamo, J. Jaramillo, R. Gomperts, R.E. Stratmann, O. Yazyev, A.J. Austin, R. Cammi, C. Pomelli, J.W. Ochterski, R.L. Martin, K. Morokuma, V.G. Zakrzewski, G.A. Voth, P. Salvador, J.J. Dannenberg, S. Dapprich, A.D. Daniels, O. Farkas, J.B. Foresman, J.V. Ortiz, J. Cioslowski, D.J. Fox, Gaussian 09, Revision D.01, Gaussian Inc., Wallingford CT (2013).
- [25] W.L. Jorgensen, D.S. Maxwell, J. Tirado-Rives, Development and testing of the opls all-atom force field on conformational energetics and properties of organic liquids, *J. Am. Chem. Soc.* 118 (1996) 11225–11236, <https://doi.org/10.1021/ja9621760>.
- [26] M. Svanberg, An improved leap-frog rotational algorithm, *Mol. Phys.* 92 (1997) 1085–1088, <https://doi.org/10.1080/002689797169727>.
- [27] D. Fincham, Leapfrog rotational algorithm, *Mol. Simul.* 24 (1992) 33–69, <https://doi.org/10.1080/08927029208022474>.
- [28] M.P. Allen, D.J. Tildesley, *Computer Simulation of Liquids*, Oxford University Press, Oxford, 1987.
- [29] A.J.C. Ladd, Monte carlo simulation of water, *Mol. Phys.* 33 (1977) 1039–1050, <https://doi.org/10.1080/00268977700100921>.
- [30] A.J.C. Ladd, Long-range dipolar interactions in computer simulations of polar liquids, *Mol. Phys.* 36 (1978) 463–474, <https://doi.org/10.1080/00268977800101701>.
- [31] M. Neumann, Dielectric properties and the convergence of multipolar lattice sums, *Mol. Phys.* 60 (1987) 225–235, <https://doi.org/10.1080/00268978700100171>.
- [32] C. Millot, J.-L. Rivail, R. Diguët, Static dielectric constant density and temperature dependence for the tips model of liquid methyl chloride, *Chem. Phys. Lett.* 160 (1989) 228–232, [https://doi.org/10.1016/0009-2614\(89\)87587-6](https://doi.org/10.1016/0009-2614(89)87587-6).
- [33] F. Dehez, M.T.C. Martins Costa, D. Rinaldi, C. Millot, Long-range electrostatic interactions in hybrid quantum and molecular mechanical dynamics using a lattice summation approach, *J. Chem. Phys.* 122 (2005) 234503, <https://doi.org/10.1063/1.1931667>.
- [34] D.J. Adams, G.S. Dubey, Taming the ewald sum in the computer simulation of charged systems, *J. Comput. Phys.* 72 (1987) 156–176, [https://doi.org/10.1016/0021-9991\(87\)90076-3](https://doi.org/10.1016/0021-9991(87)90076-3).
- [35] B. Cichocki, B.U. Felderhof, K. Hinsen, Electrostatic interactions in periodic coulomb and dipolar systems, *Phys. Rev. A* 39 (1989) 5350–5358, <https://doi.org/10.1103/PhysRevA.39.5350>.
- [36] C. Millot, J.-C. Soetens, M.T.C. Martins Costa, Static dielectric constant of the polarizable stockmayer fluid. comparison of the lattice summation and reaction field methods, *Mol. Simul.* 18 (1997) 367–383, <https://doi.org/10.1080/08927029708024131>.
- [37] K. Shimaoka, M. Kinoshita, K. Fujii, T. Tosaka, valuation of measurement data-supplement 1 to the guide to expression of uncertainty in measurement-propagation of distributions using a monte carlo method, https://www.bipm.org/documents/20126/2071204/JCGM_101_2008_E.pdf/325dcaad-c15a-407c-1105-8b7f322d651c, [Online; accessed 16-November-2021] (2008).
- [38] K. Shimaoka, M. Kinoshita, K. Fujii, T. Tosaka, Evaluation of measurement data –guide to the expression of uncertainty in measurement, https://www.bipm.org/documents/20126/2071204/JCGM_100_2008_E.pdf/cb0ef43f-baa5-11cf-3f85-4dcd86f77bd6, [Online; accessed 16-November-2021] (2008).
- [39] P.W. Bridgman, The Pressure-Volume-Temperature Relations of Fifteen Liquids, *Proc. Am. Acad. Arts Sci.* 68 (1933) 1–25, <https://doi.org/10.2307/20022928>.
- [40] A.A. Pribylov, E.B. Postnikov, Thermodynamic curvature and the thermal expansion isolines, *J. Mol. Liq.* 335 (2021) 115994, <https://doi.org/10.1016/j.molliq.2021.115994>.
- [41] M.F. Bolotnikov, Y.A. Neruchev, The enthalpies of vaporization and intermolecular interaction energies of 1-chloroalkanes, *Russ. J. Phys. Chem.* 80 (2006) 1191–1197, <https://doi.org/10.1134/S0036024406080024>.
- [42] V.V. Melent'ev, E.B. Postnikov, I. Polishuk, Experimental determination and modeling thermophysical properties of 1-chlorononane in a wide range of conditions: is it possible to predict a contribution of chlorine atom?, *Ind Eng. Chem. Res.* 57 (2018) 5142–5150, <https://doi.org/10.1021/acs.iecr.8b00174>.
- [43] J.-L. Daridon, D. Nasri, J.-P. Bazile, Computation of isobaric thermal expansivity from liquid density measurements application to toluene, *J. Chem. Eng. Data* 12 (2021), <https://doi.org/10.1021/acs.jced.1c00634>.
- [44] J.L. Lebowitz, J.K. Percus, L. Verlet, Ensemble dependence of fluctuations with application to machine computations, *Phys. Rev.* 153 (1967) 250–254, <https://doi.org/10.1103/PhysRev.153.250>.
- [45] P.S.Y. Cheung, On the calculation of specific heats, thermal pressure coefficients and compressibilities in molecular dynamics simulations, *Mol. Phys.* 33 (1977) 519–526, <https://doi.org/10.1080/00268977700100441>.
- [46] J.R. Durig, X. Zhu, S. Shen, Conformational and structural studies of 1-chloropropane and 1-bromopropane from temperature-dependant ft-ir spectra of rare gas solutions and ab initio calculations, *J. Mol. Struct.* 570 (2001) 1–23, [https://doi.org/10.1016/S0022-2860\(01\)00473-2](https://doi.org/10.1016/S0022-2860(01)00473-2).
- [47] P. Klabeo, The vibrational spectra of 2-chloro, 2-bromo, 2-iodo and 2-cyanopropane, *Spectrochim. Acta* 26A (1970) 87–108, [https://doi.org/10.1016/0584-8539\(70\)80253-7](https://doi.org/10.1016/0584-8539(70)80253-7).
- [48] D.A. Case, T.E. Cheatham III, T. Darden, H. Gohlke, R. Luo, K.M. Merz Jr., A. Onufriev, C. Simmerling, B. Wang, R.J. Woods, The amber biomolecular simulation programs, *J. Comput. Chem.* 26 (2005) 1668–1688, <https://doi.org/10.1002/jcc.20290>.
- [49] R. Salomon-Ferrer, D.A. Case, R.C. Walker, An overview of the amber biomolecular simulation package, *WIREs Comput. Mol. Sci.* 3 (2013) 198–210, <https://doi.org/10.1002/wcms.1121>.
- [50] A.P. Thompson, H.M. Aktulga, R. Berger, D.S. Bolintineanu, W.M. Brown, P.S. Crozier, P.J. in 't Veld, A. Kohlmeyer, S.G. Moore, T.D. Nguyen, R. Shan, M.J. Stevens, J. Tranchida, C. Trit, S.J. Plimpton, LAMMPS – a flexible simulation tool for particle-based materials modeling at the atomic, meso, and continuum scales, *Comput. Phys. Commun.* 271 (2022) 108171, <https://doi.org/10.1016/j.cpc.2021.108171>.

Katowice, 11.04.2023 r.

Instytut Chemii
Wydział Nauk Ścisłych i Technicznych
Uniwersytet Śląski w Katowicach
ul. Bankowa 12, 40-007 Katowice

Statement on the contribution to the publication

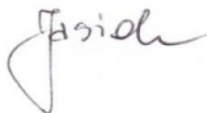
Publication:

B. Jasiok, M. Chorążewski, A.A. Pribylov, E.B. Postnikov, P. Friant-Michel, C. Millot, Thermophysical properties of chloropropanes in liquid phase: Experiments and simulations. *Journal of Molecular Liquids* **2022**, 358, 119137, DOI: 10.1016/j.molliq.2022.119137.

We hereby state that the contribution to the work published jointly with Bernadeta Jasiok is in accordance with the description below:

Bernadeta Jasiok

I was responsible for: Conceptualization, Methodology, Formal analysis, Investigation, Data Curation, Writing – Original Draft, Writing – Review & Editing, Visualization, Project administration



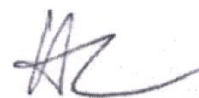
Mirosław Chorążewski

I was responsible for: Conceptualization, Writing – Original Draft, Writing – Review & Editing, Supervision, Funding acquisition



Alexander A. Pribylov

Software, Validation, Formal analysis, Writing – Original Draft, Writing – Review & Editing, Visualization



Eugene B. Postnikov

I was responsible for: Conceptualization, Methodology, Formal analysis, Investigation, Writing – Original Draft, Writing – Review & Editing, Visualization, Supervision



Pascale Friant-Michel

I was responsible for: Methodology, Software, Formal analysis, Writing – Original Draft, Writing – Review & Editing



Claude Millot

I was responsible for: Conceptualization, Methodology, Software, Formal analysis, Investigation, Data Curation, Writing – Original Draft, Writing – Review & Editing, Visualization, Supervision, Project administration



References

- [1] J. E. Proctor, *The Liquid and Supercritical Fluid States of Matter*, CRC Press, Boca Raton, FL, 2020. doi:10.1201/9780429491443.
- [2] A. Bertucco, G. Vetter (Eds.), *High Pressure Process Technology: Fundamentals and Applications*, Elsevier, Amsterdam, 2001.
- [3] E. Wilhelm, T. Letcher, *Volume Properties: Liquids, Solutions and Vapours*, Royal Society of Chemistry, Cambridge, 2014.
- [4] E. Wilhelm, T. Letcher, *Heat Capacities: Liquids, Solutions and Vapours*, Royal Society of Chemistry, Cambridge, 2010.
- [5] F. Salvador, J. Gimeno, M. Carreres, M. Crialesi-Esposito, Experimental assessment of the fuel heating and the validity of the assumption of adiabatic flow through the internal orifices of a diesel injector, *Fuel* 188 (2017) 442–451.
- [6] E. Tahmasebi, T. Lucchini, G. D’Errico, A. Onorati, G. Hardy, An investigation of the validity of a homogeneous equilibrium model for different diesel injector nozzles and flow conditions, *Energy Conversion and Management* 154 (2017) 46–55.
- [7] S. L. Randzio, From calorimetry to equations of state, *Chemical Society Reviews* 24 (5) (1995) 359–366. doi:10.1039/CS9952400359.
- [8] M. Taravillo, V. G. Baonza, M. Cáceres, J. Núñez, Thermodynamic regularities in compressed liquids: I. the thermal expansion coefficient, *Journal of Physics: Condensed Matter* 15 (19) (2003) 2979.
- [9] U. Deiters, K. De Reuck, Guidelines for publication of equations of state i. pure fluids (technical report), *Pure and applied chemistry* 69 (6) (1997) 1237–1250.

- [10] F. Aitken, J.-N. Foulc, *From Deep Sea to Laboratory 3: From Tait's Work on the Compressibility of Seawater to Equations-of-State for Liquids*, John Wiley & Sons, Hoboken, NJ, USA, 2019. doi:10.1002/9781119663362.
- [11] J.-L. Daridon, J.-P. Bazile, Computation of liquid isothermal compressibility from density measurements: an application to toluene, *Journal of Chemical & Engineering Data* 63 (6) (2018) 2162–2178.
- [12] B. A. Oakley, G. Barber, T. Worden, D. Hanna, Ultrasonic parameters as a function of absolute hydrostatic pressure. i. a review of the data for organic liquids, *Journal of Physical and Chemical Reference Data* 32 (4) (2003) 1501–1533.
- [13] M. Dzida, E. Zorębski, M. Zorębski, M. Żarska, M. Geppert-Rybczyńska, M. Chorążewski, J. Jacquemin, I. Cibulka, Speed of sound and ultrasound absorption in ionic liquids, *Chemical reviews* 117 (5) (2017) 3883–3929.
- [14] G. M. Kontogeorgis, X. Liang, A. Arya, I. Tsvintzelis, Equations of state in three centuries. are we closer to arriving to a single model for all applications?, *Chemical Engineering Science: X* 7 (2020) 100060.
- [15] J. O. Valderrama, The State of the Cubic Equations of State, *Industrial & Engineering Chemistry Research* 42 (2003) 1603–1618. doi:10.1021/ie020447b.
- [16] S. Zhou, J. R. Solana, Progress in the Perturbation Approach in Fluid and Fluid-Related Theories, *Chemical Reviews* 109 (2009) 2829–2858. doi:10.1021/cr900094p.
- [17] G. M. Kontogeorgis, G. K. Folas, *Thermodynamic Models for Industrial Applications: From Classical and Advanced Mixing Rules to Association Theories*, John Wiley & Sons, Chichester, 2009. doi:10.1002/9780470747537.
- [18] I. Polishuk, A. Mulero, The numerical challenges of SAFT EoS models, *Reviews in Chemical Engineering* 27 (2011) 241–251.

- [19] F. Shaahmadi, S. A. M. Smith, C. E. Schwarz, A. J. Burger, J. T. Cripwell, Group-Contribution SAFT Equations of State: A Review, *Fluid Phase Equilibria* (2022) 113674 doi:10.1016/j.fluid.2022.113674.
- [20] M. Chorążewski, E. B. Postnikov, B. Jasiok, Y. V. Nedyalkov, J. Jacquemin, A fluctuation equation of state for prediction of high-pressure densities of ionic liquids, *Scientific reports* 7 (1) (2017) 1–9.
- [21] B. Jasiok, E. B. Postnikov, M. Chorążewski, The prediction of high-pressure densities of different fuels using fluctuation theory-based tait-like equation of state, *Fuel* 219 (2018) 176–181.
- [22] A. R. Lowe, B. Jasiok, V. V. Melent'ev, O. S. Ryshkova, V. I. Korotkovskii, A. K. Radchenko, E. B. Postnikov, M. Spinnler, U. Ashurova, J. Safarov, et al., High-temperature and high-pressure thermophysical property measurements and thermodynamic modelling of an international oil standard: Ravenol diesel rail injector calibration fluid, *Fuel Processing Technology* 199 (2020) 106220.
- [23] B. Jasiok, A. R. Lowe, E. B. Postnikov, J. Feder-Kubis, M. Chorążewski, High-pressure densities of industrial lubricants and complex oils predicted by the fluctuation theory-based equation of state, *Industrial & Engineering Chemistry Research* 57 (34) (2018) 11797–11803.
- [24] F. Philippi, D. Rauber, K. L. Eliassen, N. Bouscharain, K. Niss, C. W. Kay, T. Welton, Pressing matter: why are ionic liquids so viscous?, *Chemical Science* 13 (9) (2022) 2735–2743.
- [25] J. Mackenzie, The elastic constants of a solid containing spherical holes, *Proceedings of the Physical Society. Section B* 63 (1) (1950) 2.
- [26] N. Ramakrishnan, V. Arunachalam, Effective elastic moduli of porous solids, *Journal of materials science* 25 (9) (1990) 3930–3937.

- [27] L. D. Landau, E. M. Lifshitz, *Statistical Physics: Volume 5*, Vol. 5, Elsevier, 2013.
- [28] <https://webbook.nist.gov/chemistry/fluid/>.
- [29] P. Walden, Molecular weights and electrical conductivity of several fused salts, *Bull. Acad. Imper. Sci.(St. Petersburg)* 1800 (1914).
- [30] D. D. Patel, J.-M. Lee, Applications of ionic liquids, *The Chemical Record* 12 (3) (2012) 329–355.
- [31] A. J. Greer, J. Jacquemin, C. Hardacre, Industrial applications of ionic liquids, *Molecules* 25 (21) (2020) 5207.
- [32] A. Ray, B. Saruhan, Application of ionic liquids for batteries and supercapacitors, *Materials* 14 (11) (2021) 2942.
- [33] P. Bridgman, Thermodynamic properties of liquid water to 80 and 12000 kgm, in: *Proceedings of the American Academy of Arts and Sciences*, Vol. 48, American Academy of Arts & Sciences, 1912, pp. 309–362.
- [34] E. B. Postnikov, M. Chorążewski, Transition in fluctuation behaviour of normal liquids under high pressures, *Physica A: Statistical Mechanics and its Applications* 449 (2016) 275–280.
- [35] B. Jasiok, E. B. Postnikov, M. Chorążewski, The prediction of high-pressure volumetric properties of compressed liquids using the two states model, *Physical Chemistry Chemical Physics* 21 (29) (2019) 15966–15973.
- [36] M. Chorążewski, E. B. Postnikov, K. Oster, I. Polishuk, Thermodynamic properties of 1, 2-dichloroethane and 1, 2-dibromoethane under elevated pressures: experimental results and predictions of a novel dippr-based version of ft-eos, pc-saft, and cp-pc-saft, *Industrial & Engineering Chemistry Research* 54 (39) (2015) 9645–9656.

- [37] H. Guerrero, L. M. Ballesteros, M. García-Mardones, C. Lafuente, I. Gascón, Volumetric properties of short-chain chloroalkanes, *Journal of Chemical & Engineering Data* 57 (7) (2012) 2076–2083.
- [38] E. B. Postnikov, B. Jasiok, V. V. Melent'ev, O. S. Ryshkova, V. I. Korotkovskii, A. K. Radchenko, A. R. Lowe, M. Chorazewski, Prediction of high pressure properties of complex mixtures without knowledge of their composition as a problem of thermodynamic linear analysis, *Journal of Molecular Liquids* (2020) 113016.
- [39] S. L. Randzio, J. P. E. Grolier, M. Chorazewski, High-pressure “maxwell relations” measurements, *Volume Properties: Liquids, Solutions and Vapours* (2014) 414–438.
- [40] S. Randzio, J.-P. Grolier, J. Quint, D. Eatough, E. Lewis, L. Hansen, n-hexane as a model for compressed simple liquids, *International journal of thermophysics* 15 (3) (1994) 415–441.

7 Appendix – author’s scientific activity

Results performed studies were published in the six papers:

- P1. **Bernadeta Jasiok**, Eugene B. Postnikov, Mirosław Chorążewski, The prediction of high-pressure volumetric properties of compressed liquids using the two states model. *Physical Chemistry Chemical Physics* 2019, 21, 15966-15973, DOI: 10.1039/C9CP02448D.
- P2. Eugene B. Postnikov, **Bernadeta Jasiok**, Mirosław Chorążewski, The CATBOOST as a tool to predict the isothermal compressibility of Ionic Liquids. *Journal of Molecular Liquids* 2021, 333, 115889, DOI: 10.1016/j.molliq.2021.115889.
- P3. Eugene B. Postnikov, **Bernadeta Jasiok**, Vyacheslav V. Melent’ev, Olga S. Ryshkova, Vadim I. Korotkovskii, Anton K. Radchenko, Alexander R. Lowe, Mirosław Chorążewski, Prediction of high pressure properties of complex mixtures without knowledge of their composition as a problem of thermodynamic linear analysis. *Journal of Molecular Liquids* 2020, 310, 113016, DOI: 10.1016/j.molliq.2020.113016.
- P4. **Bernadeta Jasiok**, Eugene B. Postnikov, Ivan Yu. Pikalov, Mirosław Chorążewski, Prediction of the speed of sound in ionic liquids as a function of pressure. *Journal of Molecular Liquids* 2022, 363, 119792, DOI: 10.1016/j.molliq.2022.119792.
- P5. **Bernadeta Jasiok**, Mirosław Chorążewski, Eugene B. Postnikov, Claude Millot, Liquid dibromomethane under pressure: a computational study. *Physical Chemistry Chemical Physics* 2021, 23, 2964-2971, DOI: 10.1039/D0CP06458K.
- P6. **Bernadeta Jasiok**, Mirosław Chorążewski, Alexander A. Pribylov, Eugene B. Postnikov, Pascale Friant-Michel, Claude Millot, Thermophysical properties of chloropropanes in liquid phase: Experiments and simulations. *Journal of Molecular Liquids* 2022, 358, 119137, DOI: 10.1016/j.molliq.2022.119137.

Mentioned papers are attached to Chapter 6. Publications with statements of co-authors on contribution. Moreover, I am a co-author of 5 following articles which are not directly linked to the topic of the dissertation:

1. Mirosław Chorążewski, Eugene B. Postnikov, **Bernadeta Jasiok**, Yuriy V. Nedyalkov, Johan Jacquemin, A fluctuation equation of state for prediction of high-pressure densities of ionic liquids. *Scientific Reports* 2017, 7(1), 1-9, DOI: 10.1038/s41598-017-14855-2.
2. **Bernadeta Jasiok**, Eugene B. Postnikov, Mirosław Chorążewski, The prediction of high-pressure densities of d fluctuation theory-based Tait-like equation of state. *Fuel* 2018, 219, 176-181, DOI: 10.1016/j.fuel.2018.01.091.
3. **Bernadeta Jasiok**, Alexander R. Lowe, Eugene B. Postnikov, Joanna Feder-Kubis, Mirosław Chorążewski, High-pressure densities of industrial lubricants and complex oils predicted by the fluctuation theory-based equation of state. *Industrial & Engineering Chemistry Research* 2018, 57, 11797-11803, DOI: 10.1021/acs.iecr.8b01542.
4. Alexander R. Lowe, **Bernadeta Jasiok**, Vyacheslav V. Melent'ev, Olga S. Ryshkova, Vadim I. Korotkovskii, Anton K. Radchenko, Eugene B. Postnikov, Monika Spinnler, Ulkar Ashurova, Javid Safarov, Egon Hassel, Mirosław Chorążewski, High-temperature and high-pressure thermophysical property measurements and thermodynamic modelling of an international oil standard: RAVENOL diesel rail injector calibration fluid. *Fuel Processing Technology* 2020, 199, 106220, DOI: 10.1016/j.fuproc.2019.106220.
5. Andrzej Grzybowski, Alexander R. Lowe, **Bernadeta Jasiok**, Mirosław Chorążewski, Volumetric and viscosity data of selected oils analyzed in the density scaling regime. *Journal of Molecular Liquids* 2022, 353, 118728, DOI: 10.1016/j.molliq.2022.118728.

List of oral presentations

1. Bernadeta Jasiok, Mirosław Chorążewski, Rao equation analysis in Ionic Liquids under high pressure, 13th Winter Workshop on Molecular Acoustics, Relaxation and Calorimetric Methods, 28 February 2017, Szczyrk
2. Bernadeta Jasiok, Eugene B. Postnikov, Mirosław Chorążewski, Nowe podejście do oceny przewidywania prędkości propagacji fali ultradźwiękowej w płynach technicznych pod ciśnieniem, 61. Zjazd Naukowy Polskiego Towarzystwa Chemicznego, 17-21 September 2018, Kraków
3. Bernadeta Jasiok, Eugene B. Postnikov, Mirosław Chorążewski, The two states model for prediction of high-pressure volumetric properties of polar and non-polar liquids, European/Japanese Molecular Liquid Group, 8-13 September 2019, Kutná Hora, Czech Republic
4. Bernadeta Jasiok, Eugene B. Postnikov, Mirosław Chorążewski, Claude Millot, Thermophysical properties of dibromomethane: a computational study, 63. Zjazd Naukowy Polskiego Towarzystwa Chemicznego, 13-17 September 2021, Łódź
5. Bernadeta Jasiok, Eugene B. Postnikov, Ivan Yu. Pikalov, Mirosław Chorążewski, Prediction of high pressure thermodynamic properties of ionic liquids, European/Japanese Molecular Liquid Group, 12-16 September 2022, Barcelona, Spain

List of poster presentations:

1. Bernadeta Jasiok, Marzena Dzida, Mirosław Chorążewski, Does the variation of the speed of sound through liquids proves correct also in ionic liquids under high pressure? 60. Zjazd Naukowy Polskiego Towarzystwa Chemicznego, 17-21 September 2017, Wrocław
2. Bernadeta Jasiok, Eugene B. Postnikov, Mirosław Chorążewski, A fluctuation equation of state for prediction of high-pressure speed of sound, Tenth Liblice Conference on the Statistical Mechanics of Liquids, 17-22 June 2018, Srni, Czech Republic

List of awarded grants:

1. Preludium 21, finansowane ze środków NCN "MEDUSA – anomalia termodynamiczne w cieczach z wykorzystaniem symulacji komputerowych" / "MEDUSA – thermodynamic anomalies in liquids Using computer Simulations", numer projektu 555934

List of internships abroad:

1. Internship at Kursk State University (Russia), Theoretical Physics Department/Research Center for Condensed Matter Physics, 10 July – 5 August 2018
2. 6 months internship at University of Lorraine, Laboratory of Theoretical Physics and Chemistry, Nancy (France), as part of Iwanowska's Program financed by the Polish National Agency for Academic Exchange (Poland) Decision No. PPN/IWA/2018/1/00054/DEC/1 "Explaining the anomalous thermodynamic properties of compressed liquids at high pressure using the Fluctuations Equation of State and Molecular Dynamics simulation", 01 September 2019 – 29 February 2020
3. Internship at Università Degli Studi di Ferrara (Italy), Department of Chemical, Pharmaceutical and Agricultural Sciences, 02 – 08 May 2022

List of workshops abroad:

1. 9 days internship at University of Lorraine, Laboratory of Theoretical Physics and Chemistry, Nancy (France), as part of Non-competition project of Polish National Agency for Academic Exchange "International scholarship exchange of PhD candidates and academic staff", Decision No. PPI/PRO/2018/1/00029/U/001 "Simulation study of the thermodynamic properties of liquid dibromomethane", 01 – 09 July 2019

Distinctions and awards

1. Grant of the Rector of the University of Silesia for the best students (2018)
2. Scholarship holder in the OPUS 12 project "Nowe doświadczalne i teoretyczne spojrzenie na właściwości termofizyczne skompresowanych cieczy. Termodynamiczne modelowanie równań stanu" / "A new experimental and theoretical insights for practical handling of pressurized liquids. Modeling using the equations of state approach" – as a Master Student
3. Rector's scholarship – the academic year 2020/2021
4. Scholarship holder in the OPUS 12 project "Nowe doświadczalne i teoretyczne spojrzenie na właściwości termofizyczne skompresowanych cieczy. Termodynamiczne modelowanie równań stanu" / "A new experimental and theoretical insights for practical handling of pressurized liquids. Modeling using the equations of state approach" – as a Ph.D. Student